MASSACHUSETTS INSTITUTE OF TECHNOLOGY

DEPARTMENT OF NUCLEAR ENGINEERING

Cambridge, Massachusetts 02139

THE REACTIVITY AND TRANSIENT ANALYSIS OF MITR-II

by

Nuh Tolga Yarman,

A. F. Henry, D. D. Lanning, J. W. Gosnell

July, 1972

MITNE - 139

THE REACTIVITY AND TRANSIENT ANALYSIS OF MITR-II

by

Nuh Tolga Yarman

B.S., M.S., Institut National des Sciences Appliquées (INSA) de Lyon (1967)

M.S., Institute for Nuclear Energy, Technical University of Istanbul (1968)

SUBMITTED IN PARTIAL FULFILLMENT OF THE REQUIREMENTS FOR THE DEGREE OF DOCTOR OF PHILOSOPHY

at the

MASSACHUSETTS INSTITUTE OF TECHNOLOGY

July 1972

Signature of Author ______________________________
Department of Nuclear Engineering, July, 1972

Certified by ______________________________
Thesis Supervisor

Certified by ______________________________
Thesis Supervisor

Accepted by ______________________________
Chairman, Departmental Committee on Graduate Students

THE REACTIVITY AND TRANSIENT ANALYSIS OF MITR-II

by

Tolga Yarman

Submitted to the Department of Nuclear Engineering on 24 July, 1972, in partial fulfillment of the requirements for the degree of Doctor of Philosophy.

ABSTRACT

The two-dimensional, time dependent, three-group diffusion equations for the proposed designed core of the MIT reactor are written with an extra source term accounting for the photoneutrons generated in the D_2O reflector. An analytical expression is developed for this term. Then an approximate flux composed of two spatial shapes chosen beforehand, each having an unknown time coefficient, is inserted into the time dependent multigroup equations and the weighted residual criteria is applied. This yields multimode kinetics equations with generalized definitions for the conventional matrix parameters: generation time, reactivity, delayed neutron (and photoneutron) fractions matrices. Computational methods for these parameters are presented. An accident concerning the withdrawal of the shim rods is examined with the code OZAN written for the purpose of the computations required by the present work. This study suggests that a space-dependent analysis is required to analyse the accident postulated.

Thesis Supervisors: A. F. Henry, Professor of Nuclear Engineering

D. D. Lanning, Professor of Nuclear Engineering

J. W. Gosnell, Assistant Professor of Nuclear Engineering

ACKNOWLEDGEMENTS

The author would like to express his gratitude to Professor A. F. Henry. He provided guidance and made himself available for discussions whenever requested.

To Professor D. D. Lanning. He shared the guidance of this work and several ideas. He provided a Research Assistantship when it was necessary and support for performing computations required by the present work, at the M.I.T. Information Processing Center.

To Professor J. W. Gosnell. He also shared the guidance of this work and several ideas.

To his parents, brothers and sisters, his friends and Pan. With their help and encouragement they made the accomplishment of this work much easier.

The author would like to extend his thanks to the Scientifical and Technical Research Council of Turkey who provided a NATO fellowship for most of the course of the present work.

BIOGRAPHICAL NOTE

Tolga Yarman was born in 1945, in Istanbul (Turkey). He attended elementary and secondary school at the "Galatasaray Lisesi", in Istanbul. He graduated in June 1963.

He entered the "Institut National des Sciences Appliquées (INSA) de Lyon" in September 1963. In June 1967 he received the "equivalent" of a B.S.-M.S. degree in Chemical Engineering.

In October 1967 he was appointed as a teaching assistant in the Chemical Engineering Department (Physical Chemistry Division) of The Technical University of Istanbul. At the same time he enrolled as a graduate student in the "Institute for Nuclear Energy" of the Technical University of Istanbul. In September 1968 he was graduated with the "equivalent" of an M.S. degree in Nuclear Engineering.

He then entered Massachusetts Institute of Technology as a graduate student in the Department of Chemistry. He transferred to the Department of Nuclear Engineering in February, 1969.

TABLE OF CONTENTS

Page

LIST OF FIGURES

LIST OF TABLES

CHAPTER I

INTRODUCTION

The reactivity and transient analysis of a reactor consists of predicting the behavior of the neutron flux at a point in the reactor during a transient. This leads ultimately to information about the behavior of the power level of the reactor, during the transient.

1-1 Point Kinetics Method

There are a number of ways of performing the analysis. The point kinetics method is the conventional one. This method assumes that the time and space dependent neutron flux, throughout a transient can be expressed in terms of the product of two functions: the first one a function of time alone, and the second one a function of space alone. Supposing that the space function is known, one can then derive (from the multigroup diffusion equations) the conventional point kinetics equations for the time function - of the time and space dependent flux expression - .

Parameters appearing in the point kinetics equations;

The point kinetics equations involve a number of parameters (reactivity, generation time and delayed neutron fractions) the value of which depend on the manipulations (weighting, integration, etc.) undertaken to get rid of the space dependency in deriving the point kinetics equations.

Thus the point kinetics method consists of fixing a space function that is supposed to express the space dependency of the time and space dependent flux, and then determining, through appropriate manipulations the conventional parameters of the point kinetics equations.

Case where the space function is the flux shape of the critical reactor;

It is customary to choose as the space function the shape of the critical reactor. In this case (and assuming that the weighting function is the same for all cases) generation time and delayed neutron fractions, are always the same for all changes in the reactor that cause the transient.

Thus the reactivity and transient analysis of a given reactor will consist of determining the reactivity that characterizes the transient in question,and solving the point kinetics equations for the time function of the flux expression. The time and space dependent flux at any point of the reactor is then predicted to be the steady state, critical shape changing in magnitude during the transient in accord with the solution of the point kinetics equations.

Hence, if possible small changes in fission cross section are neglected, the solution of the points kinetics equations characterizes the beha ior of the power level of the reactor during a transient.

1-2 Solution Techniques accounting for the space dependency of the time and space dependent flux during a transient

A number of methods that account for changes in the shape of the flux during a transient have been developed and may be used for the transient analysis of a reactor.

These methods can be placed into two broad categories [26,27].

Indirect solution techniques;

The first category involves indirect solution techniques that make some assumptions about the mathematical form of the time and space dependent flux over subregions or over the entire reactor, and perhaps also over various periods of time during the transient. These assumptions are then forced into the final solution.

Direct solution techniques;

The second category involves direct techniques that generally consist of finding the solution of the finite difference approximation to the time dependent multigroup diffusion equations.

Differences between the Indirect and Direct solution techniques;

It is worthwhile to point out that there are two major differences between the indirect techniques and direct techniques, of attacking the space-dependent kinetics equations.

The indirect techniques are reasonably fast in computing the final solution, but lack definitive error bounds. Thus whether or not a set of trial functions (assumptions made about the shape of the time and space dependent flux) will give good results for a particular perturbation, is rather intuitive. The direct finite difference techniques, in contrast, require much more time for computations, but are characterized by definitive error estimates. For this reason they are very useful as numerical standards against which the more approximate methods can be compared.

*

The very first step that must be taken for the "Reactivity and Transient Analysis of MITR-II" is to chose an appropriate method (among these summarized in the first two sections of the present chapter), or if necessary to construct one ourselves.

1-3 The reactivity and transient analysis of MITR-II; set up of the problem.

MITR-II stands for the redesign of the Massachusetts Institute of Technology research reactor. This reactor [28] (cf. also Appendix G) will be cooled and moderated by light water. The reflector is composed of heavy water. Photoneutron sources are present in the D_2O reflector because of the interaction of the radiation coming out of the core with the deuterium nuclei .

Can the point kinetics method be adequate?

There are complications in applying the point kinetics model to MITR-II. First of all it is not clear how we are going to account for the photoneutrons in the computation of the reactivity characterizing the transient in question. More serious than that, it is not guaranteed in the case of MITR-II, that the time and space dependent flux can be represented using only one shape throughout a transient.

Thus the primary purpose of this thesis is to investigate a more sophisticated method of analysis and to compare the predictions with the ones obtained through a point kinetics type of approach (accounting also for the photoneutrons).

The Basic Model;

As a basic model we assume that the time dependent multigroup diffusion equations can describe the time and space dependent flux in the MITR-II. However the presence of photoneutron sources in D_2O reflector, will require more elaboration. Thus we write

$$v^{-1}\frac{\partial \phi(\underline{r},t)}{\partial t} = [\nabla\cdot D(\underline{r},t)\nabla - A(\underline{r},t) + (1-\beta)\nu\chi_p\,\Sigma_F^T\,(\underline{r},t)]\phi(\underline{r},t)$$

$$+\sum_{j=1}^{J}\lambda_j\chi_j\eta_j\,(\underline{r},t) + S(\underline{r},t) \qquad , \qquad (1\text{-}1)$$

$$\frac{\partial \eta_j(\underline{r},t)}{\partial t} = \beta_j \nu \, \Sigma_F^T(\underline{r},t)\phi(\underline{r},t) - \lambda_j \eta_j(\underline{r},t) \quad ,$$

$$(j = 1,\ldots, J), \qquad (1\text{-}2)$$

where; $S(\underline{r},t)$ refers to the photoneutrons generated in the reflector and the familiar diffusion theory, matrix notation (spelled out in the body of the dissertation - cf. Chapter III-) is used.

An analytical solution of Equations (1-1) and (1-2), even when the photoneutron source term $S(\underline{r},t)$ is not present, is not known, and the method we are to investigate will consist of obtaining an approximate solution to these simultaneous equations. This requires first constructing an analytical expression for the photoneutron source term, $S(\underline{r},t)$.

1-4 Photoneutron source term

In the analysis of a reactor [25] , similar to MITR-II it is pointed out that the photoneutrons may be significant during a transient. The argument we develop below, supports this assumption.

A simple scheme;

Consider an atom of U^{235} fissioning in an infinite medium of heavy water. Let N_0 be the total number of delayed photons coming out of the fission products that have sufficient energy to generate photoneutrons. Let $\overline{\Sigma}$ and $\overline{\Sigma}_D$ be respectively the average macroscopic attenuation and photoneutron reaction cross sections in D_2O, for the photons of interest. Thus

$$N_0 \int_{R_1}^{R_2} \frac{1}{4\pi r^2} \overline{\Sigma}_D e^{-\overline{\Sigma} r} 4\pi r^2 \, dr = N_0 \frac{\overline{\Sigma}_D}{\overline{\Sigma}} (e^{-\overline{\Sigma} R_1} - e^{-\overline{\Sigma} R_2}), \qquad (1\text{-}3)$$

represents the total number of photoneutrons produced by the photons of interest in the volume between the two spheres of radius R_2 and R_1 centered at the point where the atom of U^{235} is located in the infinite medium of heavy water (cf. Appendix B).

Next assume that, MITR-II can be represented by a spherical model with R_1 and R_2 being the inner and outer radius of the D_2O reflector and that the radiation is coming from a point source located at the center of the reactor and embedded in pure D_2O (cf. Chapter II). We then expect

$$\text{pct} = \frac{N_0 \frac{\overline{\Sigma}_D}{\overline{\Sigma}} (e^{-\overline{\Sigma} R_1} - e^{-\overline{\Sigma} R_2}) \times 100}{N_0 \frac{\overline{\Sigma}_D}{\overline{\Sigma}}}, \qquad (1\text{-}4)$$

percent of the total amount of the delayed photoneutrons produced by delayed photons from fission products of U^{235} on D_2O, to be produced in the D_2O reflector of MITR-II. Taking $R_1 = 30$ cm, $R_2 = 60$ cm and $\overline{\Sigma} = 0.04\ cm^{-1}$, we obtain

$$\text{pct} \approx 21\% \qquad (1\text{-}5)$$

Thus the ratio of delayed photoneutrons to the total number of neutrons produced due to the fission of U^{235} in an infinite medium of heavy water being $\approx 1.\times 10^{-3}$, the MITR-II delayed photoneutrons can reach a fraction of $\approx 2.\times 10^{-4}$. This may indeed be significant compared to the total delayed neutron fraction ($\approx 7\times 10^{-3}$).

Prompt photoneutrons;

Besides the delayed photoneutrons there are also prompt photoneutrons due to prompt gamma rays (fission, capture, inelastic scattering, etc.) generated within the reactor. A quick comparison of prompt photoneutrons produced by prompt photons from the fission of U^{235} on D_2O, with delayed photoneutrons produced by delayed photons from the fission products of U^{235}, on D_2O (cf. Chapter II) will suggest that the former ones are as important as the latter ones.

These considerations require that we devote attention to the photoneutrons throughout this thesis. Thus the photoneutron source term will be studied, and Chapter II, Appendices A and B are concerned with an appropriate analytical expression for the photoneutron source term in Eq. (1-1).

1-5 Proposed method

Among the approximate ways of attacking Equations (1-1) and (1-2) summarized in the first two sections of the present chapter we intend to examine the simplest one that will account for the space dependency of the time and space dependent flux.

Time synthesis;

This method, called time synthesis, assumes that $\emptyset(\underline{r},t)$ can be expressed approximately as the sum of two fixed shapes, each having an undetermined, time dependent coefficient. We thus intend to examine a trial function of the form

$$\bar{\emptyset}\,(\underline{r},t) = \psi_1(\underline{r})\; N_1(t) + \psi_2(\underline{r})\; N_2(t), \qquad (1\text{-}7)$$

in which the flux shapes $\psi_1(\underline{r})$ and $\psi_2(\underline{r})$ do not depend on time and can be selected in a number of ways.

Application of the weighted residual method [27];

By substituting the RHS of Eq. (1-7) into Equations (1-1) and (1-2) we obtain residuals.

Chapter III describes the application of the weighted residual method to find equations for $N_1(t)$ and $N_2(t)$ from these residuals. In this chapter, in spite of the complicated expression accounting for the photoneutron source term in Eq. (1-1) we shall still be able to obtain the conventional form for the multi mode kinetics equations, with however different definitions for the various parameters.

Thus the problem will be reduced to solving for N(t)

$$\Lambda \frac{dN(t)}{dt} = [\rho_{new}(t) - \overline{\beta}_{new}(t)]\ N(t) + \sum_{j=1}^{H} \lambda_j C_j(t) \qquad (1\text{-}8)$$

$$\frac{dC_j(t)}{dt} = \overline{\beta}_{j_{new}}(t)\ N(t) - \lambda_j C_j(t) \ , \ (j=1,\ldots, H), \qquad (1\text{-}9)$$

and where the summation over the delayed neutron groups also includes delayed photoneutron groups, and Λ, ρ_{new} (t) and $\overline{\beta}_{j_{new}}$'s are [2x2] matrices.

1-6 Computation of the parameters Λ, $\rho_{new}(t)$ and $\overline{\beta}_{j_{new}}$ (t)'s; Chapter IV and V

The computation of the matrix parameters that appears in Equations (1-8) and (1-9) turned out to be a difficult problem.

In Chapter V, which is closely related to Chapter IV, methods for computing various parameters appearing in Equations (1-8) and (1-9) in a consistent way are presented.

*

A computer code OZAN* (described briefly in Appendix N, and presented in Appendix O) was created to perform computations required by the present work.

* OZAN means poet in Turkish.

1-7 Chapter VI, A problem treated by the proposed method

We attempted to use OZAN in the case of the withdrawal of the blade of shim rods and to predict the behavior of the power level. The accident of interest is presented in Chapter VI. The complications that arose - because of the particular character of the problem - are then discussed. Finally a comparison of these predictions with the ones obtained through a point kinetics type of approach is made.

1-8 Chapters VII and VIII, checks and conclusions

Tests that validate OZAN are described in Chapter VII, and conclusions about the present work are drawn in Chapter VIII.

CHAPTER II

STUDY OF THE PHOTONEUTRON SOURCE TERM $S_g(\underline{r},t)$

In this chapter our goal is to develop an analytical expression for $S_g(\underline{r},t)$ which will account for the number of photoneutrons generated per cm^3 per sec. within the g^{th} neutron group at a point $\underline{r}$ and time t in the D_2O reflector.

If we had a D_2O cooled AND reflected reactor, we could think of using the data (shown in Table 2-1) relevant to the generation of photoneutrons - in an infinite medium of heavy water by photons coming out of the fission of U^{235}-. With some effectiveness correction due to the leakage out of the reactor of photons giving rise to photoneutrons, this would have covered the production of delayed photoneutrons.

Table 2-1 [1]

Group Constants for Delayed Photoneutrons from U^{235} Fission Gammas on D_2O

Group index, i	Half-life	λ_j	$\beta_j(10^{-5})$
1	12.8 d	6.26×10^{-7}	0.05
2	53 h	3.63×10^{-6}	0.103
3	4.4 h	4.37×10^{-5}	0.323
4	1.65 h	1.17×10^{-4}	2.34
5	27 m	4.28×10^{-4}	2.07
6	7.7 m	1.50×10^{-3}	3.36
7	2.4 m	4.81×10^{-3}	7.00
8	41 s	1.69×10^{-2}	20.4
9	2.5 s	2.77×10^{-1}	65.1
			Total 100.75

Average D_2O photoneutron half-life $\equiv (\ln_e 2) \sum(\beta_j/\lambda_j)/\sum\beta_j$
$= 16.7$ min (following saturation irradiation)

Instead, in the MITR-II D_2O is present in the reflector only. In addition we have other gamma rays than the ones coming from U^{235} and causing the photoneutron reaction. We would also like to have a space dependent photoneutron source term. All this forces us to drop the previous data of Table 2-1 and to try a different approach to the solution of the problem.

To this end we will start with the production of photons within the reactor. We next compute through a shielding type of calculation the photon flux in a given energy range at a point $\underline{r}$ in the reflector, and finally make use of the photoneutron reaction cross sections.

Let then $I(\underline{r},\Lambda,t)$ be the non-directional flux of photons of energy Λ per cm^2 per Mev per second in the reflector at $\underline{r}$ and time t.

Let $\Sigma_D(\underline{r},\Lambda,t)$ be the macroscopic photoneutron reaction cross section of deuterium in the reflector at $\underline{r}$ and time t, for the incident photons of energy Λ.

Let $P_\Lambda(E)dE$ be the probability for the photoneutron generated by an incident photon of energy Λ to be emitted within the energy dE around E. ($P_\Lambda(E)$ - with some pertinent forms- is described in Appendix C).

Thus the product

$$I(\underline{r},\Lambda,t)\ \Sigma_D(\underline{r},\Lambda,t)P_\Lambda(E)dE\ d\Lambda, \qquad (2\text{-}1)$$

gives the number of photoneutrons per cm^3 per sec. generated in the reflector, at $\underline{r}$ and time t in the range dE about E, by incident photons of energy lying within $d\Lambda$ around Λ.

This is the first step in obtaining $S_g(\underline{r},t)$, the photoneutron source term. However there are a number of problems hidden in Eq. (2-1). How are we going to determine $I(\underline{r},\Lambda,t)$? Trying to solve the transport equation for the directional photon flux over the reactor volume [9] is impractical and also ill advised unless we have reason to believe photoneutrons are very important.

It would in fact be a great simplification if we could work only with the uncollided photons. But would this approximation be valid? In other words, can the photoneutrons generated by photons having had collisions, especially by photons having had one and only one collision, be neglected as compared to photoneutrons generated by the uncollided photons?

The answer to the latter question is developed in Appendix A and is yes (within an approximation of a few per cent).

A second problem concerns the accuracy of the data specifying the production and attenuation of photons, and the accuracy of photoneutron reaction cross sections. Are these data consistent? If so, one should be able to generate theoretically the results of Table 2-1 starting with the data for the production of photons coming out of the fission of U^{235}.

The latter question has been studied in Appendix B, and the data we shall work with, has been found satisfactorily consistent.

Furthermore this checking procedure led us to establish an analytical expression for the decay curves of fission photons having an energy above 2.23 Mev (the threshold energy for the photoneutron reaction in heavy water) - Fig. B-1 - in terms of - the time wise - group decay constants of photoneutrons shown in Table 2-1. This correlation becomes clear when we recognize that the appearance of a photoneutron of a given half life, implies there must be a photon having that same half life to generate the photoneutron in question.

Our next problem concerns the geometry of the system. Even though we use the uncollided photon flux approximation the expression for $I(\underline{r},\Lambda,t)$ is extremely complicated. Again, since we do not expect photoneutrons to be very important, we make a gross approximation.

Thus if $S_f(\underline{r},\Lambda,t)$ is the number of photons of "f^{th} type" (this terminology will become more clear shortly) emitted per cm^3 per Mev per second at location $\underline{r}$ in the reactor, with energy Λ and at time t, we define

$$S_f(\Lambda,t) = \int_{\underline{r},\text{reactor}} S_f(\underline{r},\Lambda,t)\, d\underline{r} \qquad (2\text{-}2)$$

We then assume for the purpose of computing $I(\underline{r},\Lambda,t)$ in the reflector that the extended source, $S_f(\underline{r},\Lambda,t)$, throughout the reactor may be replaced by the point source, $S_f(\Lambda,t)$, located at the center of the reactor, and embedded in pure D_2O.†

† This simplification has two consequences that tend to cancel each other: the intensity of photons from a source that is moved back, will be decreased at a point (r,z) in the reflector; but also the attenuation through D_2O instead of the heavier core material, is now easier.

For the purpose of comparing these two consequences we suppose we have reason to adopt the scheme shown on the next page.

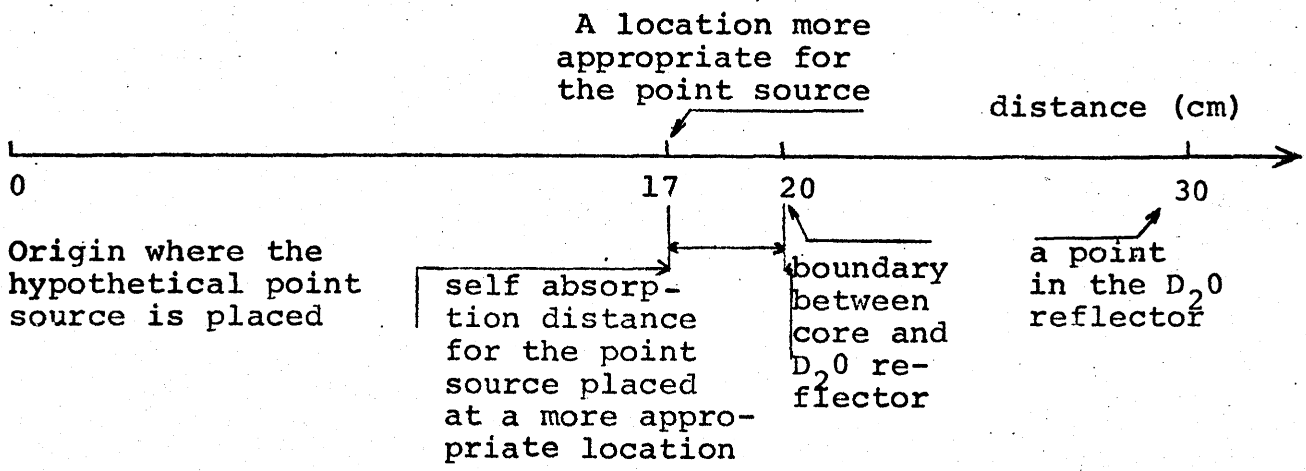

In addition assume we deal with photons of energy, approximately, 3 Mev, for which the total macroscopic attenuation cross section in the heavy core material and in the D_2O is taken to be, respectively, 0.2 and 0.04 cm^{-1}.

Then the attenuation coefficient for both of the cases (point source placed at the center of the reactor and embedded in pure D_2O, and point source placed at a more appropriate location within the core - where the self absorption distance can be figured out through a shielding type of information -), - assuming that the photons are emitted isotropically - , is

$$\frac{1}{4\pi(900)} e^{-(30 \times 0.04)} ,$$

and

$$\frac{1}{4\pi(169)} e^{-(3 \times 0.8 + 10 \times 0.04)} .$$

Hence supposing that the second description for the attenuation is closer to the reality than the first one, we can see that

- Moving back the point source to the center of the reactor decreases the intensity of photons at a point in the reflector as much as: $\frac{900}{169} \approx 5$;

- But also, the attenuation is now easier as much as

$$\frac{e^{-(30 \times 0.04)}}{e^{-(3 \times 0.8 + 10 \times 0.04)}} \approx 5.$$

†

We are now ready to work out an expression for $I(\underline{r},\Lambda,t)$. This photon flux has two components, one due to the prompt gamma rays, the other due to delayed gamma rays, that, we believe, deserve equal attention.†

† To see that consider one atom of U^{235} fissionning in the middle of an infinite medium of D_2O. Both prompt and delayed gamma rays will be emitted due to that fission. Thus we intend to compare the number of photoneutrons generated by the uncollided prompt photons, with the number of photoneutrons generated by the uncollided delayed photons, from respectively, the fission, and fission products of U^{235} on D_2O.

For the purpose of calculation we recall the results given in Appendix B for the two-group scheme of photons, and the output of the Code POPOP IV (cf. Appendix D) for the prompt fission gamma rays from U^{235} (that is, 0.163 photons for the higher energy group - Λ_0 = 7 Mev - and 0.483 photons for the second group - Λ_1 = 3.5 Mev -, per fission). Then it is found:

- $\sim$ 2. x 10^{-3} prompt photoneutrons due to uncollided prompt photons, per fission of U^{235}, and;

- $\sim$ 1.4 x 10^{-3} delayed photoneutrons due to uncollided delayed photons (emitted between t=1 sec. and t=∞ sec.), per fission of U^{235}.

As will be seen below, there are also other prompt gamma rays than the fission prompt gamma rays. Hence an equal attenuation will be paid to the study of the prompt photoneutron source term as well as the study of the delayed photoneutron source term.

†

2-1 Component of $I(r,z,\Lambda,t)^*$ due to Prompt gamma rays and the corresponding photoneutron source term

The prompt gamma rays are emitted within 10^{-7} sec. and can be coming from the fission event, inelastic scattering of neutrons, or capture of neutrons.

Let $\emptyset(r,z,E,t)$ be the scalar neutron flux at (r,z) of neutrons having an energy within an interval of energy of 1 Mev around E, and at time t.

Let $\Sigma_f(r,z,E,t)$ be the macroscopic neutron cross section for f^{th} type of reaction (either fission or inelastic scattering or capture), at (r,z), of neutrons of energy E, at time t, and let $\Gamma_{f_E}^{n}(\Lambda)d\Lambda$ be the yield of photons of energy within $d\Lambda$ and Λ

* To be more specific, instead of $I(\underline{r},\Lambda,t)$ the notation has been changed to $I(r,Z,\Lambda,t)$ for the $(\overline{r,Z})$ geometry.

resulting from the f^{th} type of reaction induced by neutrons of energy E, in nuclei n [that takes place at (r,z)].

Next we define

$$\phi_g(r,z,t) = \int_{E_g}^{E_{g-1}} \phi(r,z,E,t)\, dE, \tag{2-3}$$

$$\Sigma_{f_g}(r,z,t) = \frac{1}{\phi_g(r,z,t)} \int_{E_g}^{E_{g-1}} \Sigma_f(r,z,E,t)\phi(r,z,E,t)\, dE, \tag{2-4}$$

$$\Gamma_{f_g}^{n}(\Lambda) = \frac{1}{\Sigma_{f_g}(r,z,t)\phi_g(r,z,t)} \int_{E_g}^{E_{g-1}} \Sigma_f(r,z,E,t)\, \Gamma_{f_E}^{n}(\Lambda)\phi(r,z,E,t) dE, \tag{2-5}$$

where E_g and E_{g-1} are the lower and upper limits in this order of g^{th} neutron group (cf. Fig. 2-1).

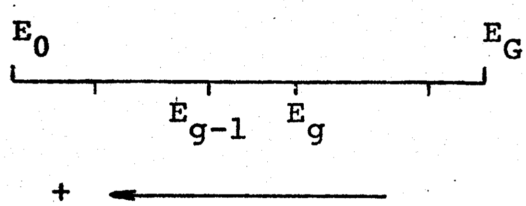

Fig. 2-1 Neutron Energy group limits for G energy groups

Then with the definitions

$$\Gamma_f^{n}(\Lambda) = \text{diag}\,(\Gamma_{f_1}^{n}(\Lambda) \ldots \Gamma_{f_G}^{n}(\Lambda)), \tag{2-6}$$

$$\Sigma_f(r,z,t) = \text{column}\,(\Sigma_{f_1}(r,z,t) \ldots \Sigma_{f_G}(r,z,t)), \tag{2-7}$$

$$\emptyset(r,z,t) = \text{column } (\emptyset_1(r,z,t)\ldots\emptyset_G(r,z,t)), \qquad (2\text{-}8)$$

We may write

$$S_{P_f}(r,z,E,t) = \frac{1}{4\pi(r^2+z^2)} \int_{\Lambda=2.23\text{ Mev}}^{\infty} d\Lambda \;\; \Sigma_D(r,z,\Lambda,t)P_\Lambda(E)e^{-\Sigma(\Lambda,t)\sqrt{r^2+z^2}}$$

$$2\pi \int_{r',\text{reactor}} r'\,dr' \int_{z',\text{reactor}} dz' \quad \Sigma_f^T(r,z,t)\;\Gamma_f(r,z,\Lambda)^{*}\emptyset(r,z,t)$$

$$(2\text{-}9)$$

for the number of photoneutrons due to photons induced by f^{th} type of neutron reaction, generated per unit energy, per cm^3 per sec. at (r,z) and time t.

In Eq. (2-9); $\Sigma_f^T(r,z,t)$ is the transpose of $\Sigma_f(r,z,t)$.

$$2\pi \int_{r',\text{reactor}} r'dr' \int_{z',\text{reactor}} dz' \quad \Sigma_f^T(r',z',t)\,\Gamma_f(r',z',\Lambda)\emptyset(r',z',t) \;,$$

is the previously defined point source $S_f(\Lambda,t)$ placed in the center of the neutron [cf. Eq. (2-2)]. The quantity $e^{-\Sigma(\Lambda,t)\sqrt{r^2+z^2}}$ is the attenuation coefficient, with $\Sigma(\Lambda,t)$ the macroscopic attenuation cross section, for photons of energy Λ, at time t for the heavy water medium.

The term $\frac{1}{4\pi(r^2+z^2)}$ appears because of the assumption that photons are emitted isotropically from a point source at r=z=0.

---

* $\Gamma_f(r,z,\Lambda) \equiv \overset{n}{\Gamma}_f(\Lambda)$; In case there are N(>1) nucleis present at (r,z), $\sum_{n=1}^{N} \Sigma_f^{n^T}(r,z,t)\,\overset{n}{\Gamma}_f(\Lambda)$ shall replace $\Sigma_f^T(r,z,t)\,\overset{n}{\Gamma}_f(\Lambda)$.

We define now

$$\Sigma_{D_\ell}(r,z,t) = \frac{1}{\Delta\Lambda_\ell} \int_{\Lambda_\ell}^{\Lambda_{\ell-1}} \Sigma_D(r,z,\Lambda,t)\, d\Lambda, \qquad (2\text{-}10)$$

where Λ_ℓ and $\Lambda_{\ell-1}$ are the lower and upper limits of ℓ^{th} photon group (cf. Fig. 2-2).

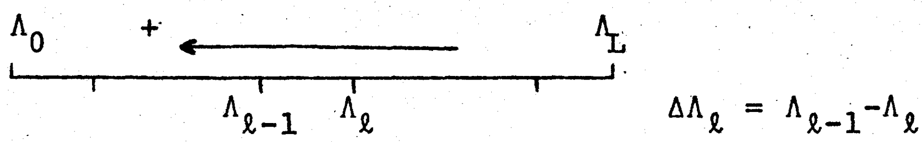

Fig. 2-2 Photon Energy Group limits for L energy groups

$$\Sigma_D(r,z,t) = \text{column}\ (\Sigma_{D_1}(r,z,t) \ldots \Sigma_{D_L}(r,z,t)), \qquad (2\text{-}11)$$

$$P_\ell(E) = \frac{1}{\Delta\Lambda_\ell} \int_{\Lambda_\ell}^{\Lambda_{\ell-1}} P_\Lambda(E)\, d\Lambda\ , \qquad (2\text{-}12)$$

$$P(E) = \text{diag.}\ (P_1(E) \ldots P_L(E)), \qquad (2\text{-}13)$$

$$\Sigma_\ell(t) = \frac{1}{\Delta\Lambda_\ell} \int_{\Lambda_\ell}^{\Lambda_{\ell-\Lambda}} \Sigma(\Lambda,t)\, d\Lambda\ , \qquad (2\text{-}14)$$

$$E(r,z,t) = \text{diag.} \left(e^{-\Sigma_1(t)(r^2+z^2)^{\frac{1}{2}}} \ldots e^{-\Sigma_L(t)(r^2+z^2)^{\frac{1}{2}}} \right), \qquad (2\text{-}15)$$

$$\Gamma^n_{f_\ell} = \int_{\Lambda\ell}^{\Lambda_{\ell-1}} \Gamma^n_f(\Lambda)\ d\Lambda\ , \qquad (2\text{-}16)$$

$$\Gamma^n_f = \text{column}\ (\Gamma^n_{f_1} \ldots \Gamma^n_{f_L})\ , \qquad (2\text{-}17)$$

$$\mathcal{P}_g = \int_{E_g}^{E_{g-1}} p(E)\, dE \quad , \tag{2-18}$$

$$q_f(r',z',t) = \text{column } (\Sigma_f^T(r',z',t)\Gamma_{f_1}(r,z) \ldots \Sigma_f^T(r',z',t)\Gamma_{f_L}(r,z)) \tag{2-19}$$

With integrations over Λ from Λ_ℓ to $\Lambda_{\ell-1}$(ℓ varying from L to 1) and over E from E_g to E_{g-1}, summation over the three types of prompt photon production and the above definitions Eq. (2-9) finally becomes

$$S_{P_g}(r,z,t) = \frac{1}{4\pi(r^2+z^2)} \Sigma_D^T(r,z,t)\mathcal{P}_g E(r,z,t) \times$$

$$2\pi \int_{r',\text{reactor}} r'dr' \int_{z',\text{reactor}} dz' \sum_{f=1}^{3} q_f(r',z',t)\phi(r',z',t), \tag{2-20}$$

which is the component of $S_g(r,z,t)$ due to prompt photons.

To get more insight into Eq. (2-20) choose two energy groups of photons and define

$$Q(r,z,t) = \frac{1}{2(r^2+z^2)} \int_{r',\text{reactor}} r'\,dr' \int_{z',\text{reactor}} dz' \sum_{f=1}^{3}$$

$$q_f(r',z',t)\phi(r',z',t) \quad . \tag{2-21}$$

Then Eq. (2-20) yields

$$S_{P_g}(r,z,t) = \Sigma_{D_1}(r,z,t)\; P_{1_g} E_\Lambda(r,z,t)\;\; Q_1(r,z,t)$$

$$+ \Sigma_{D_2}(r,z,t)\; P_{2_g} E_2(r,z,t)\; Q_2(r,z,t) \; . \qquad (2\text{-}22)$$

In Eq. (2-22) the first term gives the number of prompt photoneutrons born at (r,z) and time t per cm^3 per sec. within the g^{th} group of neutrons, induced by photons belonging to the first energy group of photons. Similarly the second term in Eq. (2-22) gives the number of prompt photoneutrons born at (r,z) and time t per cm^3 per sec. within the g^{th} group of neutrons, induced by photons belonging to the second energy group of photons.

The quantities

$$\Sigma_{f_g}(r',z',t)\; \Gamma_{f_{\ell g}}(r,z), (\ell=1,\ldots,L)$$

appearing in Eq. (2-22) through Eq. (2-21) and Eq. (2-19) are to be determined for all the locations (or materials present in MITRII) and any of the three types of neutron reaction inducing prompt photons. Fortunately there is a code with its own library for doing this.

Thus the code POPOP IV [2] computes

$$SGCS_{\ell g}(r,z,t) = \sum_{f=1}^{3} \Sigma_{f_g}(r,z,t)\; \Gamma_{f_{\ell g}}(r,z) \; , \qquad (2\text{-}23)$$

the secondary gamma ray cross sections for photons of ℓ^{th} group, induced by neutrons of g^{th} group. In Appendix D POPOP IV is briefly discussed and the relevant numbers are presented.

2-2 Component of $I(r,z,\Lambda,t)$ due to Delayed gamma rays and the corresponding photoneutron source term

Delayed gamma rays can be due to fission products decay and activation of the material leading to delayed gamma ray emission.

Activation gamma rays of sufficient energy happen not to be significant in MITR II. Hence we need to consider only the decay of fission products.

To this end we turn our attention to the fission product having the decay constant λ_j. The photons that will follow will appear with the same decay constant. Any photoneutrons caused by these photoneutrons will show up with that decay constant too.

We let then, $L_j(r,z,t)$, be the concentration per cm^3, per sec. of the j^{th} delayed photon precursor (the fission product having the decay constant λ_j) at (r,z) and t.

Let N_0 be the total number of delayed photon precursors created per fission that may decay with one of the λ_j's, and let y_j be the fraction of these N_0 delayed photon precursors that decay with the decay constant λ_j.

Let $\Sigma_F(r,z,E,t)$ be the macroscopic fission cross section for neutrons of energy E, at (r,z) and t, and define

$$\Sigma_{F_g}(r,z,t) = \frac{1}{\phi_g(r,z,t)} \int_{E_g}^{E_{g-1}} \Sigma_F(r,z,E,t)\phi(r,z,E,t)\, dE, \quad (2\text{-}24)$$

$$\Sigma_F^T(r,z,t) = \text{row}\ (\Sigma_{F_1} \dots \Sigma_{F_G}) \quad . \quad (2\text{-}25)$$

$L_j(r,z,t)$ can now be obtained from

$$\frac{\partial L_j(r,z,t)}{\partial t} = \Sigma_F^T(r,z,t)\phi(r,z,t)y_j N_0 - \lambda_j L_j(r,z,t) \quad . \quad (2\text{-}26)$$

The total rate at which delayed photons of the j^{th} kind are emitted from the core is then

$$S_e^j(t) = 2\pi \int_{r',\text{core}} r'\, dr' \int_{z',\text{core}} dz' \quad \lambda_j L_j(r',z',t) \quad . \quad (2\text{-}27)$$

We let Y_{j_ℓ} be the probability that the photons of sufficient energy to produce photoneutron reaction in D_2O, emitted from the j^{th} precursor appear in the ℓ^{th} photon group and define

$$Y_j = \text{column}\ (Y_{j_\ell} \dots y_{j_L}) \quad , \quad (2\text{-}28)$$

Then as we did with the prompt photons, we assume that all the delayed photons are born at the center of the reactor and are attenuated in reaching to the reflector as if they were travelling through pure D_2O. As a result, in complete analogy with Eq. (2-2) we obtain the delayed photoneutron source;

$$S_{D_g}^{j}(r,z,t) = \frac{1}{4\pi(r^2+z^2)} \; \Sigma_D^T(r,z,t) \; \rho_g E(r,z,t) Y_j \lambda_j \; \times$$

$$2\pi \int_{r',\,core} r'\,dr' \int_{z',\,core} dz' \quad L_j(r',z',t), \qquad (2\text{-}29)$$

at which the-energy wise-group-g photoneutrons appear per unit volume and per unit time at point (r,z) in the reflector and time t due to the -time wise-group j delayed photons.

The total rate of delayed photoneutrons emitted in neutron group g is then

$$S_{D_g}(r,z,t) = \sum_{j=7}^{15} S_{D_g}^{j}(r,z,t) \quad , \qquad (2\text{-}30)$$

where having reserved j from 1 to 6 for delayed neutron groups, we use j from 7 to 15 for 9 groups of delayed photoneutrons.

The form of Eq. (2-29) suggests that we picture the delayed photoneutrons appearing at (r,z) as coming from fictitious precursors actually present at (r,z). Accordingly we define a concentration $\theta_g^j(r,z,t)$ of "delayed photoneutron precursors" in relation with the delayed photoneutron group j, and emitting neutrons into neutron group g at time t;

$$\theta_g^j(r,z,t) = \frac{S_{D_g}^{j}(r,z,t)}{\lambda_j} \quad , \qquad (2\text{-}31)$$

so that from Eq. (2-30),

$$S_{D_g}(r,z,t) = \sum_{j=7}^{15} \lambda_j \; \theta_j(r,z,t) \qquad (2\text{-}32)$$

To find equations for the $\theta_g^j(r,z,t)$ we integrate Eq. (2-26) over the core volume and multiply it at the left by

$\frac{1}{4\pi(r^2+z^2)} \Sigma_D^T(r,z,t)\, P_g\, E(r,z,t)\, Y$, where we omit the subscript j on the column vector [cf. Eq. (2-28)] since the experimental data (cf. Appendix B) indicates this approximation is justified.

The first term of Eq. (2-26) then becomes

$$\frac{1}{4\pi(r^2+z^2)} \Sigma_D^T\,(r,z,t)\, P_g\, E(r,z,t)\, Y \quad x$$

$$2\pi \int_{r',core} r'\, dr' \int_{z',core} dz' \;\frac{\partial L_j}{\partial t}\; (r',z',t) = \frac{\partial \theta_D^j(r,z,t)}{\partial t}$$

$$- \frac{\frac{\partial}{\partial t}\,(\Sigma_D^T(r,z,t)\, P_g\, E(r,z,t))\, Y}{\Sigma_D^T(r,z,t)\, P_g\, E(r,z,t) Y}\, \theta_g^j(r,z,t) \qquad (2\text{-}33)$$

and the last term becomes

$$\frac{1}{4\pi(r^2+z^2)} \Sigma_D^T(r,z,t)\, P_g E(r,z,t) Y\, \lambda_j \quad x$$

$$2\pi \int_{r',core} r' dr' \int_{z',core} dz' \;\; L_j(r',z',t) = \lambda_j \theta_g^j\,(r,z,t)\;. \qquad (2\text{-}34)$$

It appears legitimate to ignore the time dependence of

$\Sigma_D(r,z,t)$ and $E(r,z,t)$. In Eq. (2-33), accordingly we drop the last term and obtain

$$\frac{\partial \theta_g^j(r,z,t)}{\partial t} = \frac{1}{4\pi(r^2+z^2)} y_j N_0 \Sigma_D^T(r,z,t) P_g E(r,z,t) \; Y \quad x$$

$$2\pi \int_{r',core} r'dr' \int_{z',core} dz' \; \Sigma_F^T(r',z',t)\phi(r',z',t) - \lambda_j \theta_g^j(r,z,t), \quad (2\text{-}35)$$

We discuss in Appendix B how values of λ_j, y_j, N_0 and Y may be obtained from experimental data.

2.3 Summary

In order to find an analytical expression for the photoneutron source term in the D_2O reflector of MITR-II we have first computed the production of prompt and delayed photons and then, by making a very gross approximation have estimated their attenuation through the core.

Eq. (2-20) (prompt photoneutrons) and Eq. (2-32) coupled with Eq. (2-35) (delayed photoneutrons) are the end products of this procedure. We thus have;

$$S_g(r,z,t) = S_{P_g}(r,z,t) + \sum_{j=7}^{15} \lambda_j \theta_g^j(r,z,t) \quad . \quad (2\text{-}36)$$

CHAPTER III

APPLICATION OF THE WEIGHTED RESIDUAL METHOD

We shall use the weighted residual method to describe the space and time dependent flux in terms of spatial shapes chosen beforehand and unknown time coefficients.

To carry out this procedure, we begin with the time dependent multigroup diffusion equation with our extra photoneutron source term

$$V^{-1}\frac{\partial \emptyset(r,z,t)}{\partial t} = [\nabla . D(r,z,t)\nabla - A(r,z,t) + (1-\beta)\nu\chi_p\Sigma_F^T(r,z,t)]\emptyset(r,z,t)$$

$$+ \sum_{j=1}^{J}\lambda_j\chi_j\eta_j(r,z,t) + \frac{\alpha}{4\pi(r^2+z^2)}\text{ column }\Bigg(\Sigma_D^T\ (r,z,t)\ P_g E(r,z,t)$$

$$2\pi\int_{r',\text{reactor}} r'dr' \int_{z',\text{reactor}} dz'$$

$$\sum_{f=1}^{3}\text{column } [\Sigma_f^T(r',z',t)\ \Pi_{f_\ell}(r',z')]\emptyset(r',z',t)\Bigg) + \sum_{j=J+1}^{H}\lambda_j\theta_j(r,z,t), \quad (3\text{-}1)$$

$$\frac{\partial \eta_j(r,z,t)}{\partial t} = \beta_j\nu\Sigma_F^T(r,z,t)\emptyset(r,z,t) - \lambda_j\eta_j(r,z,t)\ , \quad (3\text{-}2)$$

$$\frac{\partial \Theta_j(r,z,t)}{\partial t} = \frac{\alpha}{4\pi(r^2+z^2)} y_j N_0 \text{ column} \left(\Sigma_D^T(r,z,t)\, P_g E(r,z,t)\; Y \right.$$

$$\left. 2\pi \int_{r',core} r'dr' \int_{z',core} dz' \quad \Sigma_F^T(r',z',t)\, \phi(r',z',t) \right) - \lambda_j \Theta_j(r,z,t) \quad ,(3\text{-}3)$$

where

$$V^{-1} = \text{diag} \quad (\frac{1}{V_1} \ldots \frac{1}{V_G}) \quad , \qquad (3\text{-}4)$$

$$D(r,z,t) = \text{diag} \; (D_1(r,z,t) \;\ldots\; D_G(r,z,t)) \quad , \qquad (3\text{-}5)$$

$$A(r,z,t) = \begin{bmatrix} \Sigma a_1(r,z,t) + \sum_{h=1}^{G} \Sigma_{s_{h \leftarrow 1}}(r,z,t) & & \\ & \ddots & \\ & & \Sigma a_G(r,z,t) + \sum_{h=1}^{G} \Sigma_{s_{h \leftarrow G}}(r,z,t) \end{bmatrix}$$

$$- \begin{bmatrix} \Sigma_{1 \leftarrow 1}(r,z,t) & \ldots & \Sigma_{1 \leftarrow G}(r,z,t) \\ \vdots & & \vdots \\ \Sigma_{G \leftarrow 1}(r,z,t) & \ldots & \Sigma_{G \leftarrow G}(r,z,t) \end{bmatrix} \quad ; \qquad (3\text{-}6)$$

$\Sigma a_g(r,z,t)$: macroscopic absorption cross section of neutrons belonging to g^{th} group at (r,z) and t ;

α: correction factor (generated or empirical) for overcoming the error introduced by the approximations made for the computation of the photoneutron source term in the reflector;

$\Sigma_{s_{h \leftarrow g}}(r,z,t)$: macroscopic scattering cross section of neutrons from group g into group h at(r,z)and t.

β_j : delayed neutron fraction for group j,(j=1,..., J),

$$\beta = \sum_{j=1}^{J} \beta_j \quad . \tag{3-7}$$

There are J delayed neutron group(s).

ν : number of neutrons created per fission ,

$$\chi_p = \text{column } (\chi_{p_1} \cdots \chi_{p_G}) \quad . \tag{3-8}$$

λ_j : delayed neutron precursor decay constant for j^{th} group (j=1,...,J); delayed photoneutron group decay constant for j^{th} group [j=(J+1),...,H].

There are (H-J) delayed photoneutron group(s).

$\eta_j(r,z,t)$: delayed neutron precursor concentration for j^{th} group at(r,z)and t.

$$\chi_j = \text{column } (\chi_{j_1} \cdots \chi_{j_G}) \quad . \tag{3-9}$$

χ_{p_g} and χ_{j_g} are the probabilities, respectively for prompt and delayed neutrons of j^{th} group, to appear within the g^{th} neutron group.

By column $\left(\quad \right)$ in Eq. (3-1) and Eq. (3-3) is meant the column matrix obtained by varying g in P_g of the expression in between the brackets from 1 to G. In the same way column [ ] in Eq. (3-1) describes the column matrix obtained by varying ℓ in Γ_{f_ℓ} from 1 to L.

Finally

$$\Theta_j(r,z,t) = \text{column } (\Theta_1^j(r,z,t) \ \ldots \ \Theta_G^j(r,z,t)) \ . \qquad (3\text{-}10)$$

Other symbols appearing in eqs. (3-1),(3-2) and (3-3) have been defined previously.

Since it is impractical to obtain an analytical solution to the system of equations (3-1), (3-2) and (3-3), we shall employ an approximation method based on expressing $\phi(\underline{r},t)$ by a trial function of the form

$$\phi(\underline{r},t) = \sum_{i=1}^{I} \psi_i(\underline{r}) \ N_i(t) \ , \qquad (3\text{-}11)$$

where $\psi_i(\underline{r})$ is the i^{th} mode, a column matrix having G elements ($\psi_{ig}(\underline{r})$, g=1,...,G) that are spatial functions selected beforehand, and $N_i(t)$ is an unknown time coefficient. We then have I unknown time coefficients to be determined.

The idea behind the expression (3-11) consists in choosing $\psi_i(\underline{r})$'s that are linearly independent functions (cf. Appendix E) so that various combinations of them will provide a good approximation to the flux shape expected during the transient. [3] . The accuracy of the solution will naturally depend on the good choice of these spatial shapes.

3-1 Formulation of the residuals

We now rewrite Eq. (3-11) using the matrix notation

$$\bar{\phi}(r,z,t) = \psi(r,z) \ N(t) \ , \qquad (3\text{-}12)$$

with

$$\psi(r,z) = \begin{bmatrix} \psi_{11}(r,z) & \dots & \psi_{1I}(r,z) \\ \vdots & & \vdots \\ \psi_{G1}(r,z) & \dots & \psi_{GI}(r,z) \end{bmatrix} , \qquad (3\text{-}13)$$

$$N(t) = \text{column } (N_1(t) \dots N_I(t)) \quad . \qquad (3\text{-}14)$$

The bar on top of $\phi(r,z,t)$ is to indicate that this is an approximate solution. Thus when we insert it into Eq. (3-1), Eq. (3-2) and Eq. (3-3) the left hand sides of these equations are no longer exactly equal to their right hand sides. The differences are called residuals;

$$\mathcal{R}(r,z,t) = V^{-1}\frac{dN(t)}{dt}\,\psi(r,z)$$

$$-[\nabla.D(r,z,t)\nabla - A(r,z,t) + (1-\beta)\nu\chi_p\Sigma_F^T(r,z,t)]\;\psi(r,z)N(t) -$$

$$\sum_{j=1}^{J} \lambda_j\chi_j\,\eta_j(r,z,t) - \frac{\alpha}{4\pi(r^2+z^2)}\text{column}\Big(\Sigma_D^T(r,z,t)\;P_g E(r,z,t)$$

$$2\pi\int_{r',\text{reactor}} r'dr' \int_{z',\text{reactor}} dz' \sum_{f=1}^{3} \text{column } [\Sigma_f^T(r',z',t)\,\Gamma_{f_\ell}(r',z')]\,\psi$$

$$\psi(r',z')N(t) \;-\; \sum_{j=J+1}^{H} \lambda_j\theta_j(r,z,t) \quad , \qquad (3\text{-}15)$$

$$R_{p_j}(r,z,t) = \frac{\partial \eta_j(r,z,t)}{\partial t} - \beta_j \nu \Sigma_F^T(r,z,t)\psi(r,z)N(t) + \lambda_j \eta_j(r,z,t),$$

$$(j=1,\ldots,J), \qquad (3\text{-}16)$$

$$R_{H_j}(r,z,t) = \frac{\partial \Theta_j(r,z,t)}{\partial t} - \frac{\alpha}{4\pi(r^2+z^2)} Y_j N_0 \text{ column}\Bigg(\Sigma_D^T(r,z,t)P_g E(r,z,t)$$

$$Y\ 2\pi \int_{r',\text{core}} r'dr' \int_{z',\text{core}} dz' \quad \Sigma_F^T(r',z',t)\psi(r',z')N(t)\Bigg) + \lambda_j \Theta_j(r,z,t),$$

$$(j=(J+1),\ldots,H) \qquad (3\text{-}17)$$

In addition to these three residuals we should in general have interface, boundary and initial condition residuals. However we intend to use good trial functions that will not leave interface residuals and that will satisfy boundary and initial conditions; namely

$$\bar{\phi}(R_0,z,t) = \bar{\phi}(r,Z_+,t) = \bar{\phi}(r,Z_-,t) = 0, \qquad (3\text{-}18)$$

$$\bar{\phi}(r,z,0) = \phi(r,z,0) \qquad , \qquad (3\text{-}19)$$

where R_0 is the extrapolated radius of the reactor (the one which is taken for criticality calculations). Similarly Z_+ and Z_- are the upper and lower levels where the flux is taken to be zero.

3-2 Weighting of the residuals and preparation of the equations for the unknown time coefficients

Because of the inherent inaccuracy of Eq. (3-12) we cannot make the residuals (3-15), (3-16) and (3-17) vanish at all points $\underline{r}$. However we can choose the N(t) so that the residuals vanish in an integral sense. Accordingly we define the GxI matrix of weighting shapes;

$$W(r,z) = \begin{bmatrix} W_{11}(r,z) & \dots & W_{1I}(r,z) \\ \vdots & & \vdots \\ W_{G1}(r,z) & \dots & W_{GI}(r,z) \end{bmatrix} , \qquad (3\text{-}20)$$

where the i^{th} column is the i^{th} weighting mode and no two weighting modes can be proportional to one another. W_{gi} is chosen to be continuous and defined* throughout the entire reactor.

We then require;

$$0 = 2\pi \int_{r,\text{reactor}} r\, dr' \int_{z,\text{reactor}} dz \quad W^T(r,z)\,\mathcal{R}\,(r,z,t) , \qquad (3\text{-}21)$$

---

* These conditions will be automatically satisfied since we intend to use the adjoint fluxes as weighting functions.

$$O = 2\pi \int_{r,\text{reactor}} r\,dr \int_{z,\text{reactor}} dz \quad W^T(r,z)\chi_j \mathcal{R}_{P_j}(r,z,t),$$

$$(j=1,\ldots,J), \qquad (3\text{-}22)$$

$$O = 2\pi \int_{r,\text{reactor}} r\,dr \int_{z,\text{reactor}} dz \quad W^T(r,z)\ \mathcal{R}_{H_j}(r,z,t),$$

$$[j=(J+1),\ldots,H), \qquad (3\text{-}23)$$

3-3 Formulation of the system of equations for the time dependent coefficients

In order to abstract the equations for N(t) implied by equations (3-21), (3-22) and (3-23) we introduce the definitions;

$$\xi_{P_g}(r,z,t) = \frac{1}{4\pi(r^2+z^2)} \Sigma_D^T(r,z,t) \mathcal{P}_g E(r,z,t)\, 2\pi \int_{r',\text{reactor}} r'dr' \int_{z',\text{reactor}} dr' \sum_{f=1}^{3}$$

$$\text{column } [\Sigma_f^T(r',z',t) \quad \Gamma_{f_\ell}(r',z')]\psi(r',z') \qquad , \qquad (3\text{-}24)$$

$$\xi_P(r,z,t) = \text{column } (\xi_{P_1}(r,z,t) \ \ldots \ \xi_{P_G}(r,z,t)), \qquad (3\text{-}25)$$

$$\beta_g^j(r,z,t) = \frac{1}{4\pi(r^2+z^2)} y_j N_0 \Sigma_D^T(r,z,t)\ \mathcal{P}_g E(r,z,t) Y\ 2\pi \int_{r',\text{core}} r'dr' \int_{z',\text{core}} dz'$$

$$\Sigma_F^T(r',z',t)\ \psi(r',z') \qquad (3\text{-}26)$$

$$\beta_j(r,z,t) = \text{column } [\beta_1^j(r,z,t) \ldots \beta_G^j(r,z,t)] \;, \tag{3-27}$$

$$\Lambda = 2\pi \int_{r,\text{reactor}} r\,dr \int_{z,\text{reactor}} dz \quad W^T(r,z)\; V^{-1}\psi(r,z) \;, \tag{3-28}$$

$$\rho(t) = 2\pi \int_{r,\text{reactor}} r\,dr \int_{z,\text{reactor}} dz \quad W^T(r,z) \quad [\nabla . D(r,z,t) - A(r,z,t)$$

$$+ (1-\beta)\chi_p \nu \Sigma_F^T(r,z,t)]\psi(r,z) + \alpha\xi_p(r,z,t) \quad , \tag{3-29}$$

$$\overline{\beta}_j(t) = \beta_j 2\pi \int_{r,\text{core}} r\,dr \int_{z,\text{core}} dz \quad W^T(r,z)\nu\Sigma_F^T(r,z,t)\psi(r,z),$$

$$(j = 1,\ldots, J), \tag{3-30}$$

$$D_{j_i}(t) = 2\pi \int_{r,\text{core}} r\,dr \int_{z,\text{core}} dz \quad W_i^T(r,z)\chi_j\, \eta_j(r,z,t) \;,$$

$$(i = 1,\ldots, I),\; (j = 1,\ldots, J), \tag{3-31}$$

$$D_j(t) = \text{column } (D_{j_1}(t) \ldots D_{j_I}(t)) \;, (j = 1,\ldots, J), \tag{3-32}$$

$$\overline{\beta}_j(t) = 2\pi \int_{r,\text{reflector}} r\,dr \int_{z,\text{reflector}} dz \quad W^T(r,z)\; \beta_j\; (r,z,t),$$

$$[j = (J+1),\ldots, H] \;, \tag{3-33}$$

$$\Theta_j(t) = 2\pi \int_{r,\mathrm{reflector}} r\,dr \int_{z,\mathrm{reflector}} dz \quad W^T(r,z)\Theta_j(r,z,t), \tag{3-34}$$

With these definitions Eq. (3-21) becomes:

$$\Lambda \frac{dN(t)}{dt} = \rho(t)N(t) + \sum_{j=1}^{J} \lambda_j D_j(t) + \sum_{j=J+1}^{H} \lambda_j \; \Theta_j(t) \; . \tag{3-35}$$

Eq. (3-22) becomes

$$\frac{D_j(t)}{dt} = \overline{\beta}_j(t) \; N(t) - \lambda_j D_j(t), \; (j=1,\ldots,J). \tag{3-36}$$

Finally Eq. (3-23) becomes

$$\frac{d\Theta_j(t)}{dt} = \alpha \; \overline{\beta}_j(t) \; N(t) \; - \; \lambda_j \Theta_j(t), \; (j = (J+1),\ldots, H). \tag{3-37}$$

In order to simplify further we define

$$\overline{\beta}_{j_{new}}(t) \equiv \overline{\beta}_j(t) \quad , (j = 1,\ldots, J) \quad , \tag{3-38}$$

$$\overline{\beta}_{j_{new}}(t) = \alpha \; \overline{\beta}_j(t), \; (j = (J+1), \ldots, H) \; , \tag{3-39}$$

$$\overline{\beta}_{new}(t) = \sum_{j=1}^{H} \overline{\beta}_{j_{new}}(t) \quad , \tag{3-40}$$

$$\rho_{new}(t) = \rho(t) + \overline{\beta}_{new}(t) \quad , \tag{3-41}$$

so that $\rho_{new}(t)$ has four components;

1. The prompt neutron reactivity:

$$2\pi \int_{r,core} r\, dr \int_{z,core} dz \quad W^T(r,z)\,[\nabla.D(r,z,t)\nabla - A(r,z,t)$$

$$+(1-\beta)\ \nu\chi_p\ \Sigma_F^T(r,z,t)]\ \psi\ (r,z);$$

2. The prompt photoneutron reactivity:

$$2\pi \int_{r,reflector} r\, dr \int_{z,reflector} dx \quad W^T(r,z)\ \xi_p(r,z,t);$$

3. The delayed neutron reactivity:

$$\sum_{j=1}^{J} \bar{\beta}_j(t) = \sum_{j=1}^{J} \beta_j 2\pi \int_{r,core} r\, dr \int_{z,core} dz \quad W^T(r,z)\,\nu\chi_j\Sigma_F^T(r,z,t)\,\psi(r,z);$$

4. The delayed photoneutron reactivity:

$$\sum_{j=J+1}^{H} \alpha\bar{\beta}_j(t) = \sum_{j=J+1}^{H} 2\pi \int_{r,reflector} r\ \ dr \int_{z,reflector} dz \quad W^T(r,z)\,\beta_j(r,z,t).$$

Both prompt and delayed photoneutron reactivities are produced in the reflector.

We finally define

$$C_j(t) \equiv D_j(t) \qquad ,\ (j = 1,\ \ldots,\ J) \quad , \qquad (3\text{-}42)$$

$$C_j(t) \equiv \Theta_j(t) \qquad ,\ (j = (J+1),\ldots,\ H) \quad , \qquad (3\text{-}43)$$

With the new definitions we obtain from Eq. (3-35), Eq. (3-36) and Eq.(3-37) a system of equations for the unknown time coeffients that has the familiar point kinetics form;

$$\Lambda \frac{dN(t)}{dt} = [\rho_{new}(t) - \overline{\beta}_{new}(t)]\, N(t) + \sum_{j=1}^{H} \lambda_j C_j(t) \ , \qquad (3\text{-}44)$$

$$\frac{dC_j(t)}{dt} = \overline{\beta}_{j_{new}}(t)\, N\,(t) - \lambda_j C_j(t) \ , \ (j=1,\ldots, H) \ . \qquad (3\text{-}45)$$

By analogy with the point kinetics equations Λ(IxI) will be called the generation time matrix; $\rho_{new}(t)$ (IxI), the reactivity matrix; $\overline{\beta}_{j_{new}}(t)$ (IxI), the delayed neutron fraction matrix for the j^{th} group and $C_j(t)$ (Ix1), the precursor amplitude function matrix for the j^{th} group.

It is worthwhile to point out that the form obtained for the above equations does not depend on the formulation of the energy and time dependent photon flux or the choice of the geometry in the course of the calculation of the photoneutron source term in the reflector. In a different case the same form would be found with however different expressions for the parameters Λ, $\rho(t)$ and $\beta_j(t)$'s.

Equations (3-44) and (3-45) represent a set of I (H+1) equations for I time coefficients and IxH precursor amplitude functions.

There are several ways of solving these equations [4]. That topic is outside of the scope of the present work. One of these ways based on the weighted residual method with subdomain weighting has been adopted since it was the only method implemented by an available computer program, when we first needed a solution. This method is briefly described in Appendix F.

3-4 Summary

In order to find a solution for the space and time dependent flux we have used an expression in prechosen spatial shapes and unknown time dependent coefficients. The insertion of this approximate flux into the equations gave us residuals. Then we have chosen as many weighting modes as the number of unknown time coefficients, weighted the residuals and integrated over the reactor volume. That procedure furnished us equations of the point kinetics type for the unknown time coefficients.

We must describe now a method of computing the very complicated integral expressions for Λ, $\rho_{new}(t)$ and $\overline{\beta}_{j_{new}}(t)$'s (subject to Chapter V). This however shall require that we know the way the spatial shapes have been selected, that is done next.

CHAPTER IV

SELECTION OF OUR SPATIAL FUNCTIONS

To describe in the simplest way the time and space dependent flux during a transient in MITR-II, we shall choose two trial modes and two weighting modes. Each of the modes is a G-element column vector of spatial functions (G being the number of neutron groups).

Thus

$$\bar{\phi}(r,t) = \psi_1(\underline{r})\ N_1(t) + \psi_2(\underline{r})\ N_2(t), \qquad (4\text{-}1)$$

where $N_1(t)$ and $N_2(t)$ will be determined through the manipulations involving $W_1(\underline{r})$ and $W_2(\underline{r})$, described in the previous chapter.

Following former criticality calculations done for MITR-II, a three-group model in (r,z) geometry (cf. Appendix G) with no upscattering and down scattering to the closest lower group only, is adopted. That model has 40 mesh points in the r direction and 48 mesh points in the z direction. The boundaries for neutron energy groups are given in Table 4-1.

Table 4-1

Group boundaries for three-group scheme

Group	Group boundaries in Mev
Fast	3×10^{-3} - ∞
Epithermal	4×10^{-7} - 3×10^{-3}
Thermal	2.5×10^{-10} - 4×10^{-7}

The code Exterminator II[5] was used to obtain the spatial functions.

4-1. The Selection of the First Trial and Weighting Modes

The first trial mode is taken to be the solution of

$$\{\nabla.D_1(\underline{r})\nabla - A_1(\underline{r}) + [(1-\beta)\chi_p + \sum_{j=1}^{J}\beta_j\chi_j]\nu\Sigma^T_{F_1}(\underline{r})\}\psi_1(\underline{r}) = 0, \tag{4-2}$$

where $D_1(\underline{r}) = D(\underline{r},0)$, $A_1(\underline{r}) = A(\underline{r},0)$, $\Sigma_{F_1}(\underline{r}) = \Sigma_F(\underline{r},0)$ and $D(\underline{r},t)$, $A(\underline{r},t)$, $\Sigma_F(\underline{r},t)$ have been defined previously.

That is physically, (ignoring the photoneutrons) $\psi_1(\underline{r})$ is the flux shape of MITR-II in a steady state critical condition.

Both prompt and delayed neutrons appear in the fast group of the three-group scheme shown in Table 4-1. Therefore

$$\chi = \chi_p = \chi_j = \begin{pmatrix} 1 \\ 0 \\ 0 \end{pmatrix} \tag{4-3}$$

Thus Eq.(4-2) will be written as

$$[\nabla.D_1(\underline{r})\nabla-A_1(\underline{r}) + \nu\chi\,\Sigma^T_{F_1}(\underline{r})]\,\psi_1(\underline{r})=0. \qquad (4\text{-}4)$$

$W_1(\underline{r})$ is chosen to be $\psi_1^*(\underline{r})$; the solution of the equation adjoint to Eq.(4-4), namely

$$H_1^+(\underline{r})\;\psi_1^*(\underline{r}) = 0\;, \qquad (4\text{-}5)$$

with

$$\langle\psi_1(\underline{r})|H_1^+(\underline{r})|\psi_1^*(\underline{r})\rangle = \langle\psi_1^*(\underline{r})|H_1(\underline{r})|\psi_1(\underline{r})\rangle\,, \qquad (4\text{-}6)$$

and

$$H_1(\underline{r}) = \nabla.D_1(\underline{r})\;\nabla-A_1(\underline{r}) + \nu\chi\;\Sigma^T_{F_1}(\underline{r}) \qquad (4\text{-}7)$$

4-2 The Selection of the second trial and weighting modes

The selection of the second trial and weighting modes will be undertaken in the case of a particular transient where a control rod has been withdrawn. We intend to study the transient up to time t=T; by then the reactor is presumed to be on a prompt critical period.

Thus the rod being in its withdrawn position at time t=T, we select as the second expansion mode a vector such that in the vicinity of time t=T;

$$\phi(\underline{r},t) = \psi_2(\underline{r})e^{\omega t}\;, \qquad (4\text{-}8)$$

with

$$v^{-1}\frac{\partial \phi(r,t)}{\partial t}=[\nabla . D(\underline{r},t)\nabla - A(\underline{r},t) + (1-\beta)\chi_p \nu\, \Sigma_F^T(\underline{r},t)]\phi(\underline{r},t)$$

$$+\sum_{j=1}^{J}\lambda_j \chi_j \eta_j(\underline{r},t) \quad , \qquad (4\text{-}9)$$

$$\frac{\partial \eta_j(\underline{r},t)}{\partial t} = \beta_j\ \nu\ \Sigma_F^T \phi(\underline{r},t)-\lambda_j\, \eta_j(\underline{r},t),\ (j=1,\ldots,J), \qquad (4\text{-}10)$$

and

$$\eta_j(\underline{r},t) = M_j(\underline{r})e^{\omega t} \qquad (4\text{-}11)$$

Eq. (4-10) with Equations (4-9) and (4-11) then gives;

$$M_j(\underline{r}) = \frac{\beta_j \nu\ \ \Sigma_F^T\ (\underline{r},t)\psi_2(\underline{r})}{\omega + \lambda_j} \qquad (4\text{-}12)$$

and Eq. (4-9) with Equations (4-8), (4-12) and (4-3) becomes

$$\{\nabla . D(\underline{r},t)\nabla - A(\underline{r},t) - v^{-1}\omega + \chi\nu\left(1-\sum_{j=1}^{J}\frac{\omega\beta_j}{\omega+\lambda_j}\right)\Sigma_F^T(\underline{r},t)\ \}\psi_2(\underline{r})=0$$

$$(4\text{-}13)$$

In the case of a prompt run away we expect to find $\omega >> \lambda_j$ so that, at t=T,

$$\{\nabla . D_2(\underline{r})\nabla - [A_2(\underline{r})+\omega V^{-1}] + (1-\beta)\chi\nu\ \Sigma_{F_2}^T(\underline{r})\}\ \ \psi_2(\underline{r})=0, \qquad (4\text{-}14)$$

where $D_2(\underline{r}) = D(\underline{r},t)$, $A_2(\underline{r}) = A(\underline{r},T)$ and $\Sigma_{F_2}(\underline{r}) = \Sigma_F(\underline{r},T)$.

An eigenvalue ω can be found such that Eq.(4-14) is satisfied at every point.

The numerical procedure for finding a value of ω that satisfies Eq.(4-14) is called a poison search, one introducing a $(\frac{1}{V})$ - poison (i.e. an effective neutron absorber whose cross section varies inversely with the incident neutron velocity) which is spread uniformly throughout the supercritical reactor until criticality calculation for the reactor yields an eigenvalue of $\frac{1}{1-\beta}$.

Thus our second trial mode is determined through a poison search procedure.

*

$W_2(\underline{r})$ is chosen to be $\psi_2^*(\underline{r})$; the solution of the equation adjoint to Eq.(4-14). Thus as with Equations (4-5), (4-6) and (4-7) we have;

$$H_2^+(\underline{r})\ \psi_2^*(\underline{r}) = 0 \quad , \tag{4-15}$$

$$\langle\psi_2(\underline{r})|H_2^+(\underline{r})|\psi_2^*(\underline{r})\rangle = \langle\psi_2^*(\underline{r})|H_2(\underline{r})|\psi_2(\underline{r})\rangle \quad , \tag{4-16}$$

$$H_2(\underline{r}) = \nabla.D_2(\underline{r})\nabla - A_2(\underline{r}) - \omega V^{-1} + (1-\beta)\nu\ \chi\ \Sigma_{F_2}^T(\underline{r}) \ . \tag{4-17}$$

4-3 Recomputation, in an integral sense, of the eigenvalue relative to the trial mode

In Section 4-1 we have tacitly assumed that the reactor is critical; also both in sections 4-1 and 4-2 a well converged solution was supposed to be available so that Equations (4-4) and (4-14) are valid at every point of the reactor.

The fact that the reactor may not be critical could be dismissed by merely assuming that the eigenvalue of the reactor is already within $\nu\chi\,\Sigma^T_{F_1}(\underline{r})$, the same way $\frac{1}{1-\beta}$ divides $\nu\chi\,\Sigma^T_{F_2}(\underline{r})$ in the case of Eq. (4-14). More serious than that is the fact that we may not have a converged solution. Then the eigenvalue [assumed to be unity in case of Eq. (4-4) and $\frac{1}{1-\beta}$ in case of Eq. (4-14)] coming from a criticality calculation does not anymore insure the balance - in Equations (4-4) and (4-14) - at every point of the reactor.

In addition, the fact that we drop some of the figures of the fluxes coming out of Exterminator-II run or we might use a slightly different scheme of calculation as compared to the one used in Exterminator-II, may also disturb the balance in Equations (4-4) and (4-14). That is if $\psi_1(\underline{r})$, for example, as it is punched out on cards from an Exterminator-II run, is inserted in Eq. (4-4) and the latter being weighted by $\psi_1^*(\underline{r})$, is integrated over the reactor volume, a finite value results rather than exactly zero.

This is an undesirable situation for we intend to make use further (cf. Chapter V section 5-2), of the balance equations (4-4) and (4-14).

Thus it was necessary to recompute

$$k_k = \frac{\int_{\underline{r},\text{reactor}} W_1^T(\underline{r})\ F_k(\underline{r})\psi_k(\underline{r})d\underline{r}}{\int_{\underline{r},\text{reactor}} W_1^T(\underline{r})\,[A_k'(\underline{r})-\nabla.D_k(\underline{r})\nabla]\,\psi_k(\underline{r})d\underline{r}}, \tag{4-18}$$

where for k=1; $F_k(\underline{r}) = \nu\chi\ \Sigma_{F_1}^T(\underline{r})$, $A_k'(\underline{r})=A_1(\underline{r})$; for k=2; $F_k(\underline{r}) = \nu\ \Sigma_{F_2}^T\ (\underline{r})$ and $A_k'(\underline{r}) = A_2(\underline{r}) + \omega V^{-1}$, so that we assume we could write;

$$[\nabla.D_k(\underline{r})-A_k'(r) + \frac{1}{k_k}\nu\ \chi\ \ \Sigma_{F_k}^T(\underline{r})]\ \ \psi_k(\underline{r})=0,\ k=1,2\ . \tag{4-19}$$

4-4 Summary

We intend to use two trial modes for the expression of the time and space dependent flux. The first one is composed of the flux shape at the beginning of the transient and the second one, the flux shape at the end of the transient (the end of the time during which we wanted to study the transient). Thus along the bracketing idea, the flux shape will run from the steady state shape onto the shape at the end of the transient.

Both of the modes and the corresponding weighting modes for MITR-II will be computed for a 40x48 mesh point-cylindrical model and three-group scheme, from a steady state type of equations.

The computation of the second mode and its adjoint in the particular case of withdrawal of a control rod, required a poison search.

The computations will be performed with the code Exterminator-II. Thereafter it was necessary to recompute in an integral sense, the eigenvalue relative to the trial mode, to overcome the disturbance of the balance in equations giving $\psi_1(\underline{r})$ and $\psi_2(\underline{r})$, due to numerical disagreements.

CHAPTER V

METHODS FOR COMPUTING THE PARAMETERS APPEARING IN THE FINAL EQUATIONS FOR THE UNDETERMINED TIME COEFFICIENTS

The aim in this chapter is to formulate a way for computing Λ, $\rho(t)_{new}$ and $\overline{\beta}_j(t)_{new}$'s in

$$\Lambda \frac{dN(t)}{dt} = \left(\rho(t)_{new} - \overline{\beta}(t)_{new}\right) N(t) + \sum_{j=1}^{H} \lambda_j C_j(t), \qquad (5\text{-}1)$$

$$\frac{dC_j(t)}{dt} = \overline{\beta}_j(t)_{new} N(t) - \lambda_j C_j(t), \quad (j=1,\ldots,H), \qquad (5\text{-}2)$$

where

$$\overline{\beta}(t)_{new} = \sum_{j=1}^{H} \overline{\beta}_j(t)_{new} \,. \qquad (5\text{-}3)$$

The expressions giving the coefficients Λ, $\rho(t)$, $\overline{\beta}_j(t)_{new}$'s involve two main forms:

1. $$2\pi \int_{r,reactor} rdr \int_{z,reactor} dz \quad W^T(r,z)\underline{F}(r,z,t) = \underline{C}_1(t), \qquad (5\text{-}4)$$

where $\underline{F}(r,z,t)$ is a known function of r, z, and t; and

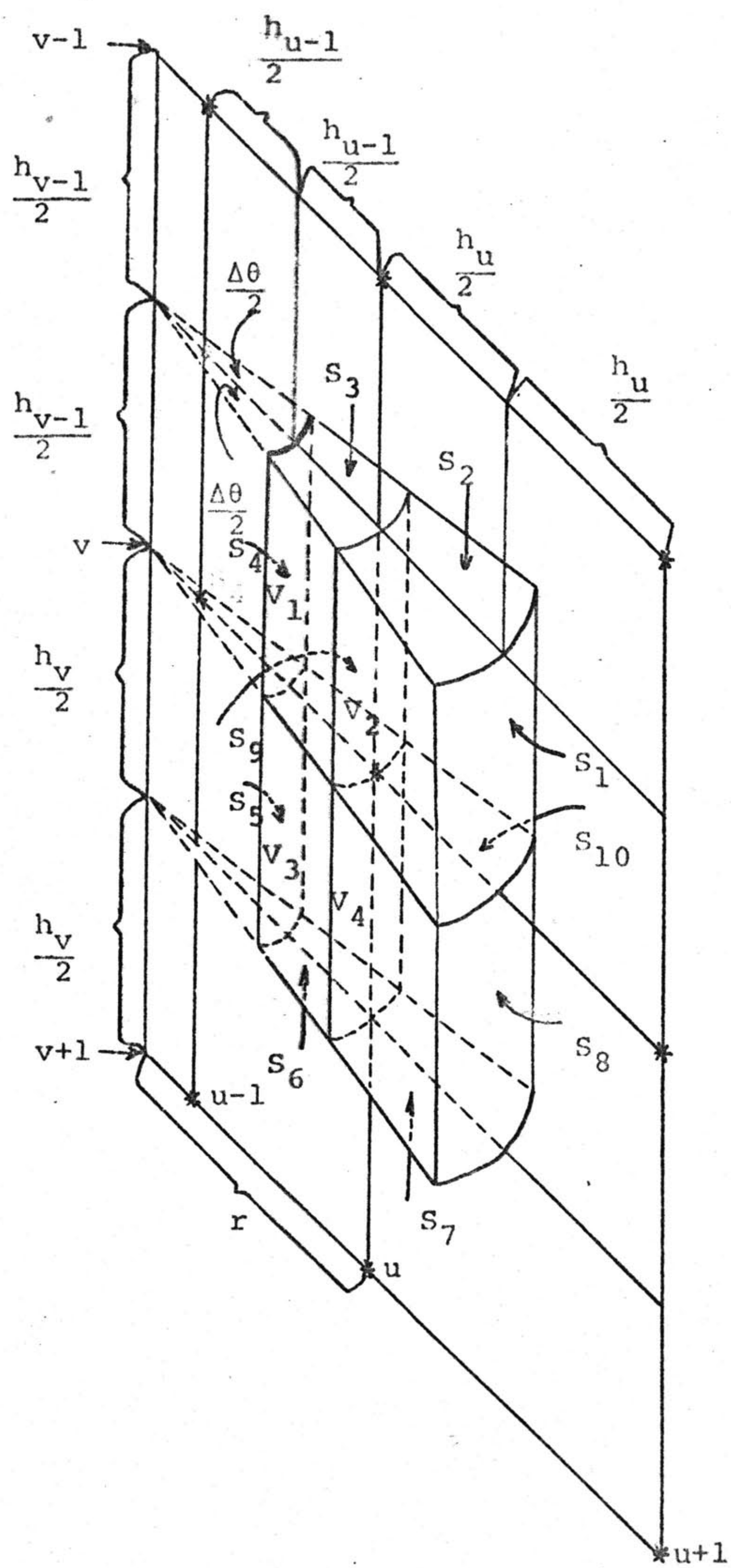

Fig. 5-1 Mesh Scheme in (r,z) Geometry

(5-5)

2. $$2\pi \int_{r,\text{reactor}} r\,dr \int_{z,\text{reactor}} dz \quad W^T(r,z)\left(\nabla . D(r,z,t)\nabla\psi(r,z)\right) = \underline{C}_2(t).$$

For the purpose of calculating $\underline{C}_1(t)$ and $\underline{C}_2(t)$ consider the Fig. 5-1 [6], where in two dimensions an equivalent mesh volume, V_{eq} composed of four submesh volumes: V_1, V_2, V_3, and V_4, is shown around the mesh point (v,u).

As is customary, we define for each mesh volume a constant neutron cross section for any event (fission, absorption, etc.), hence a constant diffusion coefficient, for each neutron group. Also, a constant value for $\psi_{gi}(r,z)$* and $W_{gi}(r,z)$ is fixed within the equivalent mesh volume around the mesh point (v,u) (cf. Fig. 5-2).

As shown in Fig. 5-2, there are $U\times V$ mesh points and $(U-1)\times(V-1)$ mesh volumes.

5-1 Calculation of $\underline{C}_1(t)$

In terms of the coordinate system described above $\underline{C}_1(t)$ can be written as

$$\underline{C}_1(t) = 2\pi \sum_{v=2}^{V-1} \sum_{u=1}^{U-1} W^T_{v,u} \quad \int_{V_{eq}} r\,dr \int_{V_{eq}} dz\ \underline{F}(r,z,t), \qquad (5\text{-}6)$$

where the integration is performed over the equivalent mesh volume V_{eq} around the mesh point (v,u) and the summation

---

* The g^{th} element of the i^{th} mode, as it is computed by the Code Exterminator II.

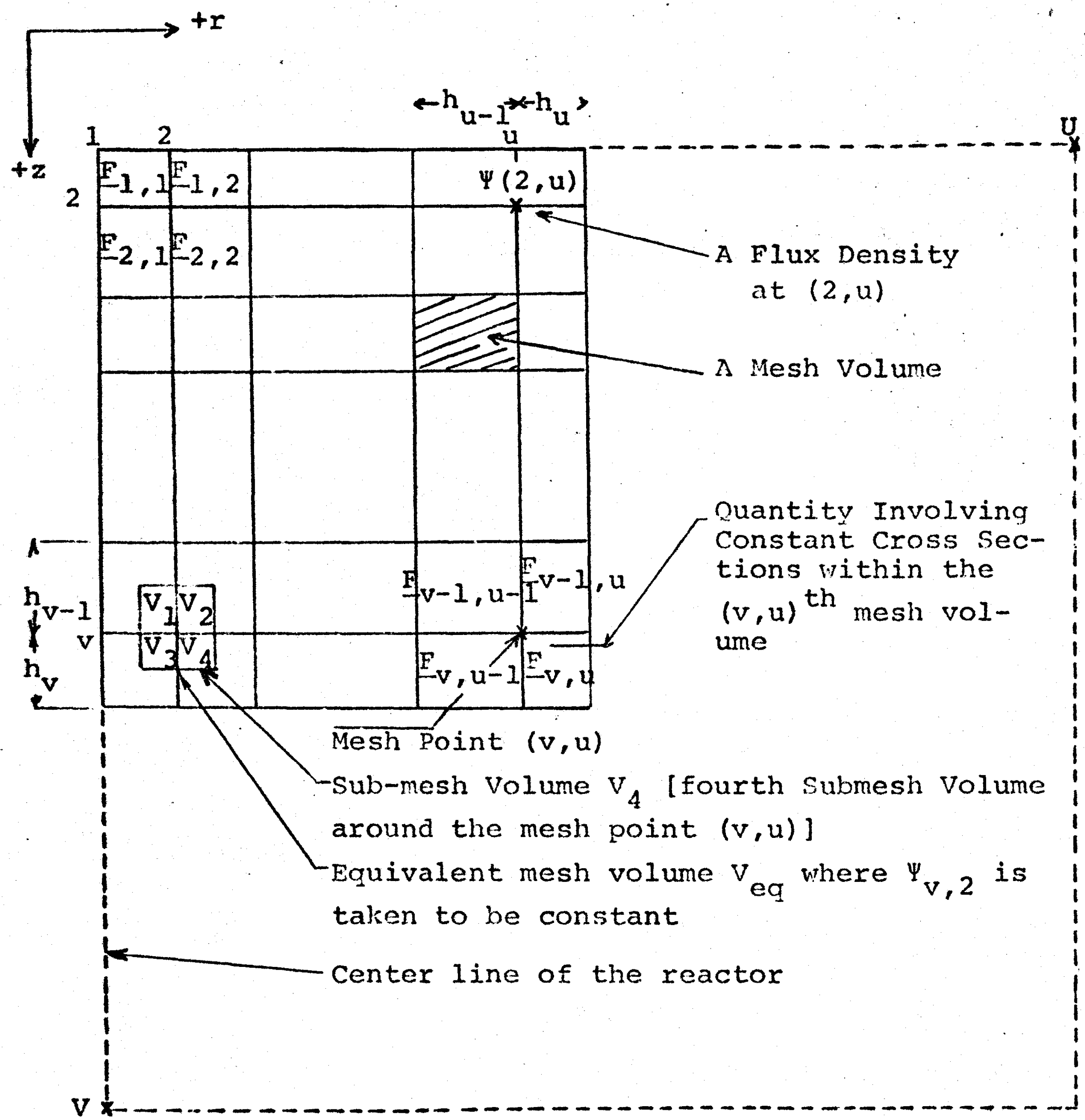

Fig. 5-2 Set Up of the Mesh Scheme

is carried up to U-1 and V-1 only, since $W^T_{v,u}$ vanishes at $u = U$ for all values of v, and at $v = 1$ and $v = V$ for all values of u.

In accord with Eq. (5-6) we then have

$$\underline{C}_1(t) \tag{5-7}$$

$$= \sum_{v=2}^{V-1} \sum_{u=1}^{U-1} W^T_{v,u} \left(\underline{F}_{v-1,u-1}(t)V_1 + \underline{F}_{v-1,u}(t)V_2 + \underline{F}_{v,u-1}(t)V_3 + \underline{F}_{v,u}(t)V_4 \right)$$

where $\underline{F}_{v,u}(t)$ is the constant quantity involving cross sections within the $(v,u)^{th}$ mesh volume at time t; and

$$V_1 = \Delta\theta \, \frac{h_{v-1}}{2} \cdot \frac{h_{u-1}}{2} \left(r - \frac{h_{u-1}}{4} \right), \tag{5-8}$$

with $r = \sum_{u=1}^{U-1} h_u$,

$$V_2 = \Delta\theta \, \frac{h_{v-1}}{2} \cdot \frac{h_u}{2} \left(r + \frac{h_u}{4} \right), \tag{5-9}$$

$$V_3 = \Delta\theta \, \frac{h_v}{2} \cdot \frac{h_{u-1}}{2} \left(r - \frac{h_{u-1}}{4} \right), \tag{5-10}$$

$$V_4 = \Delta\theta \, \frac{h_v}{2} \cdot \frac{h_u}{2} \left(r + \frac{h_u}{4} \right). \tag{5-11}$$

In addition, the cross sections at the left-hand side of the center line are taken to be zero.

Integrating Eq. (5-7) over the angle (θ from 0 to 2π) and using the expressions (5-9), (5-10), and (5-11), we arrive at

$$\underline{C}_1(t) = \frac{\pi}{2} \sum_{v=2}^{V-1} \sum_{u=1}^{U-1} W_{v,u}^T \left\{ \left(\underline{F}_{v-1,u-1}(t) h_{v-1} h_{u-1} + \underline{F}_{v,u-1}(t) h_v h_{u-1} \right) \left(r - \frac{h_{u-1}}{4} \right) + \left(\underline{F}_{v-1,u}(t) h_{v-1} h_u + \underline{F}_{v,u}(t) h_v h_u \right) \left(r + \frac{h_u}{4} \right) \right\}. \tag{5-12}$$

5-2 Calculation of $\underline{C}_2(t)$

$\underline{C}_2(t)$ is an I×I matrix (I being the number of expansion modes) composed of elements:

$$\underline{C}_{2_{ik}}(t) = 2\pi \int_{r,\text{reactor}} rdr \int_{z,\text{reactor}} dz \quad W_i^T(r,z) \left[\nabla . D(r,z,t) \nabla \psi_k(r,z) \right], \tag{5-13}$$

$$i = 1,2,\ k = 1,2.$$

We know from the previous chapter (Eq. (4-19)) that the two $\psi_k(r,z)$'s are the solutions of

$$\left[\nabla . D_k(r,z) \nabla - A_k'(r,z) + \frac{F_k(r,z)}{k_k} \right] \psi_k(r,z) = 0,\ k = 1,2 \tag{5-14}$$

Because of the assumed spatial independence of $D(r,z,t)$ in the b^{th} submesh volume around the mesh point (v,u), we can write

$$\nabla . D(r,z,t)\nabla\psi_k(r,z) = D_{b_{v,u}}(t)\nabla . \nabla\psi_k(r,z), \tag{5-15}$$

but also from Eq. (5-14),

$$D_{k_{b_{v,u}}} \nabla . \nabla\psi_k(r,z) = \left(A'_{k_{b_{v,u}}} - \frac{F_{k_{b_{v,u}}}}{k_k} \right) \psi_k(r,z). \tag{5-16}$$

Thus, combining Equations (5-15) and (5-16), we have in the b^{th} submesh volume around the mesh point (v,u)

$$\nabla . D(r,z,t)\nabla\psi_k(r,z) = D_{b_{v,u}}(t) D^{-1}_{k_{b_{v,u}}} \left(A'_{k_{b_{v,u}}} - \frac{1}{k_k} F_{k_{b_{v,u}}} \right) \psi_k(r,z), \tag{5-17}$$

such that, through Eq. (5-12),

$$\underline{C}_2(t) = \frac{\pi}{2} \sum_{v=2}^{V-1} \sum_{u=1}^{U-1} W^T_{v,u} \quad \text{row} \Bigg\{ \tag{5-18}$$

$$\Bigg[\Big(D_{v-1,u-1}(t) M_{k_{v-1,u-1}} h_{v-1} + D_{v,u-1}(t) M_{k_{v,u-1}} h_v \Big) h_{u-1} \left(r - \frac{h_{u-1}}{4} \right) +$$

$$\Big(D_{v-1,u}(t) M_{k_{v-1,u}} h_{v-1} + D_{v,u}(t) M_{k_{v,u}} h_v \Big) h_u \left(r + \frac{h_u}{4} \right) \Bigg] \psi_{k_{v,u}} \Bigg\},$$

where row { } denotes the row matrix whose k^{th} $(k=1,\ldots,K)$ element stands in between { }. (Note that this element is a $G\times 1$ matrix), and

$$M_{k_{b_{v,u}}} = D^{-1}_{k_{b_{v,u}}}\left(A'_{k_{b_{v,u}}} - \frac{F_{k_{b_{v,u}}}}{k_k}\right). \tag{5-19}$$

The column vector $D_{b_{v,u}}(t)M_{k_{b_{v,u}}}\psi_{k_{v,u}}$ encountered in Eq. (5-18) when written explicitly is

$$D_{b_{v,u}}(t)M_{k_{b_{v,u}}}\psi_{k_{v,u}}$$

$$= \begin{pmatrix} \left[\left(\Sigma_{a_{1k_{b_{v,u}}}} + \Sigma_{\overleftarrow{21}k_{b_{v,u}}} - \dfrac{\nu\Sigma_{F_{1k_{b_{v,u}}}}}{k_k}\right)\psi_{1k_{v,u}} - \dfrac{\nu\Sigma_{F_{2k_{b_{v,u}}}}}{k_k}\psi_{2k_{v,u}} - \dfrac{\nu\Sigma_{F_{3k_{b_{v,u}}}}}{k_k}\psi_{3k_{v,u}}\right]\dfrac{D_{1_{b_{v,u}}}(t)}{D_{1_{k_{b_{v,u}}}}} \\[2ex] \left[-\Sigma_{\overleftarrow{21}k_{b_{v,u}}}\psi_{1k_{v,u}} + \left(\Sigma_{a_{2k_{b_{v,u}}}} + \Sigma_{\overleftarrow{32}k_{b_{v,u}}}\right)\psi_{2k_{v,u}}\right]\dfrac{D_{1_{b_{v,u}}}(t)}{D_{1_{k_{b_{v,u}}}}} \\[2ex] \left[-\Sigma_{\overleftarrow{32}k_{b_{v,u}}}\psi_{2k_{v,u}} + \Sigma_{a_{3k_{b_{v,u}}}}\psi_{3k_{v,u}}\right]\dfrac{D_{3_{b_{v,u}}}(t)}{D_{3_{k_{b_{v,u}}}}} \end{pmatrix} \tag{5-20}$$

The $\underline{C}_{2_{ik}}(t)$ can be presented as

(5-21)

$$\underline{C}_{2_{ik}}(t) \equiv LAP_{ik}(t) = \frac{\pi}{2}\sum_{v=2}^{V-1}\sum_{u=1}^{U-1}\left[W_{i1_{v,u}}X_{1k_{v,u}}(t) + W_{i2_{v,u}}X_{2k_{v,u}}(t) + W_{i3_{v,u}}X_{3k_{v,u}}(t)\right],$$

where the notation $LAP_{ik}(t)$ (cf. laplacian) is introduced with

(5-22)

$$X_{1k_{v,u}}(t)$$

$$= \Bigg\{\Bigg[\left[\left(\Sigma_{a_{1_{k_{v-1,u-1}}}} + \Sigma_{21_{k_{v-1,u-1}}} - \frac{\nu\Sigma_{F_{1_{k_{v-1,u-1}}}}}{k_k}\right)COEF_{1_{k_{v-1,u-1}}}(t)h_{v-1}\right.$$

$$\left.+ \left(\Sigma_{a_{1_{k_{v,u-1}}}} + \Sigma_{21_{k_{v,u-1}}} - \frac{\nu\Sigma_{F_{1_{k_{v,u-1}}}}}{k_k}\right)COEF_{1_{k_{v,u-1}}}(t)h_v\right]h_{u-1}\left(r-\frac{h_{u-1}}{4}\right)$$

$$+ \left[\left(\Sigma_{a_{1_{k_{v-1,u}}}} + \Sigma_{21_{k_{v-1,u}}} - \frac{\nu\Sigma_{F_{1_{k_{v-1,u}}}}}{k_k}\right)COEF_{1_{k_{v-1,u}}}(t)h_{v-1}\right.$$

$$\left.+ \left(\Sigma_{a_{1_{k_{v,u}}}} + \Sigma_{21_{k_{v,u}}} - \frac{\nu\Sigma_{F_{1_{k_{v,u}}}}}{k_k}\right)COEF_{1_{k_{v,u}}}(t)h_v\right]h_u\left(r+\frac{h_u}{4}\right)\Bigg\}\psi_{1_{k_{v,u}}}$$

$$- \Bigg[\left(\nu\Sigma_{F_{2_{k_{v-1,u-1}}}}COEF_{1_{k_{v-1,u-1}}}(t)h_{v-1} + \nu\Sigma_{F_{2_{k_{v,u-1}}}}COEF_{1_{k_{v,u-1}}}(t)h_v\right)$$

$$h_{u-1}\left(r-\frac{h_{u-1}}{4}\right) +$$

(equation continued on next page)

(5-22 cont.)

$$+ \left(\left(\nu\Sigma_{F_{2_{k_{v-1,u}}}} COEF_{1_{k_{v-1,u}}}(t)h_{v-1} + \nu\Sigma_{F_{2_{k_{v,u}}}} COEF_{1_{k_{v,u}}}(t)h_v\right)h_u\left(r+\frac{h_u}{4}\right)\right)$$

$$\frac{1}{k_k}\psi_{2_{k_{v,u}}}$$

$$-\left(\left(\nu\Sigma_{F_{3_{k_{v-1,u-1}}}} COEF_{1_{k_{v-1,u-1}}}(t)h_{v-1} + \nu\Sigma_{F_{3_{k_{v,u-1}}}} COEF_{1_{k_{v,u-1}}}(t)h_v\right)\right.$$

$$h_{u-1}\left(r-\frac{h_{u-1}}{4}\right)$$

$$+ \left(\left(\nu\Sigma_{F_{3_{k_{v-1,u}}}} COEF_{1_{k_{v-1,u}}}(t)h_{v-1} + \nu\Sigma_{F_{3_{k_{v,u}}}} COEF_{1_{k_{v,u}}}(t)h_v\right)h_u\left(r+\frac{h_u}{4}\right)\right)$$

$$\frac{1}{k_k}\psi_{3_{k_{v,u}}},$$

where

$$COEF_{1_{k_{b_{v,u}}}}(t) = \frac{D_{1_{b_{v,u}}}(t)}{D_{1_{k_{b_{v,u}}}}}, \qquad (5\text{-}23)$$

(5-24)

$$
\begin{aligned}
&X_{2k_{v,u}}(t) \\
&= -\Bigg[\bigg(\Sigma\overleftarrow{21}_{k_{v-1,u-1}}\,COEF_{2_{k_{v-1,u-1}}}(t)h_{v-1} + \Sigma\overleftarrow{21}_{k_{v,u-1}}\,COEF_{2_{k_{v,u-1}}}(t)h_{v}\bigg) \\
&\quad h_{u-1}\left(r-\frac{h_{u-1}}{4}\right) + \bigg(\Sigma\overleftarrow{21}_{k_{v-1,u}}\,COEF_{2_{k_{v-1,u}}}(t)h_{v-1} + \Sigma\overleftarrow{21}_{k_{v,u}}\,COEF_{2_{k_{v,u}}}(t)h_{v}\bigg) \\
&\quad h_{u}\left(r+\frac{h_{u}}{4}\right)\Bigg]\psi_{1_{k_{v,u}}} + \Bigg\{\Bigg[\bigg(\Sigma a_{2_{k_{v-1,u-1}}} + \Sigma\overleftarrow{32}_{k_{v-1,u-1}}\bigg)COEF_{2_{k_{v-1,u-1}}}(t)h_{v-1} \\
&\quad + \bigg(\Sigma a_{2_{k_{v,u-1}}} + \Sigma\overleftarrow{32}_{k_{v,u-1}}\bigg)COEF_{2_{k_{v-1,u-1}}}(t)h_{v}\Bigg]h_{u-1}\left(r-\frac{h_{u-1}}{4}\right) \\
&\quad + \Bigg[\bigg(\Sigma a_{2_{k_{v-1,u}}} + \Sigma\overleftarrow{32}_{k_{v-1,u}}\bigg)COEF_{2_{k_{v-1,u}}}(t)h_{v-1} \\
&\quad + \bigg(\Sigma a_{2_{k_{v,u}}} + \Sigma\overleftarrow{32}_{k_{v,u}}\bigg)COEF_{2_{k_{v,u}}}(t)h_{v}\Bigg]h_{u}\left(r+\frac{h_{u}}{4}\right)\Bigg\}\psi_{2_{k_{v,u}}},
\end{aligned}
$$

and,

(5-25)

$$X_{3k_{v,u}}(t)$$

$$= -\Bigg[\Bigg(\Bigg[\Sigma_{\overleftarrow{3}2_{k_{v-1,u-1}}} \mathrm{COEF}_{3_{k_{v-1,u-1}}}(t)h_{v-1} + \Sigma_{\overleftarrow{3}2_{k_{v,u-1}}} \mathrm{COEF}_{3_{k_{v,u-1}}}(t)h_{v}\Bigg]$$

$$h_{u-1}\left(r-\frac{h_{u-1}}{4}\right) + \Bigg[\Sigma_{\overleftarrow{3}2_{k_{v-1,u}}} \mathrm{COEF}_{3_{k_{v-1,u}}}(t)h_{v-1} + \Sigma_{\overleftarrow{3}2_{k_{v,u}}} \mathrm{COEF}_{3_{k_{v,u}}}(t)h_{v}\Bigg]$$

$$h_{u}\left(r+\frac{h_{u}}{4}\right)\Bigg)\psi_{2_{k_{v,u}}} + \Bigg(\Bigg[\Sigma_{a_{3_{k_{v-1,u-1}}}} \mathrm{COEF}_{3_{k_{v-1,u-1}}}(t)h_{v-1}$$

$$+ \Sigma_{a_{3_{k_{v,u-1}}}} \mathrm{COEF}_{3_{k_{v,u-1}}}(t)h_{v}\Bigg] h_{u-1}\left(r-\frac{h_{u-1}}{4}\right)$$

$$+ \Bigg[\Sigma_{a_{3_{k_{v-1,u}}}} \mathrm{COEF}_{3_{k_{v-1,u}}}(t)h_{v-1} + \Sigma_{a_{3_{k_{v,u}}}} \mathrm{COEF}_{3_{k_{v,u}}}(t)h_{v}\Bigg] h_{u}\left(r+\frac{h_{u}}{4}\right)\Bigg)\psi_{3_{k_{v,u}}}\Bigg].$$

5-3 A different approach to the leakage integral for a special case

The indirect method just described avoids the use of the finite difference technique to determine the laplacian part of $\underline{C}_{2_{ik}}(t)$. However, a direct approach to the leakage integral is necessary when we want to compute k_k, the eigenvalue of the balance equation for ψ_k (cf. Eq. (4-18)). That quantity was assumed to be known in the course of the previous section.

Thus we want to compute

$$\underline{L}_k = \int_{V_1,\text{reactor}} d\underline{r} \quad W_1^T(\underline{r})\nabla . D_k(\underline{r})\psi_k(\underline{r}). \tag{5-26}$$

With the help of Fig. 5-1, Eq. (5-26) can be written as

$$\begin{aligned}\underline{L}_k = \sum_{v=2}^{V-1}\sum_{u=1}^{U-1} W^T_{1_{v,u}} \Bigg(& D_{k_{v-1,u-1}} 2\pi \int_{V_1} rdr \int_{V_1} dz \ \nabla.\nabla\psi_k(r,z) \\ & + D_{k_{v-1,u}} 2\pi \int_{V_2} rdr \int_{V_2} dz \ \nabla.\nabla\psi_k(r,z) \\ & + D_{k_{v,u-1}} 2\pi \int_{V_3} rdr \int_{V_3} dz \ \nabla.\nabla\psi_k(r,z) \\ & + D_{k_{v,u}} 2\pi \int_{V_4} rdr \int_{V_4} dz \ \nabla.\nabla\psi_k(r,z)\Bigg).\end{aligned} \tag{5-27}$$

By the divergence theorem the integrals in Eq. (5-27) can be reduced to surface integrals of $\frac{\partial\psi_k}{\partial n}(r,z)$ (the derivative of $\psi_k(r,z)$ in the direction of outward normal to the surface) over the six surfaces which enclose the equivalent mesh volume.

Making this transformation on, for instance, the second integral in Eq. (5-27) yields

$$2\pi \int_{V_2} rdr \int_{V_2} dz\ \nabla . \nabla\psi(r,z) \tag{5-28}$$

$$= \int_{S_1} \frac{\partial\psi\ (r,z)}{\partial n} dS + \int_{S_2} \frac{\partial\psi\ (r,z)}{\partial n} dS + \int_{S_9} \frac{\partial\psi(r,z)}{\partial n} dS$$

$$+ \int_{S_{10}} \frac{\partial\psi(r,z)}{\partial n} dS .$$

Since the neutron current, $D_{g_k}(r,z)\ \frac{\psi\partial_{gk}(r,z)}{\partial n}$ is assumed to be continuous across interfaces, the surface integrals over the common surfaces to the submesh volumes cancel when the four expressions similar to Eq. (5-28) are added. Then Eq. (5-27) becomes,

$$\underline{L}_k = \sum_{v=2}^{V-1} \sum_{u=1}^{U-1} W^T_{1_{v,u}} \Bigg(D_{k_{v-1,u}} \sum_{b=1}^{2} \int_{S_b} \frac{\partial\psi_k(r,z)}{\partial n} dS \tag{5-29}$$

$$+ D_{k_{v-1,u-1}} \sum_{b=3}^{4} \int_{S_b} \frac{\partial\psi_k(r,z)}{\partial n} dS + D_{k_{v,u-1}} \sum_{b=5}^{6} \int_{S_b} \frac{\partial\psi_k(r,z)}{\partial n} dS$$

(equation continued on next page)

$$+ D_{k_{v,u}} \sum_{b=7}^{8} \int_{S_b} \frac{\partial \psi_k(r,z)}{\partial n} \, dS \; . \qquad \text{(5-29) cont.}$$

Next we let $\underline{I}_{p_k}$ stand for $\int_{S_p} \frac{\partial\psi_k(r,z)}{\partial n} dS$ and note that

$$\underline{I}_{1_k} = \frac{\psi_{k_{v,u+1}} - \psi_{k_{v,u}}}{h_u} \, \Delta\theta \, \frac{h_{v-1}}{2} \left[r + \frac{h_u}{2} \right], \quad (k=1,2), \qquad (5\text{-}30)$$

$$\underline{I}_{2_k} = \frac{\psi_{k_{v-1,u}} - \psi_{k_{v,u}}}{h_{v-1}} \, \Delta\theta \, \frac{h_u}{2} \left[r + \frac{h_u}{4} \right], \quad (k=1,2), \qquad (5\text{-}31)$$

$$\underline{I}_{3_k} = \frac{\psi_{k_{v-1,u}} - \psi_{k_{v,u}}}{h_{v-1}} \, \Delta\theta \, \frac{h_{u-1}}{2} \left[r - \frac{h_{u-1}}{4} \right], (k=1,2), \qquad (5\text{-}32)$$

$$\underline{I}_{4_k} = \frac{\psi_{k_{v,u-1}} - \psi_{k_{v,u}}}{h_{u-1}} \, \Delta\theta \, \frac{h_{v-1}}{2} \left[r - \frac{h_{u-1}}{2} \right], (k=1,2), \qquad (5\text{-}33)$$

$$\underline{I}_{5_k} = \frac{\psi_{k_{v,u-1}} - \psi_{k_{v,u}}}{h_{u-1}} \, \Delta\theta \, \frac{h_v}{2} \left[r - \frac{h_{u-1}}{2} \right], \quad (k=1,2), \qquad (5\text{-}34)$$

$$\underline{I}_{6_k} = \frac{\psi_{k_{v+1,u}} - \psi_{k_{v,u}}}{h_v} \, \Delta\theta \, \frac{h_{u-1}}{2} \left[r - \frac{h_{u-1}}{4} \right], (k=1,2), \qquad (5\text{-}35)$$

$$\underline{I}_{7_k} = \frac{\psi_{k_{v+1,u}} - \psi_{k_{v,u}}}{h_v} \, \Delta\theta \, \frac{h_u}{\;} \left[r + \frac{h_u}{4} \right], \quad (k=1,2), \qquad (5\text{-}36)$$

$$\underline{I}_{8_k} = \frac{\psi_{k_{v,u+1}} - \psi_{k_{v,u}}}{h_u} \quad \frac{h_v}{2} \left(r + \frac{h_u}{2}\right), \quad (k=1,2). \qquad (5\text{-}37)$$

Inserting Equations (5-30) up to (5-37) into Eq. (5-27) and integrating over the angle (θ from 0 to 2π) one gets

$$(5\text{-}38)$$

$$\underline{L}_k = \sum_{v=2}^{V-1} \sum_{u=1}^{U-1} W^T_{1_{v,u}} \left\{ \frac{\psi_{k_{v,u+1}}}{h_u} \left(D_{k_{v-1,u}} h_{v-1} + D_{k_{v,u}} h_v\right) \left(r + \frac{h_u}{2}\right) \right.$$

$$+ \frac{\psi_{k_{v-1,u}}}{h_{v-1}} \left[D_{k_{v-1,u}} h_u \left(r + \frac{h_u}{4}\right) + D_{k_{v-1,u-1}} h_{u-1} \left(r - \frac{h_{u-1}}{4}\right) \right]$$

$$+ \frac{\psi_{k_{v,u-1}}}{h_{u-1}} \left(D_{k_{v-1,u-1}} h_{v-1} + D_{k_{v,u-1}} h_v\right) \left(r - \frac{h_{u-1}}{2}\right)$$

$$+ \frac{\psi_{k_{v+1,u}}}{h_v} \left[D_{k_{v,u-1}} h_{u-1} \left(r - \frac{h_{u-1}}{4}\right) + D_{k_{v,u}} h_v \left(r + \frac{h_u}{4}\right) \right]$$

$$- \psi_{k_{v,u}} \left[\left(D_{k_{v-1,u}} h_{v-1} + D_{k_{v,u}} h_v\right) \frac{1}{h_u} \left(r + \frac{h_u}{2}\right) + \left[D_{k_{v-1,u}} h_v \left(r + \frac{h_u}{4}\right) \right.\right.$$

$$\left. + D_{k_{v-1,u-1}} h_{u-1} \left(r - \frac{h_{u-1}}{4}\right) \right] \frac{1}{h_{v-1}} + \left(D_{k_{v-1,u-1}} h_{v-1} + D_{k_{v,u-1}} h_v\right) \times$$

(equation continued on next page)

(5-38 cont.)

$$\times \frac{1}{h_{u-1}} \left(r - \frac{h_{u-1}}{2}\right) \left[D_{k_{v,u-1}} h_{u-1} \left(r - \frac{h_{u-1}}{4}\right) + D_{k_{v,u}} h_u \left(r + \frac{h_u}{4}\right) \right] \frac{1}{h_v} \Bigg] \Bigg\} .$$

This method of evaluating the leakage integral has not been used to calculate $\underline{C}_2(t)$ because we cannot insure that it is valid to write relationships such as

$$D^L_{g_k}(r,z,t) \frac{\partial \psi_{gk}(r,z)}{\partial n} = D^R_{g_k}(r,z,t) \frac{\partial \psi_{gk}}{\partial n} \qquad (5\text{-}39)$$

with L and R indicating the left and right hand sides of an interface, respectively, and n being either r or z.

Whereas with a diffusion coefficient belonging to the space function in question, an equation like Eq. (5-39) is true, it will not in general hold for any other diffusion coefficient. Hence we had to work out the method described in the previous section.

5-4 Computation of k_k

The calculation of $\underline{C}_2(t)$ cannot be completed unless k_k is known. For this purpose, besides the leakage integral [Eq. (5-38)] we need the fission and absorption integrals. These quantities are given by

$$\underline{F}_k = \frac{\pi}{2} \sum_{v}\sum_{u}{}_{\text{over the core}} W_{11_{v,u}} \nu \Bigg\{\Bigg[\Big(\Sigma_{F_{1_{k_{v-1,u-1}}}} h_{v-1} + \Sigma_{F_{1_{k_{v,u-1}}}} h_v\Big) h_u\Big(r-\frac{h_{u-1}}{4}\Big) + \Big(\Sigma_{F_{1_{k_{v-1,u}}}} h_{v-1} + \Sigma_{F_{1_{k_{v,u}}}} h_v\Big) h_u\Big(r+\frac{h_u}{4}\Big)\Bigg]\psi_{1_{k_{v,u}}}$$

$$+ \Bigg[\Big(\Sigma_{F_{2_{k_{v-1,u-1}}}} h_{v-1} + \Sigma_{F_{2_{k_{v,u-1}}}} h_v\Big) h_u\Big(r-\frac{h_{u-1}}{4}\Big)$$

$$+ \Big(\Sigma_{F_{2_{k_{v-1,u}}}} h_{v-1} + \Sigma_{F_{2_{k_{v,u}}}} h_v\Big) h_u\Big(r+\frac{h_u}{4}\Big)\Bigg]\psi_{2_{k_{v,u}}}$$

$$+ \Bigg[\Big(\Sigma_{F_{3_{k_{v-1,u-1}}}} h_{v-1} + \Sigma_{F_{3_{k_{v,u-1}}}} h_v\Big) h_u\Big(r-\frac{h_{u-1}}{4}\Big)$$

$$+ \Big(\Sigma_{F_{3_{k_{v-1,u}}}} h_{v-1} + \Sigma_{F_{3_{k_{v,u}}}} h_v\Big) h_u\Big(r+\frac{h_u}{4}\Big)\Bigg]\psi_{3_{k_{v,u}}}\Bigg\}, \qquad (5\text{-}40)$$

$$(5\text{-}41)$$

$$\underline{A} = \frac{\pi}{2} \sum_{v=2}^{V-1} \sum_{u=2}^{U-1} \Big(W_{11_{v,u}} Z_{1k_{v,u}} W_{12_{v,u}} Z_{2k_{v,u}} W_{13_{v,u}} Z_{3k_{v,u}}\Big)$$

where $Z_{1k_{v,u}}$, $Z_{2k_{v,u}}$, and $Z_{3k_{v,u}}$ can be found from Equations (5-23), (5-24), and (5-25) by taking out the terms involving the fission cross sections, omitting

$COEF_{g_{k_b}}$'s and changing the signs.

Finally we have

$$k_k = \frac{\underline{F}_k}{\underline{A}_k - \underline{L}_k} \quad . \tag{5-42}$$

5-5 Final expressions for the parameters Λ, $\rho(t)_{new}$, $\overline{\beta}_j(t)_{new}$

Using the final integral expressions found for Λ, $\rho(t)_{new}$, and $\overline{\beta}_j(t)_{new}$'s in Chapter III, and Equations (5-12) and (5-21), one obtains

$$\Lambda_{ik} = \frac{\pi}{2} \sum_{v=2}^{V-1} \sum_{u=1}^{U-1} \left(\sum_{g=1}^{G} W_{ig_{v,u}} V_g^{-1} \psi_{kg_{v,u}} \right) \left[\left(h_{v-1} + h_v \right) h_{u-1} \left(r - \frac{h_{u-1}}{4} \right) + \left(h_{v-1} + h_v \right) h_u \left(r + \frac{h_u}{4} \right) \right], \tag{5-43}$$

$$\rho(t)_{new_{ik}} = PPR_{ik}(t) + LAP_{ik}(t) + FMA_{ik}(t) + DPR_{ik}(t), \tag{5-44}$$

where the prompt photoneutron reactivity matrix is defined by its i^{th} row, k^{th} column element;

$$
\begin{aligned}
&PPR_{ik}(t) \qquad\qquad\qquad\qquad\qquad\qquad\qquad\qquad\qquad\qquad\qquad\qquad\qquad (5\text{-}45)\\
&= \frac{\pi}{2}\sum_{re=1}^{RE} ATT_{re} \underbrace{\sum_{v}\sum_{u}}_{\text{over the reflector}} W_{il_{v,u}} \Bigg\{ \sum_{\ell=1}^{L} \\
&\Bigg[\Bigg[\Big[\Sigma_{D_{\ell_{v-1,u-1}}}(t)h_{v-1} + \Sigma_{D_{\ell_{v,u-1}}}(t)h_v\Big]h_{u-1}\left(r-\frac{h_{u-1}}{4}\right) \\
&+ \Big[\Sigma_{D_{\ell_{v-1,u}}}(t)h_{v-1} + \Sigma_{D_{\ell_{v,u}}}(t)h_v\Big]h_u\left(r+\frac{h_u}{4}\right)\Bigg] \\
&\times \frac{\pi}{2}\sum_{v=2}^{V-1}\sum_{u=1}^{U-1}\sum_{g=1}^{G}\Bigg[\Bigg[\Big[SGCS_{g\ell_{v-1,u-1}}(t)h_{v-1} \\
&+ SGCS_{g\ell_{v,u-1}}(t)h_v\Big]h_{u-1}\left(r-\frac{h_{u-1}}{4}\right) + \Big[SGCS_{g\ell_{v-1,u}}(t)h_{v-1} \\
&+ SGCS_{g_{v,u}}(t)h_v\Big]h_u\left(r+\frac{h_u}{4}\right)\Bigg]\Bigg]\psi_{gk_{v,u}}\Bigg\},
\end{aligned}
$$

RE being the number of regions in the reflector, each coupled with a constant attenuation factor for photons to simplify the computation. That is, ATT_{re} replaces $\frac{1}{4\pi(r^2+z^2)} e^{-\Sigma_\ell (r^2+z^2)^{\frac{1}{2}}}$ within the re^{th} region (cf. Appendix H); and

$$SGCS_{g\ell_{v,u}}(t) = \sum_{f=1}^{3} \Sigma_{f_{g_{v,u}}}(t) \prod_{f_{\ell g}}^{n} ; \qquad (5\text{-}46)$$

where n stands for the nuclei n present at (v,u). The computation of $LAP_{ik}(t)$ is described in Section 5-2 above; and $FMA_{ik}(t)$ can be found from the expression for $LAP_{ik}(t)$ by omitting $COEF_{g_{k_b}}$'s and the dependency of the cross sections on k, making the cross sections time-dependent and changing all the signs.

The delayed photoneutron reactivity matrix is defined by its i^{th} row, k^{th} column element;

$$DPR_{ik}(t) = \sum_{j=J+1}^{H} \bar{\beta}_{j}(t)_{new_{ik}} , \qquad (5\text{-}47)$$

with

(5-48)

$$\overline{\beta}_{j_{new_{ik}}}(t) = \frac{\pi}{2} y_j N_0 \sum_{re=1}^{RE} ATT_{re} \underset{\text{over the reflector}}{\sum_v \sum_u} W_{i1_{v,u}} \left\{ \sum_{\ell=1}^{L} Y_\ell \right.$$

$$\left[\left[\left(\Sigma_{D_{v-1,u-1}}(t)h_{v-1} + \Sigma_{D_{v,u-1}}(t)h_v\right)h_{u-1}\left(r-\frac{h_{u-1}}{4}\right)\right.\right.$$

$$\left.+\left(\Sigma_{D_{v-1,u}}(t)h_{v-1} + \Sigma_{D_{v,u}}(t)h_v\right)h_u\left(r+\frac{h_u}{4}\right)\right]$$

$$\times \frac{\pi}{2} \underset{\text{over the core}}{\sum_v \sum_u} \left[\sum_{g=1}^{G} \nu \left[\left[\left(\Sigma_{F_{g_{v-1,u-1}}}(t)h_{v-1}\right.\right.\right.\right.$$

$$\left.+ \Sigma_{F_{g_{v,u-1}}}(t)h_v\right)h_{u-1}\left(r-\frac{h_{u-1}}{4}\right) + \left(\Sigma_{F_{g_{v-1,u}}}(t)h_{v-1}\right.$$

$$\left.\left.\left.\left.+ \Sigma_{F_{g_{v,u}}}(t)h_v\right)h_u\left(r+\frac{h_u}{4}\right)\right]\right]\psi_{gk_{v,u}}\right\}, \; (j = (g+1),\ldots,H).$$

We finally have,

(5-49)

$$\overline{\beta}_{j_{new_{ik}}}(t) = \overline{\beta}_j \frac{\pi}{2} \underset{\text{over the core}}{\sum_v \sum_u} W_{i1_{v,u}} \nu \left[\left[\left(\Sigma_{F_{1_{v-1,u-1}}}(t)h_{v-1}\right.\right.\right.$$

(equation continued on next page)

(5-49 cont.)

$$+ \Sigma_{F_{1_{v,u-1}}}(t)h_v\Bigg] h_{u-1}\left(r - \frac{h_{u-1}}{4}\right) + \Bigg[\Sigma_{F_{1_{v-1,u}}}(t)h_{v-1}$$

$$+ \Sigma_{F_{1_{v,u}}}(t)h_v\Bigg] h_u\left(r + \frac{h_u}{4}\right)\Bigg\}\psi_{1k_{v,u}} + \Bigg\{\Bigg[\Sigma_{F_{2_{v-1,u-1}}}(t)h_{v-1}$$

$$+ \Sigma_{F_{2_{v,u-1}}}(t)h_v\Bigg] h_{u-1}\left(r - \frac{h_{u-1}}{4}\right) + \Bigg[\Sigma_{F_{2_{v-1,u}}}(t)h_{v-1}$$

$$+ \Sigma_{F_{2_{v,u}}}(t)h_v\Bigg] h_u\left(r + \frac{h_u}{4}\right)\Bigg\}\psi_{2k_{v,u}} + \Bigg\{\Bigg[\Sigma_{F_{3_{v-1,u-1}}}(t)h_{v-1}$$

$$+ \Sigma_{F_{3_{v,u-1}}}(t)h_v\Bigg] h_{u-1}\left(r - \frac{h_{u-1}}{4}\right) + \Bigg[\Sigma_{F_{3_{v-1,u}}}(t)h_{v-1}$$

$$+ \Sigma_{F_{3_{v,u}}}(t)h_v\Bigg] h_u\left(r + \frac{h_u}{4}\right)\Bigg\}\psi_{3k}\Bigg], \quad (j = 1,\ldots,J).$$

5-6 Computation of k_{OZAN}* for $\rho_{new_{11}}(0)$

For clarity assume we have only one expansion mode (point kinetics case) that is composed of the steady state shape of the reactor and the reactor is critical. Had then $\rho_{new_{11}}$ [Eq.(5-44)] failed to vanish, the time-dependent

---

* OZAN is the name of the computer code written to perform calculations required by the present work.

equations will predict a change in the power level that must remain constant. To remedy this erroneous behavior we shall compute a quantity k_{OZAN} that divides the fission integral in Eq. (5-44), and insures that $\rho_{new_{11}}(0) = 0$. Thus if the reactor is critical at the beginning of the transient we define

$$k_{OZAN} = \frac{F_{11}(0)}{A_{11}(0) - [LAP_{11}(0)+PPR_{11}(0)+DPR_{11}(0)]} \tag{5-50}$$

with

$$F_{11}(t) - A_{11}(t) = FMA_{11}(t). \tag{5-51}$$

Note that in case the photoneutrons are neglected $k_{OZAN} \equiv k_1$ [cf. Eq. (4-18)].

We point out that while k_k $(k = 1,2)$ was introduced to make use of the balance equation furnishing $\psi_k(\underline{r})$ in order to compute $LAP_{ik}(t)$ [Eq. (5-21)], k_{OZAN} is physically the eigenvalue of the reactor (at $t = 0$), computed in an integral sense. Hence the fission cross sections of the critical reactor are supposed to be equal to

$$\frac{\Sigma_{F_1}(\underline{r})}{k_{OZAN}} .$$

5-7 Representation of the time dependency of the parameters $\rho_{new}(t)$ and $\bar{\beta}_{j_{new}}(t)$'s

The solution to the system of equations for the time coefficients will require analytical representations for the parameters $\rho_{new}(t)$ and $\bar{\beta}_{j_{new}}(t)$'s. For this purpose we shall assume that throughout the transient

$$\rho_{new}(t) = \rho_{new}(0) + \rho_1 t, \tag{5-52}$$

$$\bar{\beta}_{j_{new}}(t) = \bar{\beta}_{j_{new}}(0) + \bar{\beta}_{j_1} t, \; (j = 1,\ldots,H), \tag{5-53}$$

where $\rho_{new}(0)$ and $\bar{\beta}_{j_{new}}(0)$ are the initial values of $\rho_{new}(t)$ and $\bar{\beta}_{j_{new}}(t)$, and

$$\rho_1 = \frac{\rho_{new}(T) - \rho_{new}(0)}{T}, \tag{5-54}$$

$$\bar{\beta}_{j_1} = \frac{\bar{\beta}_{j_{new}}(T) - \bar{\beta}_{j_{new}}(0)}{T}, \tag{5-55}$$

where T in seconds is the duration of the transient beginning at $t = 0$.

5-8 Summary

In this chapter we have developed a method for computing various parameters appearing in the equations for the unknown time coefficients. For this purpose a finite difference technique is used in keeping with the way the spatial functions are computed.

The leakage part of the reactivity matrix requires a special treatment since the time-dependent diffusion coefficient in the desired integral is not the one associated with the expansion modes and the continuity condition across interfaces fails. This procedure, however, requires knowing the eigenvalue that balances the equation from which the trial mode is generated. In calculating this eigenvalue we were able to use a direct way of attacking the leakage integral.

If the reactor was critical at the beginning of the transient and the photoneutrons were felt to be significant, it was then necessary to introduce an eigenvalue k_{OZAN} so that the initial value of the first element of the reactivity matrix vanishes. Thus k_{OZAN} is the eigenvalue of the reactor (at $t = 0$).

CHAPTER VI

A PROBLEM HANDLED BY THE PROPOSED METHOD

To compare the proposed synthesis method (use of two spatial modes in the expansion of the space and time dependent flux) with the point kinetics type of approach (use of only one spatial mode for the same expansion), we have considered the following problem:

The MITR-II operator looses control on the shim rods during the start up of the reactor. It is assumed that all six shim blades begin moving out at once rather than the usual operation of a single blade at a time. - It is worthwhile to mention that this is a very improbable accident, involving a simultaneous short circuit of six contacts. - That is the bank of shim rods starts from its shutdown position - correspoinding to a -0.12 of reactivity (we will further clarify what we mean by the word "reactivity") - going up with a constant insertion rate, 0.003 in reactivity per sec. (that notion of ramp insertion of reactivity will also be further clarified).

The bank continues going up until the reactor reaches the power level of 6 MW (assuming even further that the high rate-of-rise shut down system does not operate). Once the powermeter reads 6 MW, the shim rods receive automatically the order to scram. However there is a delay of

0.1 sec. due to the instrumentation. That is from 6 MW on the power level will continue to increase for 0.1 second more. The question is: What will be the maximum power level of the reactor during this incident?

6-1 Further Theoretical Preparations

There are a number of hidden difficulties, that we must overcome to be able to attack the problem by our proposed method. All of these difficulties, except one, are due to the fact that the reactor is subcritical at the beginning of the transient.

The first difficulty involves the fact that we need an external source to start up the reactor. Yet nowhere in the course of the development of the proposed method have we taken into account an external source.

6-1-1 Overcoming the Difficulty Due to the Presence of an External Source

Adding an external source term to the diffusion equation (3-1) and carrying out the calculations from there is impractical. Instead we found it easier to describe the source by the activity of a fictitious delayed neutron precursor that has a relatively long half life. The strength of this activity can be computed in the following way:

Consider the point kinetics equations with the familiar notation:

$$\frac{dN_{PK}(t)}{dt} = \frac{\rho_{PK}(t) - \beta_{PK}}{\Lambda_{PK}} N_{PK}(t) + \sum_{j=1}^{H} \lambda_j C_{PK_j}(t) + S_{PK} , \qquad (6\text{-}1)$$

$$\frac{dC_{PK_j}(t)}{dt} = \frac{\beta_{PK_j}}{\Lambda_{PK}} N_{PK}(t) - \lambda_j C_{PK_j}(t), \ (j = 1,\ldots, H), \qquad (6\text{-}2)$$

where the subscript PK stands for point kinetics, and everything is a scalar. At this stage the initial reactivity and the constant reactivity insertion we have pointed out above, should be understood merely as two quantities used to determine $\rho_{PK}(t)$ - in case of a ramp change. (We will later consider the way they are obtained.)

We take the time origin at the time the reactor becomes critical with the given motion of the rods (i.e., $-t_s$ = 40 sec. after the transient has started; the initial reactivity being -0.12 and the insertion rate 0.003 per sec.). In addition we assume the reactor is at 1 milliwatt power level at the beginning of the transient. That is, 5 MW being the power level of the critical reactor working under normal circumstances, at the start up the power level is,

$$N_{PK}\ (t_s) = \frac{1 \times 10^{-3}}{5 \times 10^{-6}} = 2 \times 10^{-10}\ , \tag{6-3}$$

times smaller than the normal power level (5 MW) of the reactor.

Thus assuming that the reactor is at a steady state with the external source in, prior to the change, we obtain from Eq. (6-2)

$$\frac{\beta_{PK_j}}{\Lambda_{PK}} N_{PK}(t_s) = \lambda_j\ C_{PK_j}(t_s),\ (j = 1, \ldots, H)\ . \tag{6-4}$$

Next with $\left.\frac{dN_{PK}(t)}{dt}\right|_{t_s} = 0,$ Equations (6-4) and (6-1) yield (for the source, S_{PK}, represented as a fictitious precursor concentration, $C_{PK_{(H+1)}}(t_s)$, decaying with a time constant, λ_{H+1})

$$S_{PK} \equiv \lambda_{H+1}\ C_{PK_{(H+1)}}(t_s) = \frac{-\rho_{PK}(t_s)}{\Lambda_{PK}} N_{PK}(\ t_s) \tag{6-5}$$

with

$$\beta_{PK_{(H+1)}} = 0 \tag{6-6}$$

We can pick λ_{H+1} as small as we want so that

$$C_{PK_{(H+1)}}(t) = C_{PK_{(H+1)}}(t_s)\, e^{\lambda_{H+1}(t-t_s)}, \qquad (6-7)$$

stays constant throughout the transient. Thus we choose arbitrarily $\lambda_{H+1} = 1 \times 10^{-13}$ sec.$^{-1}$.

Λ_{PK} is taken ($1. \times 10^{-4}$), - as it will be justified later - to be the first row, first column element of the generation time matrix [cf. Eq. (3-44)].

Hence we can compute $C_{PK_{(H+1)}}(t_s)$ (to be $\dfrac{0.12 \times 2 \times 10^{-10}}{1 \times 10^{-4} \times 1 \times 10^{-13}} = 2.4 \times 10^{6}$) and express S_{PK} in terms of the $(H+1)^{th}$ fictitious precursor concentration.

6-1-2 Selection of the First Spatial Mode

A second difficulty arises when we come to choose a spatial shape to describe the flux at the beginning of the transient. The period of time while the reactor is still subcritical - during the transient - is not of interest. Also the computations may be unnecessarily time consuming if we took a look at the transient with the two-shape method starting subcritical. Thus we choose as the first trial mode the flux shape of the critical reactor, and start studying the transient with the two-shape method at the time when the reactor becomes - momentarily - critical under the given accident. That, however, brings up a major difficulty:

Since the reactor is not at a steady state when it becomes critical, how do we compute the precursor concentrations at time t = 0 ($-t_s$ seconds after the transient took off)? This is answered in the next two sections.

6-1-3 Calculation of the Initial Value of the First Precursor Amplitude Function

We need to compute $C_j(0)$'s, j = 1,..., (H+1), of Eq. (3-45). $C_j(t)$ is a column matrix having two elements in the case of two trial modes. The calculation of the first element will be done in this section whereas we save the calculation of the second element for the next section.

Over the period of time $t_s \leq t \leq 0$, only one trial mode (the flux shape of the critical reactor) is used to describe the flux. Then at t = 0 we can write

$$C_{j_1}(0) = \Lambda_{PK}\, C_{PK_j}(0), \; [j = 1,\ldots, (H+1)], \quad (6\text{-}8)$$

where $C_j(t)$ is the solution of Eq. (3-45), C_{PK_j} the solution of Eq. (6-2), and the subscript 1 stands for the first element of the column matrix $C_j(0)$.

Thus with Equations (6-3), (6-5), (6-6), (6-8) and $\rho_{PK}(t) = -0.12 + 3 \times 10^{-3}(t-t_s)$, $\Lambda_{PK}(\equiv \Lambda_{11}) \simeq 1. \times 10^{-4}$, the Equations (6-1) and (6-2) will furnish $C_{j_1}(0)$'s. For the purpose of the calculation we have run a points kinetics computer code [18] to find $N_{PK}(0) \equiv N_1(0)$, the factor that multiplies the power level when the reactor becomes - momentarily - critical under the given accident.

We emphasize that while writing the Equation (6-8), we have tacitly assumed that the reactivity $\rho_{PK}(t)$ is the same as $\rho_{new_{11}}(t)$ of Eq. (3-44) for $t_s \leq t \leq 0$. That is, for instance, if we computed the reactivity corresponding to "bank of shim rods completely inserted", through Equations (3-41) and (3-29) we assume we would find -0.12 (the number taken above as the negative reactivity of the shutdown reactor). However this is not necessarily true for that reactivity may be determined through other procedures (weighting by unity instead of a weighting function, taking the relative difference of the eigenvalues of the reactor at the shutdown and critical positions - thus abandoning the perturbation type of calculation where the flux shape of the critical reactor is used alone -, etc.).

Now we turn our attention to the second element of the column matrix $C_j(0)$.

6-1-4 Calculation of the Initial Value of the Second Precursor Amplitude Function

To compute $C_{j_2}(0)$, $j = 1,\ldots,(H+1)$, we recall through Equations (3-42), (3-43), (3-31) and (3-34)

$$C_{j_i}(t) \equiv D_{j_i} = 2\pi \int_{r,\text{core}} r\,dr \int_{z,\text{core}} dz \quad W_i^T(r,z)\ \chi_j\ \eta_j\ (r,z,t),$$

$$(i = 1,\ 2),\ (j = 1,\ldots,J), \qquad (6\text{-}9)$$

$$C_{j_i}(t) \equiv \Theta_{j_i}(t) = 2\pi \int_{r,\text{reflector}} r\,dr \int_{z,\text{reflector}} dz \quad W_i^T(r,z)$$

$$\theta_j(r,z,t),\ (i = 1,2),\ [j = (J+1),\ldots,H], \qquad (6\text{-}10)$$

$$C_{(H+1)_i}(t) = s\ 2\pi \int_{r,\text{reactor}} r\,dr \int_{z,\text{reactor}} dz \quad W_i^T(r,z)\ \chi,\ (i = 1,2), \qquad (6\text{-}11)$$

where s is the constant source spread out uniformly throughout the reactor such that

$$\lambda_{H+1} \frac{C_{(H+1)}}{\Lambda_{11}} (t_s) = S_{PK}\ , \qquad (6\text{-}12)$$

first mentioned in Eq. (6-1), and χ is defined through Eq. (4-3).

The initial conditions for the undetermined time coefficients being $N(t) = \begin{pmatrix} 2 \times 10^{-10} \\ 0 \end{pmatrix}$, we find it legitimate to assume;

- At times very close to t = 0 (t > 0), the second shape contributes practically nothing, and, with one shape and one undetermined time coefficient, it is appropriate to write

$$\eta_j\,(r,z,t) = M_j(r,z)\ e^{\omega t},\ (j = 1,\ldots,\ J)\ ,\qquad (6\text{-}13)$$

and

$$\theta_j\,(r,z,t) = T_j(r,z)\ e^{\omega t},\ [j = (J+1),\ldots,\ H], \qquad (6\text{-}14)$$

- ω at times close to t = 0 can be considered independent of t.

Then one can through Equations (3-45), (6-9), (6-10), (6-13) and (6-14), arrive at

$$C_{j_i}(t) = C_{j_i}(0)\ e^{\omega t},\ (i = 1,2),\ (j = 1,\ldots,\ H), \qquad (6\text{-}15)$$

where

$$C_{j_i}(0) = 2\pi \int_{r,core} r\ dr \int_{z,core} dz\ \ W_i^T(r,z)\ \chi_j\ M_j\ (r,z),$$
$$(i = 1,2),\ (j = 1,\ldots,\ J), \qquad (6\text{-}16)$$

$$C_{j_i}(0) = 2\pi \int_{r,\text{reflector}} r\,dr \int_{z,\text{reflector}} dz \quad W_i^T(r,z)\ x$$

$$T_j(r,z),\ (i = 1,2),\ [j = (J+1),\ldots, H], \tag{6-17}$$

and

$$(\omega + \lambda_j)\ C_{j_i}(t) = \left(\overline{\beta}_{j_{new}}(t)\ N(t)\right)_i, (i = 1,2),$$

$$(j = 1,\ldots, H), \tag{6-18}$$

where $C_{j_i}(t)$, $(i = 1,2)$ and $\overline{\beta}_{j_{new}}(t)$'s, $(i = 1,2)$, were defined in Chapter III.

Thus taking the ratio of the equation obtained with $i = 1$, in Eq. (6-18), to the equation obtained with $i = 2$, in Eq. (6-18), we finally have, near time $t = 0$

$$\frac{C_{j_1}(t)}{C_{j_2}(t)} = \frac{\overline{\beta}_{j_{new_{11}}}(t)}{\overline{\beta}_{j_{new_{21}}}(t)},\ (j = 1,\ldots, H). \tag{6-19}$$

Knowing $C_{j_1}(0)$, $(j = 1,\ldots, H)$, we then can compute from Eq. (6-19)

$$C_{j_2}(0) = C_{j_1}(0)\,\frac{\overline{\beta}_{j_{new_{21}}}(0)}{\overline{\beta}_{j_{new_{11}}}(0)}\,. \qquad (6\text{-}20)$$

The calculation of $C_{(H+1)_2}(0)$ is straightforward from Eq. (6-11). Taking $\chi = \begin{pmatrix}1\\0\\0\end{pmatrix}$, we have

$$C_{(H+1)_2}(0) = C_{(H+1)_1}(0)\,\frac{2\pi \int_{r,reactor} r\,dr \int_{z,reactor} dz \quad W_{12}(r,z)}{2\pi \int_{r,reactor} dr \int_{z,reactor} dz \quad W_{11}(r,z)}\,. \qquad (6\text{-}21)$$

6-1-5 Determination of the Position of the Bank of Shim Rods at the Time the Signal for Scram is Received

The last difficulty to overcome is how to determine the position of the bank of shim rods at the time the signal for scram is received. We must estimate this position in order to choose the second trial mode for the expansion of the flux (poison search, cf. Chapter IV, section 4-2).

This last question is resolved by using the point kinetics approach. A point kinetics code [18] is applied in order to determine the time at which $N_{PK}(t)$ [cf. Eqs. (6-1) and (6-2)] is 1.2, that is the time at which the power level reaches a 6 MW (5 x 1.2) level. We then add 0.1 second to find the time, T, at which the bank of shim rod will scram. To determine the bank position at that time T, we write

$$\rho_{PK}(T) = \rho_{PK}(0) + \rho_{1_{PK}} T \quad , \qquad (6\text{-}22)$$

with $\rho_{PK}(0) = 0.$ and $\rho_{1_{PK}} = 3 \times 10^{-3}$ [The terms in Eq. (6-22) are equal to the corresponding first row, first column elements of the matrix equation (5-52).], Now we consider Fig. 6-1 [19] where for MITR-II the reactivity versus the position of the shim rods bank is shown. Knowing $\rho_{PK}(T)$ permits us to use this figure to determine the approximate position of the shim bank at time T. (One should however keep in mind that, the reactivity appearing in Fig. 6-1 does not exactly correspond to that defined previously. The reactivity of Fig. 6-1 was calculated by computing the eigenvalue of the reactor with the bank of shim rods at different positions; then taking the relative difference $\Delta k/k$ for that position.)

The ramp change slope of the reactivity matrix, ρ_1 [cf. Eq. (5-52)], can be calculated by computing first

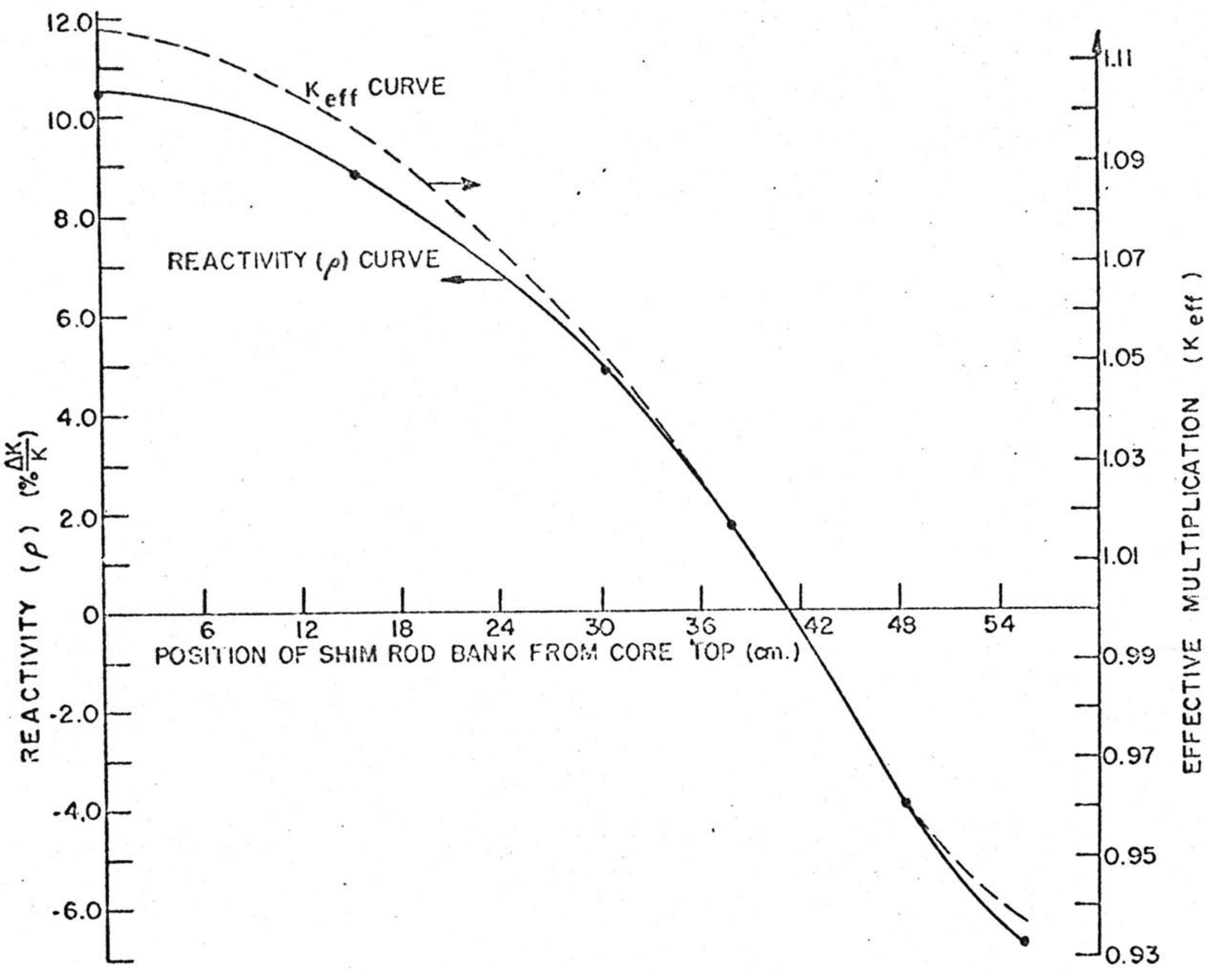

Fig. 6-1 The Bank of Shim Rods Worth Curve for MITR-II [19]

$\rho_{new}(0)$, the reactivity matrix at time t = 0 (the time the reactor becomes momentarily critical and we begin studying the transient with the two-trial mode method); next by determining the reactivity matrix at time T, through the integral expression for reactivity formulated in Chapter III, and finally by writing

$$\rho_1 = \frac{\rho_{new}(T) - \rho_{new}(0)}{T} . \qquad (6\text{-}23)$$

We note that within our scheme of attacking the transient if only one trial mode is chosen to describe the spatial shape of the flux we will use for the ramp change slope of the reactivity, the first row, first column element of the matrix ρ_1 [cf. Eq. (6-23)]. That will not necessarily equal $\rho_{1_{PK}}$ (3×10^{-3}) of Eq. (6-22) because of the difference in the definitions of our reactivity and the reactivity of Fig. 6-1.

*

Now that we have overcome the difficulties encountered because of the special nature of the problem, we can proceed with it by our proposed method. The code OZAN (cf. Appendices N and O) has been created to perform the computations required by the present work. It has been used along with the code Exterminator-II [5] and the point kinetics code [18]. The relevant results are presented in the next section.

*

6-2 Results

The point kinetics code [18] is run first to furnish the precursor concentrations [hence through Eq. (6-8), the first element of the column matrix $C_j(0)$, $j = 1,\ldots,(H+1)$] and the time T at which the bank of shim rods receive the signal to scram. (The transient will be studied by the two-trial mode method throughout the period of time $0 \leq t \leq T$.) The relevant input and output are presented below.

6-2-1 Input to the Point Kinetics Code [18]

Table 6-1-1 Input (1) to the Point Kinetics Code [18]

Generation time: Λ_{PK}	1.2980×10^{-4} sec.
Initial Reactivity: $\rho_{PK}(t_s)$	-0.12
Ramp change slope of Reactivity: $\frac{d\rho_{PK}(t)}{dt}$	3×10^{-3} sec.$^{-1}$

Table 6-1-2 Input (2) to the Point Kinetics Code [18]

Delayed Photoneutron Group: j	β_{PK_j}	λ_j (sec^{-1})
1	3.010 E-4	1.27 E-2
2	1.709 E-3	3.17 E-2
3	1.529 E-3	0.115
4	3.082 E-3	0.311
5	8.980 E-4	1.40
6	3.280 E-4	3.87
7	3.255 E-5	0.277
8	1.020 E-5	1.69 E-2
9	3.500 E-6	4.81 E-3
10	1.680 E-6	1.50 E-3
11	1.035 E-6	4.28 E-4
12	1.170 E-6	1.17 E-4
13	1.615 E-7	4.37 E-5
14	5.15 E-8	3.63 E-6
15	0.	1. E-13

y E-n stands for: $y \times 10^{-n}$

6-2-2 Comments on the Input to the Point Kinetics Code, Correction Factor for the Delayed Neutron Fractions

In Table 6-1-1 Λ_{PK} appears to be 1.298×10^{-4} (rather than 1.0107×10^{-4} as computed by OZAN for the first row, first column element of the matrix Λ). The reason is that Λ_{PK} was obtained by a previous run where, as the weighting function, the flux, instead of the adjoint flux, was used. For the same reason the delayed photoneutron fractions shown in Table 6-1-2 ($j = 7, \ldots, 14$) differ from those given subsequently in this chapter. These differences are not very important since the run with the point kinetics code was made only to estimate the quantities - $C_{PK_j}(0)$'s, $N(0)$, and T - and not to determine them precisely. In addition, because of the nature of the transient, the delayed neutrons (chiefly the delayed photoneutrons) are not very significant. Thus, the fact that the numbers for the delayed photoneutron fractions, shown in Table 6-1-2, differ from the ones presented subsequently (obtained by using the adjoint flux as the weighting function), is even more tolerable.

α (the correction factor introduced in Chapter III for overcoming the error due to approximations made in calculating the photoneutron source term - see Chapter II) was taken equal to 10 (approximately).

Correction Factor for the Delayed Neutron Fractions

The delayed neutron fractions shown in Table 6-1-2 (j = 1,..., 6) are not exactly the ones given by the nuclear data [20]. The reason for that is as follows: At emission, the energy of a delayed neutron is generally less than the energy of a prompt neutron. Therefore during the thermalization, a delayed neutron has less chance to leak out of the reactor, than a prompt neutron. That is, in causing fission, a delayed neutron is more effective than a prompt neutron. However, in the three-group scheme that we have adopted, both delayed and prompt neutrons are born in the same - fast - group. The fact that the delayed neutrons are worth more is, then, not taken into account automatically.

An adequate way to correct for this condition would be to multiply the β_j by the factor

$$\frac{\int_{\underline{r},\mathrm{core}} d\underline{r}\ \psi_1^*(\underline{r})\ \Sigma_F^T(\underline{r},o)\ \chi_j\ \psi_1(\underline{r})}{\int_{\underline{r},\mathrm{core}} d\underline{r}\ \psi_1^*(\underline{r})\ \Sigma_F^T(\underline{r},o)\ \chi_p\ \psi_1(\underline{r})}\ , \quad (j = 1,\ldots, 6), \qquad (6\text{-}24)$$

where a multigroup scheme is considered so that $\chi_j \neq \chi_p$. (In expression (6-24) the familiar notation is being used; i.e., the subscript 1 refers to the steady state of the reactor).

This method of computing the correction factor for the delayed neutrons was not undertaken because applying it for a fifteen-group scheme would be very expensive. Also on a theoretical ground we had reason to believe that one could estimate the correction factor by applying a neutron balance argument to the already available fifteen-group Exterminator-II output for MITR-II.

Therefore, rather than choosing the expensive, straightforward way of solving the problem, we developed a method (described briefly in Appendix K) based on the multigroup output of Exterminator-II obtained for MITR-II. The computer code embodying this method is shown in Appendix L. (It is worthwhile to mention that this code worked for less than a fiftieth of the cost estimated for the more exact calculation.)

Unfortuantely a serious difficulty was encountered: When the eigenvalue of the reactor was recomputed through the numbers obtained by the proposed method, a discrepancy (of about 8%) was found as compared to the eigenvalue given by the original output of Exterminator-II.

This is thought to be due to the fact that the convergence of the flux in the output was rather poor (relative convergence of the flux = 4.48×10^{-1}). As a result, the neutron current across interfaces was not continuous. Indeed when we computed the total leakage out of the core by means of the numbers (given in the fifteen-group output of Exterminator-II) relevant to the core and by means of the numbers relevant to the regions outside of the core we found a difference of about 10%. This fact increases confidence in our method and code, but does not change our doubts about the result;

$$CF_j = 1.2467, \; j = 1, \ldots, 5 \; ,$$

$$CF_6 = 1.4312 \; , \qquad (6\text{-}25)$$

where CF stands for correction factor (CF_6 is greater than CF_j, $j = 1, \ldots, 5$, since the 6^{th} group delayed neutrons, at the emission, are less energetic than the delayed neutrons of other groups).

With some account taken of Eq. (6-25) and in view of estimates appearing in reference [21], CF_j, ($j = 1, \ldots, 5$), was chosen to be 1.20 and accordingly CF_6, 1.38.

6-2-3 Output from the Point Kinetics Code

$N_{PK}(0)$ was found to be 4.242331×10^{-9}, and corresponging $C_{PK_j}(0)$'s are shown in Table 6-2. The behavior of the power level beyond 6 MW is sketched in Fig. 6-2. The time T, when the shim rods receive the signal to scram, is seen to be 3.77 sec. At the end of this time the point kinetics code predicts a power level of 81.80 MW.

6-2-4 The Accident Analyzed

Further Preparations for the Code OZAN;

Knowing T we compute $\rho_{PK}(T) = 1.131 \times 10^{-2}$ through Eq. (6-22). Applying the procedure discussed in section 6-1-5 above, we found from Fig. 6-1 that at time t=T the rods would be about an inch higher from their initial postion. Accordingly a poison search was made through Exterminator-II. The value ω [cf. Eq. (4-18)] was found to be 17.262131 (the eigenvalue of the reactor was required to converge to $\frac{1}{1-\beta} = 1.007896$ and turned out to be - after 90 iterations - 1.0078964). Thus the absorption cross sections throughout the reactor were increased by ωV^{-1} (the average values shown in Table 6-3 were used for V^{-1}) and a second shape and its adjoint were computed.

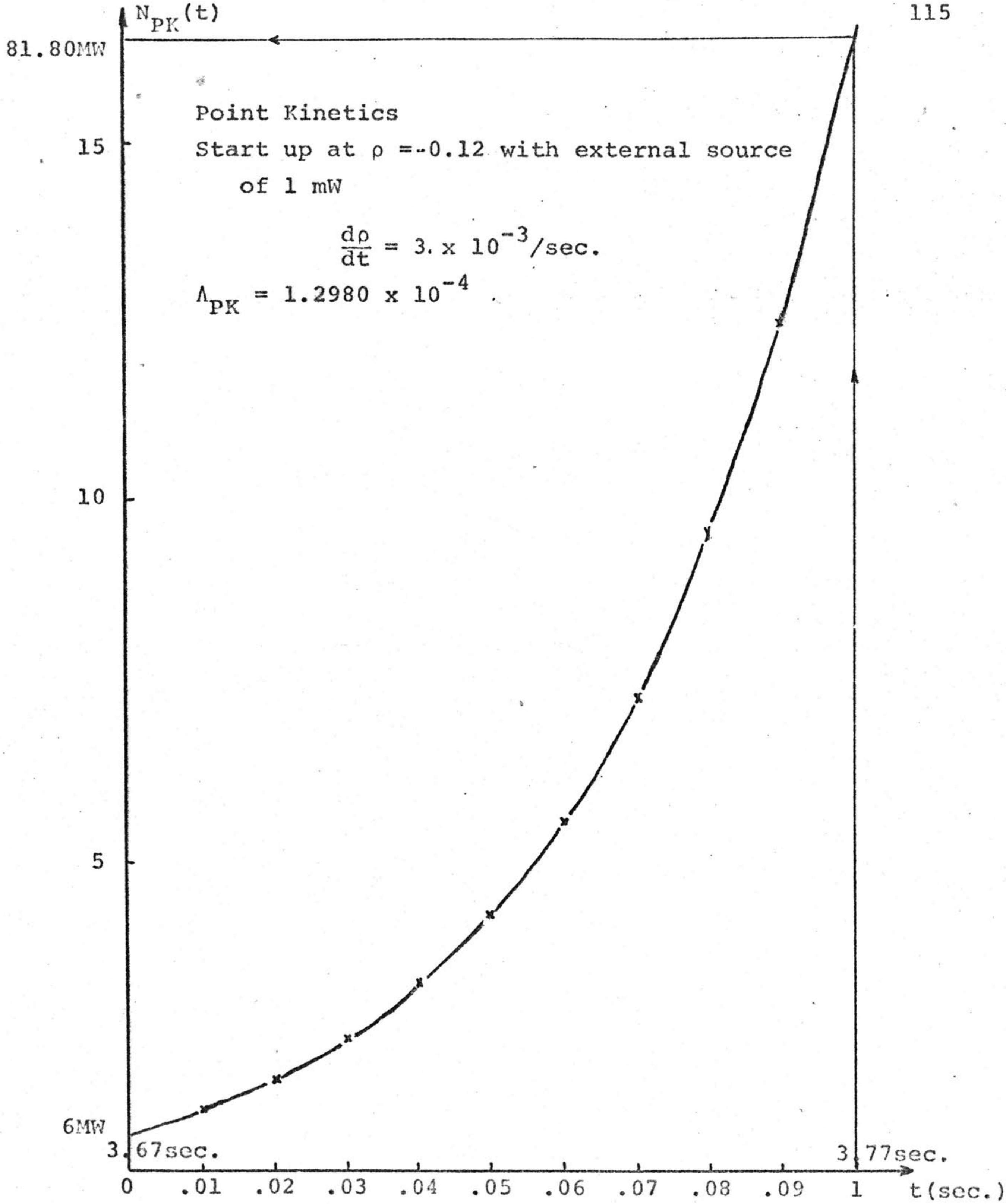

Fig. 6-2 Behavior of the Power Level Beyond 6MW under the Fictitious Accident in Question

Table 6-2 The Precursor Concentrations at Time t = 0 Under the Accident in Question, as Computed by the Point Kinetics Code

j	$C_{PK_j}(0)$
1	0.78880 E-7
2	0.29879 E-6
3	0.15651 E-6
4	0.18583 E-6
5	0.18175 E-7
6	0.26554 E-8
7	0.21027 E-8
8	0.23295 E-8
9	0.16389 E-8
10	0.19797 E-8
11	0.38836 E-8
12	0.15587 E-7
13	0.57189 E-8
14	0.21868 E-7
15	0.18490 E+7

y E n stands for y 10^n

The output from the point kinetics code will be a portion of the input to OZAN.

The value for V_g $(g = 1 \text{ to } 3)$;

An average for V_g was computed through

$$V_g^{-1} = \frac{\int_{\underline{r},\text{reactor}} d\underline{r} \int_{E_g}^{E_{g-1}} dE\, \phi\, (\underline{r}, E, o)\, V^{-1}\, (E)}{\int_{\underline{r},\text{reactor}} d\underline{r} \int_{E_g}^{E_{g-1}} dE\, \phi\, (\underline{r}, E, o)} \cdot \qquad (6\text{-}26)$$

For the purpose of the calculation the fifteen-group output of Exterminator-II for MITR-II was used with V(E)'s (for fifteen-group scheme) taken from reference [22]. We thus computed

$$V_g^{-1} = \frac{\sum_m^M \sum_{h=h_{g-1}}^{h_g} \phi_{mh}(0)\, V_h^{-1}}{\sum_m^M \sum_{h=h_{g-1}}^{h_g} \phi_{mh}(0)}, \qquad (6\text{-}27)$$

where M is the number of compositions, $\phi_{mh}(0)$ is the flux given in the output in question, for the h^{th} group and in the m^{th} material, V_h is the h^{th} group velocity as given in reference [22] and h_{g-1} and h_g are respectively the initial and final groups in the fifteen-group scheme that are framing the g^{th} group of the three-group scheme.

The computer code that was written in order to perform the computation for Eq. (6-27) is presented in Appendix M. The results are shown in Table 6-3.

Table 6-3 Average Group Velocities for MITR-II

g	V^{-1}(sec/cm)	V(cm/sec)
1	1.9903×10^{-9}	5.0244×10^{8}
2	2.3170×10^{-7}	4.3159×10^{6}
3	4.5454×10^{-6}	2.200×10^{5}

Further input data to OZAN;

In addition to data already discussed, it is necessary to input to OZAN, the mesh-volume dimensions, various cross sections at the beginning and the end of the transient, the delayed neutron fractions, etc. A complete set up of the input is discussed in Appendix N and shown in Appendix O.

6-2-5 Output from OZAN(NMODES* = 2)

The output relevant to the final step before the solution of the time dependent equations is as follows;

The generation time matrix:

$$\Lambda = \begin{pmatrix} 0.10107\ E{-3} & 0.97859\ E{-4} \\ 0.98072\ E{-4} & 0.95077\ E{-4} \end{pmatrix} \quad ; \qquad (6\text{-}28)$$

The reactivity matrix at t = 0:

$$\rho_{new}(0) = \begin{pmatrix} -0.40165523\ E{-5} & 0.14627143\ E{-2} \\ 0.19336105\ E{-4} & -0.52609537\ E{-1} \end{pmatrix} \quad ; \qquad (6\text{-}29)$$

The ramp change slope of the reactivity matrix:

$$\rho_1 = \begin{pmatrix} 0.20038732\ E{-2} & 0.22407090\ E{-2} \\ 0.15396409\ E{-1} & 0.16423021\ E{-1} \end{pmatrix} \quad ; \qquad (6\text{-}30)$$

The delayed neutron (and photoneutron) fraction matrices;

$$\overset{1}{\begin{pmatrix} 0.30100\ E{-3} & 0.29948\ E{-3} \\ 0.28180\ E{-3} & 0.28045\ E{-3} \end{pmatrix}} \;,\; \overset{2}{\begin{pmatrix} 0.17090\ E{-2} & 0.17003\ E{-2} \\ 0.16000\ E{-2} & 0.15923\ E{-2} \end{pmatrix}}$$

---

* NMODES: the number of trial modes used in expanding the flux.

$$\overset{3}{\begin{pmatrix} 0.15290\ \text{E-2} & 0.15213\ \text{E-2} \\ 0.14315\ \text{E-2} & 0.14246\ \text{E-2} \end{pmatrix}}, \quad \overset{4}{\begin{pmatrix} 0.30820\ \text{E-2} & 0.30664\ \text{E-2} \\ 0.28855\ \text{E-2} & 0.28716\ \text{E-2} \end{pmatrix}}$$

$$\overset{5}{\begin{pmatrix} 0.89800\ \text{E-3} & 0.89345\ \text{E-3} \\ 0.84073\ \text{E-3} & 0.83669\ \text{E-3} \end{pmatrix}}, \quad \overset{6}{\begin{pmatrix} 0.32800\ \text{E-3} & 0.32634\ \text{E-3} \\ 0.30708\ \text{E-3} & 0.30561\ \text{E-3} \end{pmatrix}}$$

$$\overset{7}{\begin{pmatrix} 0.11281\ \text{E-3} & 0.11271\ \text{E-3} \\ 0.11012\ \text{E-3} & 0.11003\ \text{E-3} \end{pmatrix}}, \quad \overset{8}{\begin{pmatrix} 0.35308\ \text{E-4} & 0.35278\ \text{E-4} \\ 0.34467\ \text{E-4} & 0.34438\ \text{E-4} \end{pmatrix}}$$

$$\overset{9}{\begin{pmatrix} 0.12153\ \text{E-4} & 0.12142\ \text{E-4} \\ 0.11863\ \text{E-4} & 0.11853\ \text{E-4} \end{pmatrix}}, \quad \overset{10}{\begin{pmatrix} 0.58236\ \text{E-5} & 0.58186\ \text{E-5} \\ 0.56849\ \text{E-5} & 0.56801\ \text{E-5} \end{pmatrix}}$$

$$\overset{11}{\begin{pmatrix} 0.35744\ \text{E-5} & 0.35713\ \text{E-5} \\ 0.34893\ \text{E-5} & 0.34863\ \text{E-5} \end{pmatrix}}, \quad \overset{12}{\begin{pmatrix} 0.40277\ \text{E-5} & 0.40243\ \text{E-5} \\ 0.39318\ \text{E-5} & 0.39284\ \text{E-5} \end{pmatrix}}$$

$$\overset{13}{\begin{pmatrix} 0.55621\ \text{E-6} & 0.55573\ \text{E-6} \\ 0.54296\ \text{E-6} & 0.54250\ \text{E-6} \end{pmatrix}}, \quad \overset{14}{\begin{pmatrix} 0.17575\ \text{E-6} & 0.17560\ \text{E-6} \\ 0.17157\ \text{E-6} & 0.17142\ \text{E-6} \end{pmatrix}}$$

$$\overset{15}{\begin{pmatrix} 0.0 & 0.0 \\ 0.0 & 0.0 \end{pmatrix}} , \qquad (6\text{-}31)$$

where for the delayed photoneutron fractions, a correction factor $\alpha = 10$ is used and the 15^{th} matrix elements are set to zero since the fictitious 15^{th} group delayed precursor amplitude functions are used merely to represent the external source.

Note that the first row, first column element of the matrix ρ_1 is different than 3×10^{-3} - initially input to the point kinetics code as the ramp change slope of the reactivity - because of the difference between the definition of reactivity of Fig. 6-1 and the one adopted throughout the present dissertation (cf. Chapter III).

To attack the time dependent equations, we finally have to add to Equations (6-28) up to (6-31) the $N_{PK}(0)$ and $C_j(0)$'s computed through the point kinetics code and the manipulations described in the previous sections. It was mentioned (cf. section 6-2-2) that we did not use the best values for, Λ_{PK} and $\beta_{j_{PK}}$'s in determining $N_{PK}(0)$ and the $C_{PK_j}(0)$'s earlier. For the present run (OZAN, NMODES = 2) we had a chance to recompute the initial

Table (6-4) Initial Precursor Amplitude Functions

j	$C_{j_1}(0)$	$C_{j_2}(0)$
1	0.1010 E-10	0.94559 E-11
2	0.38500 E-10	0.36045 E-10
3	0.20100 E-10	0.18818 E-10
4	0.23900 E-10	0.22376 E-10
5	0.27000 E-11	0.25278 E-11
6	0.42100 E-12	0.39415 E-12
7	0.98000 E-12	0.95666 E-12
8	0.10900 E-11	0.10640 E-11
9	0.77400 E-12	0.75557 E-12
10	0.93600 E-12	0.91371 E-12
11	0.18300 E-11	0.17864 E-11
12	0.73200 E-11	0.71457 E-11
13	0.26900 E-11	0.26259 E-11
14	0.10200 E-10	0.99571 E-11
15	0.23600 E+03	0.22763 E+03

y E n stands for $y \times 10^n$

values $N_{PK}(0)$ and C_{PK_j}'s through the point kinetics code, using this time, Λ_{11} (for Λ_{PK}), and $\beta_{j_{new}}(0)$'s (for β_{PK_j}'s) obtained from a previous OZAN run. Λ_{PK} as a result became 1.0149×10^{-4} and β_{PK} ($= \sum_{j=1}^{15} \beta_{PK_j}$), 8.03316 $\times 10^{-3}$ (instead of 7.89737×10^{-3} used for the previous point kinetics run).

The corresponding $N_{PK}(0)$ is 4.149860×10^{-3} and the final $C_{j_1}(0)$ [cf. Eq. (6-8), with H = 14] is presented along with $C_{j_2}(0)$ [cf. Equations (6-20) and (6-21)] in Table (6-4).

$C_{1_1}(0)$ computed from $C_{PK_1}(0)$ of Table 6-2 becomes for instance, 0.78880 E-7 x 1.298 E-4 ≃ 0.1020 E-10. The difference between that number and the one given for $C_{1_1}(0)$ in Table 6-4 (0.1010 E-10) is 1%. The difference between $N_{PK}(0)$ just computed and $N_{PK}(0)$ computed through the previous run is also about the same. Thus these differences are not very significant, as it was anticipated in section 6-2-2.

*

The solution of the time dependent equations is presented in Table (6-5).

Table 6-5 The Two Time Coefficients With Respect to the Time

t(sec.)	$N_1(t)$	$N_2(t)$
0	0.41499 E-08	0.
1	0.61103 E-08	0.20874 E-08
2	0.99747 E-08	0.10478 E-08
3	0.61673 E-07	0.22693 E-06
4	-0.54800 E-01	0.92655 E 00
5	-0.12375 E+19	0.47876 E+19

We note that while at the beginning of the transient $N_1(t)$ is dominant and $N_2(t)$ is small (one can show that for the initial conditions imposed $\left.\frac{dN_2(t)}{dt}\right|_{t=0} = 0$), as the rods get closer to the position 2.54 cm higher than their initial level, the second shape gradually takes over.

As will be explained in the next chapter, one can obtain an equivalent time function $N_{eq}(t)$ out of $N_1(t)$ and $N_2(t)$ with appropriate manipulations. Thus the power level follows $N_{eq}(t) = N_1(t) + \frac{\Lambda_{12}}{\Lambda_{11}} N_2(t)$.

$N_{eq}(t)$ for the present run is shown in Fig. 6-3.

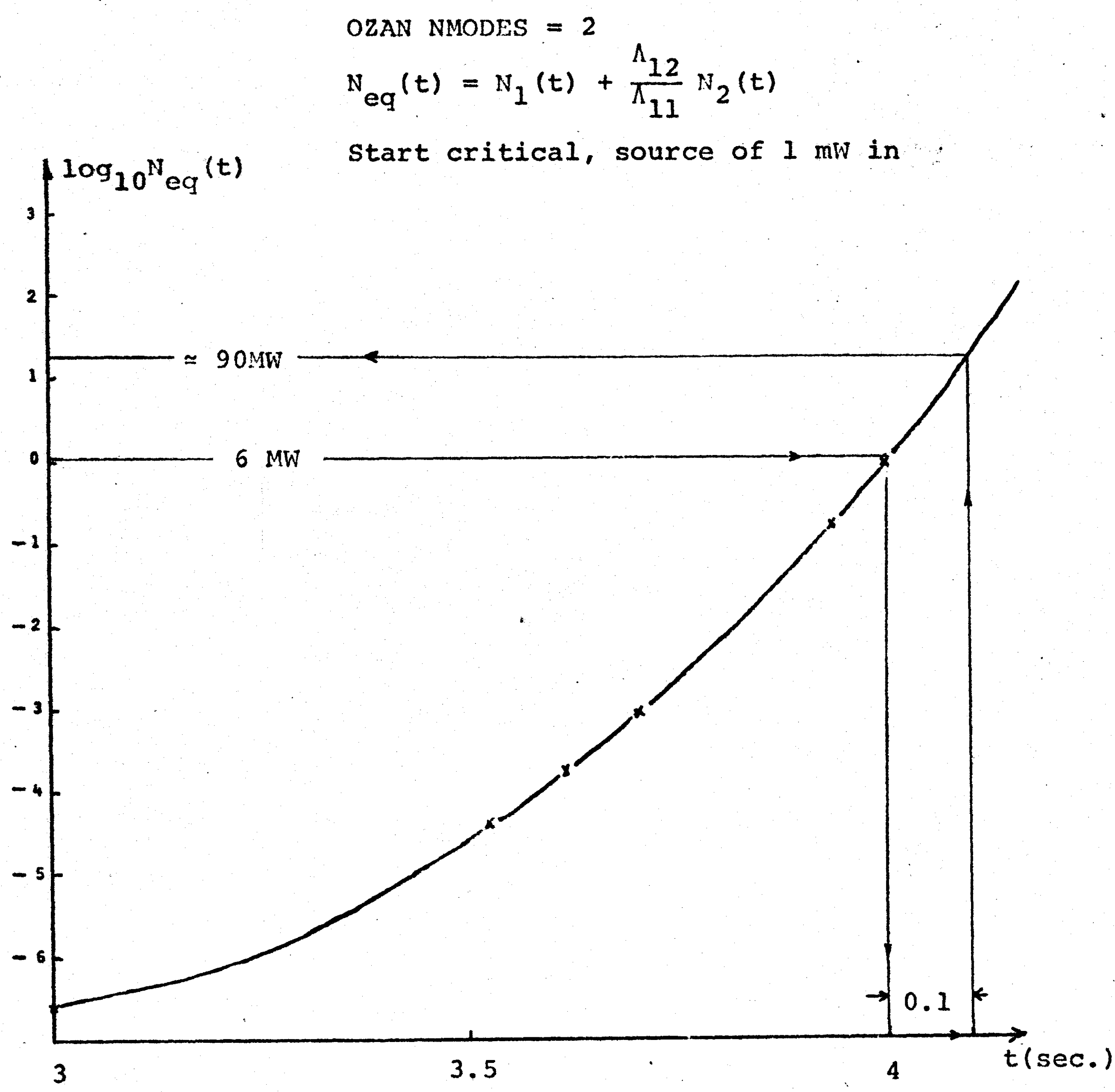

Fig. 6-3 Behavior of $N_{eq}(t)$ under the Accident in Question, Studied by the Proposed Method

In this figure we see that 6 MW level is reached at around 4 sec., and 0.1 second later the power level reaches about 90 MW.

We note that around t = T, the inverse period, ω, of the reactor is about the one predicted by the poison search made for the second trial mode $(\omega = \frac{1}{N_{eq}} \frac{dN_{eq}}{dt} \simeq 17.2$ around 3.7 sec.).

The derivation of an equivalent scalar reactivity and generation time and their variation with respect to the time, is presented in the next chapter.

6-2-6 Output from OZAN (NMODES = 1)

The same study is repeated with however only one trial function. Thus the problem is reduced to a point kinetics case. Then the solution $N_1(t)$ is searched with $\Lambda_{PK} = \Lambda_{11}$, $\rho_{PK}(0) = \rho_{new_{11}}(0)$, $\rho_{1_{PK}} = \rho_{1_{11}}$, and $\beta_{PK_j} = \overline{\beta}_{j_{new_{11}}}(0)$, [j = 1,..., (H+1)], defined through respectively equations (6-28), (6-29), (6-30) and (6-31).

The behavior of $N_1(t)$ is shown in Fig. (6-4), where we see that 6 MW level is reached at around 5.06 sec. 0.1 sec. more from there on brings the reactor onto about 60 MW power level.

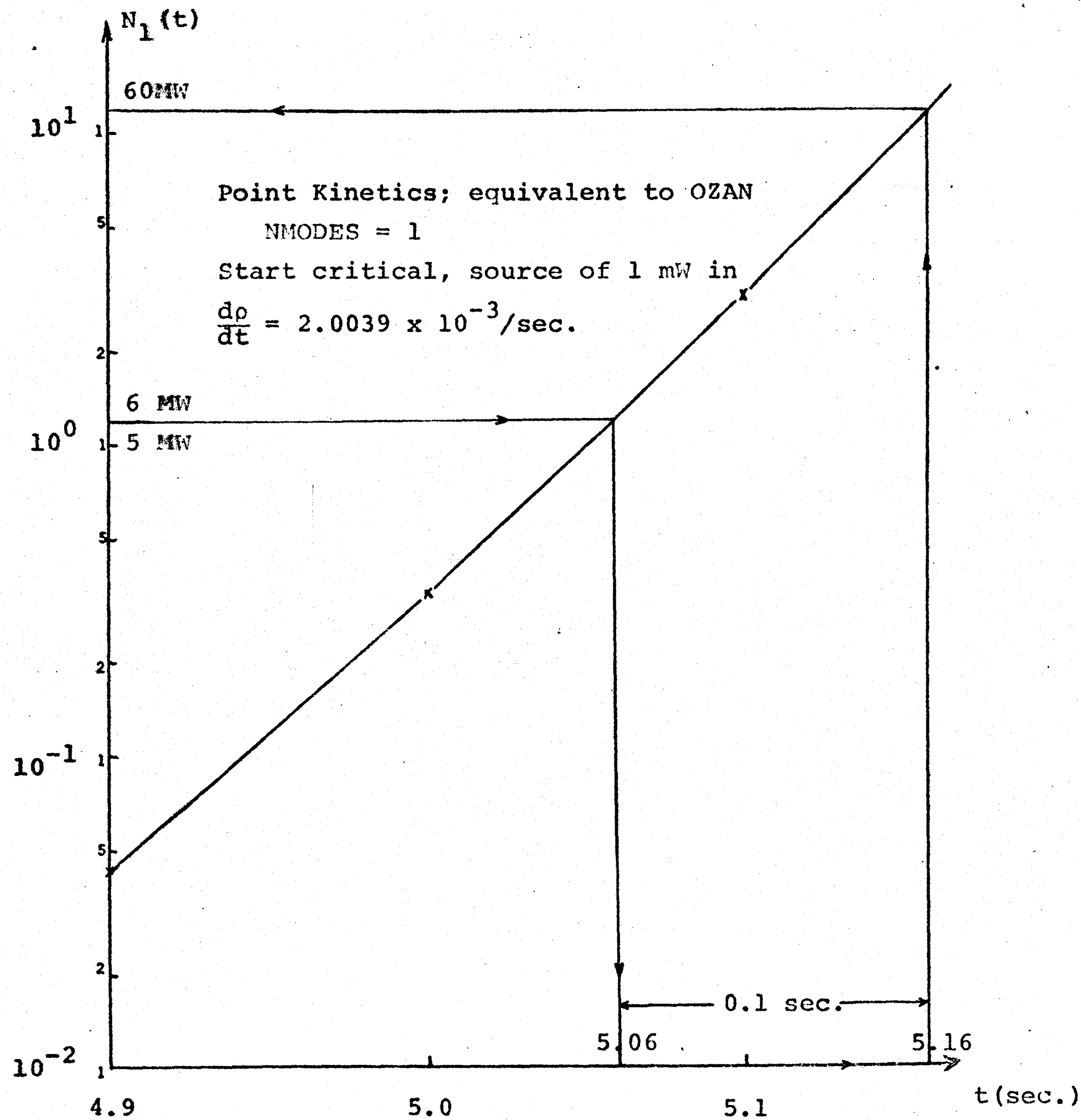

Fig. 6-4 OZAN Studying the Accident in Question with one Trial Mode Only

We note that (although $\omega \approx 23$ around 5.1 sec. in the last case) $N_1(t)$ of Fig. (6-4) is much slower than $N_{eq}(t)$ of Fig. (6-3). A comparison of these two quantities with respect to the time is shown in Table 6-6.

Table 6-6 Behavior of the Power Level Predicted by OZAN-NMODES = 2-and -NMODES = 1-

t(sec.)	$N_{eq}(t)$ (NMODES=2)	$N_1(t)$ (NMODES=1)
1	0.813 E-08	0.742 E-08
2	0.201 E-07	0.140 E-07
3	0.282 E-06	0.438 E-07
4	0.850	0.991 E-06
5	0.340 E+19	0.332

We emphasize that in both studies (cf. Table 6-6) everything was the same except for the number of trial modes used in the expansion of the flux.

In the next chapter we shall discuss in detail the validity of the numbers shown in Table 6-6. If these results are correct, there is certainly a large difference between the two predictions shown in Table 6-6.

6-3 Summary

In this chapter we aimed to study a fictitious accident with the proposed method and compare the results (NMODES = 2) with those obtained through a point kinetics approach (NMODES = 1). We also wanted to answer the question: For the given accident, how far beyond 6 MW does the power level continue to climb in 0.1 more sec.?

The problem was of a special nature [startup subcritical and requiring that we have an estimate of the answer(position of the rods when they receive the signal to scram) before beginning space-dependent analysis].

We decided to use a single critical shape until the rods were at a critical position and then use the two-shape method for the rest of the transient.

We then required more theoretical preparations. An external source was expressed in terms of an extra delayed neutron precursor concentration. The initial values (at t = 0) for the first precursor amplitude functions and the first time coefficient, as well as the duration of the transient (T) - input to OZAN - were estimated through a point kinetics code. The initial values for the second precursor amplitude functions were found in a consistent way [Equations (6-20) and (6-21)].

The position of the rods at t = T was then determined. Then a poison search was made and the second shape and its adjoint were computed.

Finally a study of the problem with OZAN (NMODES = 2 and NMODES = 1) was undertaken. The end results are summarized in Table 6-7.

Table 6-7

Summary of the Results

	the first point kinetics run	OZAN NMODES=2	OZAN NMODES=1
time t (sec.) at which the 6 MW level is reached	3.67	≃ 4.	5.06
the power level (MW) reached 0.1 sec. after time t	81.8	≃ 90	60

In conclusion it is important to recall that this is a fictitious case, not only has the assumption been made that the safety controls and instrumentation failed but also the inherent safety features of negative void and temperature coefficients have been neglected. If the negative reactivity feed back from the void formation is included, the shape of the transient would be significantly altered.

Rather than an explicit representation of the power history for the proposed problem, the results of these calculations should be viewed as study of the importance of special effects in fast transient calculations. The fact that the OZAN result with NMODES = 2 is significantly higher than the result with NMODES = 1, indicates that care must be taken if one is trying to make conservative conclusions based only on a point kinetics calculations.

CHAPTER VII

CROSS CHECKING OF THE RESULTS

The main question that arises from the previous chapter is: Do we believe in the numbers we have obtained? In fact this question has two parts:

1. Do we believe in the computer code (OZAN) written to perform the computations required by the proposed method?

2. Assuming that the answer to the first question is yes, do we believe in the prediction made by the proposed method?

Unfortunately the second question will be answered only superficially (and that will be done in the next chapter). Much more would have to be done to answer this question definitively.

In this chapter, we shall consider the validity of the computer code (OZAN) written to perform computations required by the proposed method. For this purpose five distinct tests were applied.

7-1 Some of the results computed through OZAN checked against the same quantities computed by Exterminator-II

The eigenvalues relative to the spatial shapes and the first row first column element of the generation time matrix are computed in both OZAN and Exterminator-II. In addition an Exterminator-II poison search predicted a value for ω (the inverse period that the reactor supposedly assumes near the time the rods receive the signal for scram). ω can also be estimated through the time behavior of the expansion coefficients predicted by OZAN (NMODES = 2) - cf. Fig. 6-3.

The results are summarized in Table 7-1, where $k_k (k=1,2)$ is given by Eq. (4-18) [Note that in the case of Exterminator-II the weighting function is unity. Thus, in computing $k_k (k=1,2)$ - assuming that the current across interfaces is continuous - , the leakage integral involved in the denominator of Eq. (4-18) was reduced to a surface integral over the outer surface of the reactor]. Λ_{11} is the one obtained from Eq. (3-28) through the normalization

$$\Lambda_{11} = \frac{2\pi \int_{r,\text{reactor}} r\, dr \int_{z,\text{reactor}} dz \quad \psi_1^{*T}(r,z) V^{-1} \psi_1(r,z)}{\frac{1}{k^{(*)}} 2\pi \int_{r,\text{core}} r\, dr \int_{z,\text{core}} dz \quad \psi_1^{*T}(r,z) \nu\chi \, \Sigma_F^T(r,z,0) \psi_1(r,z)} , \quad (7\text{-}1)$$

where the integrals are evaluated by the methods shown in Chapter V.

We point out that the relative convergence for the first shape, given by Exterminator-II was 3.452×10^{-4} and for the second shape, 6.199×10^{-5}; for the first weighting mode,

(*) In OZAN, instead of k_1, k_{OZAN} (1.01795673) is used. However this is a minor difference

Table 7-1

Comparison of some of the results computed through OZAN with the same quantities computed through Exterminator-II

	OZAN (NMODES=2)	Exterminator-II
k_1 (Eigenvalue of the first trial mode)	1.01737499	0.99973398
k_2 (Eigenvalue of the second trial mode)	1.02579212	1.007946
Λ_{11} (first row, first column element of the generation time matrix)	1.0107050×10^{-4}	1.043922×10^{-4}
ω (inverse period at around time t=T =3.77 sec.)	$\sim$17.2 (t=3.7 sec.)	17.262131

8.180×10^{-1} and for the second weighting mode, 8.528×10^{-1} (Note the poor degree of convergence for the weighting mode as compared to the degree of convergence for the spatial shape ; the same number of iterations were used in computing both.).

Thus the agreement of the eigenvalues (shown in Table 7-1) computed by OZAN with the ones computed by Exterminator-II is within less than 1.75%. The discrepancy between the generation time computed by one code and the generation time computed by the other code is less than 3.2%.

We conjecture that the difference between the eigenvalue computed by one code and the eigenvalue computed by the other may be due to the differences between the methods of computations used in both codes; namely differences in the evaluation of the leakage integral, use of - a rather poor - weighting function in OZAN, in comparison to use of unity as weighting function in Exterminator-II, etc. It is nevertheless possible that programming or input errors in OZAN may be responsible for the discrepancies observed between the two codes. We note however that k_1 and k_2 computed by OZAN are consistent with respect to k_1 and k_2 computed by Exterminator-II in that $(k_2-k_1)_{OZAN} = 8.41713 \times 10^{-3}$ while $(k_2-k_1)_{Ext.II} = 8.212 \times 10^{-3}$.

7-2 Cross checking of the elements of the matrix ρ_1 [The ramp change slope of the reactivity matrix - Eq. (6-30)], against the same quantities computed by a perturbation type of approach handled by an independent code written for this purpose

We recall that ρ_1 is computed through Eq. (5.54) in OZAN. That is specifically, we have (in terms of the notation adopted throughout the dissertation);

$$T\rho_1 = (2\pi \int_{r,reactor} r\, dr \int_{z,reactor} dz \quad W^T(r,z)\{[\nabla . D(r,z,T) - A(r,z,T)$$

$$+\chi_p \nu \Sigma_F^T(r,z,T)]\}\psi(r,z) + \alpha\xi_p(r,z,T) + \sum_{j=J+1}^{H} \overline{\beta}_{j_{new}}(T))$$

$$-(2\pi \int_{r,reactor} r\, dr \int_{z,reactor} dz \quad W^T(r,z)\{[\nabla . D(r,z,0) - A(r,z,0)$$

$$+\chi_p \nu \Sigma_F^T(r,z,0)]\}\psi(r,z) + \alpha\ \xi_p(r,z,0) + \sum_{j=J+1}^{H} \overline{\beta}_{j_{new}}(0)) \quad . \qquad (7\text{-}2)$$

Actually OZAN will test each component (D, A, Σ_F, ξ_p and $\overline{\beta}_{new}$) and will then form the differences.

$$\{2\pi \int_{r,reactor} r,dr \int_{z,reactor} dz \quad W^T(r,z)[COMP(r,z,T)]\ \psi\ (r,z)\}$$

$$-\{2\pi \int_{r,reactor} r\, dr \int_{z,reactor} dz \quad W^T(r,z)\ [COMP(r,z,0)]\ \psi\ (r,z)\}\ , \qquad (7\text{-}3)$$

(where COMP stands for D, A, Σ_F etc.) only if the component in question is subject to a change during the transient.

Thus, since only D and A vary during the accident (withdrawal of the control rods) we have studied, OZAN has computed as $T\rho_1$ the quantity

$$T\rho_1 = \{2\pi \int_{r,\text{reactor}} r\,dr \int_{z,\text{reactor}} dz \quad W^T(r,z)[\nabla.D(r,z,T)-A(r,z,T)]$$

$$\psi(r,z)\}-\{2\pi \int_{r,\text{reactor}} r\,dr \int_{z,\text{reactor}} dz \quad W^T(r,z)[\nabla.D(r,z,0)-A(r,z,0)]$$

$$\psi(r,z)\} \qquad (7\text{-}4)$$

That is, OZAN does not consider the particular-perturbation-nature of the problem, according to which Eq. (7-4) can be written

$$T\rho_1 = 2\pi \int_{r,\text{perturbed area}} r\,dr \int_{z,\text{perturbed area}} dz\ W^T(r,z)\ [\nabla.\delta D(r,z)$$

$$-\delta A(r,z)]\psi(r,z) \quad , \qquad (7\text{-}5)$$

where $\delta D(r,z)=D(r,z,T)-D(r,z,0)$, $\delta A(r,z)=A(r,z,T)-A(r,z,0)$, and the "perturbed area" refers to the location of the reactor being perturbed by the withdrawal of the rods. Thus instead of computing the integrals shown in Eq. (7-5) over only one mesh volume (for the problem studied the perturbation takes place in one mesh volume), OZAN deals with the problem as though it were general and computes $T\rho_1$ from Eq. (7-4) with the integrals performed over the entire reactor volume.

Thus we can check the results obtained by OZAN through Eq. (7-4), against results obtained by applying Eq. (7-5). For the purpose of this calculation a separate code was written (shown in Appendix 0, next to the code OZAN). Results are compared in Table 7-2.

Table 7-2

The matrix ρ_1 computed by OZAN and by a perturbation type of approach

	OZAN	Perturbation type of approach
ρ_{1_A}	$\begin{pmatrix} 0.20929807E29 & 0.12860273E30 \\ 0.12197004E30 & 0.90442634E30 \end{pmatrix}$	$\begin{pmatrix} 0.20932522E29 & 0.12861792E30 \\ 0.12199029E30 & 0.90486858E30 \end{pmatrix}$
ρ_{1_A}	$\begin{pmatrix} 0.88040249E29 & -0.67456125E28 \\ 0.71528204E30 & -0.11339531E29 \end{pmatrix}$	$\begin{pmatrix} 0.88058761E29 & -0.67489701E28 \\ 0.71562643E30 & -0.11343823E29 \end{pmatrix}$

$yEx \equiv yx10^x$

In Table 7-2 ρ_{1_A} and ρ_{1_D} refer to the components of ρ_1 due to absorption and leakage so that

$$\rho_1 = \rho_{1_A} + \rho_{1_D} \quad ; \qquad (7\text{-}6)$$

In order to normalize, these quantities must be divided by the denominator of Eq. (7-1).

We note that the two sets of numbers shown in Table 7-2 agree with each other very closely. This is, we believe, strong evidence that, the matrix elements (-at least-of ρ_1) are correctly computed in OZAN.

7-3 The matrix ρ_1 calculated algebraically in terms of quantities output from OZAN; comments on $\rho_{new}(0)$: the initial value of the reactivity matrix

Our third way of cross-checking consists of calculating ρ_1 through an algebraic relationship that involves quantities output from OZAN. We first develop that relationship.

7-3-1 Algebraic relationship

For this purpose define

$$H_1(\underline{r}) = \nabla.D_1(\underline{r})\nabla - A_1(\underline{r}) + \frac{F_1(\underline{r})}{k_1} , \qquad (7\text{-}7)$$

and

$$H_2(\underline{r}) = \nabla.D_2(\underline{r})\nabla - A_2(\underline{r}) + \frac{F_2(\underline{r})}{k_2} - \omega v^{-1} , \qquad (7\text{-}7)$$

with the notation used in Chapter IV.

$H_1(\underline{r})$ and $H_2(\underline{r})$ are the operators used in computing $\psi_1(\underline{r})$ and $\psi_2(\underline{r})$.

We next substract Eq. (7-7) from Eq. (7-8) to obtain

$$H_2(\underline{r}) - H_1(\underline{r}) = \nabla\delta D(\underline{r})\nabla - \delta A(\underline{r}) + F_1(\underline{r})\left(\frac{1}{k_2} - \frac{1}{k_1}\right) - \omega v^{-1}, \tag{7-9}$$

where $\delta D(\underline{r}) = D_2(\underline{r}) - D_1(\underline{r})$; $\delta A(\underline{r}) = A_2(\underline{r}) - A_1(\underline{r})$, and we have used the fact that $F_1(\underline{r}) = F_2(\underline{r})$.

Further define

$$\delta(\underline{r}) = \nabla\delta D(\underline{r})\nabla - \delta A(\underline{r}) \quad , \tag{7-10}$$

and

$$H_B(\underline{r}) = \frac{F_1(\underline{r})}{k_{OZAN}} \, BET \tag{7-11}$$

(where $BET = \sum_{j=1}^{6} \overline{\beta}_{j_{new_{11}}}(0)$)

Then with convenient manipulations we arrive at

$$\delta(\underline{r}) = H_2(\underline{r}) - H_1(\underline{r}) + H_B(\underline{r}) \frac{k_2 - k_1}{k_2 k_1 BET} k_{OZAN} + \omega v^{-1} \quad . \tag{7-12}$$

The matrix ρ_1 can now be written as

$$\rho_1 = \frac{\langle \psi^{*T}(\underline{r}) | \delta(\underline{r}) | \psi(\underline{r}) \rangle}{T} \quad . \tag{7-13}$$

Thus we are able to express ρ_1 in terms of

$$\langle \psi^{*T}(\underline{r}) | H_2(\underline{r}) | \psi(\underline{r}) \rangle \quad , \tag{7-14}$$

$$\langle \psi^{*T}(\underline{r}) | H_1(\underline{r}) | \psi(\underline{r}) \rangle \quad , \tag{7-15}$$

$$\langle \psi^{*T}(\underline{r}) | H_B(\underline{r}) | \psi(\underline{r}) \rangle \quad , \tag{7-16}$$

$$\langle \psi^{*T}(\underline{r}) | \omega v^{-1} | \psi(\underline{r}) \rangle \quad (\equiv \Lambda) \quad , \tag{7-17}$$

and k_1, k_2, k_{OZAN} and $\overline{\beta}_{new_{11}}(0)$. These quantities are output from OZAN except for some of the matrix elements of expressions (7-14) and (7-15) that are the subject of the next subsection.

7-3-2 Review of elements of the matrices (7-14) and (7-15)

This review will be done in five stages;

1. The first-row, first-column element of the matrix (7-14) cannot be evaluated:

Apparently there is no possibility of evaluating the element, $\langle \psi_1^{*T}(\underline{r}) | H_2(\underline{r}) | \psi_1(\underline{r}) \rangle$ under the circumstances we are working with.

2. Two elements are zero by definition:

The elements $\langle \psi_1^{*T}(\underline{r}) | H_1(\underline{r}) | \psi_1(\underline{r}) \rangle$ and $\langle \psi_1^{*T}(\underline{r}) | H_2(\underline{r}) | \psi_2(\underline{r}) \rangle$ vanish because of Eq. (4-19) [cf. the definition of k_k $(k = 1, 2)$].

3. Two elements should vanish in view of the definition for k_k $(k = 1, 2)$:

If $\psi_1(\underline{r})$ and $\psi_2(\underline{r})$ were well converged, we could write (at all points in the reactor)

$$H_1(\underline{r})|\psi_1(\underline{r})> = 0 \quad , \quad (7\text{-}18)$$

and

$$H_2(\underline{r})|\psi_2(\underline{r})> = 0 \quad , \quad (7\text{-}19)$$

through the definitions

$$<\psi_1^{*T}(\underline{r})|H_1(\underline{r})|\psi_1(\underline{r})> = 0 \quad , \quad (7\text{-}20)$$

and

$$<\psi_1^{*T}(\underline{r})|H_2(\underline{r})|\psi_2(\underline{r})> = 0 \quad , \quad (7\text{-}21)$$

Equations (7-18) and (7-19) would then imply respectively

$$<\psi_2^{*T}(\underline{r})|H_1(\underline{r})|\psi_1(\underline{r})> = 0 \quad , \quad (7\text{-}22)$$

and

$$<\psi_2^{*T}(\underline{r})|H_2(\underline{r})|\psi_2(\underline{r})> = 0 \quad . \quad (7\text{-}23)$$

4. Two elements should vanish in view of the definition of the adjoint mode:

Provided proper continuity properties exist, the elements $<\psi_2^{*T}(\underline{r})|H_2(\underline{r})|\psi_1(\underline{r})>$ and $<\psi_1^{*T}(\underline{r})|H_1(\underline{r})|\psi_2(\underline{r})>$ can be written respectively

$$<\psi_1^T(\underline{r})|H_2^+(\underline{r})|\psi_2^*(\underline{r})> \quad , \quad (7\text{-}24)$$

and

$$<\psi_2^T(\underline{r})|H_1^+(\underline{r})|\psi_1^*(\underline{r})> \quad , \quad (7\text{-}25)$$

with $H_1^+(\underline{r})$ and $H_2^+(\underline{r})$ defined in Chapter IV.

If $\psi_2^*(\underline{r})$ and $\psi_1^*(\underline{r})$ were well converged we would have

$$H_2^+(\underline{r})|\psi_2^*(\underline{r})\rangle = 0 \quad , \tag{7-26}$$

and

$$H_1^+(\underline{r})|\psi_1^*(\underline{r})\rangle = 0 \quad , \tag{7-27}$$

at all the points of the reactor. Thus expressions (7-24) and (7-25) would vanish.

5. $\langle\psi_2^{*T}(\underline{r})|H_1(\underline{r})|\psi_2(\underline{r})\rangle$:

To calculate this element we consider

$$H_{OZAN}(\underline{r}) = \nabla.D_1(\underline{r})\nabla - A_1(\underline{r}) + \frac{F_1(\underline{r})}{k_{OZAN}} + H_{PPN}(\underline{r}) + H_{DPN}(\underline{r}), \tag{7-28}$$

where $H_{PPN}(\underline{r})$ and $H_{DPN}(\underline{r})$ are respectively the prompt <u>and</u> the delayed photoneutron operators defined through

$$\langle\psi^{*T}(\underline{r})|H_{PPN}(\underline{r})|\psi(\underline{r})\rangle \quad , \tag{7-29}$$

and

$$\langle\psi^{*T}(\underline{r})|H_{DPN}(\underline{r})|\psi(\underline{r})\rangle \quad , \tag{7-30}$$

that is, the prompt <u>and</u> the delayed photoneutron reactivity matrices introduced in Chapter III. Both matrices (7-29) and (7-30) are output from OZAN.

With appropriate manipulations we obtain

$$H_1(\underline{r}) = H_{OZAN}(\underline{r}) + H_B(\underline{r}) \left(\frac{1}{k_1} - \frac{1}{k_{OZAN}}\right) \frac{k_{OZAN}}{BET} - H_{PPN}(\underline{r})$$

$$- H_{DPN}(\underline{r}) \quad , \qquad (7\text{-}31)$$

such that

$$<\psi^{*T} | H_{OZAN}(\underline{r}) | \psi(\underline{r}) >= \rho_{new}(0) \quad ; \qquad (7\text{-}32)$$

the initial value of the reactivity matrix (comments about $\rho(0)$ are saved for the subsection 7-3-4).

Thus using Eq. (7-31), Eq. (7-12) can be written as

$$\delta(\underline{r}) = H_2(\underline{r}) - H_{OZAN}(\underline{r}) + \frac{H_B(\underline{r})}{BET} \left(1 - \frac{k_{OZ}}{k_2}\right) + H_{PPN}(\underline{r}) + H_{DPN}(\underline{r}) + \omega v^{-1} \ .$$

$$(7\text{-}33)$$

*

Hence ρ_1 will be calculated through Eq. (7-13) by making use of Eq. (7-12) (for the first row, second column, and second row, first column; elements) and Eq. (7-33) (for the second row, second column element) in conjunction with the comments made for the matrices (7-14) and (7-15). Further information is given in Table 7-3.

In numbers (appearing in Table 7-3) relevant to the photoneutrons a correction factor $\alpha = 10$ is present.

Table 7-3 Further information for the purpose of the algebraic calculation

k_{OZAN}	1.01795673
$\overline{\beta}_{new_{11}}(0)$	0.78469925E-2
The delayed neutron fraction matrix [that corresponds to $H_B(\underline{r})$]	$\begin{pmatrix} 0.78469925E-2 & 0.78072660E-2 \\ 0.73465705E-2 & 0.73112361E-2 \end{pmatrix}$
The prompt photoneutron production matrix [that corresponds to $H_{PPN}(\underline{r})$]	$\begin{pmatrix} 0.21412867E29 & 0.24675711E29 \\ 0.20902955E29 & 0.24088097E29 \end{pmatrix}$
The delayed photoneutron fraction matrix [that corresponds to $H_{DPN}(\underline{r})$]	$\begin{pmatrix} 0.17435974E-3 & 0.17421108E-3 \\ 0.17020771E-3 & 0.1700626E-4 \end{pmatrix}$

$$y \; E \; x \equiv y \times 10^{x}$$

For purposes of normalization the numbers for the prompt photoneutron should be divided by $0.54379688 \times 10^{32}$.

7-3-3 Results

Results are regrouped in Table 7-4.

Table 7-4 Elements of the matrix ρ_1 calculated algebraically (by hand) compared with the same elements computed through OZAN

	Algebra	OZAN
Second row first column (21) element	0.254 E-2	0.15396 E-1
First row second column (12) element	0.2241 E-2	0.22409 E-2
Second row second column (22) element	0.1643 E-1	0.16423 E-1

$y \text{ E } x \equiv y \times 10^{x}$

We note that the agreement between the last two elements of Table 7-4 is very good. However the first element computed through OZAN is badly off as compared to the result given by the algebra for the same element. This, we believe, is due to the incorrectness of the assumption that expression (7-24) vanishes -this expression is computed nowhere in OZAN . Similarly, if indeed we assume, throughout the calculation of the (12) element that $<\psi_1^{*T}(\underline{r})|H_1(\underline{r})|\psi_2(\underline{r})>$ (which can be calculated based on the output from OZAN, to be 1.404×10^{-3}) vanishes [cf. Eq. (7-20)], then we find - through the algebra for the (12) element- 0.2610×10^{-2} instead of 0.2241×10^{-2}.

The error in assumptions such as Eq. (7-20) implies that the fluxes determined by Exterminator-II are not well converged. The degree of convergence for the two adjoint modes are shown in Table 7-5. $\psi_1^*(\underline{r})$ was computed in 60 iterations and $\psi_2^*(\underline{r})$, 50 iterations. For a comparison the degree of convergence for $\psi_1^*(\underline{r})$ after 50 iterations, is also shown.

Table 7-5 Degree of convergence of the adjoint modes

Fluxes	Iteration number	Relative convergence	Absolute convergence
$\psi_1^*(\underline{r})$	60	8.1799 E-1	-9.5230 E-1
$\psi_2^*(\underline{r})$	50	8.5283 E-1	-9.9201 E-1
$\psi_1^*(\underline{r})$	50	8.5275 E-1	-9.9206 E-1

We note the worse convergence for $\psi_2^*(\underline{r})$. We also note that if $\psi_1^*(\underline{r})$ were computed out of 50 iterations (instead of 60), then its convergence would be as bad as the one for $\psi_2^*(\underline{r})$. These facts may be responsible for the greater divergence from zero of $\langle\psi_2^{*T}(\underline{r})|H_2(\underline{r})|\psi_1(\underline{r})\rangle$ [this can be computed - see Eq. (7-34) - making use of Eq. (7-12) to be ≈ 0.048] than the divergence from zero of $\langle\psi_1^{*T}(\underline{r})|H_1(\underline{r})|\psi_2(\underline{r})\rangle$ (≈ 0.0014).

We have calculated $\langle\psi_2^{*T}(\underline{r})|H_2(\underline{r})|\psi_2(\underline{r})\rangle$ from

$$\langle\psi_2^{*T}(\underline{r})|H_2(\underline{r})|\psi_1(\underline{r})\rangle = \langle\psi_2^{*T}(\underline{r})|\delta(\underline{r})|\psi_1(\underline{r})\rangle$$

$$+ \langle\psi_2^{*T}(\underline{r})|H_1(\underline{r})-H_B(\underline{r})\ \frac{k_2 - k_1}{k_2 k_1 \bar{\beta}_{new_{11}}(0)}\ k_{OZAN}|\psi_1(\underline{r})\rangle - \Lambda_{22}\ , \tag{7-34}$$

[cf. Eq. (7-12)], where $\langle\psi_2^{*T}(\underline{r})|\delta(\underline{r})|\psi_1(\underline{r})\rangle$ is taken to be the (21) element of the matrix ρ_1 as computed by OZAN.

*

We shall defer discussion of some suggestions based on the results just derived until the next chapter.

However, because it is closely related to the algebra developed within the present section, we take the opportunity in the following section to comment on $\rho_{new}(0)$, the initial value of the reactivity matrix.

7-3-4 Comments on $\rho_{new}(0)$, the initial value of the reactivity matrix

The matrix $\rho_{new}(0)$ [cf. Eq. (7-32)] deserves special attention. Starting to apply the time dependent

Equations (3-44) and (3-45) with some residual reactivity - although this may be small - , while the reactor is critical, is undesirable numerically. Thus to avoid an erroneous prediction, k_{OZAN} was introduced in Chapter V, so that, if the reactor is critical at the beginning of the transient, we have $\rho_{new_{11}}(0) = 0$. The purpose of k_{OZAN} is then to compensate for the extra reactivity due to the presence of photoneutrons (the balance for the equilibrium trial mode, $\psi_1(\underline{r})$, being maintained by dividing the fission cross sections by k_1 - eigenvalue of the first trial mode computed through OZAN).

If k_{OZAN} were the eigenvalue of a well converged first trial mode coming out of Exterminator II, we would have $\rho_{new_{11}}(0) = \rho_{new_{21}}(0) = \rho_{new_{12}}(0) = 0$ [cf. respectively Equations (7-20), (7-22) and (7-25)], since $H_{OZAN}(\underline{r})$ [cf. Eq. (7-27)] would then be identical to $H_1(\underline{r})$ [cf. Eq. (7-31)]. Failing that, we have numbers presented in Eq. (6-29).

Comments about the (11), (21) and (12) elements of $\rho_{new}(0)$.

On the RHS of Eq. (6-29) note that by definition the (11) element is zero (within the accuracy that the machine can insure on single precision).

We would like the (21) element to be as close to zero as the (11) element in view of Eq. (7-18) - written for $H_{OZAN}(\underline{r})$ instead of $H_1(\underline{r})$ - . However not only the fact that the eigenvalue computed for $\psi_1(\underline{r})$ through OZAN diverges from the one given by Exterminator-II (for $\approx$ 1.75%) but also the presence of the photoneutrons makes k_{OZAN} a rather artificial eigenvalue computed just to insure $[\rho_{new_{11}}(0) = 0]$. Thus unfortunately a relationship such as Eq. (7-18) does not hold for $H_{OZAN}(\underline{r})$. Hence the value of the LHS of Eq. (7-22) is closely bound to the character of the weighting function. We also note that the second adjoint, having the worse degree of convergence (cf. Table 7-5), makes the divergence from zero, of the (21) element about five times worse than the divergence from zero of the (11) element.

Fortunately the (21) element is still satisfactorily close to zero.

Finally note that we would not expect the (12) element to vanish even if $H_{OZAN}(\underline{r})$ and $H_1(\underline{r})$ were identical since it was pointed out - in subsection 7-3-3 - that presumably, because of the bad convergence of $\psi_1^*(\underline{r})$, $<\psi_1^{*T}(\underline{r})|H_1(\underline{r})|\psi_1(\underline{r})>$ is equal to 1.404×10^{-3} [rather than zero, cf. Eq. (7-25)].

Steady State Predictions;

It is important to determine whether or not the expansion coefficients $N_1(t)$ and $N_2(t)$ will stay steady if the reactor remains in its critical state, that is if we solve Equations (3-44) and (3-45) for expansion coefficients with $[\rho_{new}(t) = \rho_{new}(0)]^*$.

---

* The answer to this question more properly belongs to the next chapter (since it rather deals with the second question we have introduced at the beginning of the present chapter). However we find it easier to give the answer here.

To answer this question the solution of Equations (3-44) and (3-45) with $\rho_{new}(t) = \rho_{new}(0)$, the Λ and $\bar{\beta}_{j_{new}}$'s of Equations (6-28) and (6-31) and the precursor amplitude functions found from $\frac{dC_j(t)}{dt} = 0$, (j=1,..., H), was determined [by applying the subroutine [24] that takes care of the solution of the time dependent Equations (3-44) and (3-45), in OZAN]. The time coefficients $N_1(t)$ and $N_2(t)$ were found to be satisfactorily steady for the period of interest.

Further comments;

It is recognized that in the previous test, $N_2(0) = 0$. Thus the (12) element has no effect on the result. Hence during the normal run - when $N_2(t)$ becomes greater - the divergence from zero of this element may be of importance. We save the discussion of this point for the next chapter (section 8-3).

7-4 Cross checking the subroutine that solves the time dependent equations

The code [24] that solves the time dependent Equations (3-44) and (3-45) was installed in OZAN after necessary modifications were made. This code has been checked against an other code in the work cited in reference [4] that also solves the multimode kinetics equations. Good agreement was found in the special case of one group of delayed neutrons.

In case only one trial mode is used the multimode kinetics equations reduce to the conventional point kinetics equations.

Thus the prediction made through OZAN (NMODES=1) with 15 groups of delayed neutrons should agree with the one obtained through a point kinetics code if the same parameters are supplied. We were able to obtain good agreement between the point kinetics code [18] and OZAN (NMODES=1).

7-5 The point kinetics model equivalent to the multimode synthesis scheme; cross checking the behavior of the power level predicted by OZAN.

In this section we shall first show that one is able to compute a scalar generation time, reactivity, delayed neutron fractions and a time coefficient equivalent to respectively; generation time matrix, Λ, reactivity matrix $\rho_{new}(t)$, delayed neutron fraction matrices, $\overline{\beta}_{j_{new}}(t)$, [j=1,...,(H+1)] and time coefficient matrix N(t). Thus the point kinetics model described by Λ_{eq}, $\rho_{eq}(t)$ and $\beta_{eq_j}(t)$'s should predict a change in power level from $N_{eq}(t)$ equivalent to that defined by $N_1(t)$ and $N_2(t)$.

$N_{eq}(t)$ will thus be checked against the behavior of the power level computed through the point kinetics code run with Λ_{eq}, $\rho_{eq}(t)$ and $\beta_{eq_j}(t)$'s.

7-5-1 The equivalent point kinetics model

For the purpose of developing the equivalent point kinetics model we express the neutron flux as

$$\bar{\phi}(r,z,t) = \psi_{eq}(r,z,t)\ N_{eq}(t)\ [\equiv \psi_1(r,z)N_1(t)+\psi_2(r,z)N_2(t)], \tag{7-35}$$

where now the shape, $\psi_{eq}(r,z,t)$ is a function of time, since we use only one time coefficient $N_{eq}(t)$ to represent $[\psi_1(r,z)N_1(t) + \psi_2(r,z)N_2(t)]$.

Derivation;

Replacing $\phi(r,z,t)$ in Equations (3-1), (3-2) and (3-3) by $\psi_{eq}(r,z,t)\ N_{eq}(t)$ - this expression being identical to $\psi_1(r,z)N_1(t) + \psi_2(r,z)N_2(t)$ - leads us to the residuals defined through Equations (3-15), (3-16) and (3-17), where $\psi(r,z)N(t)$ should now be read: $\psi_{eq}(r,z,t)N_{eq}(t)$. Thus the first term of of the right hand side of Eq. (3-15) becomes $V^{-1}\dfrac{\partial[\psi_{eq}(r,z,t)N_{eq}(t)]}{\partial t}$. We weight the residuals [Eq. (3-15), (3-16) and (3-19)] with the first weighting mode. Thus the first term of the RHS of Eq. (3-15) becomes

$$N_{eq}(t) \int_{\underline{r},reactor} d\underline{r} \quad W_1^T(\underline{r})\ V^{-1} \frac{\partial \psi_{eq}(\underline{r},t)}{\partial t} \ +$$

$$\frac{dN_{eq}(t)}{dt} \int_{\underline{r},reactor} d\underline{r} \quad W_1^T(\underline{r})\ V^{-1} \psi_{eq}(\underline{r},t) \ . \qquad (7\text{-}36)$$

For the amplitude function, $N_{eq}(t)$, to contain most of the time dependence, $\psi_{eq}(\underline{r},t)$ should embody only slowly varying time functions for all $\underline{r}$ and t. One way of insuring this is to impose the constraint condition [23]. That is

$$\int_{\underline{r},reactor} d\underline{r} \quad W_1^T(\underline{r})\ V^{-1} \frac{\partial \psi_{eq}(\underline{r},t)}{\partial t} = 0 \qquad . \qquad (7\text{-}37)$$

That means

$$\int_{\underline{r},reactor} d\underline{r}\ W_1^T(\underline{r})\ V^{-1}\ \psi_{eq}(\underline{r},t) = cste \qquad , \qquad (7\text{-}38)$$

where cste stands for a constante number that is determined by merely setting t to zero - in Eq. (7-38) - . Thus

$$cste = \int_{\underline{r},reactor} d\underline{r}\ W_1^T(\underline{r})\ V^{-1} \psi_{eq}(\underline{r},0)$$

$$\equiv \int_{\underline{r},reactor} d\underline{r}\ W_1^T\ (\underline{r})\ V^{-1}\ \psi_1(\underline{r}) \equiv \Lambda_{11} \qquad . \qquad (7\text{-}39)$$

Then multiply both sides of Eq. (7-38) by $N_{eq}(t)$ to obtain

$$\int_{\underline{r},\text{reactor}} d\underline{r} \quad W_1^T(\underline{r})\ V^{-1}\ \bar{\phi}(\underline{r},t) \equiv N_1(t) \int_{\underline{r},\text{reactor}} d\underline{r} \quad W_1^T(\underline{r})\ V^{-1}\psi_1(\underline{r})$$

$$+N_2(t) \int_{\underline{r},\text{reactor}} d\underline{r} \quad W_1^T(\underline{r})V^{-1}\psi_2(\underline{r}) \equiv N_1(t)\Lambda_{11}+N_2(t)\Lambda_{12}(t)=\Lambda_{11}N_{eq}(t). \tag{7-40}$$

Thus $N_{eq}(t)$ is defined as

$$N_{eq}(t) = N_1(t) + \frac{\Lambda_{12}}{\Lambda_{11}} N_2(t) \quad , \tag{7-41}$$

and can be calculated at various times based on the output from OZAN.

Next multiply both sides of Eq. (7-41) by Λ_{11} and take the derivative of both sides with respect the time. The result is

$$\Lambda_{eq} \frac{dN_{eq}(t)}{dt} = \Lambda_{11} \frac{dN_1(t)}{dt} + \Lambda_{12} \frac{dN_2(t)}{dt} \quad , \tag{7-42}$$

with

$$\Lambda_{eq} \equiv \Lambda_{11} \quad . \tag{7-43}$$

Furthermore we note that the procedure of weighting the residuals analogous to those given by Equations (3-15), (3-16) and (3-19) [the only difference being that $\psi_{eq}(\underline{r},t)N_{eq}(t)$ replaces $\psi(\underline{r})\ N(t)$] by $W_1^T(\underline{r})$, leads us to equations for $N_{eq}(t)$

that are identical to the first scalar equations of the matrix equations (3-44) and (3-45); namely the equations

$$\Lambda_{11} \frac{dN_1(t)}{dt} + \Lambda_{12} \frac{dN_2(t)}{dt} = [\rho_{new_{11}}(t) - \overline{\beta}_{new_{11}}(t)]N_1(t) +$$

$$[\rho_{new_{12}}(t) - \overline{\beta}_{new_{12}}(t)]N_2(t) + \sum_{j=1}^{H+1} \lambda_j C_{j_1}(t) \quad , \qquad (7\text{-}44)$$

$$\frac{dC_{j_1}(t)}{dt} = \overline{\beta}_{j_{new_{11}}}(t)N_1(t) + \overline{\beta}_{j_{new_{12}}} N_2(t) - \lambda_j C_{j_1}(t) \; ,$$

$$(j = 1, \ldots, (H+1)] \quad , \qquad (7\text{-}45)$$

where in accord with the comment made (in the previous chapter) about the external source expressed in terms of an extra delayed neutron precursor amplitude function, j's are extended to (H+1).

Next we define

$$\beta_{eq_j}(t) = \frac{\beta_{j_{new_{11}}}(t)N_1(t) + \overline{\beta}_{j_{new_{12}}}(t)N_2(t)}{N_{eq}(t)} \; , [j=1,\ldots,H] \; ,$$

(Note that $\overline{\beta}_{(H+1)_{new_{11}}} = \overline{\beta}_{(H+1)_{new_{12}}} = 0$),

$$\beta_{eq}(t) = \sum_{j=1}^{H} \beta_{eq_j}(t) \quad , \tag{7-47}$$

and

$$\rho_{eq}(t) = \frac{\rho_{new_{11}}(t)\ N_1(t) + \rho_{new_{12}}(t)N_2(t)}{N_{eq}(t)} \tag{7-48}$$

Thus the equations (7-44) and (7-45) [identical to those we would obtain by finding $N_{eq}(t)$, through weighting by $W_1^T(\underline{r})$ the residuals given by Equations (3-15), (3-16) and (3-17) with $\psi(\underline{r})N(t)$ replaced by $\psi_{eq}(\underline{r},t)N_{eq}(t)$], can now be written through Equations (7-43), (7-46), (7-47) and (7-48) as

$$\Lambda_{eq}\ \frac{dN_{eq}(t)}{dt} = [\rho_{eq}(t)-\beta_{eq}(t)]N_{eq}(t) + \sum_{j=1}^{H+1} \lambda_j C_{eq_j}(t) \quad , \tag{7-49}$$

$$\frac{dC_{eq_j}(t)}{dt} = \beta_{eq_j}(t)N_{eq}(t)-\lambda_j C_{eq_j}(t), \ [j=1,\ldots,(H+1)] \quad , \tag{7-50}$$

where $C_{eq_j}(t)$ stands for $C_{j_1}(t)$.

Thus we have been able to derive a point kinetics model equivalent to the multimode synthesis scheme.

Normalization;

Note that Λ_{eq}, $\rho_{eq}(t)$ and $\beta_{eq_j}(t)$'s as they appear in equations (7-49) and (7-50) have not been normalized. [cf. Equations (7-43), (7-46) and (7-48)]. However that does not affect the preceding derivation since we know the normalization consists merely in dividing all the matrix elements of Λ, $\rho_{new}(t)$, and $\beta_{j_{new}}(t)$'s by the same number: denominator of the RHS of Eq. (7-1) - where k_1 should be read as k_{OZAN} - . Thus dividing both sides of Equations (7-43), (7-46) and (7-48) we obtain Λ_{eq}, $\rho_{eq}(t)$, <u>and</u> $\beta_{eq_j}(t)$-(j=1,...,H) - now normalized in terms of the normalized Λ_{11}, [$\rho_{new_{11}}(t)$, and $\rho_{new_{12}}(t)$], <u>and</u> [$\beta_{j_{new_{11}}}(t)$, and $\beta_{j\ new_{12}}(t)$ - (j = 1,..., H) -] .

Naturally $N_{eq}(t)$ predicted through Equations (7-49) and (7-50) where Λ_{eq}, $\rho_{eq}(t)$, and $\beta_{eq_j}(t)$'s are normalized is the same as $N_{eq}(t)$ predicted through the same equations with Λ_{eq}, $\rho_{eq}(t)$ and $\beta_{eq_j}(t)$'s not normalized. This can be seen from Eq. (7-41). Dividing the numerator and the denominator of $(\Lambda_{12}/\Lambda_{11})$ by the same quantity, will not affect the left hand side of Eq. (7-41), that is, $N_{eq}(t)$.

Choice of the weighting function;

Note that to arrive at Equations (7-49) and (7-50) the second adjoint mode $\psi_2^*(\underline{r})$ (or any other function) could have been chosen as the weighting function. Equations (7-49) and (7-50), now with

$$\Lambda_{eq} \equiv \Lambda_{21} \quad , \qquad (7\text{-}51)$$

$$\beta_{eq_j}(t) = \frac{\overline{\beta}_{j\ new_{21}}(t)N_1(t) + \overline{\beta}_{j\ new_{22}}(t)N_2(t)}{N_{eq}(t)} ,$$

$$(j=1,\ldots, H) \quad , \qquad (7\text{-}52)$$

$$\beta_{eq}(t) = \sum_{j=1}^{H} \beta_{eq_j}(t) \quad , \qquad (7\text{-}53)$$

and

$$\rho_{eq}(t) = \frac{\rho_{new_{21}}(t)N_1(t) + \rho_{new_{22}}(t)\ N_2(t)}{N_{eq}(t)} \quad , \qquad (7\text{-}54)$$

would predict

$$N_{eq}(t) \qquad N_1(t) + \frac{\Lambda_{22}}{\Lambda_{21}} N_2(t) \quad . \qquad (7\text{-}55)$$

Note that $N_{eq}(t)$ defined through Eq. (7-41) is different from the one defined through Eq. (7-55). However the definition of $\psi_{eq}(\underline{r},t)$ [through Eq. (7-38) where now $W_1^T(\underline{r})$ is replaced by $\psi_2^{*T}(\underline{r})$] is also not the same as the one given through Eq. (7-38).

Thus denoting $\psi_{eq_1}(\underline{r},t)$; $\psi_{eq}(\underline{r},t)$ defined through Eq. (7-38) by using $\psi_1^{*T}(\underline{r})$ as the weighting function, and $\psi_{eq_2}(\underline{r},t)$; $\psi_{eq}(\underline{r},t)$ defined through Eq. (7-38) by using $\psi_2^{*T}(\underline{r})$ as the weighting function and with

$$N_{eq_1}(t) \equiv N_{eq}(t)_{Eq.(7-41)} \quad , \tag{7-56}$$

and

$$N_{eq_2}(t) \equiv N_{eq}(t)_{Eq.(7-55)} \tag{7-57}$$

We expect to have, through Eq. (7-35),

$$\bar{\phi}(\underline{r},t) \equiv \psi_{eq_1}(\underline{r},t)\; N_{eq_1}(t) = \psi_{eq_2}(\underline{r},t) N_{eq_2}(t) \tag{7-58}$$

Hence using a different weighting function in obtaining the equivalent point kinetics equations parameters, leads to a different shape function $[\psi_{eq}(\underline{r},t)]$, and a different time coefficient $[N_{eq}(t)]$. However since $|\Lambda| = 1.282\text{x}10^{-3}$, we have

$$\frac{\Lambda_{22}}{\Lambda_{21}} \approx \frac{\Lambda_{12}}{\Lambda_{11}} \quad , \tag{7-59}$$

and

$$N_{eq_1}(t) \approx N_{eq_2}(t) \quad , \tag{7-60}$$

Thus

$$\psi_{eq_1}(\underline{r},t) \quad \psi_{eq_2}(\underline{r},t) \quad . \qquad (7\text{-}61)$$

Utility of the equivalent point kinetics Model;

Since the evaluation of Λ_{eq}, $\rho_{eq}(t)$ and $\beta_{eq_j}(t)$'s require the solution of Equations (3-44) and (3-45), the utility of the equivalence between Equations (3-44), (3-45) and Equations (7-49), (7-50) lies in reducing the complicated matrix scheme to more familiar scalar equations.

The comparison of Equations (7-49) and (7-50) (description of the transient equivalent to OZAN, NMODES = 2) with Equations (3-44) and (3-45) when just one trial mode is used [-the matrix N(t) being reduced to a scalar $N_1(t)$, thus - OZAN, NMODES=1], will be presented in the next chapter.

7-5-2 Cross checking $N_{eq}(t)$ calculated through Eq. (7-41) against $N_{eq}(t)$ computed through a point kinetics code

The last cross checking undertaken for OZAN consisted of determing Λ_{eq}, $\rho_{eq}(t)$, and $\beta_{eq_j}(t)$'s from respectively the identity (7-43), and Equations (7-48) and (7-46), computing $N_{eq}(t)$ with these quantities through a point kinetics code, and comparing $N_{eq}(t)$ to the result calculated from Eq. (7-41).

Actually $\beta_{eq_j}(t)$'s can be considered to be constant throughout the transient and, since Λ_{11} is close to Λ_{12}, $N_{eq}(t) \simeq N_1(t) + N_2(t)$; moreover $\overline{\beta}_{j_{new_{11}}}$ [j=1,...,(H+1)] is almost equal to $\overline{\beta}_{j\ new_{12}}$; thus $\beta_{eq_j}(t) \approx \overline{\beta}_{j\ new_{11}}$. In addition Λ_{eq} need not be calculated. Thus we are concerned with only the calculation of $\rho_{eq}(t)$ in order to be prepared for the point kinetics code. $\rho_{eq}(t)$ is shown in Table 7-6.

Table 7-6 The equivalent scalar reactivity

time (sec.)	$\rho_{eq}(t) \times 10^3$
1	2.445
2	5.10
3	7.80
4	10.85
5	14.04

Approximating the reactivity $\rho_{eq}(t)$ by a series of ramp changes and with Λ_{11}, $\rho_{eq}(t)$, $\overline{\beta}_{j\ new_{11}}$ and also $C_{PK_j}(0)$'s from Table 6-2 used as input, $N_{eq}(t)$ was computed through the point kinetics code. For a comparison few numbers are shown in Table 7-7.

Table 7-7 Comparison of $N_{eq}(t)$ calculated through Eq. (7-39) with $N_{eq}(t)$ computed through the point kinetics code

t(sec.)	$N_{eq}(t)$ (from the point	$N_{eq}(t)$ (OZAN)
0.8	0.71210 E-8	0.713 E-8
0.9	0.75586 E-8	0.748 E-8
1.0	0.80455 E-8	0.813 E-8

$y \text{ E } x \equiv y\text{x}10^x$

We note that numbers for $N_{eq}(t)$ calculated from Eq. (7-41) based on the output from OZAN, agree satisfactorily with numbers for $N_{eq}(t)$ computed through OZAN (within an error of less than 1.15%).

7-6 Summary

In this chapter we have taken a look at five different ways of checking the results given by OZAN to answer the question: Do we believe in the computer code (OZAN) written to perform computations required by the proposed method? At some stages we have presented results that made a positive answer difficult (discrepancy in the eigenvalues and generation time,) the (21) element of the matrix ρ_1, etc.). We pointed out however, that discrepancies encountered in section (7-1) are, we believe, due to both the bad convergence of the fluxes determined by Exterminator-II and to the difference in the methods used for computations in both OZAN and Exterminator-II. The worse convergence of the second adjoint mode was found to be responsible for the anomolous divergence of $\rho_{1_{21}}$ (algebra) from $\rho_{1_{21}}$ (OZAN).

On the other hand sections 7-2, 7-4 and 7-5 as well as $\rho_{1_{12}}$ (OZAN) and $\rho_{1_{22}}$ (OZAN) that checked well against $\rho_{1_{12}}$ (algebra) and $\rho_{1_{22}}$ (algebra) very much favor a positive answer to the question of validity of the code OZAN.

Thus we are inclined to say, we believe in OZAN.

CHAPTER VIII

THE VALIDITY OF THE PROPOSED METHOD AND CONCLUSIONS

This chapter includes a discussion of the photoneutrons, a word about the reactivity concept, a tentative to answer questions concerning the validity of the two-shape method, a summary of the conclusions and recommendations for further work.

8-1 Photoneutrons

Much effort has been devoted throughout this thesis research to analyse quantitatively the generation of both prompt and delayed photoneutrons in MITR-II.

8-1-1 Prompt photoneutrons

For α (the correction factor introduced to account for the error due to various approximations made in calculating the photon intensity at a point in the reflector region) = 1 we found

$$PPR_{11}(0) \approx 3.94 \times 10^{-5} \quad , \qquad (8\text{-}1)$$

where $PPR_{11}(0)$ denotes the (11) element of the prompt photoneutron production matrix at t = 0.

This result implies that, if (assuming that α can be taken equal to 1) the prompt photoneutrons are neglected, an error of less than $4.\times 10^{-5}$ is made in computing the (initial) reactivity* of the reactor.

8-1-2 Delayed Photoneutrons

In order to see the importance of the delayed photoneutrons in determining the reactor inverse period, for various reactivity insertions we computed [28]

$$\mathrm{RHO} = \omega\left(\Lambda + \sum_{j=1}^{H} \frac{\mathrm{BETAT}_j}{\omega + \lambda_j}\right) \quad , \qquad (8\text{-}2)$$

where RHO is a reactivity that corresponds to ω, and Λ, the neutron generation time of the reactor. Λ has been taken (1.043922×10^{-4}) as given by the Exterminator-II output for the inverse velocities presented in Chapter VI. For easy reference BETAT_j's and λ_j's are presented in Table 8-1.

The computation of RHO for various values of ω was repeated changing the correction factor α for the delayed photoneutron fractions (j = 7, ..., 14). The results are presented in Table 8-2.

* i.e. $\rho_{new_{11}}(0)$ defined in Chapter III.

Table 8-1

Delayed neutron fractions and the corresponding decay constants

j	$BETAT_j$	$\lambda_j (sec^{-1})$
1	0.3010 E-3	0.1240 E-1
2	0.1709 E-2	0.3050 E-1
3	0.1529 E-2	0.111
4	0.3082 E-2	0.301
5	0.8980 E-3	1.14
6	0.3280 E-3	3.01
7	0.1128 E-4	0.277
8	0.3531 E-5	0.169 E-1
9	0.1215 E-5	0.481 E-2
10	0.5824 E-6	0.150 E-2
11	0.3574 E-6	0.428 E-3
12	0.4028 E-6	0.117 E-3
13	0.5562 E-7	0.437 E-4
14	0.1757 E-7	0.363 E-5

$y \text{ E } x \equiv y \times 10^x$

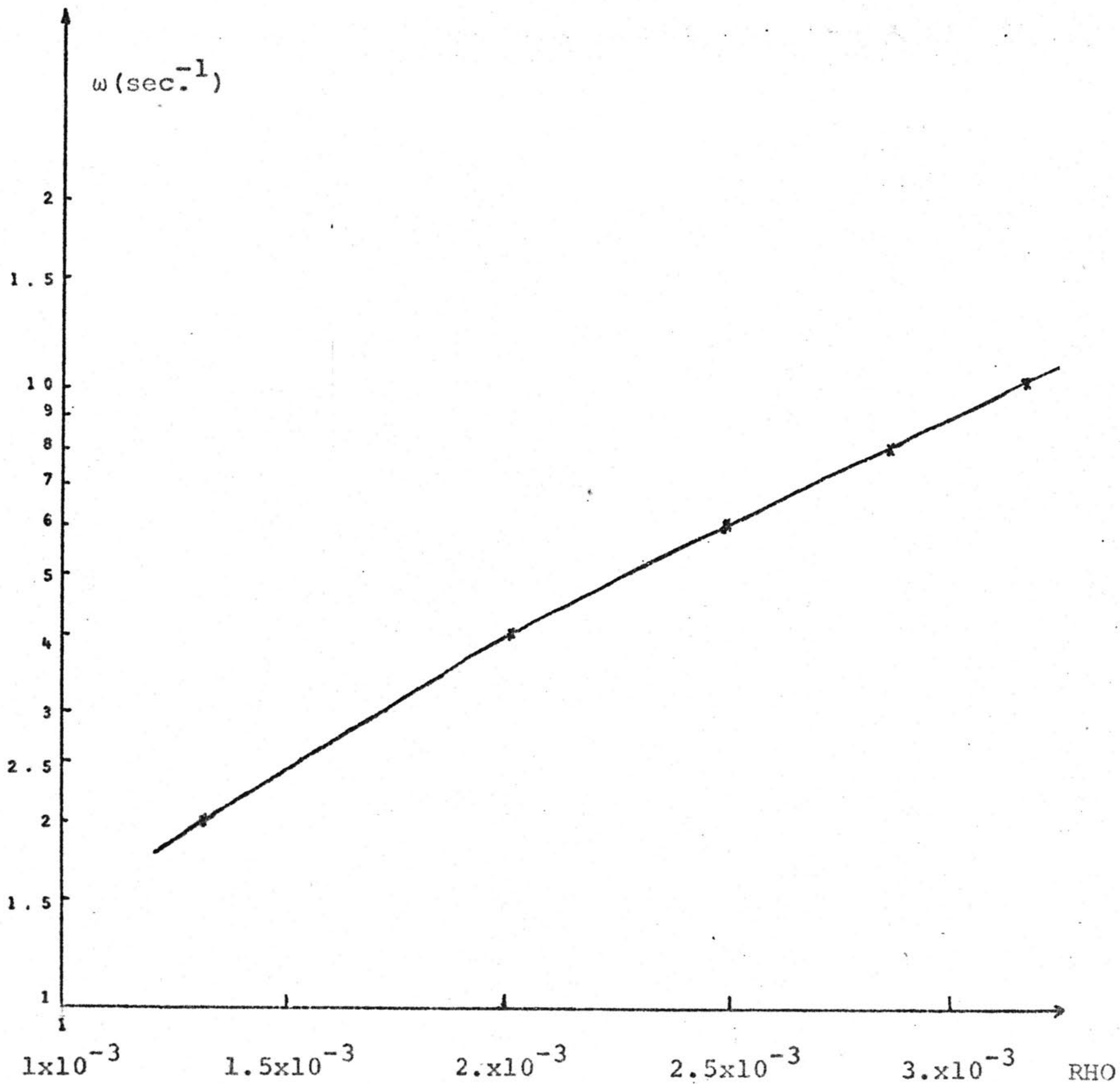

Fig. 8-1 Inverse Period versus Reactivity (α = 1)

Table 8-2 Effect of delayed photoneutrons in determining the inverse period, for various connection factors. Numbers presented are reactivities multiplied by a hundred.

α \ $\omega(sec^{-1})$	0.02	0.04	0.06	0.08	0.1
0	0.13078	0.20049	0.24888	0.28612	0.31640
1	0.13128	0.20113	0.24961	0.28692	0.31726
3	0.13229	0.20240	0.25106	0.28851	0.31897
5	0.13329	0.20368	0.25252	0.29011	0.32069

As expected we see from Table 8-2 that the delayed photoneutrons become more important for small insertions of reactivity.

$\omega(sec^{-1})$ is plotted versus RHO for $\alpha = 1$ (as shown in Chapter II) in Fig. 8-1.

8-2 The Equivalent Reactivity

In Chapter VII (section 7-5) we have shown that an equivalent generation time, set of delayed neutron fractions and reactivity can be defined so that with these parameters the P equation predicts the same solution as the one given through the multimode kinetics equations (synthesis method).

The equivalent reactivity makes it easy to visualize the difference between various predictions;

Comparing the parameters (Λ_{eq}, $\beta_{eq}(t)$ and $\rho_{eq}(t)$) of the point kinetics model equivalent to OZAN (NMODES=2), to those (Λ_{11}, $\overline{\beta}_{new_{11}}(t)$, $\rho_{new_{11}}(t)$) determined for the point kinetics type of approach; (OZAN, NMODES=1) we see that the only one that is significantly different is

$$\rho_{eq}(t) \; [\text{for } \beta_{eq}(t) = \frac{\overline{\beta}_{new_{11}}(t)N_1(t)+\overline{\beta}_{new_{12}}(t)N_2(t)}{N_{eq}(t)} \; ;$$

$$N_{eq}(t) = N_1(t) + \frac{\Lambda_{12}}{\Lambda_{11}} N_2(t); \; \frac{\Lambda_{12}}{\Lambda_{11}} \approx 1, \text{ thus } N_{eq}(t) \approx N_1(t)+N_2(t);$$

$$\overline{\beta}_{new_{11}}(t) \approx \overline{\beta}_{new_{12}}(t) \approx \overline{\beta}_{new_{11}}(0); \text{ thus } \beta_{eq}(t) \approx \overline{\beta}_{new_{11}}(0); \text{ and}$$

$$\Lambda_{eq} = \Lambda_{11}] \; .$$

Thus the three different approaches (the point kinetics Code [18], OZAN; NMODES=1, and OZAN; NMODES=2) undertaken in Chapter VI for analysing the effects of withdrawal of the bank of shim rods, are equivalent to solving equations of type

$$\frac{dN_{eq}(t)}{dt} = \frac{(\rho_{eq}(t)-\beta_{eq}(t))}{\Lambda_{eq}} N_{eq}(t) + \sum_{j=1}^{H+1} \lambda_j C_j(t) \ , \qquad (8\text{-}3)$$

$$\frac{dC_j(t)}{dt} = \frac{\beta_{eq_j}}{\Lambda_{eq}} N_{eq}(t) - \lambda_j C_j(t) \ , \ (j=1,\ldots, H) \qquad , \qquad (8\text{-}4)$$

where $\Lambda_{eq} \equiv \Lambda_{PK}$ (cf. Chapter VI) $\equiv \Lambda_{11}$ (cf. OZAN, NMODES = 1), and $\beta_{eq_j}(t) \approx \beta_{PK_j}$ (cf. Chapter VI) $\equiv \overline{\beta}_{j_{new_{11}}}(0)$ (cf. OZAN, NMODES=1), for respectively $\rho_{eq}(t) = \rho_{PK}(t)$ (cf. Chapter VI), $\rho_{eq}(t) = \rho_{new_{11}}(t)$ (cf. OZAN, NMODES=1), and

$$\rho_{eq}(t) = \frac{\rho_{new_{11}}(t)N_1(t)+\rho_{new_{12}}(t)N_2(t)}{N_{eq}(t)}$$ [cf. Eq. (7-41), OZAN, NMODES = 2].

Comparison of various reactivities;

The comparison of these various reactivities, that have been defined for the same transient (withdrawal of the control rods, cf. Chapter VI) is shown in Table 8-3. This table also includes values of two other definitions of reactivity obtained by making the first weighting function unity throughout the entire reactor, first in OZAN (NMODES=1) and then in OZAN (NMODES=2). (We will later come back to the latter study to point out the importance of the weighting function in the weighted residual technique.)

Table 8-3 Comparison of various reactivities defined for the same transient (cf. Chapter VI) through different approaches

t(sec.)	PK	OZAN (NMODES =1)	OZAN (NMODES =2)	OZAN (NMODES =1) $W_1(\underline{r})=1.$	OZAN (NMODES =2) $W_1(\underline{r})=1.$
0.	0.	0.	0.	0.	0.
1	0.3×10^{-2}	0.2×10^{-2}	0.2445×10^{-2}	0.627×10^{-2}	0.585×10^{-2}
2	0.6×10^{-2}	0.4×10^{-2}	0.510×10^{-2}	1.253×10^{-2}	0.855×10^{-2}
3	0.9×10^{-2}	0.6×10^{-2}	0.788×10^{-2}	1.88×10^{-2}	-
4	1.2×10^{-2}	0.8×10^{-2}	1.085×10^{-2}	2.51×10^{-2}	-
5	1.5×10^{-2}	1.0×10^{-2}	1.404×10^{-2}	3.14×10^{-2}	-

P_K stands for the reactivity determined by the first approach undertaken in Chapter VI in the course of the study of the withdrawal of the rods by the point kinetics code [18].

Numbers presented in the last two columns of Table 8-3;

The numbers presented in the last two columns of Table 8-3 were obtained in the following way;

A calculation has been made with the first weighting function unity throughout the reactor (and everything else being the same) for the problem (withdrawal of control rods) subject to

Chapter VI. The relevant initial value and the ramp change shape of the reactivity matrices, $\rho_{new}(0)$ and ρ_1 were taken from the output OZAN (NMODES=2). A normalization factor (cf. Chapter VIII, section 7-5)

$\int_{\underline{r},core} d\underline{r}\ (1)^T \nu\ \chi\ \Sigma_F^T(\underline{r},0)\ \psi_1(\underline{r})$ [$(1)^T$ denoting the transpose of the column matrix composed of G (number of neutron groups) elements that are unity] is already present in these matrix elements. On the other hand a normalization factor

$\int_{\underline{r},core} d\underline{r}\ \psi_1^{*T}(\underline{r}) \nu\ \chi\ \Sigma_F^T(\underline{r},0)\psi_1(\underline{r})$ is present in the numbers shown in second, third and fourth columns of the Table 8-3. Thus for the purpose of the comparison an adjustment of the $\rho_{new}(0)$ and ρ_1 relevant to the study; $W_1(\underline{r}) = 1$, OZAN (NMODES=2) is made such that the (11) element of the generation time matrix relevant to this study becomes equal to the (11) element of the generation time matrix obtained through the study where $\psi_1^*(\underline{r})$ is used (as the weighting function).

Then the fifth column numbers of Table 8-3 were obtained by writing, with the adjusted (11) elements of $\rho_{new}(0)$ and ρ_1 relevant to the study; $W_1(\underline{r}) = 1$, OZAN (NMODES=2);

$$\rho_{eq}(t) = \rho_{new_{11}}(0) + t\ \rho_{1_{11}} \qquad ;$$

and the last column numbers of Table 8-3 were obtained by using the Eq. (7-48) along $\rho_{new_{11}}(0)$, $\rho_{new_{12}}(0)$, $\rho_{1_{11}}$, and $\rho_{1_{12}}$

relevant to the same study.

*

We recognize that different sets of numbers for reactivity versus time, shown in Table 8-3 are responsible for different predictions about the transient studied. Thus the interpretation of a prediction in terms of the equivalent parameters (and mainly equivalent reactivity) makes us better understand, how this prediction is different from others.

8-3 The Validity of the two-shape calculations

In the previous chapter we examined the correctness of the code OZAN and defined the question of the validity of the proposed method. Specifically one has to examine what conditions must be fulfilled in order to make an accurate prediction for a transient through the weighted residual method and whether or not we fulfilled those conditions for the present study.
Are two shapes sufficient for the purpose of analyzing the accident mentioned in Chapter VI? Even further, in Chapter VII it is pointed out that we used the two-shape method to observe the transient only after the reactor had become critical.
If the two shape method had been used for the entire transient would the result be significantly different from those given in Chapter VI ?

Unfortunately we will not be able to give a definitive answer to these questions without further study.

We intend, however to discuss two points that relate to the character of the weighted residual method and are for consideration to resolve some of the obscurities.

a) It was pointed out earlier (cf. Chapters IV and V) that in order to compute the leakage integral $\int_{\underline{r},\text{reactor}} d\underline{r}\ W^T(\underline{r})$ $\nabla . D(\underline{r},t)\nabla\psi(\underline{r})$ (in matrix notation) we needed the balance equations through which $\psi_1(\underline{r})$ and $\psi_2(\underline{r})$ [column vectors, components of $\psi(\underline{r})$] are generated. Thus the eigenvalues k_1 and k_2 for the balance equations in question were computed through OZAN, in an integral sense. For the eigenvalues relative to $\psi_1(\underline{r})$ and $\psi_2(\underline{r})$ computed through the code (Exterminator-II) would not insure these balance equations (due to the poor convergence of the fluxes and differences in computations used in both codes, etc.) when applied to OZAN.

In addition k_{OZAN} was introduced to compensate the photoneutrons and insure that at time the reactor becomes critical the (11) element of the reactivity matrix, $\rho_{new_{11}}(0)$ vanishes so that we do not go to the time dependent equations with a residual reactivity at that time. Otherwise an erroneous prediction would result.

The examination of possible errors arising from these (somewhat artificial) manipulations is made below throughout the subsection 8-3-1.

b) A second point of this validity consideration is a study of the effect of the weighting on the prediction through the weighted residual method. This is done in the subsection 8-3-2.

8-3-1 Eigenvalues computed in an integral sense

For the purpose of studying the possible errors arising from the introduction of the eigenvalues k_1, k_2 and k_{OZAN}, computed in an integral sense (to satisfy the required balances) we develop arguments about k_{OZAN} and k_2. We then try to show that we do not have to fear the artificialities introduced by the definition of these quantities.

1. k_{OZAN};

The purpose of defining a quantity k_{OZAN} was to compensate for the presence of the photoneutrons (Neither of the operators that generated the trial shapes through Exterminator-II included the photoneutrons) by forcing $\rho_{new_{11}}(0)$ to vanish. However since $k_{OZAN}(\underline{r})$ then differs from $H_1(\underline{r})$ (a correction factor $\alpha = 10$ has been used for photoneutrons throughout the OZAN studies), a relationship such as $H_1(\underline{r})|\psi_1(\underline{r})>=0$ does not hold for $H_{OZAN}(\underline{r})$. Thus we expect $<\psi_2^{*T}(\underline{r})|H_{OZAN}(\underline{r})|\psi_1(\underline{r})>$ [the (21) element of the initial value of the reactivity matrix] to differ from zero. This quantity turned out to be 1.93×10^{-5}, which is still satisfactorily close to zero. Thus we feel the error in the (21) element introduced by this approximation is negligible.

The (12) element of the initial value of the reactivity matrix; $\psi_1^{*T}(\underline{r})|H_{OZAN}(\underline{r})|\psi_2(\underline{r})>$ is $\approx$ $1.463\text{x}10^{-3}$. If there were no photoneutrons it would be $<\psi_1^{*T}(\underline{r})|H_1(\underline{r})|\psi_2(\underline{r})>$ which should vanish if $\psi_1^*(\underline{r})$ were well converged. Numerically for the unconverged values used, the (12) element without photoneutrons is $1.404\text{x}10^{-3}$. The difference between $<\psi_1^{*T}(\underline{r})|H_{OZAN}(\underline{r})|\psi_2(\underline{r})>$ and $<\psi_1^{*T}(\underline{r})\ H_1(\underline{r})|\psi_2(\underline{r})>$ is then of a minor importance in view of the (12) element of the ramp change slope of the reactivity matrix: $2.241\text{x}10^{-3}$.

*

Thus the introduction of k_{OZAN} is a small correction and apparently gives its expected result.

2. It does not matter if the reactor has not been poisoned to compute k_2 through OZAN.

The second trial mode was generated through Exterminator-II) by increasing the absorption cross sections by the quantity ωv^{-1} throughout the reactor (cf. Chapter IV). To be rigorous we should do the same thing when we come to compute k_2 through OZAN. Failure to do so the eigenvalue k_2 (computed in an integral sense through OZAN) will be different (greater) than the one obtained if the reactor was poisoned. $k_{2_{NP}}$ (NP standing for "nonpoisoned") will then be rather artificial (for it is computed so that the balance - cf. Chapter IV - is insured for a flux through some cross sections that does not belong to this flux).

A sensitivity study was made to see the effect on the matrix elements of not poisoning the reactor in computing the eigenvalue k_2 through OZAN. A comparison is presented in Table 8-4-1.

Table 8-4-1 Comparison of reactivity matrix elements in cases the reactor has been poisoned for the computation of k_2 through OZAN, and the reactor has not been poisoned for the same computation

	P	NP
k_2	1.02579212	1.02754307
$\rho_{new}(0)$	$\begin{pmatrix} x & 0.14621585\ E{-}2 \\ x & -0.52545846\ E{-}1 \end{pmatrix}$	$\begin{pmatrix} x & 0.14627143\ E{-}2 \\ x & -0.52609537\ E{-}1 \end{pmatrix}$
ρ_1	$\begin{pmatrix} x & 0.22408564\ E{-}2 \\ x & 0.16423166\ E{-}1 \end{pmatrix}$	$\begin{pmatrix} x & 0.22407090\ E{-}2 \\ x & 0.16423021\ E{-}1 \end{pmatrix}$

$$y\ E\ x \equiv y \times 10^x$$

P stands for the case the reactor was poisoned for OZAN to compute k_2, NP for the case the reactor was not poisoned for the same computation.

The crosses in Table 8-4-1 refer to the (11) and (21) elements of the matrices in question that are not affected at all (since these elements do not involve the second trial mode).

The numbers shown in Table 8-4-1 affirm that the differences due to computing k_2 by poisoning the reactor and not poisoning it, are minor. This can also be seen from Table 8-4-2 where we give numbers for $N_1(t)$ and $N_2(t)$ for both cases.

Table 8-4-2 The time coefficients $N_1(t)$ and $N_2(t)$ for both cases: the reactor has been poisoned to compute k_2 through OZAN, and it has not been poisoned for the same computation

t(sec.)	P	NP	
1	0.61083 E-8	0.611027 E-8	$N_1(t)$
	0.20901 E-8	0.20874 E-8	$N_2(t)$
2	0.99663 E-8	0.99747 E-8	$N_1(t)$
	0.10495 E-7	0.10478 E-7	$N_2(t)$
3	0.61598 E-7	0.61673 E-7	$N_1(t)$
	0.22798 E-6	0.22693 E-6	$N_2(t)$

P, NP and y E x that stand in Table 8-4-2 were defined for Table 8-4-1.

*

The results presented throughout both parts of this subsection suggest that we do not have to fear artificialities introduced during the course of the proposed method, due to the definitions in an integral sense of k_1, k_2 and k_{OZAN}. An undesirable perturbation (photoneutrons, small variations in the cross sections, etc.) is then successfully absorbed in the definition of the eigenvalue of interest, to reassure the required balance equation. For the study undertaken in part 2 of this subsection this can be clearly seen from the algebraic relationship obtained in Chapter VII (section 7-3) for the elements of the ramp change slope of the reactivity matrix [cf. Eq.(7-33)],

$$\delta(\underline{r}) = H_2(\underline{r}) + \frac{H_B(\underline{r})}{BET} \times \frac{k_2 - k_{OZAN}}{k_2} - H_{OZAN}(\underline{r}) + H_{PPN}(\underline{r})$$

$$+ \quad H_{DPN}(\underline{r}) + \omega v^{-1} . \qquad (8\text{-}5)$$

(We recall that $\rho_1 = \dfrac{\langle \psi^{*T}(\underline{r}) | \delta(\underline{r}) | \psi(\underline{r}) \rangle}{T}$)

In case the reactor has not been poisoned to compute ρ_1 the last term in the RHS of Eq. (8-5) will be omitted, but since $k_{2_{NP}}$ is now greater than k_{2_P} (P standing for the case the reactor is poisoned to compute k_2 through OZAN), $\left(\rho_{1_{12}}\right)_{NP}$ and $\left(\rho_{1_{22}}\right)_{NP}$ are still approximately equal to respectively $\left(\rho_{1_{12}}\right)_P$ and $\left(\rho_{1_{22}}\right)_P$ (cf. Table 8-4-1). This implies that a relationship such as

$$\omega v^{-1} = \frac{1}{k_{2_P}} - \frac{1}{k_{2_{NP}}} \; H_B(\underline{r}) \; \frac{k_{OZAN}}{\bar{\beta}_{new_{11}}(0)} \quad , \qquad (8\text{-}6)$$

is approximately true; that gives (through the values for k_{2_P}, $k_{2_{NP}}$, k_{OZAN}, BET, and ω given ealier);

$$\Lambda \approx 1.305 \; \langle \psi^{*^T}(\underline{r}) \,|\, H_B(\underline{r}) \,|\, \psi(\underline{r}) \rangle \quad . \qquad (8\text{-}7)$$

which happens to be indeed right (cf. Table 8-5).

Table 8-5 Comparison of the elements of the generation time matrix with the ones obtained through the approximate Relationship (8-7)

Λ	$\Lambda_{Eq.(8-7)}$
$\begin{pmatrix} 0.1011\text{ E-3} & 0.9786\text{ E-4} \\ 0.9807\text{ E-4} & 0.9508\text{ E-4} \end{pmatrix}$	$\begin{pmatrix} 0.1023\text{ E-3} & 0.1020\text{ E-3} \\ 0.960\text{ E-4} & 0.955\text{ E-4} \end{pmatrix}$

Throughout this subsection we will try to emphasize the importance of the weighting functions in the weighted residual method. This is done in three parts.

1. The (12) element of the initial value of the reactivity matrix is not small enough;

It was pointed out earlier that (cf. Chapter VII section 7-3-4) the (12) element of the initial value of the reactivity matrix is not close enough to zero due to the bad convergence of $\psi_1^*(r)$ ($<\psi_1^{*T}(\underline{r})|H_1(\underline{r})|\psi_2(\underline{r})> \approx 1.4 \times 10^{-3}$, and the photoneutrons are shown - cf. part 1. of the previous subsection - not to play a major role in this divergence from zero), and may be a source of trouble. Through Eq. (7-48) one can indeed see that, because the (12) element of the initial value of the reactivity matrix is not negligible as compared to tx $\rho_{1_{12}}$ (for the period of time of interest), there is a certain contribution of $\rho_{new_{12}}(0)$ in the computation of the equivalent reactivity, $\rho_{eq}(t)$. Equivalent reactivity $\rho_{eq}(t)$ is calculated assuming that $\rho_{new_{12}}(0)$ vanishes, and compared in Table 8-6, to the numbers obtained by taking the finite value - for $\rho_{new_{12}}(0)$ - computed through OZAN.

Thus apparently the prediction about the transient would not be as severe if the first adjoint mode were well converged so that $<\psi_1^{*T}(\underline{r})|H_1(\underline{r})|\psi_1(\underline{r})>$ vanishes and $\rho_{new_{12}}(0)$ is close

Table 8-6 Comparison of $\rho_{eq}(t)$ of Table 7-6 with $\rho_{eq}(t)$ calculated by making $\rho_{new_{12}}(0)$, zero.

t(sec.)	$\rho_{eq}(t)$ [with $\rho_{new_{12}}(0)\approx$ 0.1463E-2]	$\rho_{eq}(t)$ [with $\rho_{new_{12}}(0)=0$]
1	2.445 E-3	2.075 E-3
2	5.100 E-3	4.33 E-3
3	7.880 E-3	6.70 E-3
4	10.850 E-3	9.25 E-3
5	14.04 E-3	12.15 E-3

$y\ \text{Ex} \equiv j \times 10^{x}$

enough to zero.

We note that in any case;

- A space-dependent analysis (for the transient we have studied) results in a different (and hopefully more accurate) prediction than a point kinetic analysis (cf. numbers presented in Table 8-6 compared to the numbers presented in the third column of Table 8-3);

- The reactivity $\rho_{eq}(t)$ versus time is initially lower than $\rho_{PK}(t)$ (cf. the second column of Table 8-3) for sometime and finally intercepts it [at around 5 sec. in case we have numbers presented in the second column of Table 8-6 and later in case we have numbers presented in the third column of the same table].

2. A comment about the (21) element of the ramp change slope of the reactivity matrix that was found badly off as compared to the prediction made by the algebra (cf. Chapter VII, section 7-3);

It may be thought that we can overcome the divergence of $\rho_{1_{21}}$ computed through OZAN (NMODES=2), from the value given by the algebraic relationship (developed in Chapter VII, section 7-3), by simply setting $\rho_{1_{21}}$ to this algebraic result. This is not as simple for the reasons we give below;

The divergence in question was found due to the bad convergence of the second adjoint made [specifically $\langle\psi_2^{*T}(\underline{r})|H_2(\underline{r})|\psi_1(\underline{r})\rangle$ was found to be $\approx 5. \times 10^{-2}$, whereas it is expected to vanish].

On the other hand in section 7-2 (Chapter VII) it was shown that the elements of the matrix ρ_1 can be merely computed by taking into account the perturbed area only (that is four points <u>and</u> the relevant fluxes and cross sections). That means, since setting $\rho_{1_{21}}$ to the value found by the algebra implies $\langle\psi_2^{*T}(\underline{r})|H_2(\underline{r})|\psi_1(\underline{r})\rangle = 0$, convenient values for $\psi_2^*(\underline{r})$ over the four points (of the perturbed area) in question, are then tacitly assumed (so that the relationship of interest is now satisfied). This in return implies all the matrix elements that involve $\psi_2^*(\underline{r})$ must be accordingly adjusted, or an erroneous prediction will result.

We may think from a different point of view that the nature of the weighted residual method does not require relationships such as $<\psi_2^{*T}(\underline{r})|H_2(\underline{r})|\psi_1(\underline{r})> = 0$, so that a bad converged adjoint function can be allowed as a weighting function. This is shown to be incorrect throughout the final part of this subsection.

3. Effect of Changing the weighting function

Changing the weighting function makes a large difference. We have examined a case where $W_1(\underline{r})$ is chosen to be unity for all the points of the reactor, for the same accident presented in Chapter VI. The equivalent reactivity, $\rho_{eq}(t)$ for this case is already presented in the last column of Table 8-3.

We will be content here by giving the final predictions as compared to the ones obtained through the run where $W_1(\underline{r})$ was $\psi_1^*(\underline{r})$ (cf. Table 8-7).

Table 8-7 Comparison of the results obtained by making $W_1(\underline{r}) = 1$ with those obtained by making $W_1(\underline{r}) = \psi_1^*(\underline{r})$

t(sec.)	OZAN (NMODES=2) $W_1(\underline{r}) = 1$	OZAN (NMODES=2) $W_1(\underline{r})=\psi_1^*(\underline{r})$	
1	0.554 E9 0.128 E8	0.611 E-8 0.209 E-8	$N_1(t)$ $N_2(t)$
2	0.257 E27 0.116 E27	0.997 E-8 0.105 E-7	$N_1(t)$ $N_2(t)$

The prediction with $W_1(\underline{r}) = 1$ is erroneous. The reason is that the reactivity insertion $\rho_{eq}(t)$, estimated for the accident is much higher with $W_1(\underline{r}) = 1$. (cf. Table 8-3).

*

Apparently it is inappropriate to use just any weighting function in the weighted residual method. As suggested by the perturbation theory or variational method, the adjoint modes that correspond to the spatial shapes are more properly used as weighting functions. Moreover it is important to have reasonably well converged adjoint functions (as well converged as the spatial shapes) in order to make an accurate prediction.

We find it interesting to note that $\rho_{eq}(t)$, $W_1(\underline{r}) = 1.$, NMODES=2 behaves better than $\rho_{eq}(t)$, $W_1(\underline{r}) = 1$, NMODES=1 (cf. the last two columns of Table 8-3). It seems then that the two-shape method (NMODES=2) improves the results as compared to a point kinetics type of approach (NMODES=1). However the prediction is still far beyond being realistic.

**

We conclude in this section thus, that the answer of the question: Do we believe in the proposed method?, lies in answering the question: Did we use well converged weighting functions?, everything else, we believe, working correctly. A positive answer to the latter question is not available due to lack of funds, and it seems, better results would be obtained if we had more converged weighting functions, that remains however to be shown.

***

In any case one unfortunately cannot tell whether or not he made a good prediction through the weighted residual method until he compares his results with the exact solution, although the method was proven to give successful results (for a much simpler case however) [27], if care is taken to insure "good" working conditions.

It is believed that for some cases, obtaining the exact solution may be even easier. For the generation of well converged trial shapes and weighting functions along the application of the weighted residual criteria, may be as time consuming as 90 minutes of computation (case of the present study) on an IBM 360/65 computer. Even if the exact solution is thought to be "little" more costly than that, we believe it may be worth spending the computation time to obtain a reassuring prediction.

8-4 SUMMARY

It was shown that equivalent point kinetics parameters can be defined so that the same prediction made through the multimode kinetics equations about a transient, can be made through a point kinetics equations. It was emphasized that the equivalent reactivity is the predominant parameter in the kind of accident undertaken. Thus it was pointed out that the equivalent reactivity concept makes it easier to visualize the differences in the procedures used by various methods.

We were concerned that erroneous prediction may be caused by the definitions of the eigenvalues k_1, k_2 and k_{OZAN} in an integral sense. The artificialities introduced through the definitions (in an integral sense) of k_1, k_2 and k_{OZAN} are proven to be of a minor importance.

Finally a study about the importance of the weighting functions used in the weighted residual method is presented. It is shown that not just any function can be used as a weighting function, and the adjoint functions are the most appropriate ones for this purpose. Furthermore the weighting functions are required to be as converged as the trial shapes. Otherwise an erroneous prediction may result.

8-5 Recommendations for further work

The concern about the proposed technique has always been the fact that it lacks definitive error bounds.

We recognize that for a good set of fluxes (trial shapes and their adjoint modes) the algebraic relationships presented in Chapter VII (section 7-3) would be satisfied and we would feel much more comfortable about the predictions under these circumstances.

We suggest a study should be done to see the effect of the convergence of the fluxes on the predictions (however in a much simpler case than the one we have undertaken for the present work). Then we thought a line may be drawn between the divergence of the predictions from the exact solution and the degree at which the algebraic relationships are satisfied.

It may, then, also be possible without having to generate more converged fluxes, to adjust in a consistent way the "bad" matrix elements so that a better prediction can be made quickly. The proposed method would be more fruitful and more satisfactory under these circumstances.

The effect, on the prediction, of more trial shapes and more neutron groups remains to be seen. However the limitations of the available facilities (computer care storage, use of input output devices, etc.) may impede the combination of such studies.

A comparison between the multimode method with OZAN and an exact solution for a simplified transient problem would give valuable information about the validity and usefulness of the proposed method.

REFERENCES

1. G. Robert Keepin, Physics of Nuclear Kinetics, Table 5-3.

-Walter E. Ford, III, David H. Wallace, POPOP4, A Code For Converting Gamma-Ray Spectra to Secondary Gamma-Ray Production Cross Sections, CTC-12.

-W. E. Ford, III, David H. Wallace, The Use and "Testing" of Al, Fe, Ni, Cu, and Secondary Gamma-Ray Production Data Sets from the POPOP4 Library, CTC-20.

-W. E. Ford, III, The POPOP4 Library of Neutron-Induced Secondary Gamma-Ray Yield and Cross Section Data (POPOP4 Memo No. 1), CTC-42.

-POPLIB, A Compendium of Neutron-Induced Secondary Gamma-Ray Yield and Cross Section Data, DLC-12.

3. S. Kaplan, O. J. Marlow, and J. Berwick, Application of Synthesis Techniques to Problems Involving Time Dependence, Nucl. Sci. Eng. 18, 163 (1964).

4. Joe Turuage, A New Approach to solving the Multimode Kinetics Equations, M.I.T., Nuclear Engineering Department, Thesis, (1972).

5. Fowler, Toblas, Vondy, Exterminator-2, Argonne National Laboratory, Argonne Code Center, Reference Material, Abstract 156.

6. L. A. Hugemer, Numerical Methods and Techniques Used in Two Dimensional Neutron Diffusion Program PDQ-5, WAPD-TM 364 UC-32, Fig. 5-1.

7. Reactor Physics Constants, ANL 5800, 1.3.1, 1.3.2.

8. Kernforschungzentrum, Karlsruhe, KFK 770, EUR 3953 d.

9. Melville Clark, Jr., and Kent F. Hansen, Numerical Methods of Reactor Analysis, Appendix A (The Boltzmann equation for photons).

10. Klaus Scharmer, ALIZE III, First Critical Experiment for the Franco-German High Flux Reactor-Calculations-, CEA-R-3393(E), Section 13.

11. Edward L. Fuller III, Weighted Residual Methods in Space-Dependent Reactor Dynamics, ANL-7565 (Chapter VI).

12. G. Robert Keepin, Physics of Nuclear Kinetics, Fig. 5-4.

13. G. Robert Keepin, Physics of Nuclear Kinetics, Fig. 5-1.

14. Reactor Physics Constants, ANL 5800, Table 8-10.

15. Reactor Physics Constants, ANL 5800, Fig. 8-6.

16. G. Robert Keepin, Physics of Nuclear Kinetics, Table 5-1.

17. Goldstein, Shielding, page 60.

18. Jose Nobrega, personnel communication: A code developed during the course of the thesis; Time Integration Methods for Reactor Kinetics, M.I.T., Nuclear Engineering Department (1972).

19. A. K. Addae, The Reactor Physics of the Massachusetts Institute of Technology Reactor Redesign, MITNE-118 (1970).

20. Lamarsh, Nuclear Reactor Theory, Table 3-7 and 3-8.

21. Lamarsh, Nuclear Reactor Theory, Section 12-5.

22. Reactor Physics Constants, ANL-5800, Tables 1-9 and 1-11.

23. M. Becker, A Generalized Formulation of Point Nuclear Reactor Kinetics Equation, Nucl. Sci. Eng. 31, 458 (1968).

24. Edward L. Fuller III, personnel communication: A code developed during the course of the thesis; Weighted Residual Methods in Space-Dependent Reactor Dynamics, University of Arizona, Nuclear Engineering Department (1969).

25. Klaus Scharmer, ALIZE III, First Critical Experiment for the Franco-German High Flux Reactor - Calculations - , CEA-R-3393 (E), Section 15.

26. Edward L. Fuller III, Weighted Residual Methods in Space-Dependent Reactor Dynamics, ANL-7565 (Chapter I).

27. Donald R. Ferguson, Solution of the Space-Dependent Reactor Kinetics Equations in Three Dimensions, MITNE-132 (Chapter I).

28. Lamarsh, Nuclear Reactor Theory, Section 12-9.

APPENDIX A

PHOTONEUTRONS GENERATED BY PHOTONS HAVING HAD ONE AND ONLY ONE COLLISION, FROM U^{235} ON D_2O

The purpose in this Appendix is to investigate whether the photoneutrons generated in D_2O by photons from U^{235}, having had one and only one collision, could be neglected as compared to photoneutrons produced by uncollided photons under the same circumstances.

To this end we seek an estimate of photoneutrons generated by photons having had one and only one collision, from U^{235} on D_2O.

Assume then that we know the directional flux of uncollided photons of energy Λ', per cm^2, per Mev, per steradian, per sec., from an atom of U^{235} at a central location, in an infinite medium of D_2O, at r', in the direction $\underline{\Omega}'$ and at time t': $\xi'(r',\Lambda',\Omega',t')$ photons per cm^2 × Mev × steradian × sec.

Thus

$$\psi'(r',\Lambda',\Omega',t) = \int_0^t \xi'(r',\Lambda',\Omega',t')dt', \qquad \text{(A-1)}$$

gives the total number of uncollided photons of energy within a unit interval of energy around Λ', crossing a unit area at r' perpendicular to the direction $\underline{\Omega}'$, within a unit solid angle around $\underline{\Omega}'$, between $t' = 0$ and $t' = t$, from an atom of U^{235} placed in a central location in an infinite medium of D_2O.

Define now the microscopic Compton scattering cross section

$$d^2{}_e\sigma(\Lambda' \to \Lambda) = \frac{r_0^2}{2}\left(\frac{\Lambda}{\Lambda'}\right)^2\left(\frac{\Lambda'}{\Lambda} + \frac{\Lambda}{\Lambda'} - \sin^2\theta\right)d\mu \sin\theta\, d\theta, \tag{A-2}$$

where r_0 is the classical radius of the electron, Λ' and Λ are the energies of the photon respectively before and after the scattering; in addition, various angles $(\theta, \mu, \Omega, \Omega')$ are shown in Fig. A-1.

Let $\underline{N}_{D_2O}$ be the number of D_2O molecules per cm^3 and Z be the number of electrons present in one molecule of D_2O, $(Z = 10)$; such that,

$$\phi'(r', \Lambda' \to \Lambda, \Omega', t)d\underline{r}' = \psi'(r', \Lambda', \Omega', t)d\underline{r}' \; d^2{}_e\sigma(\Lambda' \to \Lambda)\underline{N}_{D_2O}Z, \tag{A-3}$$

is the number of photons among those described by the Eq. (A-1), scattered in the elementary volume $d\underline{r}'$, into the solid angle $d\Omega = d\mu \sin\theta\, d\theta$.

Furthermore through the study of Compton collision,

$$\frac{1}{\Lambda'} - \frac{1}{\Lambda} = \frac{1-\cos\,\theta}{E_0}\,, \qquad \text{(A-4)}$$

where E_0 = 0.51 Mev, and considering Λ' to be constant,

$$E_0\,\frac{d\Lambda}{\Lambda^2} = \sin\,\theta\;d\theta\,, \qquad \text{(A-5)}$$

so that the energy of the scattered photon stays within $d\Lambda$ around Λ; once the solid angle $d\Omega$ is chosen, Λ being determined through Eq. (A-4) and $d\Lambda$ through Eq. (A-5).

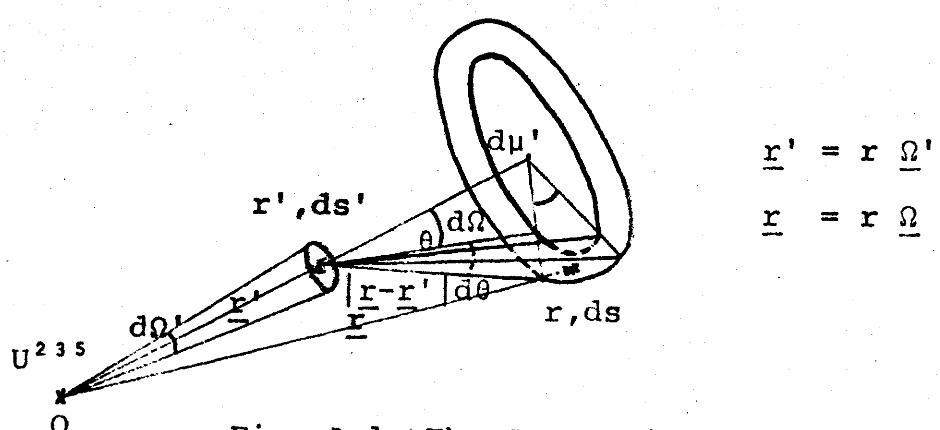

Fig. A-1 The Scattering of the Photon, at r' from $d\Omega'$ into $d\Omega = d\mu\,\sin\theta\;d\theta$

The photon flux due to photons described in Eq. (A-3) is $\phi'(r',\Lambda' \rightarrow \Lambda,\Omega',t)dr'$ divided by ds, the surface area seen by $d\Omega$, at r and,

$$ds = d\Omega|\underline{r}-\underline{r}'|^2 \qquad \text{(A-6)}$$

Define now, $\Sigma_D(\Lambda)$ and $\Sigma(\Lambda)$ to be respectively the photoneutron reaction and the attenuation cross section for photons of energy Λ in D_2O.

We can, then, write the total number of photoneutrons generated by photons having had one and only one collision, from an atom of U^{235} on an infinite medium of D_2O to be

$$S_1 = \int_{r',r,\Lambda',\Omega',\Omega} d\underline{r}'d\underline{r}d\Lambda'd\Omega'\psi'(r',\Lambda',\Omega',\infty)d^2{}_e\sigma(\Lambda' \rightarrow \Lambda)\underline{N}_{D_2O}Z \times \qquad \text{(A-7)}$$

$$\frac{1}{ds} e^{-\Sigma(\Lambda)|\underline{r}-\underline{r}'|} \Sigma_D(\Lambda),$$

where $\int_{r',r,\Lambda',\Omega',\Omega}$ denotes the integrations over the variables r',r,Λ',Ω' and Ω, and ∞ in $\psi'(r',\Lambda,\Omega',\infty)$ stands for $t = \infty$; that is, the atom of U^{235} being fissioned, we wait for all the gamma rays to come out of the fission products.

A-1 Calculation of S_1

To perform the calculation of S_1 we consider the Fig. B-2 (of Appendix B) where we have $a(\Lambda',t)$, the number of photons of energy Λ' emitted per sec., per Mev, t second(s) after the fission of an atom of U^{235} took place.

Then,

$$\psi'(r',\Lambda',\Omega',t) = \left\{\int_0^t a(\Lambda',t')dt'\right\} \frac{1}{4\pi} \times \frac{1}{ds'} e^{-\Sigma(\Lambda')r'}, \tag{A-8}$$

where

$$ds' = d\Omega' r'^2, \tag{A-9}$$

and

$$d\underline{r}' = r'^2 \sin\theta' \, d\theta' d\mu' dr' \tag{A-10}$$

in the spherical coordinate system relative to $0(U^{235})$.

Next notice,

$$d\underline{r} = ds\,d|\underline{r}-\underline{r}'|. \tag{A-11}$$

Eq. (A-7), through Equations (A-8) up to (A-11), thus becomes,

(A-12)

$$S_1 = \int_{r'=0}^{\infty} \int_{|\underline{r}-\underline{r}'|=0}^{\infty} \int_{\theta'=0}^{\pi} \int_{\theta=0}^{\pi} \int_{\mu'=0}^{\pi} \int_{\mu=0}^{\pi} \int_{\Lambda'=E_{th}}^{\infty}$$

$$\left\{\int^{\infty} a(\Lambda',t')dt'\right\} \frac{1}{4\pi} \sin\theta'\, d\theta' d\mu' dr' e^{-\Sigma(\Lambda')r'} d\Lambda'$$

$$d^2{}_e\sigma(\Lambda' \rightarrow \Lambda)\underline{N}_{D_2O} Z\Sigma_D(\Lambda) d|\underline{r}-\underline{r}'| e^{-\Sigma(\Lambda)|\underline{r}-\underline{r}'|}$$

where E_{th} is for the threshold energy for photoneutron reaction in D_2O (2.23 Mev).

Note that r', θ', μ' and $|\underline{r}-\underline{r}'|$ are independent variables and that μ comes into play within $d^2{}_e\,(\Lambda' \rightarrow \Lambda)$ only; thus define

$$d_e\sigma = \int_{\mu=0}^{2\pi} d^2{}_e\sigma. \tag{A-13}$$

Further define

$$A(\Lambda') = \int_0^\infty a(\Lambda',t)dt \qquad \text{(A-14)}$$

Next consider L photon groups (Fig. A-2) such that $\Lambda_\ell = \Lambda_{\ell-1} - \Lambda_\ell$ $(\ell = 1,\ldots,L)$ is small enough to replace $d\Lambda$.

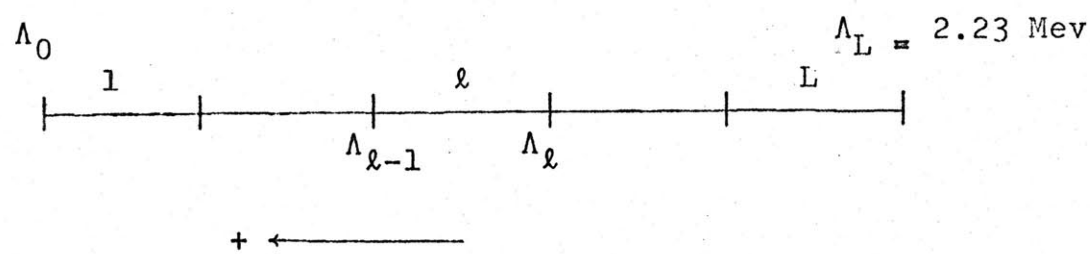

Fig. A-2 Photon energy groups

Then the scattering can be assumed to remove the photon into a lower energy group. Also the scattering cross section for photons of energy within such group, into a lower energy group, can be taken as constant and equal to $d^2{}_e\sigma(\bar{\Lambda}_\ell' \rightarrow \bar{\Lambda}_\ell)$, $\bar{\Lambda}_\ell'$ and $\bar{\Lambda}_\ell$ being the representative energies of the photon energy groups to which the photon belongs respectively before and after the scattering.

We define

$$A_\ell = \frac{1}{\Delta\Lambda_\ell}\int_{\Lambda_\ell}^{\Lambda_{\ell-1}} A(\Lambda)d\Lambda, \tag{A-15}$$

$$\Sigma_{D_\ell} = \frac{1}{\Delta\Lambda_\ell}\int_{\Lambda_\ell}^{\Lambda_{\ell-1}} \Sigma_D(\Lambda)d\Lambda \tag{A-16}$$

$$\Sigma_\ell = \frac{1}{\Delta\Lambda_\ell}\int_{\Lambda_\ell}^{\Lambda_{\ell-1}} \Sigma(\Lambda)d\Lambda \tag{A-17}$$

With the above remarks and definitions Eq. (A-12) can then be written as

$$S_1 = \underline{N}_{D_2O}Z \sum_{\ell'=1}^{L} A_{\ell'}\Delta\Lambda_{\ell'} \frac{1}{\Sigma_{\ell'}} \sum_{\ell=\ell'+1}^{L} d_e\sigma(\ell' \rightarrow \ell)\Sigma_{D_\ell} \times \frac{1}{\Sigma_\ell}, \tag{A-18}$$

where

$$d_e\sigma(\ell' \rightarrow \ell) \equiv \int_{\mu=0}^{2\pi} d^2{}_e\sigma(\overline{\Lambda}_{\ell'} \rightarrow \overline{\Lambda}_\ell) \text{ or precisely}$$

(A-19)

$$d_e\sigma(\ell' \rightarrow \ell) = \pi r_0^2\left(\frac{\overline{\Lambda}_\ell}{\overline{\Lambda}_{\ell'}}\right)^2\left(\frac{\overline{\Lambda}_{\ell'}}{\overline{\Lambda}_\ell} + \frac{\overline{\Lambda}_\ell}{\overline{\Lambda}_{\ell'}} - \sin^2\theta\right)\sin\theta\, d\theta,$$

with

$$\frac{1}{\bar{\Lambda}_\ell'} - \frac{1}{\bar{\Lambda}_\ell} = \frac{1-\cos\theta}{E_0} , \qquad \text{(A-20)}$$

$$\sin\theta\, d\theta = E_0 \frac{\Delta\Lambda_\ell}{\bar{\Lambda}_\ell^{\,2}} . \qquad \text{(A-21)}$$

Combining Equations (A-18) through (A-21) we finally have

$$S_1 = \pi \underline{N}_{D_2O} Z r_0^2 \sum_{\ell'=1}^{L-1} \underline{A}_\ell' \frac{1}{\Sigma_\ell'} \sum_{\ell=\ell'+1}^{L} \left(\frac{\bar{\Lambda}_\ell}{\bar{\Lambda}_\ell'}\right)^2 \left\{\frac{\bar{\Lambda}_\ell'}{\bar{\Lambda}_\ell} + \frac{\bar{\Lambda}_\ell}{\bar{\Lambda}_\ell'} - 1 + E_0^2\left(\frac{1}{E_0} + \frac{1}{\bar{\Lambda}_\ell} - \frac{1}{\bar{\Lambda}_\ell'}\right)^2\right\} E_0 \frac{\Delta\Lambda_\ell}{\bar{\Lambda}_\ell^{\,2}} \Sigma_{D_\ell} \times \frac{1}{\Sigma_\ell}, \qquad \text{(A-22)}$$

where

$$\underline{A}_\ell' = A_\ell' \Delta\Lambda_\ell' . \qquad \text{(A-23)}$$

A-2 Scheme for numerical application

The scheme presented in Table A-1 was the one adopted for numerical calculations and the

Table A-1

Photon Energy Groups to Compute S_1

ℓ	$\Lambda_{\ell-1}$ (Mev)	$\bar{\Lambda}_\ell$ (Mev)
1	6.00	5.000
2	4.00	3.500
3	3.00	2.875
4	2.75	2.625
5	2.50	2.365

Λ_ℓ: lower limit of energy group ℓ

$\bar{\Lambda}_\ell$: representative energy of group ℓ

determination of the relevant data ($\underline{A}_\ell$, Σ_{D_ℓ}, Σ_ℓ, $\ell=1,\ldots,5$) is discussed in the Appendix B.

Results are grouped in Table A-2.

Table A-2

Data to Compute S_1

ℓ	$\underline{A}_\ell$	$\sigma_{D_\ell} \times 10^{27}$ (cm^2)	Σ_ℓ (cm^2)
1	0.0692	----	---
2	0.141	2.25	0.0366
3	0.0518	1.70	0.0405
4	0.0804	1.20	0.0424
5	---	0.60	0.0448

Note that the number for $\underline{A}_{\ell}$'s* given in Table A-2 has been calculated for the time interval $2 \text{ sec.} \leq t \leq 10^3$ sec. To speak rigorously a correction ought to be made for those photoneutrons generated (by photons having had collisions) within 2 sec. and after 10^3 sec. the fission event took place. Nevertheless we show in this Appendix that photoneutrons generated by photons having had collisions can be neglected. Thus the time correction in question is omitted.

---

* The value, $\underline{A}_1$, of Table A-2 is 0.0692 whereas it would be 0.0650 as calculated from the last column of Table B-4. The difference is due to the fact that the latter number accounts for photons of the first energy group with an upper limit of only 6 Mev. Yet there are photons of energy beyond 6 Mev. An effort is made to include those photons in the first group. Thus an estimate of the number of photons, emitted from the fission products of an atom of U^{235}, of energy beyond 6 Mev is made through the enery dependence formula for photons of interest (cf. Appendix B, Fig. B-6): $6.22\, e^{-1.1\Lambda}$ $(\Lambda > 4 \text{ Mev})$. The number $\int_0^\infty 6.22\, e^{-1.1\Lambda}\, d\Lambda = 0.421 \times 10^2$, is then added to 0.0650 to obtain 0.0692. Note that $\frac{\sigma_D(\Lambda)}{\Sigma(\Lambda)}$ beyond 6 Mev is approximately constant.

In addition r_0 is taken to be 2.818×10^{-13} and $\underline{N}_{D_2O}$, 3.32×10^{22}.

A-3 Result and conclusion

The calculation for Equation (A-20) was carried out with a computer program shown in Appendix J. The result is

$$S_1 = 0.93 \times 10^{-4} \text{ photoneutrons/fission of } U^{235} \qquad \text{(A-24)}$$

On the other hand we learn from the Table B-1 of Appendix B that the total number of photoneutrons produced by photons from U^{235} fission products interacting with D_2O is 2.44×10^{-3}. We assume that the difference $(2.44 \times 10^{-3} - 0.093 \times 10^{-3})$ is due to those photoneutrons produced by the uncollided photons (that is an approximation of about 12% according to section B-2 of Appendix B). Thus, with an error of a few percent, — we note that this will be even less for a finite system as in the case of MITR-II, because of the leakage of a considerable number of photons out of the reactor (about 20% only of the fission photons are absorbed in the D_2O reflector of the Franco-German reactor ALIZE III) —, the photoneutrons due to photons having had collisions can be neglected.

APPENDIX B

CORRELATION BETWEEN THE DATA RELEVANT TO THE DELAYED PHOTONS FROM U^{235} FISSION PRODUCTS AND THE DATA RELEVANT TO THE DELAYED PHOTONEUTRONS GENERATED BY THOSE PHOTONS, IN D_2O

The purpose of this Appendix is to determine whether the data relevant to the generation of delayed photons from U^{235} fission products (Fig. B-1 and Fig. B-2) is consistent with the attenuation and photoneutron reaction cross sections of photons in D_2O (Fig. B-3 and Fig. B-4). If this is the case, then through those data one should be able to obtain the data relevant to the production of delayed photoneutrons by photons from U^{235} fission products in D_2O (cf. Table B-1).

To this end we consider the fission of one atom of U^{235} in an infinite medium of D_2O.

Let then $\underline{A}_\ell$ be the total number of photons within ℓ^{th} group of photons coming from the fission products of one atom of U^{235}, between 2 and 10^3 sec. after the fission event took place. For these photons let Σ_ℓ and Σ_{D_ℓ} be the attenuation and photoneutron reaction cross sections in D_2O.

Thus, taking into account only uncollided photons,

$$S_0 = \sum_{\ell=1}^{L} \underline{A}_\ell \Sigma_{D_\ell} \int_0^\infty \frac{1}{4\pi r^2} e^{-\Sigma_\ell r} 4\pi r^2 dr = \sum_{\ell=1}^{L} \underline{A}_\ell \frac{\Sigma_{D_\ell}}{\Sigma_\ell} \quad ,\text{(B-1)}$$

is the number of photoneutrons generated by photons coming from

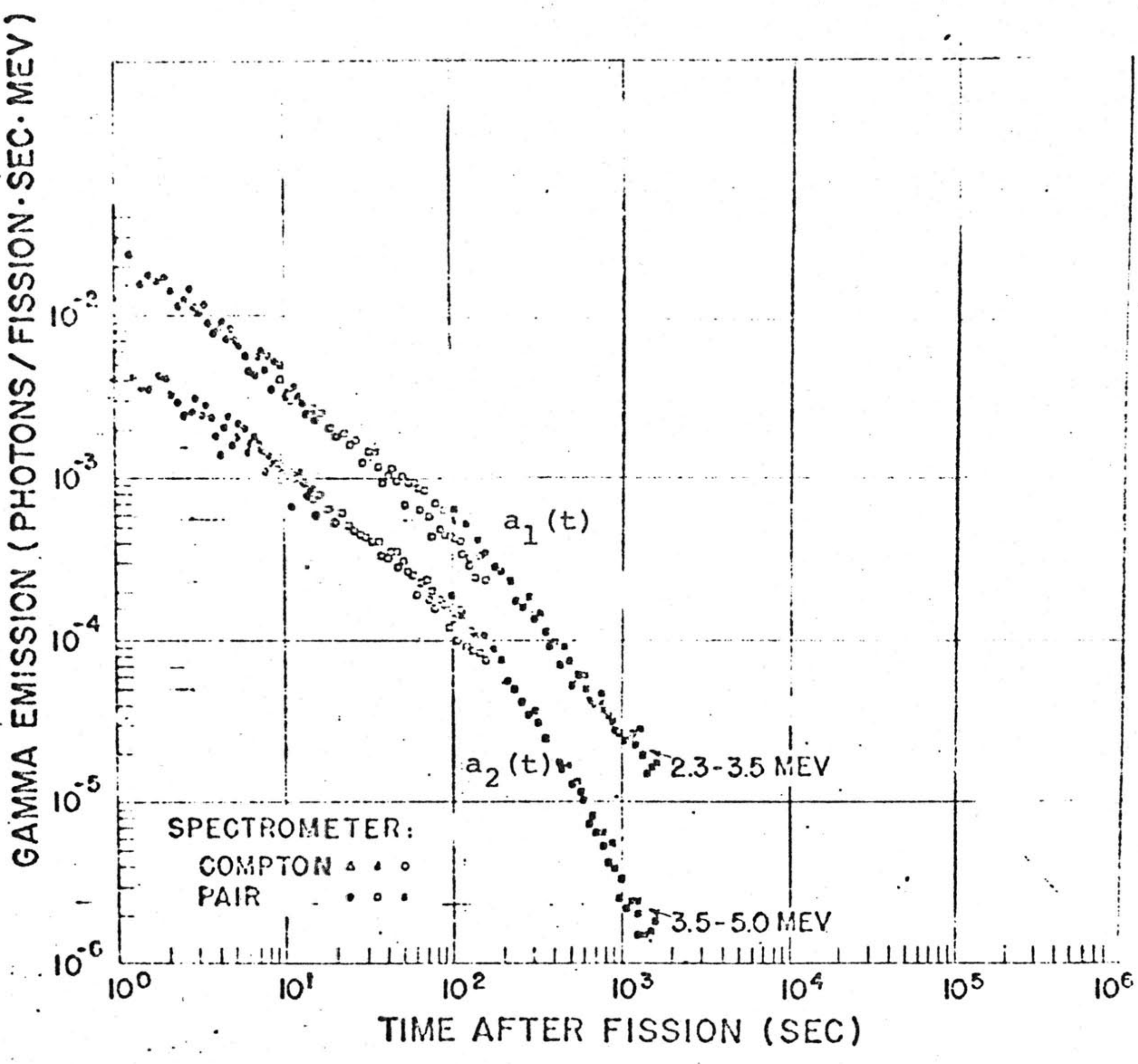

Fig. B-1 Time dependence of the emission of gamma rays that can give rise to the photoneutron reaction in D_2O, for long times after fission [12].

Table B-1 [16]

Half-Lives and Yields of Photoneutrons from U^{235} Fission Products in D_2O

Half-life	Photoneutron yield / 22-sec delayed-neutron yield	Photoneutrons(10^{-5}) / Fission
53 h	0.00074	0.25
4.4 h	0.00232	0.78
1.65 h	0.0168	5.65
27 m	0.0149	5.01
7.7 m	0.0242	8.14
2.4 m	0.0504	17.0
41 s	0.147	49.5
2.5 s	0.469	158.0

Sum $= 244.33 \times 10^{-5}$

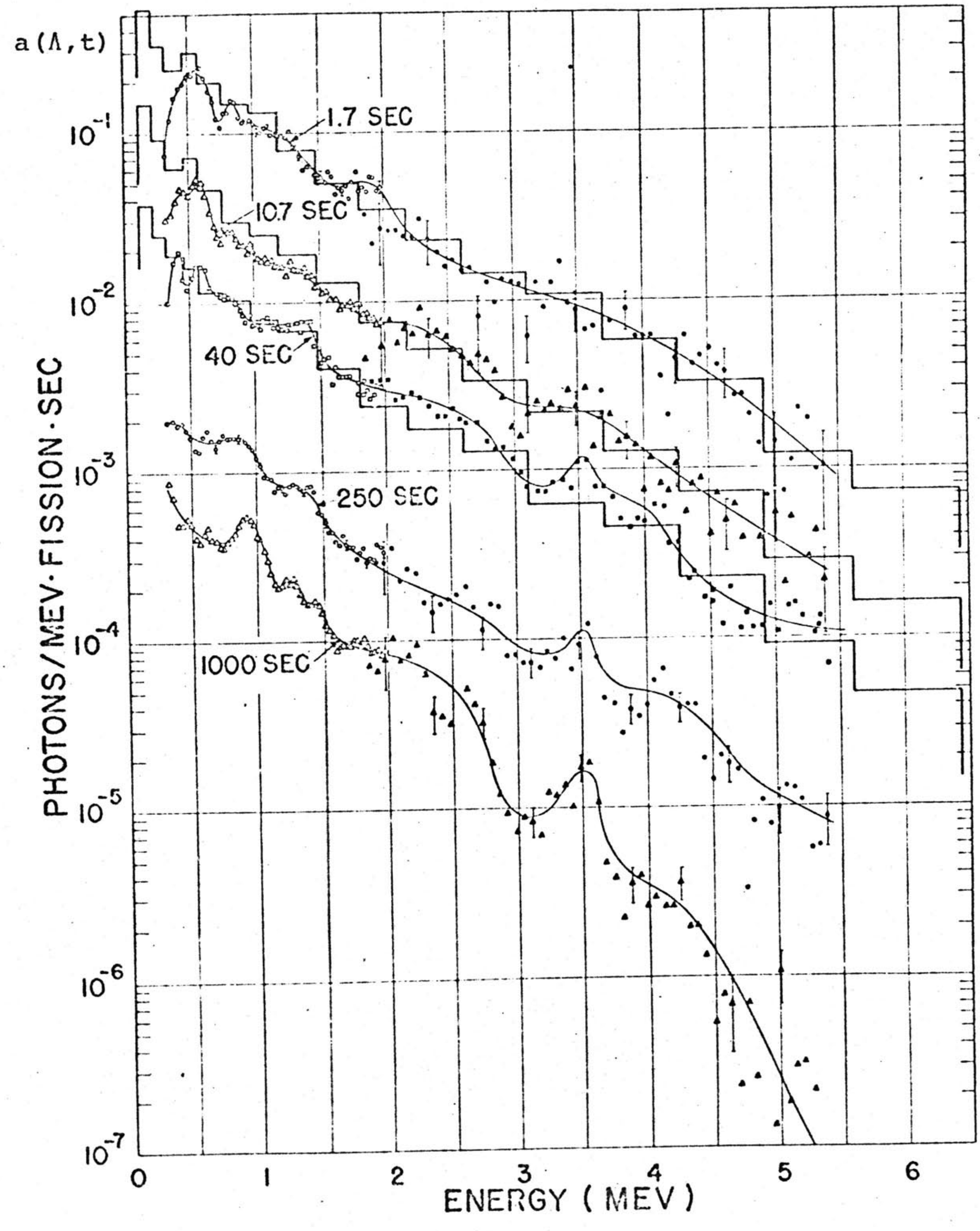

Fig. B-2 Gamma-ray spectra observed as a function of time after neutron fission of U^{235} [13]

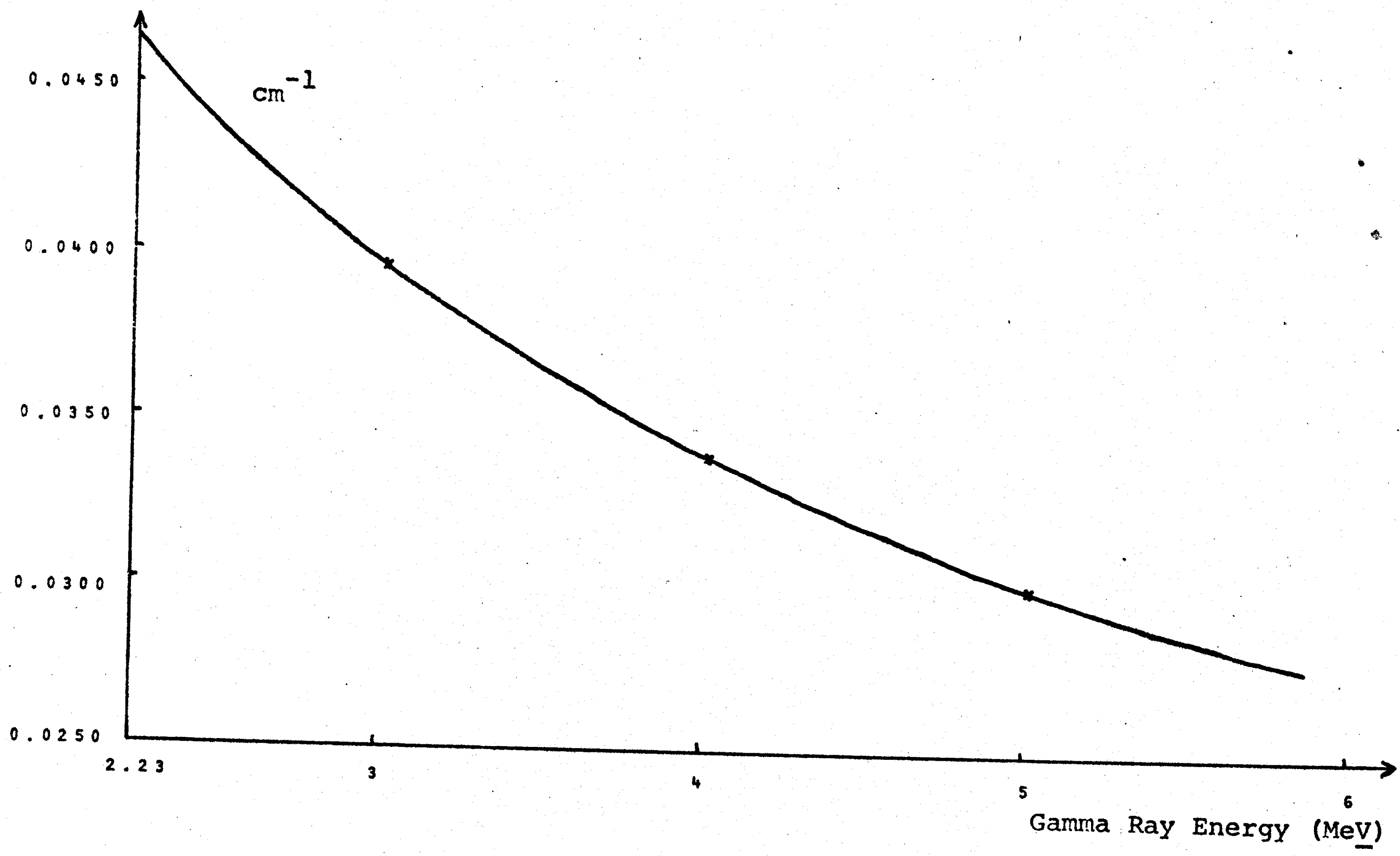

Fig. B-3 Total Gamma Ray Attenuation Cross Section in H_2O [14]

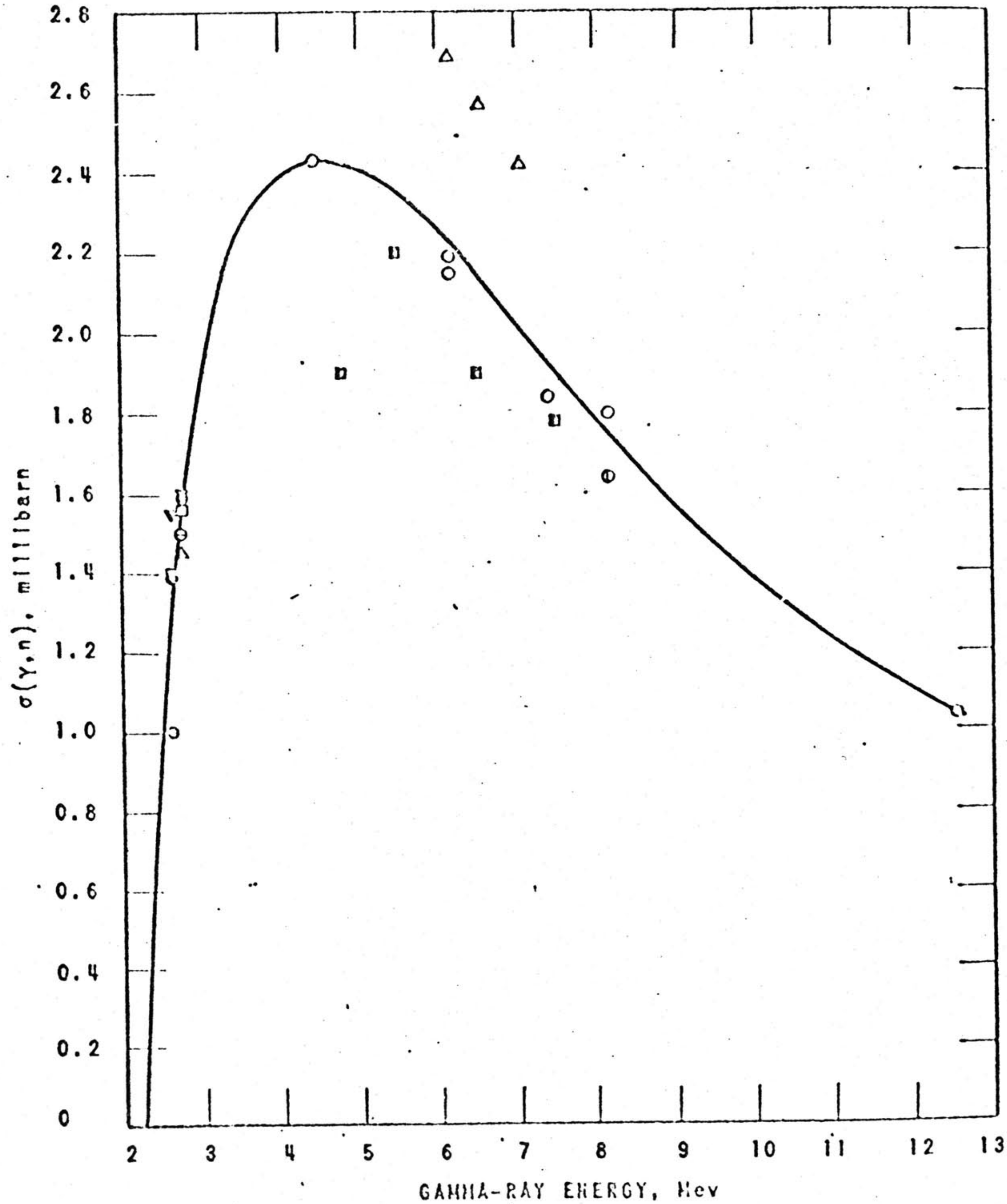

Fig. B-4 Photoneutron production cross section for deuterium [15] the fission products of one atom of U^{235}, placed in an infinite medium of D_2O, in the interval 2 sec. to 10^3 sec. after the fission event took place. (L is the number of photon groups.).

B-1 Calculation of $\underline{A}_\ell$

For the calculation of $\underline{A}_\ell$ we aim to obtain, starting with Fig. B-2, curves similar to the ones of Fig. B-1, but for more than two groups of photons. $\underline{A}_\ell$ will be then, the area under the ℓ^{th} curve (2 sec. $\leq t \leq 10^3$ sec.) multiplied by the width of the ℓ^{th} group of photons.

Actually we shall end by adopting the two-group scheme (cf. Fig. B-1). However at this stage of the development we do not know whether or not the photoneutrons produced in D_2O by photons of energy beyond 5 Mev (upper energy limit of photons sketched in Fig. B-1) can be neglected as compared to the photoneutrons produced by the less energetic photons. In addition we must prepare the material to be used in Appendix A (study of the photoneutrons produced by photons having had collisions), and that will require a scheme with more than two-group of photons. Also for a consistency check of the data we try to avoid possible errors due to the calculation of average cross sections for a few-group scheme.

$\underline{A}_\ell$ is accordingly first calculated in the following way for fifteen-groups of photons;

- Make up Table B-2 out of Fig. B-2, with $P_\ell(t)$ being the number of photons/Mev x fission x sec., belonging to the ℓ^{th} group of photons, versus time after fission;

- Then similarly to Fig. B-1, draw Fig. B-5, where we have for each of fifteen groups of photons, the decay of the fission products photons.

- Finally integrate graphically each of the curves of Fig. B-5 between t=2 sec. and $t=10^3$ sec. (cf. Table B-3) to make up Table B-4, where the product of this procedure, A_ℓ's (ℓ=1,..., 15 - the most energetic group bearing the number 15 -) are given, so that

$$\underline{A}_\ell = \Delta\Lambda_\ell A_\ell = \Delta\Lambda_\ell \int_2^{1000} P_\ell(t)\, dt, \quad \ell=1,\ldots, 15, \qquad \text{(B-2)}$$

where $\Delta\Lambda_\ell$ is the width of the ℓ^{th} group of photons.

Table B-2 Photon activity from Fission products of U^{235} versus time after the fission, for 15-group scheme

Energy group ℓ	Representative Energy (Mev) $\bar{\Lambda}_\ell$	Group Width (Mev)	Time after Fission (sec)	Photons/ Mev x fission x sec.
1	2.365	0.27	1.7	2.3×10^{-2}
			10.7	7.0×10^{-3}
			40	2.5×10^{-3}
			250	1.5×10^{-4}
			1000	4.0×10^{-5}
2	2.625	0.25	1.7	1.5×10^{-2}
			10.7	4.4×10^{-3}
			40	2.0×10^{-3}
			250	1.4×10^{-4}
			1000	4.0×10^{-5}
3	2.875	0.25	1.7	1.2×10^{-2}
			10.7	2.5×10^{-3}
			40	1.2×10^{-3}
			250	1.5×10^{-4}
			1000	1.0×10^{-5}
4	3.125	0.25	1.7	1.2×10^{-2}
			10.7	2.5×10^{-3}
			40	8.0×10^{-4}
			250	8.0×10^{-5}
			1000	9.0×10^{-6}

Energy group ℓ	Representative Energy (Mev) $\bar{\Lambda}_{\ell}$	Group Width (Mev)	Time after Fission (sec)	Photons/ Mev x fission x sec.
5	3.375	0.25	1.7	1.0×10^{-2}
			10.7	2.0×10^{-3}
			40	9.0×10^{-4}
			250	1.0×10^{-4}
			1000	3.0×10^{-5}
6	3.625	0.25	1.7	1.0×10^{-2}
			10.7	2.0×10^{-3}
			40	1.0×10^{-3}
			250	8.0×10^{-5}
			1000	1.0×10^{-5}
7	3.825	0.25	1.7	9.0×10^{-3}
			10.7	1.5×10^{-3}
			40	7.0×10^{-4}
			250	4.0×10^{-5}
			1000	4.0×10^{-6}
8	4.125	0.25	1.7	6.0×10^{-3}
			10.7	1.0×10^{-3}
			40	6.0×10^{-4}
			250	7.0×10^{-5}
			1000	3.0×10^{-6}

Table (B-2) (continued)

Energy group ℓ	Representative Energy (Mev) $\overline{\Lambda}_{\ell}$	Group Width (Mev)	Time after Fission (sec)	Photons/ Mev x fission x sec.
9	4.375	0.25	1.7	4.0×10^{-3}
			10.7	8.0×10^{-4}
			40	2.0×10^{-4}
			250	4.0×10^{-5}
			1000	2.0×10^{-6}
10	4.625	0.25	1.7	3.0×10^{-3}
			10.7	6.0×10^{-4}
			40	1.8×10^{-4}
			250	2.0×10^{-5}
			1000	1.0×10^{-6}
11	4.875	0.25	1.7	2.2×10^{-3}
			10.7	4.2×10^{-4}
			40	1.4×10^{-4}
			250	1.3×10^{-5}
			1000	4.0×10^{-7}
12	5.125	0.25	1.7	1.8×10^{-3}
			10.7	5.0×10^{-4}
			40	1.1×10^{-4}
			250	1.0×10^{-5}
			1000	1.8×10^{-7}

Energy group ℓ	Representative Energy (Mev) $\overline{\Lambda}_\ell$	Group Width (Mev)	Time after Fission (sec)	Photons/ Mev x fission x sec.
13	5.375	0.25	1.7	2.0×10^{-3}
			10.7	3.0×10^{-4}
			40	1.8×10^{-4}
			250	9.0×10^{-6}
			1000	1.0×10^{-7}
14	5.625	0.25	1.7	8.0×10^{-4}
			10.7	2.0×10^{-4}
			40	1.0×10^{-4}
			250	7.0×10^{-6}
			1000	3.0×10^{-8}
15	5.875	0.25	1.7	5.0×10^{-4}
			10.7	1.5×10^{-4}
			40	6.0×10^{-5}
			250	6.0×10^{-6}
			1000	1.0×10^{-8}

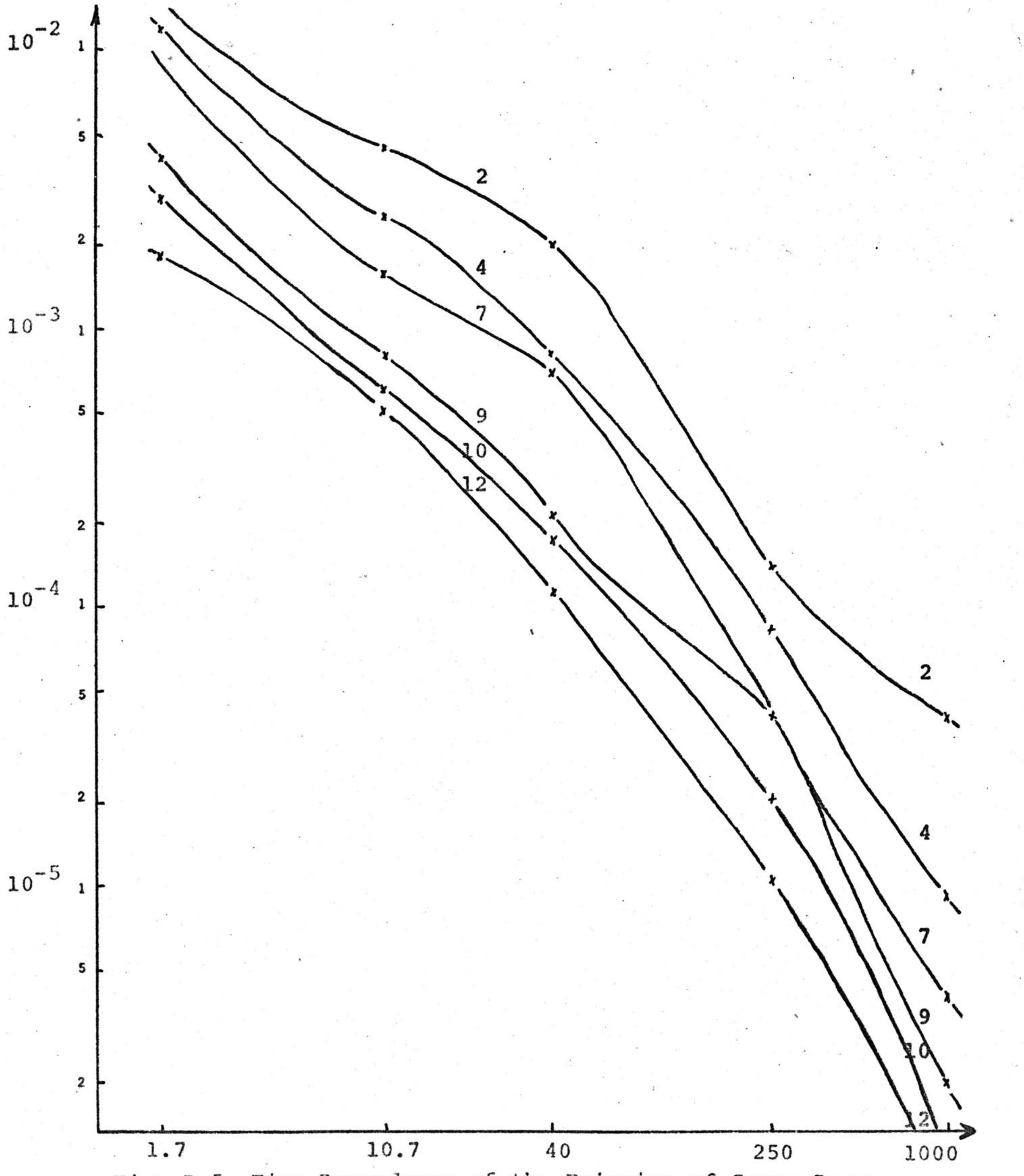

Fig. B-5 Time Dependence of the Emission of Gamma Rays Belonging to Various Energy Groups (cf. Table B-2)

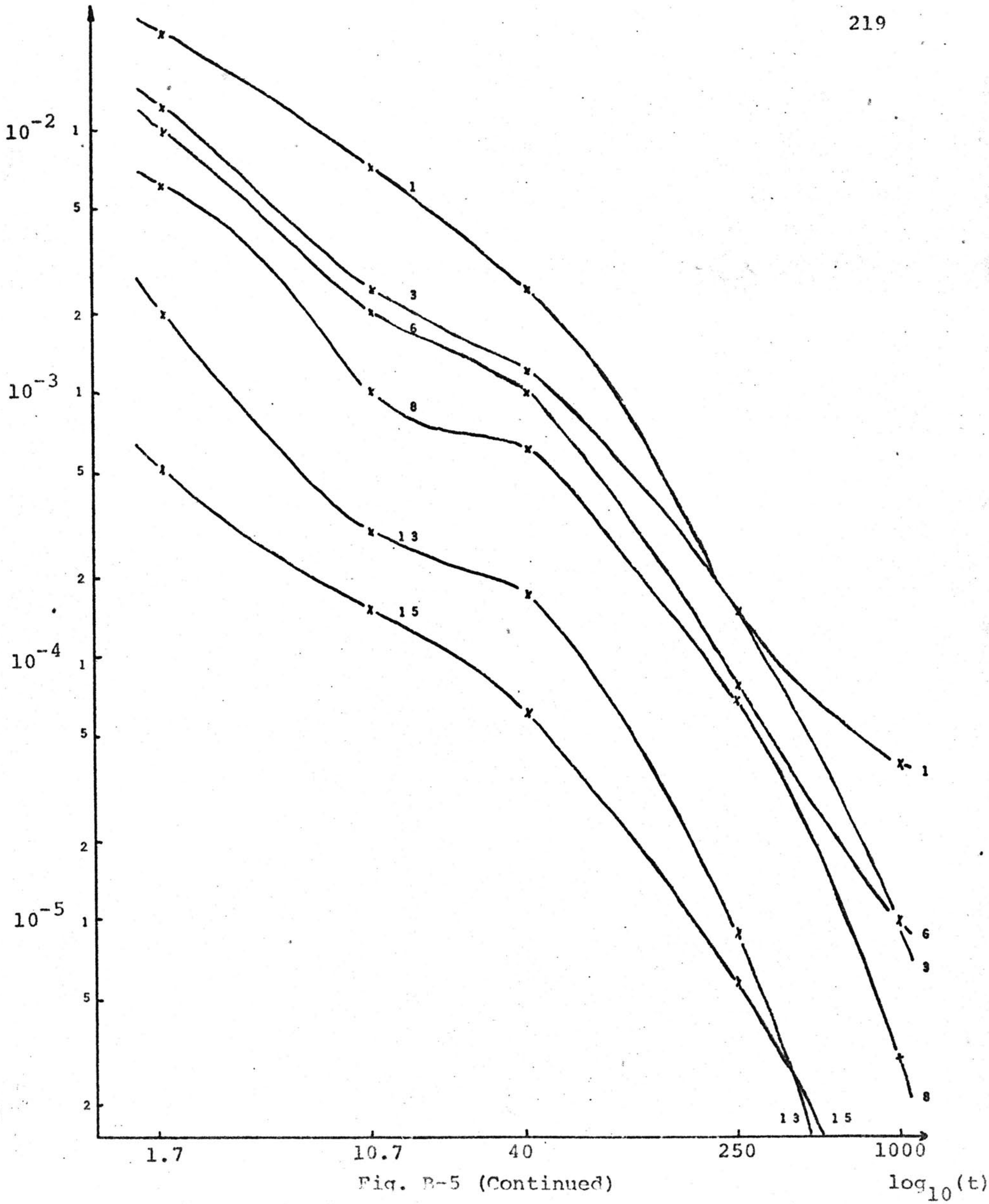

Fig. B-5 (Continued)

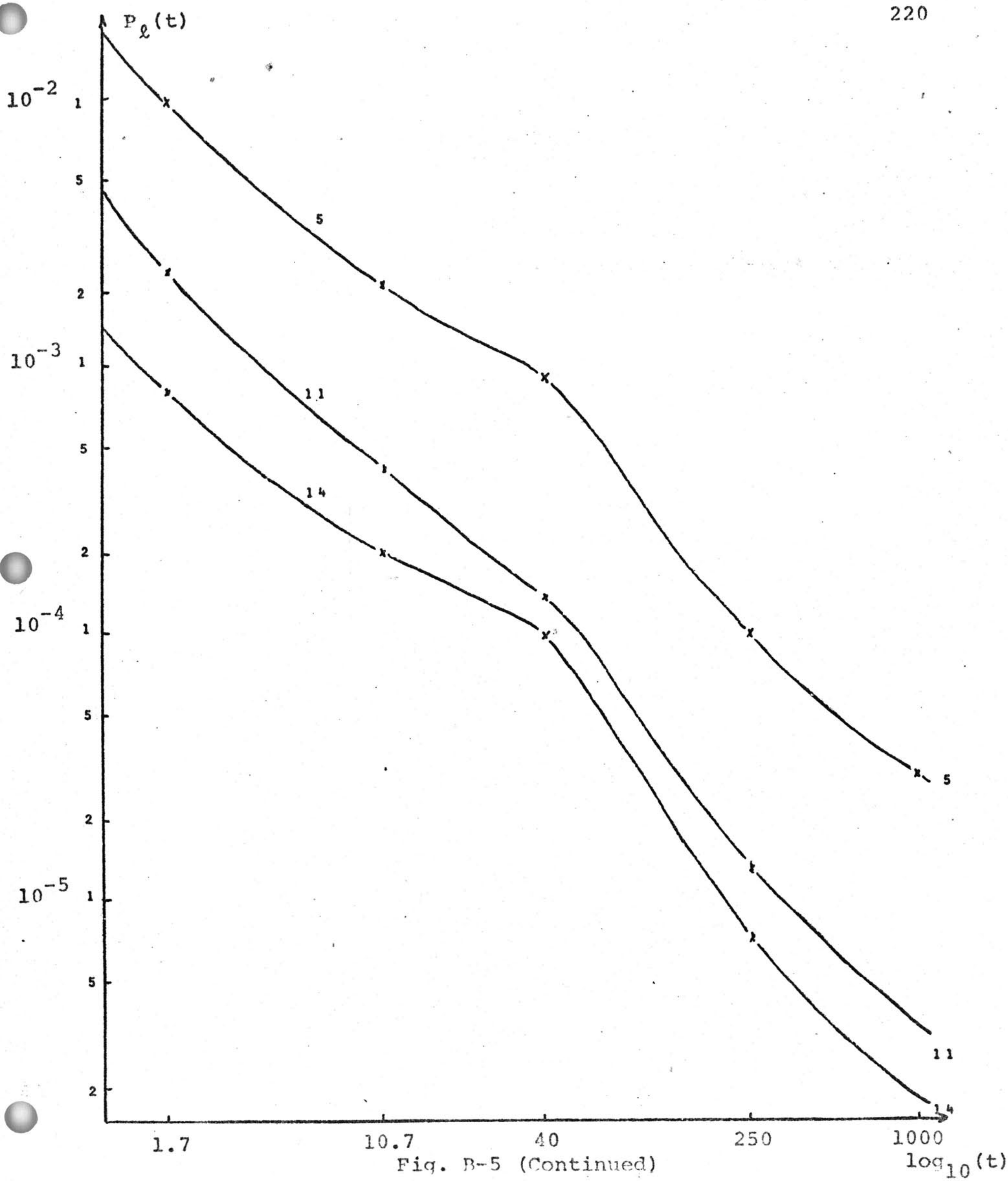

Fig. B-5 (Continued)

Table B-3 Graphical Integration of curves of Fig. B-5

t(sec) after fission	Δt (sec)	$P_1(t)$	$P_1(t)\Delta t$ $x10^2$	t(sec) after fission	Δt (sec)	$P_2(t)$	$P_2(t)\Delta t$ $x10^2$
2.5	1	$1.8x10^{-2}$	1.80	2.5	1	$1.3x10^{-2}$	1.30
3.5	1	$1.5x10^{-2}$	1.50	3.5	1	$1.1x10^{-2}$	1.10
5	2	$1.2x10^{-2}$	2.40	5	2	$9.\ x10^{-3}$	1.80
7	2	$1.0x10^{-2}$	2.00	7	2	$7.6x10^{-3}$	1.52
9	2	$8.\ x10^{-3}$	1.60	9	2	$6.5x10^{-3}$	1.30
15	10	$5.6x10^{-3}$	5.60	15	10	$4.5x10^{-3}$	4.50
25	10	$3.8x10^{-3}$	3.80	25	10	$3.0x10^{-3}$	3.00
35	10	$2.8x10^{-3}$	2.80	35	10	$2.3x10^{-3}$	2.30
50	20	$1.9x10^{-3}$	3.80	50	20	$1.5x10^{-3}$	3.00
70	20	$1.3x10^{-3}$	2.60	70	20	$1.0x10^{-3}$	2.00
90	20	$7.5x10^{-4}$	1.50	90	20	$7.0x10^{-3}$	1.40
125	50	$5.2x10^{-4}$	2.60	125	50	$4.5x10^{-4}$	2.25
175	50	$2.8x10^{-4}$	1.40	175	50	$2.5x10^{-4}$	1.25
250	100	$1.5x10^{-4}$	1.50	250	100	$1.4x10^{-4}$	1.40
350	100	$9.5x10^{-5}$	0.95	350	100	$9.0x10^{-4}$	0.90
450	100	$7.5x10^{-5}$	0.75	450	100	$7.0x10^{-5}$	0.70
600	200	$5.6x10^{-5}$	1.12	600	200	$5.5x10^{-5}$	1.10
850	300	$4.5x10^{-5}$	1.35	850	300	$4.4x10^{-5}$	1.32

$\int_2^{1000} P_1(t)dt \approx 39.07x10^{-2}$ $\int_2^{1000} P_2(t)dt \approx 32.14x10^{-2}$

Table B-3 (continued)

t(sec) after fis-sion	Δt (sec)	$P_3(t)$	$P_3(t)\Delta t$ $x10^2$	t(sec) after fis-sion	Δt (sec)	$P_4(t)$	$P_4(t)\Delta t$ $x10^2$
2.5	1	$7.0x10^{-3}$	7.0	2.5	1	$8.5x10^{-3}$	8.5
3.5	1	$6.0x10^{-3}$	6.0	3.5	1	$6.5x10^{-3}$	6.5
5	2	$4.5x10^{-3}$	9.0	5	2	$5.0x10^{-3}$	10.0
7	2	$3.5x10^{-3}$	7.0	7	2	$3.5x10^{-3}$	7.0
9	2	$3.0x10^{-3}$	6.0	9	2	$3.0x10^{-3}$	6.0
15	10	$2.0x10^{-3}$	20.0	15	10	$1.9x10^{-3}$	19.0
25	10	$1.5x10^{-3}$	15.0	25	10	$1.2x10^{-3}$	12.0
35	10	$1.3x10^{-3}$	13.0	35	10	$9.0x10^{-4}$	9.0
50	20	$1.0x10^{-3}$	20.0	50	20	$6.4x10^{-4}$	12.8
70	20	$8.0x10^{-4}$	16.0	70	20	$4.5x10^{-4}$	9.0
90	20	$6.0x10^{-4}$	12.0	90	20	$3.4x10^{-4}$	6.8
125	50	$4.5x10^{-4}$	22.5	125	50	$2.3x10^{-4}$	11.5
175	50	$2.7x10^{-4}$	13.5	175	50	$1.5x10^{-4}$	7.5
250	100	$1.5x10^{-4}$	15.0	250	100	$8.0x10^{-5}$	8.0
350	100	$9.0x10^{-5}$	9.0	350	100	$5.0x10^{-5}$	5.0
450	100	$5.5x10^{-5}$	5.5	450	100	$3.3x10^{-5}$	3.3
600	200	$3.2x10^{-5}$	6.4	600	200	$2.0x10^{-5}$	4.0
850	300	$1.5x10^{-5}$	4.5	850	300	$1.2x10^{-5}$	3.6

$$\int_2^{1000} P_3(t)dt \approx 207.4x10^{-3} \qquad \int_2^{1000} P_4(t)dt \approx 149.5x10^{-3}$$

Table B-3 (continued)

t(sec) after fission	Δt (sec)	$P_5(t)$	$P_5(t)\Delta t$ $\times 10^2$	t(sec) after fission	Δt (sec)	$P_6(t)$	$P_6(t)\Delta t$ $\times 10^2$
2.5	1	7.0×10^{-3}	7.0	2.5	1	7.0×10^{-3}	7.0
3.5	1	5.0×10^{-3}	5.0	3.5	1	5.0×10^{-3}	5.0
5	2	3.7×10^{-3}	7.4	5	2	3.7×10^{-3}	7.4
7	2	2.8×10^{-3}	5.6	7	2	2.8×10^{-3}	5.6
9	2	2.3×10^{-3}	4.6	9	2	2.3×10^{-3}	4.6
15	10	1.6×10^{-3}	16.0	15	10	1.6×10^{-3}	16.0
25	10	1.2×10^{-3}	12.0	25	10	1.25×10^{-3}	12.5
35	10	9.6×10^{-4}	9.6	35	10	1.1×10^{-3}	11.0
50	20	7.5×10^{-4}	15.0	50	20	8.0×10^{-4}	16.0
70	20	6.0×10^{-4}	12.0	70	20	6.0×10^{-4}	12.0
90	20	4.5×10^{-4}	9.0	90	20	4.5×10^{-4}	9.0
125	50	3.0×10^{-4}	15.0	125	50	2.6×10^{-4}	13.0
175	50	1.9×10^{-4}	9.5	175	50	1.5×10^{-4}	7.5
250	100	1.0×10^{-4}	10.0	250	100	7.0×10^{-4}	7.0
350	100	7.0×10^{-5}	7.0	350	100	5.0×10^{-5}	5.0
450	100	5.5×10^{-5}	5.5	450	100	3.5×10^{-5}	3.5
600	200	4.4×10^{-5}	8.8	600	200	2.2×10^{-5}	4.4
850	300	3.4×10^{-5}	13.2	800	300	1.3×10^{-5}	3.9

$$\int_2^{1000} P_5(t)\,dt \approx 172.2\times10^{-3} \qquad \int_2^{1000} P_6(t)\,dt \approx 150.4\times10^{-3}$$

Table B-3 (continued)

t(sec) after fission	Δt (sec)	$P_7(t)$	$P_7(t)\Delta t$ x10^3	t(sec) after fission	Δt (sec)	$P_8(t)$	$P_8(t)\Delta t$ x10^3
2.5	1	5.0×10^{-3}	5.0	2.5	1	3.2×10^{-3}	3.2
3.5	1	3.5×10^{-3}	3.5	3.5	1	2.3×10^{-3}	2.3
5	2	2.6×10^{-3}	5.2	5	2	1.7×10^{-3}	3.4
7	2	2.0×10^{-3}	4.0	7	2	1.3×10^{-3}	2.6
9	2	1.8×10^{-3}	3.6	9	2	1.2×10^{-3}	2.4
15	10	1.3×10^{-3}	13.0	15	10	8.6×10^{-3}	8.6
25	10	1.0×10^{-3}	10.0	25	10	7.0×10^{-4}	7.0
35	10	8.5×10^{-4}	8.5	35	10	6.4×10^{-4}	6.4
50	20	6.0×10^{-4}	12.0	50	20	5.0×10^{-4}	10.0
70	20	3.5×10^{-4}	7.0	70	20	3.5×10^{-4}	7.0
90	20	2.0×10^{-4}	4.0	90	20	2.5×10^{-4}	5.0
125	50	1.0×10^{-4}	5.0	125	50	1.5×10^{-4}	7.5
175	50	5.0×10^{-5}	2.5	175	50	9.0×10^{-5}	4.5
250	100	2.6×10^{-5}	2.6	250	100	5.0×10^{-5}	5.0
350	100	1.5×10^{-5}	1.5	350	100	2.8×10^{-5}	2.8
450	100	1.0×10^{-5}	1.0	450	100	1.8×10^{-5}	1.8
600	200	7.0×10^{-6}	1.4	600	200	1.0×10^{-5}	2.0
850	300	4.6×10^{-6}	1.38	850	300	3.0×10^{-6}	0.9

$$\int_2^{1000} P_7(t)dt \approx 90.18 \times 10^{-3} \qquad \int_2^{1000} P_8(t)dt \approx 82.4 \times 10^{-3}$$

Table B-3 (continued)

t(sec) after fission	Δt (sec)	$P_9(t)$	$P_9(t)\Delta t$ x10^3	t(sec) after fission	Δt (sec)	$P_{10}(t)$	$P_{10}(t)\Delta t$ x10^3
2.5	1	3.0×10^{-3}	3.00	2.5	1	2.2×10^{-3}	2.20
3.5	1	2.1×10^{-3}	2.10	3.5	1	1.6×10^{-3}	1.60
5	2	1.5×10^{-3}	3.00	5	2	1.2×10^{-3}	2.40
7	2	1.1×10^{-3}	2.20	7	2	9.0×10^{-4}	1.80
9	2	9.5×10^{-4}	1.90	9	2	7.5×10^{-4}	1.50
15	10	5.8×10^{-4}	5.80	15	10	4.6×10^{-4}	4.60
25	10	3.6×10^{-4}	3.60	25	10	2.9×10^{-4}	2.90
35	10	2.7×10^{-4}	2.70	35	10	2.1×10^{-4}	2.10
50	20	2.0×10^{-4}	4.00	50	20	1.5×10^{-4}	3.00
70	20	1.4×10^{-4}	2.80	70	20	1.0×10^{-4}	2.00
90	20	1.1×10^{-4}	2.20	90	20	8.0×10^{-5}	1.60
125	50	8.5×10^{-5}	4.25	125	50	5.2×10^{-5}	2.60
175	50	6.0×10^{-5}	3.00	175	50	3.5×10^{-5}	1.75
250	100	4.0×10^{-5}	4.00	250	100	2.1×10^{-5}	2.10
350	100	2.5×10^{-5}	2.50	350	100	1.2×10^{-5}	1.20
450	100	1.4×10^{-5}	2.80	450	100	7.0×10^{-6}	1.40
600	200	7.0×10^{-6}	1.40	600	200	3.5×10^{-6}	0.70
850	300	3.3×10^{-6}	0.66	850	300	1.7×10^{-6}	0.34

$\int_2^{1000} P_9(t)dt \approx 51.91\times10^{-3}$ $\int_2^{1000} P_{10}(t)dt \approx 35.79\times10^{-3}$

Table B-3 (continued)

t(sec) after fis-sion	Δt (sec)	$P_{11}(t)$	$P_{11}(t)\Delta t$ $x10^3$	t(sec) after fis-sion	Δt (sec)	$P_{12}(t)$	$P_{12}(t)\Delta t$ $x10^3$
2.5	1	$1.6x10^{-3}$	1.60	2.5	1	$1.4x10^{-3}$	1.40
3.5	1	$1.2x10^{-3}$	1.20	3.5	1	$1.15x10^{-3}$	1.15
5	2	$8.5x10^{-4}$	1.70	5	2	$9.0x10^{-4}$	1.80
7	2	$6.5x10^{-4}$	1.30	7	2	$7.0x10^{-4}$	1.40
9	2	$5.3x10^{-4}$	1.06	9	2	$6.0x10^{-4}$	1.20
15	10	$3.3x10^{-4}$	3.30	15	10	$3.7x10^{-4}$	3.70
25	10	$2.1x10^{-4}$	2.10	25	10	$2.0x10^{-4}$	2.00
35	10	$1.5x10^{-4}$	1.50	35	10	$1.3x10^{-4}$	1.30
50	20	$1.1x10^{-4}$	2.20	50	20	$8.5x10^{-5}$	1.70
70	20	$7.5x10^{-5}$	1.50	70	20	$5.5x10^{-5}$	1.10
90	20	$5.8x10^{-5}$	1.16	90	20	$4.0x10^{-5}$	0.80
125	50	$3.8x10^{-5}$	1.90	125	50	$2.5x10^{-5}$	1.25
175	50	$2.5x10^{-5}$	1.25	175	50	$1.7x10^{-5}$	0.85
250	100	$1.3x10^{-5}$	1.30	250	100	$1.0x10^{-5}$	1.00
350	100	$7.0x10^{-6}$	0.70	350	100	$5.0x10^{-6}$	0.50
450	100	$3.5x10^{-6}$	0.70	450	100	$2.0x10^{-6}$	0.40
600	200	$1.6x10^{-6}$	0.32	600	200	$8.0x10^{-7}$	0.16
850	300	$6.8x10^{-7}$	0.14	850	300	$3.0x10^{-7}$	0.06

$$\int_2^{1000} P_{11}(t)dt \approx 24.93x10^{-3} \qquad \int_2^{1000} P_{12}(t)dt \approx 21.77x10^{-3}$$

Table B-3 (continued)

t(sec) after fis- sion	Δt (sec)	$P_{13}(t)$	$P_{13}(t)\Delta t$ $x10^{3}$	t(sec) after fis- sion	Δt (sec)	$P_{14}(t)$	$P_{14}(t)\Delta t$ $x10^{4}$
2.5	1	$1.4x10^{-3}$	1.40	2.5	1	$5.5x10^{-4}$	5.5
3.5	1	$9.5x10^{-4}$	0.95	3.5	1	$4.0x10^{-4}$	4.0
5	2	$6.5x10^{-4}$	1.30	5	2	$3.2x10^{-4}$	6.4
7	2	$4.5x10^{-4}$	0.90	7	2	$2.5x10^{-4}$	5.0
9	2	$3.7x10^{-4}$	0.74	9	2	$2.3x10^{-4}$	4.6
15	10	$2.6x10^{-4}$	2.60	15	10	$1.7x10^{-4}$	17.0
25	10	$2.1x10^{-4}$	2.10	25	10	$1.3x10^{-4}$	13.0
35	10	$1.9x10^{-4}$	1.90	35	10	$1.1x10^{-4}$	11.0
50	20	$1.3x10^{-4}$	2.60	50	20	$7.0x10^{-5}$	14.0
70	20	$6.5x10^{-5}$	1.30	70	20	$4.5x10^{-5}$	9.0
90	20	$5.0x10^{-5}$	1.00	90	20	$3.3x10^{-5}$	6.6
125	50	$3.0x10^{-5}$	1.50	125	50	$2.0x10^{-5}$	10.0
175	50	$1.7x10^{-5}$	0.85	175	50	$1.2x10^{-5}$	6.0
250	100	$9.0x10^{-6}$	0.90	250	100	$6.0x10^{-6}$	6.0
350	100	$4.5x10^{-6}$	0.45	350	100	$2.7x10^{-6}$	2.7
450	100	$1.7x10^{-6}$	0.34	450	100	$8.0x10^{-6}$	1.6
600	200	$5.5x10^{7}$	0.11	600	200	$2.3x10^{-6}$	0.5
850	300	$1.7x10^{-7}$	0.04	850	300	$7.0x10^{-6}$	0.1

$$\int_2^{1000} P_{13}(t)dt \approx 20.98x10^{-3} \qquad \int_2^{1000} P_{14}(t)dt \approx 12.30x10^{-3}$$

Table B-3 (continued)

t(sec) after fission	Δt(sec)	$P_{15}(t)$	$P_{15}(t)\Delta t \times 10^4$
2.5	1	3.5×10^{-4}	3.5
3.5	1	1.8×10^{-4}	1.8
5	2	2.2×10^{-4}	4.4
7	2	1.8×10^{-4}	3.6
9	2	1.7×10^{-4}	3.4
15	10	1.2×10^{-4}	12.0
25	10	8.5×10^{-5}	8.5
35	10	6.5×10^{-5}	6.5
50	20	5.0×10^{-5}	10.0
70	20	3.5×10^{-5}	7.0
90	20	2.6×10^{-5}	5.2
125	50	1.7×10^{-5}	8.5
175	50	1.0×10^{-5}	5.0
250	100	5.5×10^{-6}	5.5
350	100	2.5×10^{-6}	2.5
450	100	9.0×10^{-7}	1.8
600	200	2.1×10^{-7}	0.44
850	300	4.0×10^{-8}	0.08

$$\int_{2}^{1000} P_{15}(t)dt \approx 89.72 \times 10^{-4}$$

Table (B-4) A_ℓ's for fifteen groups of photons

Energy group ℓ	Representative energy $\bar{\Lambda}_\ell$ (Mev)	$\Delta\bar{\Lambda}_\ell$ (Mev)	A_ℓ: Photons/Mev x fission
1	2.365	0.27	0.3907
2	2.625	0.25	0.3214
3	2.875	0.25	0.2074
4	3.125	0.25	0.1495
5	3.375	0.25	0.1722
6	3.625	0.25	0.1504
7	3.825	0.25	0.0902
8	4.125	0.25	0.0824
9	4.375	0.25	0.0519
10	4.625	0.25	0.0358
11	4.875	0.25	0.0249
12	5.125	0.25	0.0218
13	5.375	0.25	0.0210
14	5.625	0.25	0.0123
15	5.825	0.25	0.0090

$\Delta\bar{\Lambda}_\ell$; width of ℓ^{th} group

We point out that later in the library of the code POPOP IV (cf. Appendix D) we found numbers for $\underline{A}_\ell$'s (photons from the fission of U^{235}, t $\geq$ 1 sec.) presented below;

ℓ	Λ_ℓ (Mev)	$\underline{A}_\ell$
1	2.2	3.40500 E-1
2	2.6	2.27500 E-1
3	3.0	1.27860 E-1
4	3.5	9.41499 E-2
5	4.0	6.93300 E-2
6	4.5	3.36500 E-2
7	5.0	1.61900 E-2
8	5.5	7.77000 E-3
9	6.0	0.

where Λ_ℓ refers to the upper energy limit of the ℓ^{th} group, and yE-n stands for y x 10^{-n}.

We note that (although slightly higher) these numbers check against our results (11.917 E-2 and 39.264 E-2 against 9.9 E-2 and 34.8 E-2 of Table B-7 - presented further -.In addition according to those numbers of the library of the code POPOP IV we have: 12.694 E-2 for the energy interval 3.5 Mev - 10 Mev, and 43.246 E-2 for the energy interval 2.23 Mev - 3.5 Mev.).

B-2 Calculation of $S_0 = \sum_{\ell=1}^{L} \underline{A}_\ell \frac{\Sigma_{D\ell}}{\Sigma_\ell}$

One can then with the help of Fig. B-3 , Fig. B-6 and Table B-4 , make up the Table B-5 , where the last column multiplied by $\Delta\Lambda_\ell$ and summed over ℓ furnishes the result of Eq. (B-1) .

Table B-5 Calculation of $A_\ell\ \sigma_{D_\ell}/\Sigma_\ell$

Energy group ℓ	$\Sigma_\ell \times 10^2$ (cm^{-1})	σ_{D_ℓ} (mb)	$A_\ell \frac{\sigma_{D_\ell}(mb)}{\Sigma_\ell(cm^{-1})}$
1	4.48	0.60	5.24
2	4.24	1.20	9.10
3	4.05	1.70	8.72
4	3.88	2.10	8.11
5	3.73	2.20	10.15
6	3.58	2.30	9.66
7	3.45	2.37	6.21
8	3.33	2.40	5.93
9	3.23	2.44	3.92
10	3.13	2.42	2.87
11	3.05	2.41	1.965
12	2.96	2.40	1.770
13	2.90	2.37	1.720
14	2.83	2.30	1.00
15	2.77	2.26	0.735

That is, $S_0 = (\sum_{\ell=1}^{15} A_\ell \frac{\sigma_{D_\ell}}{\Sigma_\ell} \Delta\Lambda_\ell) \times 2 \times \underline{N}_{D_2O} = 19.42 \times 2 \times 3.32 \times 10^{-5}$

$= 1.29 \times 10^{-3}$ photoneutrons/fission of U^{235}, 2 sec.$\leq t \leq 10^3$ sec.

This answer is to be compared to the summation of the number presented in the last column of Table B-1, that is 2.44×10^{-3} photoneutrons/fission of U^{235}. However one should notice that in the course of the calculation of the number S_0 above, we have dealt with photons of energy up to 6 Mev only, whereas some of the photoneutrons will be produced by photons of energy beyond 6 Mev. In addition we have taken into account photons generated between t = 2 sec. and t = 10^3 sec. only, whereas delayed photons appearing within 2 sec. or 10^3 sec. after the fission, will also give rise to photoneutrons. Thus the number for S_0, found above should be corrected accordingly before being compared to 2.44×10^{-3}, result of Table B-1.

B-2-1 Estimation of photoneutrons produced by photons of energy beyond 6 Mev.

In order to estimate the number of photoneutrons produced by photons of energy beyond 6 Mev, coming from the fission products of U^{235}, in an infinite medium of D_20 between t=2 sec. and t=10^3 sec. after fission, we draw the last column of Table B-5 versus the second column of Table B-4 for $\bar{\Lambda}_\ell \geq$ 4 Mev , that is Fig. B-6 (where, the last column of Table B-4 versus the second column of Table B-4 is also plotted-bottom curves- for $\bar{\Lambda}_\ell \geq$ Mev., for use in Appendix A, section A-2). We then approximate the photoneutrons produced by photons of energy beyond

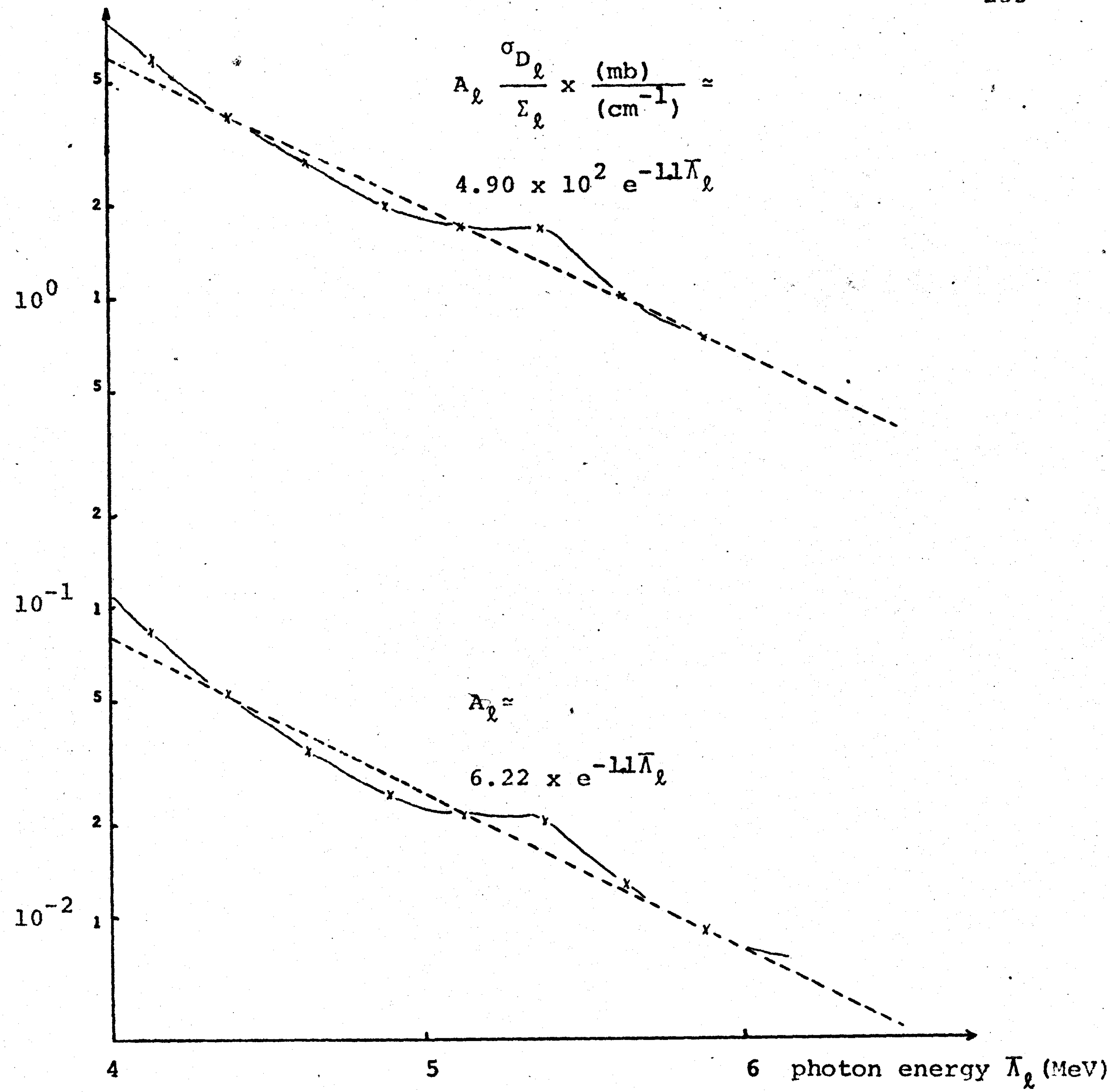

Fig. B-6 For extrapolation beyond 6 MW, the total number of photons from fission products of U^{235} versus energy ($\geq$ 4MeV) - bottom curve and the total number of photoneutrons produced by those photons - upper curve are approximated by straight lines

6 Mev by $\int_{6}^{\infty} 4.9 \times 10^{2} e^{-1.1\Lambda} d\Lambda \approx 0.62$, that is to be added to 19.42. With this S_0 becomes 1.34×10^{-3} photoneutrons/fission of U^{235}, 2 sec. $\leq t \leq 10^3$ sec.

B-2-2 Time correction brought to the total number of photoneutrons produced per fission of U^{235}.

In order to compare the result of Table B-1, that is the number 2.44×10^{-3}, to the number S_0 we obtained, we have to remove from the former,the number of photoneutrons produced within 2 sec. and after 10^3 sec. the fission of U^{235} took place; since N has been calculated for the interval of time 2 sec. $\leq t \leq 10^3$ sec.

We assume that, a photoneutron decaying with one of the half lifes shown in Table B-1, implies there must be a photon appearing with that same half life, that creates the photoneutron in question. Thus we let $N_{0_j}(1-e^{-\lambda_j t})$ be the total number of j^{th} -time wise- group of photons emitted until t. Then, assuming that there is only one energy-group of photons with $\overline{\Sigma}$ and $\overline{\Sigma}_D$ being the average attenuation and photoneutron reaction cross sections of photons in D_2O, to achieve the "time correction" the number 2.44×10^{-3} should be multiplied by

$$C = \frac{\frac{\overline{\Sigma}_D}{\overline{\Sigma}} \sum_j \left[N_{0_j}(1-e^{-\lambda_j x 10^3}) - N_{0_j}(1-e^{-\lambda_j x 2}) \right]}{\frac{\overline{\Sigma}_D}{\overline{\Sigma}} \sum_j N_{0_j}} \qquad \text{(B-3)}$$

Defining y_j to be the yield of a photon of j^{th} time group, and noting

$$N_{0_j} = N_o\, y_j \quad , \tag{B-4}$$

where

$$N_0 = \sum_j N_{0_j} \quad , \tag{B-5}$$

and $\sum_j y_j = 1$, we find that C becomes

$$C = \sum_j y_j \left(e^{-\lambda_j \times 2} - e^{-\lambda_j \times 10^3}\right) \quad . \tag{B-6}$$

y_j's are presented in Table B-6, being calculated from the information of Table B-1.

Table B-6 Yield of a photoneutron of -time wise-group j

j	λ_j	y_j
1	2.77×10^{-1}	0.647
2	1.69×10^{-2}	0.2025
3	4.81×10^{-3}	6.97×10^{-2}
4	1.50×10^{-3}	3.34×10^{-2}
5	4.28×10^{-4}	2.05×10^{-2}
6	1.17×10^{-4}	2.31×10^{-2}
7	4.37×10^{-5}	3.19×10^{-3}
8	3.63×10^{-6}	1.008×10^{-3}
9	6.26×10^{-7}	0.496×10^{-3}

The calculation of C from Eq. (B-6) then gives $C \approx 0.67$.

*

We should also include with the number S_0 the number of photoneutrons produced by photons having had one and only one collision (calculated in Appendix A), that is $S \approx 1.345 \times 10^{-3} + 0.93 \times 10^{-4} = 1.44 \times 10^{-3}$ photoneutrons/fission of U^{235}. This is now to be compared to the number $2.44 \times 10^{-3} \times 0.673 \approx 1.64 \times 10^{-3}$ photoneutrons/fission of U^{235}. The agreement is satisfactory (for a difference of about 12%, which is we think, partially due to the procedure of calculation, graphical integrations etc.).

Hence we conclude the data relevant to the generation of photons from U^{235} fission products and the attenuation and photoneutron reaction cross sections of those photons in D_2O, are consistent.

B-3 The two group scheme of Fig. B-1

The upper curve of Fig. B-6 suggests that the photoneutrons produced by photons of energy beyond 5 Mev (that is $\int_5^\infty 4.9 \times 10^2 \, e^{-1.1\Lambda} d\Lambda$) can be neglected (within an error of about 8%). We also have shown we do not have to carry photoneutron generated by photons having had collisions (cf. Appendix A) that required a multigroup scheme. Henceforth we can adopt instead of the complicated fifteen-group scheme derived from Fig. B-2, the two-group scheme already presented in Fig. B-1 (2.3 Mev $\leq \Lambda \leq$ 5 Mev, 1 sec. $\leq t \leq 10^3$ sec).

The relevant numbers are shown in Table B-7.

Table B-7 The two-group photon scheme

ℓ	$\Lambda_{\ell-1}$ (Mev)	$\Delta\Lambda_\ell$ (Mev)	$\underline{A}_\ell \times 10^2$	$\Sigma_\ell (cm^{-1}) \times 10^2$	σ_{D_ℓ} (mb)
1	7	1.5	9.9	3.28	2.39
2	3.5	1.2	34.8	4.00	1.56

$\Lambda_2 = 2.3$ Mev

In Table B-7

$$\underline{A}_\ell = A_\ell \, \Delta\Lambda_\ell \quad , \quad \ell = 1,2, \qquad \text{(B-7)}$$

and A_ℓ is obtained by integration of the curves of Fig. B-1 between t = 1 sec. and t = 10^3 sec. For this purpose we approximated the two curves of Fig. B-1, by two equations each; specifically we found for the upper curve of Fig. B-1;

$$a_1(t) = 6 \times 10^{-3} \, t^{-0.816} \quad , \quad \text{sec} \leq t \leq 10^2 \text{ sec}, \qquad \text{(B-8)}$$

$$a_1(t) = 3.83 \quad t^{-2.084}, \quad 10^2 \text{ sec.} \leq t \leq 10^3 \text{ sec}, \qquad \text{(B-9)}$$

and for the lower curve of Fig. B-1 ;

$$a_2(t) = 3.0 \times 10^{-2} \, t^{-0.85} \quad , \quad 1 \text{ sec.} \leq t \leq 10^2 \text{ sec.}, \qquad \text{(B-10)}$$

$$a_2(t) = 3.75 \times 10^{-1} \, t^{-1.398} \quad , \quad 10^2 \text{ sec.} \leq t \leq 10^3 \text{ sec.} \qquad \text{(B-11)}$$

In addition Σ_ℓ and σ_{D_ℓ} (ℓ = 1,2) were collapsed from the fifteen-group data. We neglect the photoneutrons generated by photons of energy beyond 5 Mev. and also the photoneutrons generated by photons having had collisions. We then estimate through the two-group scheme of Table B-7 the number of the photoneutrons produced by the delayed photons from the fission products of an atom of U^{235} placed in the middle of an infinite medium of D_2O. The result agrees with the data: 2.44×10^{-3} of Table B-1, within 30% of error.

[It is worthwhile to mention that using $\underline{A}_\ell$'s computed through the numbers (presented above) of the library of the code POPOP IV ($\underline{A}_1 = 12.694 \times 10^{-2}$, $\underline{A}_2 = 43.246 \times 10^{-2}$), the data shown in Table B-7, and the result of Appendix A, the agreement with the data: 2.44×10^{-3} of Table B-1 falls within 6% of error.]

B-4 Representation of Fig. B-1 in terms of the data of Table B-1

We were able to reproduce the data of Table B-1, having started with the data relevant to Fig. B-2 or Fig. B-1. This suggests that we can describe the emission of the gamma rays from U^{235} fission products, of sufficient energy to produce photoneutron reaction in D_2O , by

$$a_\ell(t) = \frac{1}{\Delta\Lambda_\ell} Y_\ell \sum_{j=1}^{J} \lambda_j y_j N_0 e^{-\lambda_j t} , \qquad \text{(B-12)}$$

with $\Delta\Lambda_\ell$, the width of the ℓ^{th} photon group. Y_ℓ is the probability that a fission product photon of sufficient energy to produce photoneutron reaction in D_2O, appears within the ℓ^{th} group (assuming that this probability is not a function of time). λ_j is the decay constant of the j^{th} (j=1,...,j) group shown in Table B-1. y_j's are presented in Table B-6 and N_0 is defined through Eq. (B-5). Y_ℓ is represented by [17];

$$Y_\ell = \frac{\int_{\Lambda_\ell}^{\Lambda_\ell -1} 1.1\, e^{-1.1\Lambda}\, d\Lambda}{\int_{2.23}^{\infty} 1.1\, e^{-1.1\Lambda}\, d\Lambda} \tag{B-13}$$

(cf. also the lower curve of Fig. B-6). That is for the two-group scheme we make up the Table B-8.

Table B-8 Y_ℓ, ℓ = 1,2

ℓ	Y_ℓ
1	0.24
2	0.76

N_0 remains to be determined so that we can make use of Eq. B-12. Thus from Eq. B-12

$$\underline{A}_\ell = \Delta\Lambda_\ell \int_0^\infty a_\ell(t)dt = Y_\ell N_0. \tag{B-14}$$

Next insert the RHS of Eq.(B-14) in Eq.(B-1). Then with the numbers of Tables B-7 and B-8 we obtain

$$N_0 \approx 0.8 \tag{B-15}$$

Finally based on Equations (B-12),(B-15) and the Tables B-1, B-6, B-7 and B-8, we can make up the Table B-1 and Fig. B-7 where a comparison of the theoretical and experimental behavior of

$$a(t) = \sum_{\ell=1}^{2} a_{\ell}(t) \quad \Delta\Lambda_{\ell} \tag{B-16}$$

is shown

Table B-9 Comparison of the theoretical and experimental values of a(t)

t(sec)	$\sum_{j=1}^{8} \lambda_j N_{0_j} e^{-\lambda_j t}$ theoretical	a(t) experimental
1	1.1×10^{-1}	4.8×10^{-2}
10	1.2×10^{-2}	7.5×10^{-3}
10^2	1.2×10^{-3}	9.5×10^{-4}
10^3	1.8×10^{-5}	3.4×10^{-5}

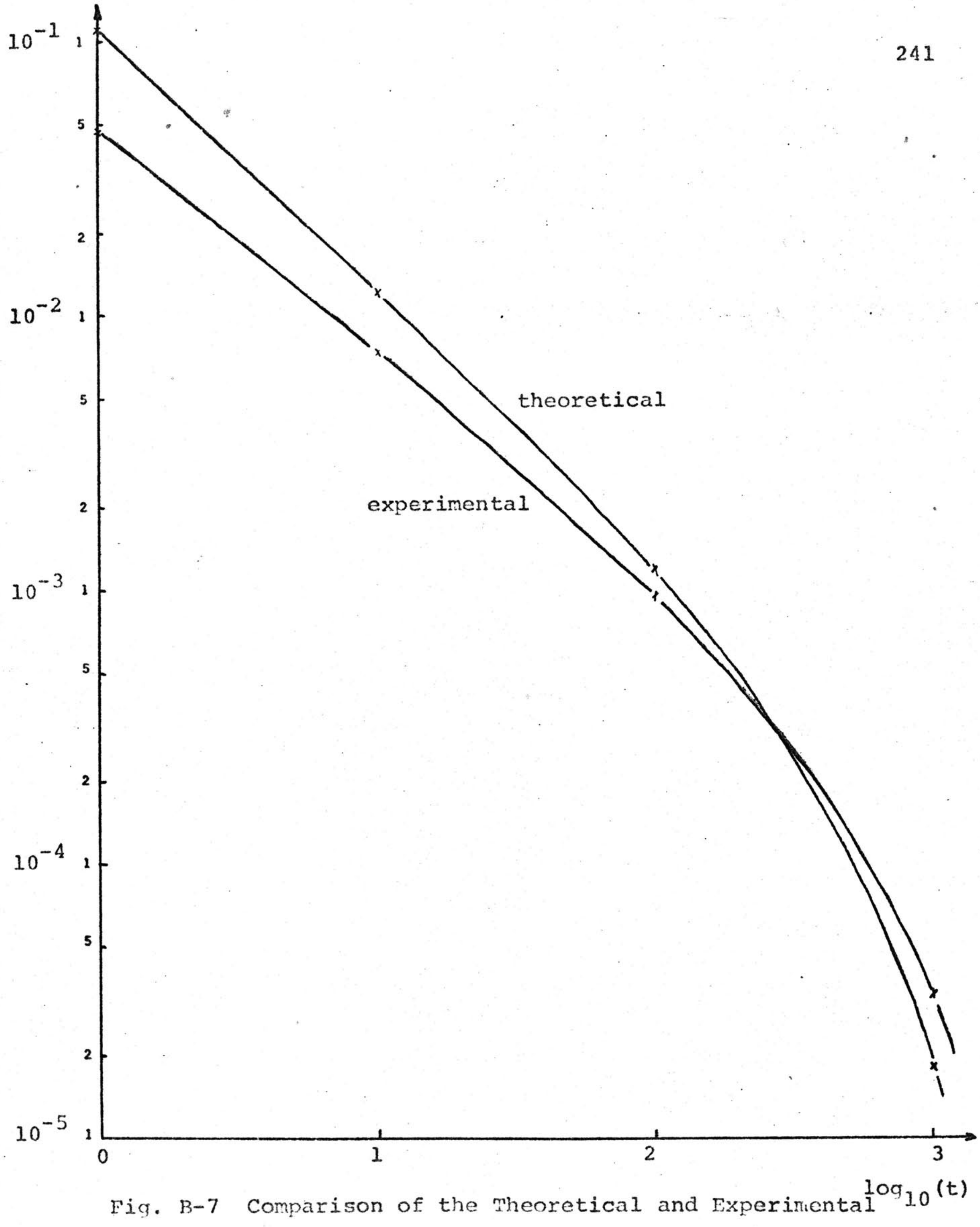

Fig. B-7 Comparison of the Theoretical and Experimental Behavior of a(t)

B-5 Conclusion

In this Appendix we have shown that the data relevant to the production of photons -from the fission products of U^{235} -and the data relevant to the attenuation of photons and photoneutron reaction (cross sections) in heavy water are consistent (within ≈ 10% of accuracy). Thus for the purpose of our calculations, we can make use of the attenuation and photoneutron reaction cross sections in D_2O, satisfactorily (at least for the photons of interest: $\Lambda \geq 2.23$ MeV).

Moreover, this checking of one data against the other led us, neglecting the photoneutrons produced by photons having had collisions, to derive an analytical representation for the curves of Fig. B-1 as the summation of nine exponential functions: $e^{-\lambda_j t}$'s, λ_j ($j = 1, \ldots, 9$) being the decay constant of the j^{th} -time wise- delayed photoneutron group (cf. Table 2-1).

Thus for the purpose of our calculations, Eq. (B-12) coupled with Eq. (B-15) will be used to express the production of delayed photons from U^{235} fission products*.

---

* It is worthwhile to mention that this enables us further to drive our equations for the unknown time coefficients (cf. Chapter III) into the familiar point kinetics form, thus

making the solution much easier to find.

APPENDIX C

THE PROBABILITY $P_\Lambda(E_\Lambda)$, THAT A PHOTONEUTRON INDUCED IN D_2O BY PHOTONS OF ENERGY Λ, WILL BE BORN WITH AN ENERGY E_Λ

A formula relating the energy E_Λ of a photoneutron induced by photons of energy Λ can be found in Reference [10] to be

$$E_\Lambda = \frac{1}{2}\left(\Lambda - 2.23 - \frac{\Lambda^2}{1862}\right) + \Lambda\left(\frac{\Lambda - 2.23}{931}\right)^{\frac{1}{2}}, \qquad \text{(C-1)}$$

where Λ and E_Λ are in MeV.

The Table C-1 and Fig. C-1 illustrate Eq. (C-1).

Table C-1

Energy E_Λ of a Photoneutron Induced by Photons of Energy Λ, in D_2O

Λ (MeV)	2.5	3	4	5
E_Λ (MeV)	0.195	0.488	1.08	1.67

According to Eq. (C-1) an appropriate analytical representation of $P_\Lambda(E_\Lambda)$ would be,

$$P_\Lambda(E) = \delta(E - E_\Lambda) \qquad \text{(C-2)}$$

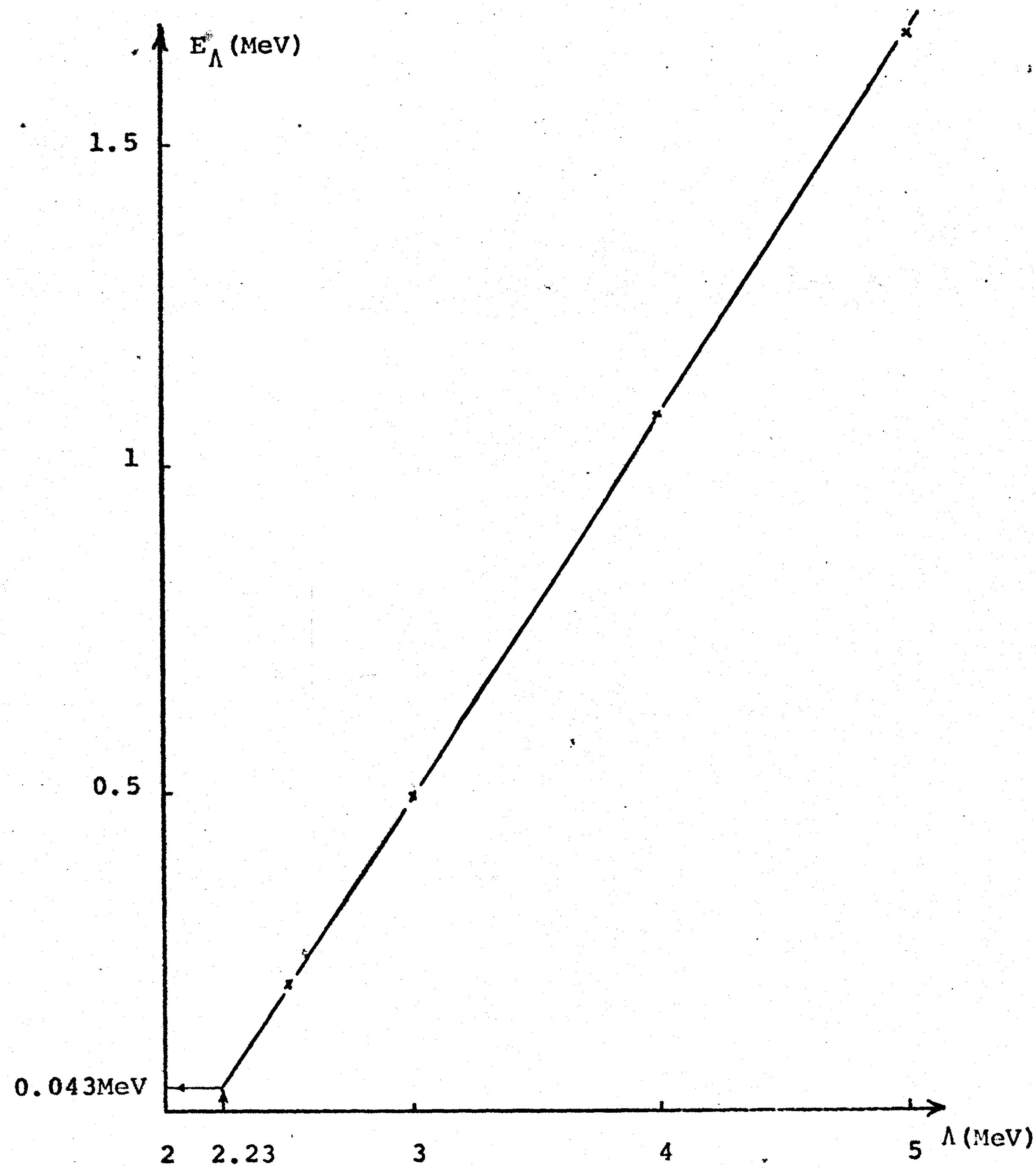

Fig. C-1 Energy of a Photoneutron as a Function of the Energy of the Incident Photon, in D_2O

Furthermore, from Fig. C-1 we can see that the minimum energy that photoneutrons born in a heavy water medium carry, is 43 keV. The lower limit of the fast energy group of our three group scheme being 3keV, all the photoneutrons, therefore, will be born in the fast group.

On the other hand, through Eqs. (2-18), (2-13), (2-12) and (C-2), we have,

$$P_g = \text{diag}\left[\frac{1}{\Delta\Lambda_1}\int_{\Lambda_1}^{\Lambda_0} d\Lambda \int_{Eg}^{Eg-1} \delta(E-E_\Lambda)\, dE \;\ldots\; \frac{1}{\Delta\Lambda_L}\int_{\Lambda_L}^{\Lambda_{L-1}} d\Lambda \int_{Eg}^{Eg-1} \delta(E-E_\Lambda)\, dE\right]. \qquad \text{(C-3)}$$

Hence,

$$P_g = \begin{pmatrix} 1 & \\ & 1 \end{pmatrix}, g = 1, \quad P_g = \begin{pmatrix} 0 & \\ & 0 \end{pmatrix}, \; g \neq 1 \qquad \text{(C-4)}$$

where only two groups of photons have been considered.

APPENDIX D

THE SECONDARY GAMMA RAY CROSS SECTIONS FROM THE CODE POPOP IV

In the expression for the prompt photoneutron source term we have quantities such as, $\Sigma_{f_g}(r,z,t)\,\Gamma_{f_{\ell g}}(r,z)$, which is the cross section for photons, induced by j^{th} type of neutron reaction (either fission or prompt capture or inelastic scattering) due to neutrons of energy group g, to appear in the photon group ℓ, at (r,z) and t.

Thus we need to evaluate

$$SGCS_{\ell g}(r,z,t) = N(r,z,t)\sum_{f=1}^{3}\sigma_{f_g}(r,z)\,\Gamma_{f_{\ell g}}(r,z) \qquad \text{(D-1)}$$

where $N(r,z,t)$ is the atom density at (r,z) and t, and $\sigma_{f_g}(r,z)$, the microscopic cross section corresponding to $\Sigma_{f_g}(r,z,t)$.

The various quantities, $\sum_{f=1}^{3}\sigma^{n}_{f_g}\,\Gamma^{n}_{f_{\ell g}}$

[where n replacing (r,z), denotes the nuclide n present at (r,z)], were computed by the code POPOP IV [2].

D-1 Input to the Code POPOP IV

Input to the code POPOP IV consists of the boundaries of the neutron and photon energy groups, the nuclei of interest, and the reaction of interest. It is also necessary to input the neutron cross sections $\sigma^n_{f_g}$'s. The code computes $\Gamma^n_{f_{\ell g}}$ out of its own library, performs the multiplication $\sigma^n_{f_g} \times \Gamma^n_{f_{\ell g}}$ and eventually sums it over f if there is more than one reaction that the nuclei n can undergo.

D-1-1 Cross sections input to the Code

The few groups fission and capture* cross sections were ready for MITR-II (cf. Appendix I), whereas we had to determine the inelastic scattering cross sections.

There are only two elements present in MITR-II that can cause inelastic scattering gamma rays having an energy above the threshold energy for photoneutron reaction in D_2O (2.23 Mev). These are carbon and oxygen. The inelastic scattering cross sections for these two elements were estimated in the following way;

---

* Capture cross section is identical to absorption cross section in case of a non fissile material. It is equal to the difference of absorption and fission cross sections in case of a fissile material.

$$\sigma_{j_{in_g}} = \frac{\int_{E_g}^{E_{g-1}} f(E)\sigma_{j_{in}}(E)\, dE}{\int_{E_g}^{E_{g-1}} f(E)\, dE} , \qquad \text{(D-2)}$$

where f(E) [7] is the fission spectrum for U^{235} and $\sigma_{j_{in}}(E)$ [8], the inelastic scattering cross section for the j^{th} nuclide at energy E.

Only fast neutrons (belonging to the fast group; $E \geq 3Kev$) can cause inelastic scattering.

Hence, assuming $\int_{3Kev}^{\infty} f(E)\, dE=1$, Eq. (D-2) becomes,

$$\sigma_{j_{in_1}} = \int_{E_{j_{threshold}}}^{\infty} f(E)\ \sigma_{j_{in}}(E)\ dE. \qquad \text{(D-3)}$$

Equation (D-3) can then be written as,

$$\sigma_{j_{in_1}} = \sum_{n=1}^{N} \sigma_{j_{in_1}} F_n \quad , \qquad \text{(D-4)}$$

where

$$F_n = \int_{E_n}^{E_{n-1}} f(E)\ dE \quad . \qquad \text{(D-5)}$$

The calculations based on this formula are presented in Table D-1.

Table D-1 Calculation of the inelastic scattering cross section of $_6C^{12}$ and $_8O^{16}$ for the fast group of our scheme

Element	$E_{threshold}$ (Mev)	n	E_n (Mev)	$F_n \times 10^2$	σ_{in_n} (barn)	$\sigma_{in_n} F_n \times 10^3$
$_6C^{12}$	4.8	1	6	3.489	0.1	3.489
		2	7	1.301	0.3	3.903
		3	8	0.615	0.3	1.845
		4	9	0.286	0.4	1.144
		5	10	0.131	0.3	0.393
						$\sum_{n=1}^{5} \sigma_{in_n} F_n =$ 10.774 mb
$_8O^{16}$	6.55	1	7	0.650	0.04	0.260
		2	8	0.615	0.20	1.230
		3	9	0.286	0.30	0.858
		4	10	0.131	0.35	0.458
						$\sum_{n=1}^{4} \sigma_{in_n} F_n =$ 2.806 mb

Thus for the inelastic microscopic scattering cross sections we input to the Code POPOP IV, the numbers in millibarn, (10.8, 0,0) for carbon and (2.8, 0,0) for oxygen.

D-1-2 Neutron and Photon energy group boundaries input to the Code POPOP IV

The neutron and photon energy group boundaries are given in Tables D-2 and D-3.

Table D-2 Upper energy limits of the neutron energy groups

g	E_{g-1} (ev)
1	1×10^{7}
2	3×10^{3}
3	4×10^{-1}

Table D-3 Upper energy limits of the photon energy groups

ℓ	$E_{\ell-1}$ (Mev)
1	7.0
2	3.5

D-2 Output from the Code POPOP IV; the microscopic secondary gamma ray cross sections

In Table D-4 are given, in barn, the final microscopic secondary gamma ray cross sections for the two-photon and three-neutron energy group, for various material present in MITR-II. The second column gives the nuclide numbers that refer to the material in question (cf. Appendix I).

The reason that two D_20's appear in Table D-4 is that the few group microscopic cross sections have been obtained through a flux weighted collapsing procedure from a multigroup scheme. We may then have two different cross sections for the same material at different locations.

In Table D-4 yE-x stands for $yx10^{-x}$.

We point out that the gamma rays born in H_20 are due to the inelastic scattering of neutrons with the oxygen nucleis only.

D-3 Macroscopic secondary gamma ray cross sections for materials present in MITR-II.

In order to get $SGCS_{\ell g}(r,z,t)$ we have to multiply the numbers given in Table D-4 by the atom densities given in Appendix I. Table D-5 shows the macroscopic secondary gamma ray cross sections, in cm^{-1}, for the two photon and three neutron energy group, for various compositions (cf.Appendix G) in MITR-II at the steady state.

Table D-4 The microscopic secondary gamma ray cross sections (in barn) for various materials present in MITR-II

Material	Nuclide Number(s)	Photon Energy Group	Neutron Energy Group 1	Neutron Energy Group 2	Neutron Energy Group 3
H_2O	3,7,12,14,	1	1.06848E-3	0.	0.
	19,26,30,		1.40488E-6	0.	0.
	31	2			
D_2O	21	1	3.56848E-3	2.63000E-5	8.63000E-5
		2	1.40488E-6	0.	0.
D_2O	40,51	1	3.06848E-3	2.45000E-5	9.86000E-4
		2	1.40488E-6	0.	0.
U^{235}	1,5,9,15,17	1	2.87140E-1	5.08125	5.53837E+1
	23,27	2	8.48170E-1	1.51157E+1	1.63794E+2
Al	4,8,11,13,20, 22,25,29,32,	1	1.13679E-3	5.29197E-3	7.52636E-2
	34,36,38,41, 44,48,50,52, 54,55	2	8.59558E-4	4.00139E-3	5.69087E-2

Table D-4 (continued)

U^{238}	2,6,10,16,18	1	5.37749E-01	6.43148	3.54914E-01
	24,28	2	9.64999E-02	1.15414	6.36899E-02
Pb		1	1.57480E-04	4.37896E-04	2.43840E-03
	33	2	0.	0.	0.
Cd	35	1	1.22047	2.95523	4.10662E+02
		2	1.48315	3.59126	4.99046E+02
C	39,53	1	5.4455E-03	7.72509E-05	2.24250E-03
		2	0.	2.57500E-05	7.47500E-04

Table D-5 The Secondary Gamma Ray cross sections (in cm^{-1}) for various compositions in MITR-II at the steady state

Composition Number	Photon Energy Group	Neutron Energy Group 1	Neutron Energy Group 2	Neutron Energy Group 3
1	1	0.1839E-03	0.2402E-03	0.2463E-01
	2	0.3707E-03	0.6233E-02	0.6759E-01
2	1	0.5189E-04	0.1592E-02	0.2263E-02
	2	0.2588E-04	0.1204E-03	0.1713E-02
3	1	0.1900E-03	1.2508E-02	0.2565E-02
	2	0.3868E-03	0.6538E-02	0.7084E-01
7	1	0.8243E-04	0.1722E-05	0.1502E-04
	2	0.1392E-06	0.6480E-06	0.9218E-05
8	1	0.5173E-05	0.1443E-04	0.8040E-04
	2	0.	0.	0.

Table D-5 (continued)

9	1	0.8549E-02	0.2084E-01	2.8644
	2	0.1034E-01	0.2520E-01	3.4759
10	1	0.6846E-04	0.3186E-03	0.4529E-02
	2	0.5174E-04	0.2409E-03	0.3427E-02
16	1	0.4536E-03	0.6431E-05	0.1866E-03
	2	0.	0.2141E-05	0.6222E-04
17	1	0.7671E-04	0.1655E-03	0.2348E-02
	2	0.2680E-04	0.1248E-03	0.1775E-02
18	1	0.3567E-04	0.	0.
	2	0.4676E-07	0.	0.
19	1	0.3699E-04	0.1593E-04	0.2265E-03
	2	0.2631E-05	0.1205E-04	0.1714E-03
23	1	0.3888E-04	0.3185E-04	0.4527E-03
	2	0.5213E-05	0.2408E-04	0.3425E-03
24	1	0.6846E-04	0.3186E-03	0.4529E-02
	2	0.5174E-04	0.2409E-03	0.3427E-02

The Composition numbers 4,5,6,11,12,13,14,15,20,21 do not appear in Table D-5, the sets of Compositions (1,5,6,14), (2,15), (3,4,13), (10,11,12) and (18,20,21) being identical.

APPENDIX E

LINEAR DEPENDENCE OF THE SPATIAL FUNCTIONS

Obtaining the time dependent coefficients through the system of equations,

$$\Lambda \frac{dN(t)}{dt} = [\rho_{new}(t) - \overline{\beta}_{new}(t)]\, N(t) + \sum_{j=1}^{H} \lambda_j C_j(t), \qquad \text{(E-1)}$$

$$\frac{dC_j(t)}{dt} = \overline{\beta}_{j_{new}}(t) - \lambda_j C_j(t), \qquad \text{(E-2)}$$

will require inverting the generation time matrix Λ. This is possible if the determinant of the matrix Λ is not singular. Moreover, numerically an "almost" singular determinant for the matrix Λ is to be avoided. Thus the normalized determinant (Grahm determinant)

$$\det(G) = 1 - \frac{\Lambda_{12}\ \Lambda_{21}}{\Lambda_{11}\ \Lambda_{22}}, \qquad \text{(E-3)}$$

$$\Lambda_{ik} = \langle W_i^T(\underline{r}) \left| v^{-1} \right| \psi_k(\underline{r}) \rangle,\ i = 1,\ 2,\ k = 1,\ 2, \qquad \text{(E-4)}$$

should be greater than an imposed criterium.

If we fear an "almost" linear dependence, we can use the difference of the second and first trial modes as the second trial mode (if only two trial modes are used), that is

$$\psi_2'(\underline{r}) = \delta\psi(\underline{r}) = \psi_2(\underline{r}) - \psi_1(\underline{r}). \tag{E-5}$$

However, here one must be careful in computing the leakage integral subject to section 5-2 of Chapter V, since Eqs. (4-19) or (5-14) do not hold for $\psi_2'(\underline{r})$. For the integral $< W_i^T(\underline{r}) \left| \nabla . D_2(\underline{r}, t) \nabla \right| \delta\psi(\underline{r}) >$, i = 1, 2 (with the familiar notation used throughout the dissertation) over the reactor volume, an appropriate expression may be found in the following way; write from Eq. (4-18),

$$< W_i^T(\underline{r}) \left| \nabla . D_2(\underline{r}) \nabla \right| \psi_2(\underline{r}) > = < W_i^T(\underline{r}) \left| A_2'(\underline{r}) - \frac{F_2}{k_2}(\underline{r}) \right. \left| \psi_2(\underline{r}) \right>, \; i = 1, 2. \tag{E-6}$$

Nothing changes if we add at the right hand side of Eq. (E-6) the quantity $< W_i^T(\underline{r}) \left| \nabla . D_1(\underline{r}) \nabla - A_1(\underline{r}) + \frac{F_1}{k_1}(\underline{r}) \right| \psi_1(\underline{r}) >$, i = 1, 2, that is equal to zero by definition.

Next subtract from both sides of Eq. (E-6) the quantity $< W_i^T(\underline{r}) \left| \nabla . D_2(\underline{r}) \nabla \right| \psi_1(\underline{r}) >$, i = 1, 2. Also add and subtract at the same time, to and from the right hand side of

Eq. (E-6), the quantities $< W_i^T(\underline{r}) \mid A_2'(\underline{r}) \mid \psi_1(\underline{r}) >$ and $< W_i^T(\underline{r}) \mid \frac{F_2}{k_2}(\underline{r}) \mid \psi_1(\underline{r}) >$, i = 1, 2, to obtain

$$< W_i^T(\underline{r}) \mid \nabla . D_2(\underline{r}) \nabla \mid \delta\psi(\underline{r}) > = < W_i^T(\underline{r}) \mid A_2'(\underline{r}) - \frac{F_2}{k_2}(\underline{r}) \mid \delta\psi(\underline{r}) > + < W_i^T(\underline{r}) \mid - [\nabla . D_2(\underline{r})\nabla - \nabla . D_1(\underline{r})\nabla] + A_2(\underline{r}) - A_1(\underline{r}) - [\frac{F_2}{k_2}(\underline{r}) - \frac{F_1}{k_1}(\underline{r})] \mid \psi_1(\underline{r}) >, \quad i = 1, 2. \qquad \text{(E-7)}$$

Hence, if we wish to use the difference of the second and first trial modes as the second trial mode - to avoid an undesirable "almost" singular generation time matrix Λ, - we should compute the leakage integral associated with that second trial mode according to Eq. (E-7).

APPENDIX F

THE SOLUTION OF THE POINT KINETICS-TYPE OF EQUATIONS BY THE WEIGHTED RESIDUAL METHOD

We wanted to solve the system of equations

$$\Lambda \frac{dN(t)}{dt} = [\rho_{new}(t) - \overline{\beta}_{new}(t)]\, N(t) + \sum_{j=1}^{H} \lambda_j C_j(t), \tag{F-1}$$

$$\frac{dC_j(t)}{dt} = \overline{\beta}_{j_{new}}(t)\, N(t) - \lambda_j C_j \,. \tag{F-2}$$

The solution we have adopted [11] proceeds as follows: Choose a trial function,

$$\overline{N}(t) = \sum_{k=0}^{K} A_k (t-t_i)^k \,, \tag{F-3}$$

for the time step: $t_i \leq t \leq t_{i+1}$, with unknown parameters; A_k's $(k = 1,\ldots, K)$, A_0 being $N(t_i)$. The bar on top of $N(t)$ indicates an approximate expression.

Inserting Eq. (F-3) into Eq. (F-1) and Eq. (F-2) will give rise to time dependent residuals. We perform as many weighted integrals with those residuals as there are unknown parameters. One way of doing this is called subdomain weighting. We integrate the time dependent residuals first over the entire time step, then over half of the time step, and so forth as many times as the number of unknown parameters.

This way we will get a system of equations in K unknowns that will determine $\bar{N}(t)$ over $t_i \leq t \leq t_{i+1}$. We then can carry out the same attack for the next time step.

The method proposed involves a way to select the time step (halving procedure) so that the convergence of the time coefficients is ensured.

APPENDIX G

THE (R,Z) CYLINDRICAL MODEL ADOPTED

THE MODEL

1	2	3	4	5	6	7	8	9	10	11	12	13	14	15	16	17	18	19	20
1	18	19	19	18	19	18	18	18	19	19	18	18	18	18	19	18	19	18	21
2	18	19	19	18	19	19	19	18	18	18	18	18	18	18	18	18	13	18	21
3	2	2	2	2	2	2	2	2	2	2	2	2	2	2	2	2	2	2	21
4	2	2	2	2	9	9	2	2	2	2	2	2	2	2	2	2	11	11	21
5	8	9	13	13	9	9	14	14	14	14	14	14	14	14	14	14	11	11	21
6	8	9	13	13	9	9	14	14	14	14	14	14	14	14	14	14	11	11	21
7	8	8	13	13	9	9	14	14	14	14	14	14	14	14	14	14	11	11	21
8	8	9	13	13	10	10	14	14	14	14	14	14	14	14	14	14	11	11	21
9	8	9	13	13	10	10	14	14	14	14	14	14	14	14	14	14	11	11	21
10	8	9	4	4	10	10	5	5	5	5	6	6	6	6	6	6	11	11	21
11	8	9	4	4	10	10	5	5	5	5	6	6	6	6	6	6	11	11	21
12	8	9	4	4	10	10	5	5	5	5	6	6	6	6	6	6	11	11	21
13	8	8	4	4	10	10	5	5	5	5	6	6	6	6	6	6	11	11	21
14	8	8	4	4	10	10	5	5	5	5	6	6	6	6	6	6	11	11	21
15	8	8	4	4	10	10	5	5	5	5	6	6	6	6	6	6	11	11	21
16	8	8	4	4	10	10	5	5	5	5	6	6	6	6	6	6	11	11	21
17	8	9	4	4	10	10	5	5	5	5	6	6	6	6	6	6	11	11	21
18	8	9	4	4	10	10	5	5	5	5	6	6	6	6	6	6	11	11	21
19	8	8	4	4	10	10	5	5	5	5	6	6	6	6	6	6	11	11	21
20	8	8	3	3	10	10	1	1	1	1	1	1	1	1	1	1	11	11	21
21	8	8	3	3	10	10	1	1	1	1	1	1	1	1	1	1	11	11	11
22	8	8	3	3	10	10	1	1	1	1	1	1	1	1	1	1	11	11	20
23	8	8	3	3	10	10	1	1	1	1	1	1	1	1	1	1	11	11	20
24	8	8	2	2	10	10	2	2	2	2	2	2	2	2	2	2	11	20	20
25	8	9	24	24	10	10	24	24	24	24	24	24	24	24	24	24	11	20	20
26	2	2	2	2	2	2	2	2	2	2	2	2	2	2	2	2	11	20	20
27	2	2	2	2	2	2	2	2	2	2	2	2	2	2	2	2	20	20	20
28	2	2	2	2	2	2	2	2	2	2	2	2	2	2	2	2	20	20	20
29	20	20	20	20	20	20	20	20	20	20	20	20	20	20	20	20	20	20	20
30	12	12	12	12	2	2	2	20	20	20	20	20	20	20	20	20	20	12	12
31	7	7	7	7	17	17	17	12	12	2	20	20	20	20	20	20	2	7	7
32	7	7	7	7	7	7	7	7	7	17	12	12	2	20	20	12	17	7	7
33	7	7	7	7	7	7	7	7	7	7	7	7	17	12	12	7	7	7	7
34	7	7	7	7	7	7	7	7	7	7	7	7	7	7	7	7	7	7	7
35	7	7	7	7	7	7	7	7	7	7	7	7	7	7	7	7	7	7	7
36	7	7	7	7	7	7	7	7	7	7	7	7	7	7	7	7	7	7	7
37	7	7	7	7	7	7	7	7	7	7	7	7	7	7	7	7	7	7	7
38	7	7	7	7	7	7	7	7	7	7	7	7	7	7	7	7	7	7	7
39	7	7	7	7	7	7	7	7	7	7	7	7	7	7	7	7	7	7	7
40	7	7	7	7	7	7	7	7	7	7	7	7	7	7	7	7	7	7	7
41	7	7	7	7	7	7	7	7	7	7	7	7	7	7	7	7	7	7	7
42	7	7	7	7	7	7	7	7	7	7	7	7	7	7	7	7	7	7	7
43	7	7	7	7	7	7	7	7	7	7	7	7	7	7	7	7	7	7	7
44	7	7	7	7	7	7	7	7	7	7	7	7	7	7	7	7	7	7	7
45	7	7	7	7	7	7	7	7	7	7	7	7	7	7	7	7	7	7	7
46	7	7	7	7	7	7	7	7	7	7	7	7	7	7	7	7	7	7	7
47	7	7	7	7	7	7	7	7	7	7	7	7	7	7	7	7	7	7	7
48																			

20	21	22	23	24	25	26	27	28	29	30	31	32	33	34	35	36	37	38	39	40
1	0	21	19	19	18	19	18	18	18	18	18	18	18	19	15	15	16	16	16	16
2	0	21	19	19	18	18	18	18	18	19	18	19	18	18	15	16	15	16	16	16
3	0	21	7	7	7	7	7	7	7	2	2	19	19	23	15	15	16	16	16	16
4	0	21	19	19	19	19	19	19	19	19	19	19	19	23	15	15	15	16	16	16
5	0	21	12	21	21	21	12	23	23	23	23	23	23	23	15	15	16	16	16	16
6	0	21	12	21	21	21	12	23	23	23	23	23	23	23	15	15	15	16	15	16
7	0	21	12	21	21	21	12	7	7	7	7	7	7	7	15	16	16	16	16	16
8	0	21	12	21	21	21	12	7	7	7	7	7	7	7	15	15	15	16	15	16
9	0	21	12	21	21	21	12	7	7	7	7	7	7	7	15	16	15	16	16	16
10	0	21	12	21	21	21	12	7	7	7	7	7	7	7	15	16	15	16	16	16
11	0	21	12	21	21	21	12	7	7	7	7	7	7	7	15	15	16	16	16	16
12	21	21	12	21	21	21	12	7	7	7	7	7	7	7	15	15	15	16	16	16
13	21	21	12	21	21	21	12	7	7	7	7	7	7	7	15	15	16	16	16	16
14	21	21	12	21	21	21	12	7	7	7	7	7	7	7	15	15	16	16	16	16
15	21	21	12	21	21	21	12	7	7	7	7	7	7	7	15	15	16	16	16	16
16	21	21	12	21	21	21	12	7	7	7	7	7	7	7	15	15	15	16	16	16
17	21	21	12	21	21	21	12	7	7	7	7	7	7	7	15	15	16	16	16	16
18	21	21	12	21	21	21	12	7	7	7	7	7	7	7	15	16	16	16	16	16
19	21	21	20	21	21	2	17	7	7	7	7	7	7	7	15	15	15	16	16	16
20	21	21	20	21	21	12	7	7	7	7	7	7	7	7	15	15	16	15	16	16
21	11	20	20	21	21	12	7	7	7	7	7	7	7	7	15	15	16	16	16	16
22	20	20	20	21	12	7	7	7	7	7	7	7	7	7	15	16	16	16	16	16
23	20	20	20	21	12	7	7	7	7	7	7	7	7	7	15	16	16	16	16	16
24	20	20	20	7	17	7	7	7	7	7	7	7	7	7	15	15	15	16	16	16
25	20	20	20	12	7	7	7	7	7	7	7	7	7	7	15	16	16	16	16	16
26	20	20	20	12	7	7	7	7	7	7	7	7	7	7	15	16	15	16	16	16
27	20	20	12	7	7	7	7	7	7	7	7	7	7	7	15	16	16	16	16	16
28	2	17	17	7	7	7	7	7	7	7	7	7	7	7	15	16	16	16	16	16
29	12	7	7	7	7	7	7	7	7	7	7	7	7	7	15	15	16	16	16	16
30	7	7	7	7	7	7	7	7	7	7	7	7	7	7	15	15	16	15	16	16
31	7	7	7	7	7	7	7	7	7	7	7	7	7	7	15	16	16	16	16	16
32	7	7	7	7	7	7	7	7	7	7	7	7	7	7	15	16	16	15	16	16
33	7	7	7	7	7	7	7	7	7	7	7	7	7	7	15	16	15	15	16	16
34	7	7	7	7	7	7	7	7	7	7	7	7	7	7	15	16	16	16	16	16
35	7	7	7	7	7	7	7	7	7	7	7	7	7	7	15	15	16	16	15	16
36	7	7	7	7	7	7	7	7	7	7	7	7	7	7	15	16	16	16	16	16
37	7	7	7	7	7	7	7	7	7	7	7	7	7	7	15	15	16	16	16	16
38	7	7	7	7	7	7	7	7	7	7	7	7	7	7	15	15	16	15	16	16
39	7	7	7	7	7	7	7	7	7	7	7	7	7	7	15	15	16	15	16	16
40	7	7	7	7	7	7	7	7	7	7	7	7	7	7	15	15	15	16	16	16
41	7	7	7	7	7	7	7	7	7	7	7	7	7	7	15	16	16	15	15	16
42	7	7	7	7	7	7	7	7	7	7	7	7	7	7	15	16	15	16	16	16
43	7	7	7	7	7	7	7	7	7	7	7	7	7	7	15	16	16	16	16	16
44	7	7	7	7	7	7	7	7	7	7	7	7	7	7	15	15	16	16	16	16
45	7	7	7	7	7	7	7	7	7	7	7	7	7	7	15	15	16	16	16	16
46	7	7	7	7	7	7	7	7	7	7	7	7	7	7	15	16	16	16	16	16
47	7	7	7	7	7	7	7	7	7	7	7	7	7	7	15	15	16	16	16	16
48																				

The (r,z) cylindrical model, that we have adopted for the Reactivity and Transient Analysis of MITR-II is shown above. In this model 23 Compositions are shown (note that the composition number 22 does not appear, thus the numbering goes up to 24). Each composition is made of nuclei which are numbered from 1 up to 55 as they were input to the code Exterminator-II. Below is shown the composition numbers before the nuclei numbers they are made of. Below each nuclei number, is presented the nucleus that bears this number.

1	1	2	4	3
	U5	U8	Al	H_2O
2	32	37		
	Al	H_2O		
3	5	6	8	7
	U5	U8	Al	H_2O
4	9	10	11	12
	U5	U8	Al	H_2O
5	15	16	13	14
	U5	U8	Al	H_2O
6	17	18	20	19
	U5	U8	Al	H_2O
7	21	22		
	D_2O	Al		
8	33			
	Pb			
9	35	34		
	Cd	Al		
10	36			
	Al			
11	54			
	Al			
24	50	19		
	Al	H_2O		

12	55			
	Al			
13	23	24	25	26
	U5	U8	Al	H_2O
14	27	28	29	30
	U5	U8	Al	H_2O
15	38	37		
	Al	H_2O		
16	39			
	C			
17	40	41		
	D_2O	Al		
18	42			
	H_2O			
19	43	44		
	H_29	Al		
20	45			
	H_2O			
21	46			
	H_2O			
23	48	47		
	Al	H_2O		

APPENDIX H

APPROXIMATE ATTENUATION COEFFICIENTS, ATT_{re}'s, FOR PRECHOSEN REGIONS OF THE D_2O REFLECTOR

To save computer time, we do not calculate the attenuation coefficient $\frac{1}{4\pi(r^2 + z^2)} e^{-\Sigma_\ell (r^2 + z^2)^{\frac{1}{2}}}$ (ℓ = 1,..., L) at every point (r, z). Instead we divide the reflector into regions within which a constant, approximate attenuation coefficient will be used.

To proceed, we make use of Fig. H-1 to create the final Table H-1.

The macroscopic attenuation cross section is taken to be equal to 0.04 cm^{-1}, the value appropriate for photons emitted with an energy of 3 MeV.

The regions in question are rectangular and defined by four mesh point numbers; two in the r direction: $INUI_{re}$, $INUF_{re}$, and two in the z direction: $INVI_{re}$, $INVF_{re}$, as shown in Fig. H-2 (cf. Appendix G for the presentation of the mesh volume structure for MITR-II).

(See following page for Fig. H-2.)

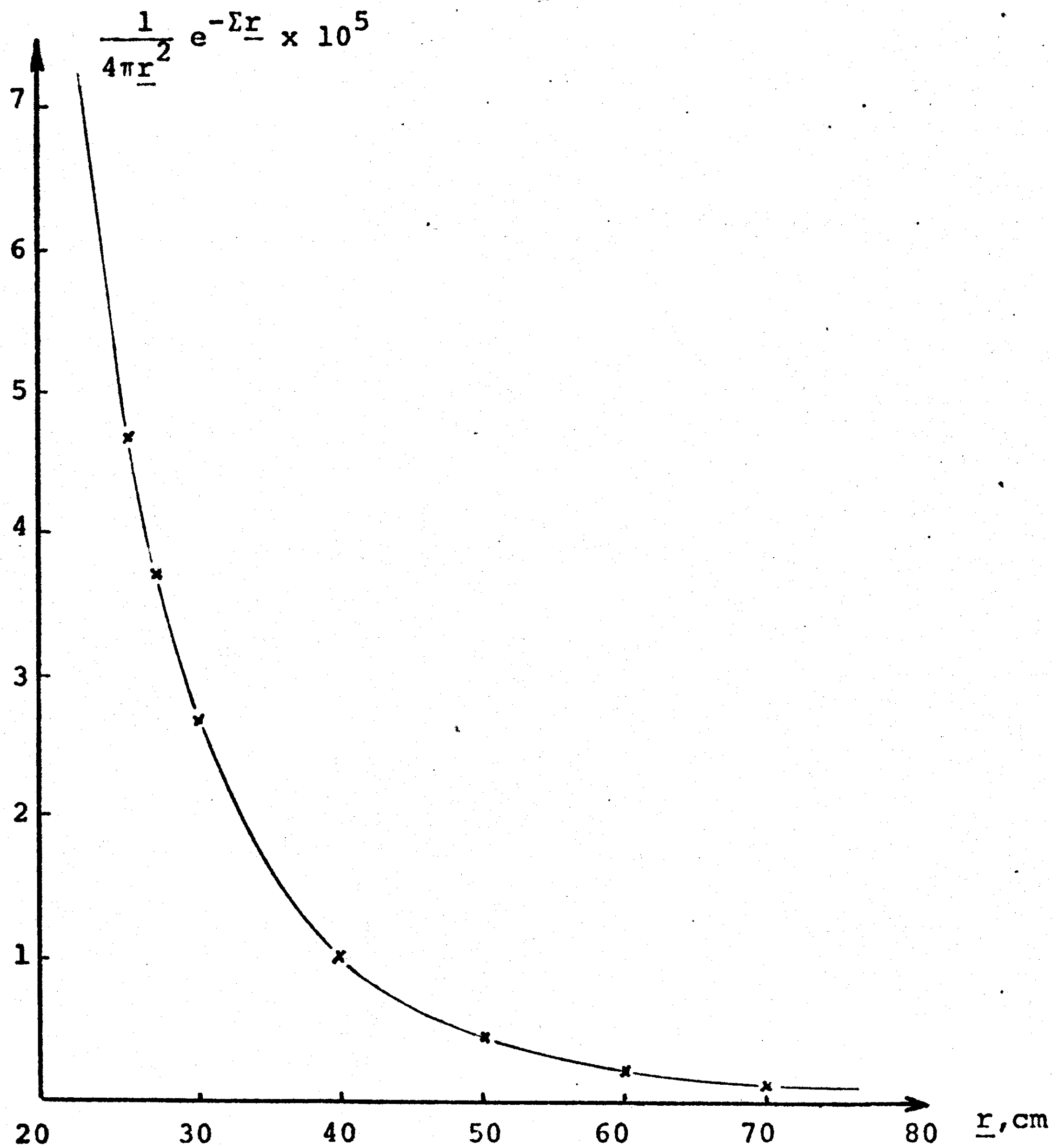

Fig. H-1 The Attenuation Factor as a Function of the Distance $\underline{r}$ of a Point in D_2O Medium, to a Central Point. The Attenuation Cross Section Σ, is Taken to be Equal to 0.04 cm^{-1}.

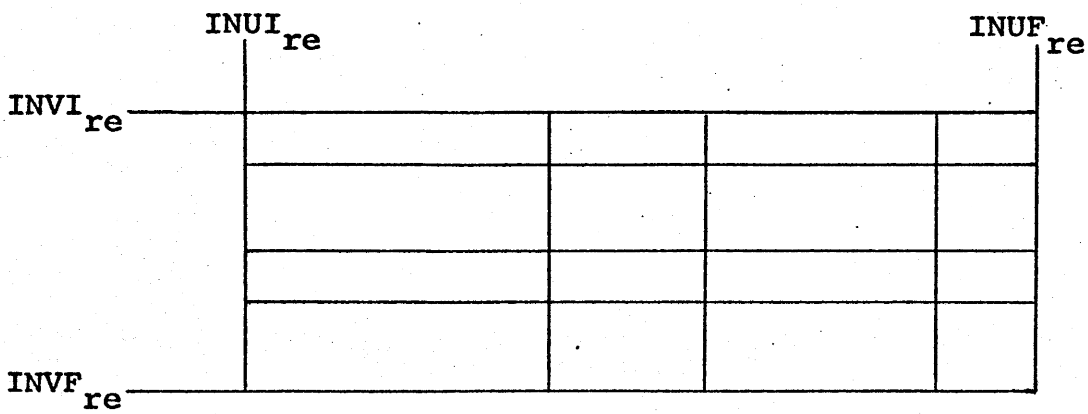

Fig. H-2 reth Region for Constant Approximate Attenuation Coefficient

Table H-1 The Constant Approximate Attenuation Coefficients, ATT_{re}'s, in Ten D_2O Reflector Regions

re	$INUI_{re}$	$INUF_{re}$	$INVI_{re}$	$INVF_{re}$	$ATT_{re} \times 10^5$
1	1	8	31	34	4.
2	9	15	32	34	2.4
3	1	15	35	39	2.4
4	16	22	29	39	1.
5	23	27	23	39	1.
6	25	27	7	22	2.7
7	28	30	7	39	1.
8	1	30	40	44	1.
9	31	33	7	44	0.3
10	1	33	45	47	0.3

APPENDIX I

EXTERMINATOR-II INPUT DATA

(FIRST TRIAL SHAPE AND ITS ADJOINT)

```
OBTAINING THE FIRST SHAPE AND ITS ADJOINT THROUGH EXTERMINATOR 2


// 'TULGA YARMAN',REGION=335K,CLASS=C
/*MITID USER=(M8696,9441)
/*SRI LOW
/*MAIN LINES=20,CARDS=30,TIME=30
/*SETUP UNIT=2314,ID=234118,A=LLD,                                      X
/*COMM='USING M7514 7728 DISKPACK'
//STEP1 EXEC FJRG,PROG='USERFILE.M7514.7728.EXTERM1.LOAD(NELIB)'
//G.FT01F001    DD  UNIT=SYSDA,DISP=(NEW,PASS),                         X
//    DCB=(RECFM=VBS,LRECL=3204,BLKSIZE=6412),SPACE=(TRK,(20,10))
//G.FT02F001    DD  UNIT=SYSDA,DISP=(NEW,PASS),                         X
//    DCB=(RECFM=VBS,LRECL=2404,BLKSIZE=4812),SPACE=(TRK,(20,10))
//G.FT03F001    DD  UNIT=SYSDA,DISP=(NEW,PASS),                         X
//    DCB=(RECFM=VBS,LRECL=1604,BLKSIZE=3212),SPACE=(TRK,(20,10))
//G.FT04F001    DD  UNIT=SYSDA,DISP=(NEW,PASS),                         X
//    DCB=(RECFM=VBS,LRECL=1604,BLKSIZE=3212),SPACE=(TRK,(20,10))
//G.FT09F001 DD DSNAME=USERFILE.M8696.9441.DENGEA.KISI,DISP=(OLD,PASS)
//G.FT10F001    DD UNIT=SYSDA,DISP=(NEW,PASS),                          X
//    DCB=(RECFM=VS,LRECL=1604,BLKSIZE=1608),SPACE=(TRK,(10,5))
//G.FT11F001    DD  UNIT=SYSDA,DISP=(NEW,PASS),                         X
//    DCB=(RECFM=VS,LRECL=804,BLKSIZE=808),SPACE=(TRK,(10,5))
//G.SYSIN DD *
MITR11 EQUILIBRIUM FLUX AND ADJOINT FLUX
 1 1 1 1 1 0 1 1 0 1 1                                  0 0 0 0 0 0 0
 0 0 0 0
 60 48 40  3 28 55 89 0 1 1 0 1 0 0 1 0 0 0 01.0E-54.125E+171.0000001.30
1.0
0.0
10.160   4 5.080   7 7.62    8 2.54   20 1.27   25 .635   26 1.164 29 .635   34
.952    35 .997   42 1.27   45 3.492 45 15.24 48
3.728    2 1.864   3 1.364   5 .317    7 1.614 11 .977   15 1.596 16   .954 19
.159    20 .635   21 .159   22 .476   23 .687   26 .635   27 4.41   34   3.0   35
9.66    37 15.24 40
  7  7 48  1 34      18  1  3  1 19      18  1  3 22 34      16  1 48 35 40
```

```
 2  3  4  1 19       2  3  4 22 31       2  4  8  1  5       2  4  8  7 17        EXT20037
19  3  4 31 33      19  4  5 22 33      23  3  5 33 34      23  5  7 27 34        EXT20038
 9  4 10  5  7      13  8 10  1  5      14  8 10  7 17       4 10 20  1  5        EXT20039
10 10 26  5  7       5 10 20  7 11       6 10 20 11 17       3 20 24  1  5        EXT20040
 1 20 24  7 17       2 24 25  1  5       2 24 25  7 17      24 25 26  1  5        EXT20041
24 25 26  7 17       2 26 29  1 17       9  1 10 20 21      21  1 21 19 20        EXT20042
21 10 21 20 21      21  1 21 21 22      11  4 27 17 18      11  4 24 18 19        EXT20043
11 21 22 19 21      12  5 19 22 23      12  5 19 26 27      15  1 48 34 35        EXT20044
12 30 31  1  5       2 30 31  5  8      17 31 32  5  8      12 31 32  8 10        EXT20045
 2 31 32 10 11      17 32 33 10 11      12 32 33 11 13       2 32 33 13 14        EXT20046
17 33 34 13 14      12 33 34 14 16      12 32 33 16 17      17 32 33 17 18        EXT20047
 2 31 32 17 18      12 30 31 18 20      12 29 30 20 21       2 28 29 20 21        EXT20048
17 28 29 21 23      12 27 28 22 23      12 25 27 23 24       2 24 25 23 24        EXT20049
17 24 25 24 25      12 22 24 24 25      12 20 22 25 26       2 19 20 25 26        EXT20050
17 19 20 26 27      20 32 33 14 16      20 31 32 11 17      20 30 31  8 18        EXT20051
20 29 30  1 20      20 28 29 17 20      20 27 28 17 22      20 24 27 18 23        EXT20052
20 22 24 19 23      20 21 22 21 23      20 19 21 22 23      21  5 24 23 24        EXT20053
21  5 22 24 25      21  5 19 25 26      25 37 40 11 12      25 36 41 12 13        EXT20054
25 35 42 13 27      26 35 42 27 29      27 35 42 29 31      28 35 42 31 35        EXT20055
22 29 45 35 40      13  5  8  1  5      10  8 10  5  7      14  5  8  7 17        EXT20056
 9  1 12 20 21       8  5 26  1  3       7 34 43 11 34      15 20 48 34 35        EXT20057
16 26 46 35 40                                                                    EXT20058
 1  1    OUTER BOT. EDGE CORE                                                     EXT20059
 14.0160E-4  23.0227E-5  43.1628E-2  31.5404E-2                                   EXT20060
 2  2    50% AL 50% H-2-O                                                         EXT20061
32 0.03012  31 0.01655                                                            EXT20062
 3  3 INNER BOT. EDGE CORE                                                        EXT20063
 54.2235E-4  63.1790E-5  83.0150E-2  71.6367E-2                                   EXT20064
 4  4    CENTRAL CORE                                                             EXT20065
 94.2235E-4 103.1790E-5 113.0150E-2 121.6367E-2                                   EXT20066
 5  5    INTERM. CORE                                                             EXT20067
154.0160E-4 163.0227E-5 133.1628E-2 141.5404E-2                                   EXT20068
 6  6    OUTER CORE                                                               EXT20069
174.0160E-4 183.0227E-5 203.1628E-2 191.5404E-2                                   EXT20070
 7  7   HEAVY WATER                                                               EXT20071
21.0329146  22.0001521                                                            EXT20072
```

```
 8  8    LEAD                                                  EXT20073
33 .3295E-1                                                    EXT20074
 9  9    15% CD 85% AL                                         EXT20075
35 0.00696  34 0.051195                                        EXT20076
10 10    INNER CORE AL                                         EXT20077
36 0.06023                                                     EXT20078
11 11    OUTER CORE AL                                         EXT20079
54 0.06023                                                     EXT20080
12 12                                                          EXT20081
55 0.06023                                                     EXT20082
13 13    CENTRAL CORE                                          EXT20083
234.2235E-4 243.1790E-5 253.0150E-2 261.6367E-2                EXT20084
14 14    OUTER CORE                                            EXT20085
274.0160E-4 283.0227E-5 293.1628E-2 301.5404E-2                EXT20086
15 15    CORE TANK                                             EXT20087
38 0.03012  37 0.01655                                         EXT20088
16 16    GRAPHITE                                              EXT20089
39 .8334E-1                                                    EXT20090
17 17    50% D-2-O,50% AL                                      EXT20091
40 0.01654  41 0.0312                                          EXT20092
18 18    REFLECTOR H-2-O                                       EXT20093
42 0.0334                                                      EXT20094
19 19                                                          EXT20095
43 .3143E-1 44 .3012E-2                                        EXT20096
20 20                                                          EXT20097
45 .03340                                                      EXT20098
21 21                                                          EXT20099
46 .03340                                                      EXT20100
22 22                                                          EXT20101
53 .8334E-1                                                    EXT20102
23 23                                                          EXT20103
48 .006023  47 .030078                                         EXT20104
24 24    50% AL 50% H-2-O                                      EXT20105
50 0.06023  49 0.03006                                         EXT20106
25 28   HEAVY WATER                                            EXT20107
51.0329146  52.0001621                                         EXT20108
```

```
                                                EXT20109
  1  1                                          EXT20110
2.0496E 01.6442E 06.5786E 02.5535E 0            EXT20111
0.0       4.7543E-30.0                          EXT20112
  1  2                                          EXT20113
4.0114E 12.6771E 14.4517E 12.4493E 0            EXT20114
0.0       0.0       4.4165E-3                   EXT20115
  1  3                                          EXT20116
4.3257E 23.4731E 24.4139E 22.4420E 0            EXT20117
0.0       0.0       0.0                         EXT20118
  2  1                                          EXT20119
3.7297E-11.1753E 06.5535E 01.1082E 0            EXT20120
0.0       5.7051E-30.0                          EXT20121
  2  2                                          EXT20122
3.0065E 10.0       2.6415E 10.0                 EXT20123
0.0       0.0       5.2998E-3                   EXT20124
  2  3                                          EXT20125
1.8136E 00.0       9.1350E 00.0                 EXT20126
0.0       0.0       0.0                         EXT20127
  3  1                                          EXT20128
3.9503E-30.0       7.4955E 00.0                 EXT20129
0.0       2.1158E 00.0                          EXT20130
  3  2                                          EXT20131
3.5490E-20.0       2.1705E 10.0                 EXT20132
0.0       0.0       4.0400E 0                   EXT20133
  3  3                                          EXT20134
5.1425E-10.0       6.6503E 10.0                 EXT20135
0.0       0.0       0.0                         EXT20136
  4  1                                          EXT20137
2.9585E-30.0       2.6894E 00.0                 EXT20138
0.0       5.9904E-30.0                          EXT20139
  4  2                                          EXT20140
1.2655E-20.0       1.3738E 00.0                 EXT20141
0.0       0.0       1.0158E-2                   EXT20142
  4  3                                          EXT20143
1.8107E-10.0       1.4662E 00.0                 EXT20144
```

```
0.0        0.0        0.0                                                   EXT20145
  5  1                                                                      EXT20146
2.0628E 01.6524E 06.6203E 02.5509E 0                                        EXT20147
0.0        4.8549E-30.0                                                     EXT20148
  5  2                                                                      EXT20149
4.0028E 12.6698E 14.4430E 12.4493E 0                                        EXT20150
0.0        0.0        4.3650E-3                                             EXT20151
  5  3                                                                      EXT20152
4.3257E 23.4731E 24.4139E 22.4420E 0                                        EXT20153
0.0        0.0        0.0                                                   EXT20154
  6  1                                                                      EXT20155
3.7109E-11.1806E 06.6000E 01.0851E 0                                        EXT20156
0.0        5.8259E-30.0                                                     EXT20157
  6  2                                                                      EXT20158
3.0029E 10.0       2.6441E 10.0                                             EXT20159
0.0        0.0        5.2380E-3                                             EXT20160
  6  3                                                                      EXT20161
1.8136E 00.0       9.1350E 00.0                                             EXT20162
0.0        0.0        0.0                                                   EXT20163
  7  1                                                                      EXT20164
3.7881E-30.0       7.5792E 00.0                                             EXT20165
0.0        2.1602E 00.0                                                     EXT20166
  7  2                                                                      EXT20167
3.5251E-20.0       2.1700E 10.0                                             EXT20168
0.0        0.0        4.0005E 0                                             EXT20169
  7  3                                                                      EXT20170
5.1425E-10.0       6.6503E 10.0                                             EXT20171
0.0        0.0        0.0                                                   EXT20172
  8  1                                                                      EXT20173
2.9157E-30.0       2.6940E 00.0                                             EXT20174
0.0        6.1172E-30.0                                                     EXT20175
  8  2                                                                      EXT20176
1.2571E-20.0       1.3738E 00.0                                             EXT20177
0.0        0.0        1.0039E-2                                             EXT20178
  8  3                                                                      EXT20179
1.8107E-10.0       1.4662E 00.0                                             EXT20180
```

```
0.0       0.0       0.0                                                                EXT20181
  9  1                                                                                 EXT20182
2.0673E 01.6554E 06.6321E 02.5507E 0                                                   EXT20183
0.0       4.8837E-30.0                                                                 EXT20184
  9  2                                                                                 EXT20185
3.9510E 12.6289E 14.3917E 12.4493E 0                                                   EXT20186
0.0       0.0       4.1198E-3                                                          EXT20187
  9  3                                                                                 EXT20188
3.5922E 22.8708E 23.6822E 22.4420E 0                                                   EXT20189
0.0       0.0       0.0                                                                EXT20190
 10  1                                                                                 EXT20191
 3.7225E-11.1723E 06.6127E 01.0832E 0                                                  EXT20192
0.0       5.8604E-30.0                                                                 EXT20193
 10  2                                                                                 EXT20194
2.9694E 10.0      2.6478E 10.0                                                         EXT20195
0.0       0.0       4.9437E-3                                                          EXT20196
 10  3                                                                                 EXT20197
1.5204E 00.0      8.9890E 00.0                                                         EXT20198
0.0       0.0       0.0                                                                EXT20199
 11  1                                                                                 EXT20200
2.8423E-30.0      2.0861E 00.0                                                         EXT20201
0.0       6.1535E-30.0                                                                 EXT20202
 11  2                                                                                 EXT20203
1.2288E-20.0      1.3768E 00.0                                                         EXT20204
0.0       0.0       9.4755E-3                                                          EXT20205
 11  3                                                                                 EXT20206
1.5807E-10.0      1.5366E 00.0                                                         EXT20207
0.0       0.0       0.0                                                                EXT20208
 12  1                                                                                 EXT20209
3.7547E-30.0      7.5854E 00.0                                                         EXT20210
0.0       2.1737E 00.0                                                                 EXT20211
 12  2                                                                                 EXT20212
3.4102E-20.0      2.1679E 10.0                                                         EXT20213
0.0       0.0       3.8151E 0                                                          EXT20214
 12  3                                                                                 EXT20215
4.2371E-10.0      5.7017E 10.0                                                         EXT20216
```

```
0.0       0.0       0.0                                                     EXT20217
 13  1                                                                      EXT20218
2.8870E-30.0        2.0843E 00.0                                            EXT20219
0.0       6.0604E-30.0                                                      EXT20220
 13  2                                                                      EXT20221
1.2215E-20.0        1.3735E 00.0                                            EXT20222
0.0       0.0       9.5483E-3                                               EXT20223
 13  3                                                                      EXT20224
1.5239E-10.0        1.4447E 00.0                                            EXT20225
0.0       0.0       0.0                                                     EXT20226
 14  1                                                                      EXT20227
3.9168E-30.0        7.5053E 00.0                                            EXT20228
0.0       2.1406E 00.0                                                      EXT20229
 14  2                                                                      EXT20230
3.4244E-20.0        2.1681E 10.0                                            EXT20231
0.0       0.0       3.8391E 0                                               EXT20232
 14  3                                                                      EXT20233
4.2913E-10.0        5.7570E 10.0                                            EXT20234
0.0       0.0       0.0                                                     EXT20235
 15  1                                                                      EXT20236
2.0574E 01.6495E 06.5969E 02.5533E 0                                        EXT20237
0.0       4.8099E-30.0                                                      EXT20238
 15  2                                                                      EXT20239
3.9558E 12.6331E 14.3966E 12.4493E 0                                        EXT20240
0.0       0.0       4.1514E-3                                               EXT20241
 15  3                                                                      EXT20242
3.6349E 22.8750E 23.7247E 22.4420E 0                                        EXT20243
0.0       0.0       0.0                                                     EXT20244
 16  1                                                                      EXT20245
3.7487E-11.1616E 06.5724E 01.1062E 0                                        EXT20246
0.0       5.7719E-30.0                                                      EXT20247
 16  2                                                                      EXT20248
2.9713E 10.0        2.6461E 10.0                                            EXT20249
0.0       0.0       4.9817E-3                                               EXT20250
 16  3                                                                      EXT20251
1.5387E 00.0        8.9989E 00.0                                            EXT20252
```

```
0.0        0.0        0.0                                 EXT20253
 17  1                                                    EXT20254
2.0435E 01.6402E 06.5655E 02.5540E 0                      EXT20255
0.0        4.6992E-30.0                                   EXT20256
 17  2                                                    EXT20257
3.9946E 12.6633E 14.4358E 12.4493E 0                      EXT20258
0.0        0.0        4.3124E-3                           EXT20259
 17  3                                                    EXT20260
4.3257E 23.4731E 24.4139E 22.4420E 0                      EXT20261
0.0        0.0        0.0                                 EXT20262
 18  1                                                    EXT20263
3.7332E-11.1740E 06.5409E 01.1131E 0                      EXT20264
0.0        5.6390E-30.0                                   EXT20265
 18  2                                                    EXT20266
3.0008E 10.0       2.6450E 10.0                           EXT20267
0.0        0.0        5.1748E-3                           EXT20268
 18  3                                                    EXT20269
1.8136E 00.0       9.1350E 00.0                           EXT20270
0.0        0.0        0.0                                 EXT20271
 19  1                                                    EXT20272
 .9522E-30.0       7.4697E 00.0                           EXT20273
0.0        2.0931E 00.0                                   EXT20274
 19  2                                                    EXT20275
3.5118E-20.0       2.1696E 10.0                           EXT20276
0.0        0.0        3.9727E 0                           EXT20277
 19  3                                                    EXT20278
 .1425E-10.0       6.6503E 10.0                           EXT20279
0.0        0.0        0.0                                 EXT20280
 20  1                                                    EXT20281
2.9535E-30.0       2.6908E 00.0                           EXT20282
0.0        5.9209E-30.0                                   EXT20283
 20  2                                                    EXT20284
1.2521E-20.0       1.3738E 00.0                           EXT20285
0.0        0.0        9.9184E-3                           EXT20286
 20  3                                                    EXT20287
1.8107E-10.0       1.4662E 00.0                           EXT20288
```

```
0.0       0.0       0.0                                                  EXT20289
 21  1                                                                   EXT20290
2.4984E-30.0        7.0599E 00.0                                         EXT20291
0.0       6.7724E-10.0                                                   EXT20292
 21  2                                                                   EXT20293
2.6314E-50.0        8.3280E 00.0                                         EXT20294
0.0       0.0       6.2333E-1                                            EXT20295
 21  3                                                                   EXT20296
 .8633E-40.0        1.2816E 10.0                                         EXT20297
0.0       0.0       0.0                                                  EXT20298
 22  1                                                                   EXT20299
3.0678E-30.0        1.9218E 00.0                                         EXT20300
0.0       1.3768E-20.0                                                   EXT20301
 22  2                                                                   EXT20302
1.4949E-20.0        1.3800E 00.0                                         EXT20303
0.0       0.0       1.3621E-2                                            EXT20304
 22  3                                                                   EXT20305
2.1166E-10.0        1.5991E 00.0                                         EXT20306
0.0       0.0       0.0                                                  EXT20307
 23  1                                                                   EXT20308
2.0869E 01.6686E 06.6716E 02.5501E 0                                     EXT20309
0.0       5.0685E-30.0                                                   EXT20310
 23  2                                                                   EXT20311
3.9430E 12.6118E 14.3898E 12.4494E 0                                     EXT20312
0.0       0.0       3.8991E-3                                            EXT20313
 23  3                                                                   EXT20314
3.5922E 22.8708E 23.6822E 22.4420E 0                                     EXT20315
0.0       0.0       0.0                                                  EXT20316
 24  1                                                                   EXT20317
3.7523E-11.1530E 06.6511E 01.0772E 0                                     EXT20318
0.0       6.0822E-30.0                                                   EXT20319
 24  2                                                                   EXT20320
3.0006E 10.0        2.6662E 10.0                                         EXT20321
0.0       0.0       4.6789E-3                                            EXT20322
 24  3                                                                   EXT20323
1.5204E 00.0        8.9890E 00.0                                         EXT20324
```

```
0.0       0.0       0.0                                                       EXT20325
 25  1                                                                        EXT20326
2.8420E-30.0        2.0792E 00.0                                              EXT20327
0.0       6.3863E-30.0                                                        EXT20328
 25  2                                                                        EXT20329
1.2178E-20.0        1.3767E 00.0                                              EXT20330
0.0       0.0       8.9680E-3                                                 EXT20331
 25  3                                                                        EXT20332
1.5807E-10.0        1.5366E 00.0                                              EXT20333
0.0       0.0       0.0                                                       EXT20334
 26  1                                                                        EXT20335
3.7140E-30.0        7.6215E 00.0                                              EXT20336
0.0       2.2475E 00.0                                                        EXT20337
 26  2                                                                        EXT20338
3.3859E-20.0        2.1662E 10.0                                              EXT20339
0.0       0.0       3.7248E 0                                                 EXT20340
 26  3                                                                        EXT20341
4.2371E-10.0        5.7017E 10.0                                              EXT20342
0.0       0.0       0.0                                                       EXT20343
 27  1                                                                        EXT20344
2.0649E 01.6547E 06.6089E 02.5534E 0                                          EXT20345
0.0       4.8899E-30.0                                                        EXT20346
 27  2                                                                        EXT20347
3.9739E 12.6425E 14.4168E 12.4493E 0                                          EXT20348
0.0       0.0       4.1611E-3                                                 EXT20349
 27  3                                                                        EXT20350
3.5922E 22.8708E 23.6822E 22.4420E 0                                          EXT20351
0.0       0.0       0.0                                                       EXT20352
 28  1                                                                        EXT20353
3.7702E-11.1495E 06.5831E 01.1079E 0                                          EXT20354
0.0       5.8679E-30.0                                                        EXT20355
 28  2                                                                        EXT20356
2.9966E 10.0        2.6521E 10.0                                              EXT20357
0.0       0.0       4.9933E-3                                                 EXT20358
 28  3                                                                        EXT20359
1.5204E 00.0        8.9890E 00.0                                              EXT20360
```

```
0.0       0.0       0.0                                   EXT20361
 29  1                                                    EXT20362
2.8845E-30.0        2.0809E 00.0                          EXT20363
0.0       6.1613E-30.0                                    EXT20364
 29  2                                                    EXT20365
1.2459E-20.0        1.3771E 00.0                          EXT20366
0.0       0.0       9.5705E-3                             EXT20367
 29  3                                                    EXT20368
1.5807E-10.0        1.5366E 00.0                          EXT20369
0.0       0.0       0.0                                   EXT20370
 30  1                                                    EXT20371
3.9034E-30.0        7.5048E 00.0                          EXT20372
0.0       2.1711E 00.0                                    EXT20373
 30  2                                                    EXT20374
3.4601E-20.0        2.1684E 10.0                          EXT20375
0.0       0.0       3.8759E 0                             EXT20376
 30  3                                                    EXT20377
4.2371E-10.0        5.7017E 10.0                          EXT20378
0.0       0.0       0.0                                   EXT20379
 31  1                                                    EXT20380
3.8287E-30.0        7.6889E 00.0                          EXT20381
0.0       2.4438E 00.0                                    EXT20382
 31  2                                                    EXT20383
3.9349E-20.0        2.1969E 10.0                          EXT20384
0.0       0.0       4.4186E 0                             EXT20385
 31  3                                                    EXT20386
6.1276E-10.0        7.7699E 10.0                          EXT20387
0.0       0.0       0.0                                   EXT20388
 32  1                                                    EXT20389
2.9243E-30.0        2.0593E 00.0                          EXT20390
0.0       7.0140E-30.0                                    EXT20391
 32  2                                                    EXT20392
1.3678E-20.0        1.3785E 00.0                          EXT20393
0.0       0.0       1.1265E-2                             EXT20394
 32  3                                                    EXT20395
2.1166E-10.0        1.5991E 00.0                          EXT20396
```

```
0.0       0.0       0.0                         EXT20397
 33  1                                          EXT20398
3.1042E-30.0        5.8792E 00.0                EXT20399
0.0       1.4549E-20.0                          EXT20400
 33  2                                          EXT20401
8.6206E-30.0        1.1134E 10.0                EXT20402
0.0       0.0       1.1662E-2                   EXT20403
 33  3                                          EXT20404
4.8000E-20.0        1.1130E 10.0                EXT20405
0.0       0.0       0.0                         EXT20406
 34  1                                          EXT20407
2.8500E-30.0        2.0590E 00.0                EXT20408
0.0       7.2065E-30.0                          EXT20409
 34  2                                          EXT20410
1.2342E-20.0        1.3770E 00.0                EXT20411
0.0       0.0       8.3502E-3                   EXT20412
 34  3                                          EXT20413
2.1166E-10.0        1.5991E 00.0                EXT20414
0.0       0.0       0.0                         EXT20415
 35  1                                          EXT20416
6.3567E 00.0        6.2660E 00.0                EXT20417
0.0       0.0       0.0                         EXT20418
 35  2                                          EXT20419
1.5368E 10.0        1.1086E 10.0                EXT20420
0.0       0.0       0.0                         EXT20421
 35  3                                          EXT20422
2.1407E 30.0        2.8590E 30.0                EXT20423
0.0       0.0       0.0                         EXT20424
 36  1                                          EXT20425
2.8564E-30.0        2.0846E 00.0                EXT20426
0.0       6.1598E-30.0                          EXT20427
 36  2                                          EXT20428
1.2340E-20.0        1.3769E 00.0                EXT20429
0.0       0.0       9.5172E-3                   EXT20430
 36  3                                          EXT20431
1.5807E-10.0        1.5366E 00.0                EXT20432
```

```
0.0         0.0         0.0                                              EXT20433
 37  1                                                                   EXT20434
2.2737E-30.0            1.0878E 10.0                                     EXT20435
0.0         6.2105E 00.0                                                 EXT20436
 37  2                                                                   EXT20437
5.2773E-20.0            2.2355E 10.0                                     EXT20438
0.0         0.0         6.5134E 0                                        EXT20439
 37  3                                                                   EXT20440
 .1276E-10.0            7.7699E 10.0                                     EXT20441
0.0         0.0         0.0                                              EXT20442
 38  1                                                                   EXT20443
3.1166E-30.0            1.8247E 00.0                                     EXT20444
0.0         1.9097E-20.0                                                 EXT20445
 38  2                                                                   EXT20446
1.8242E-20.0            1.3841E 00.0                                     EXT20447
0.0         0.0         1.7807E-2                                        EXT20448
 38  3                                                                   EXT20449
2.1166E-10.0            1.5991E 00.0                                     EXT20450
0.0         0.0         0.0                                              EXT20451
 39  1                                                                   EXT20452
0.0         0.0         3.1137E 00.0                                     EXT20453
0.0         1.1280E-10.0                                                 EXT20454
 39  2                                                                   EXT20455
1.0297E-40.0            4.4031E 00.0                                     EXT20456
0.0         0.0         1.2428E-1                                        EXT20457
 39  3                                                                   EXT20458
2.9912E-30.0            4.7187E 00.0                                     EXT20459
0.0         0.0         0.0                                              EXT20460
 40  1                                                                   EXT20461
3.3897E-30.0            6.6839E 00.0                                     EXT20462
0.0         4.3475E-10.0                                                 EXT20463
 40  2                                                                   EXT20464
2.3374E-50.0            8.3113E 00.0                                     EXT20465
0.0         0.0         5.5817E-1                                        EXT20466
 40  3                                                                   EXT20467
9.8633E-40.0            1.2816E 10.0                                     EXT20468
```

```
0.0         0.0         0.0                                                                  EXT20469
 41  1                                                                                       EXT20470
2.9910E-30.0        2.0228E 00.0                                                             EXT20471
0.0         8.8093E-30.0                                                                     EXT20472
 41  2                                                                                       EXT20473
1.4062E-20.0        1.3789E 00.0                                                             EXT20474
0.0         0.0         1.2100E-2                                                            EXT20475
 41  3                                                                                       EXT20476
2.1166E-10.0        1.5991E 00.0                                                             EXT20477
0.0         0.0         0.0                                                                  EXT20478
 42  1                                                                                       EXT20479
 .3466E-30.0        7.3682E 00.0                                                             EXT20480
0.0         2.4319E 00.0                                                                     EXT20481
 42  2                                                                                       EXT20482
4.2248E-20.0        2.2043E 10.0                                                             EXT20483
0.0         0.0         4.8494E 0                                                            EXT20484
 42  3                                                                                       EXT20485
6.1276E-10.0        7.7699E 10.0                                                             EXT20486
0.0         0.0         0.0                                                                  EXT20487
 43  1                                                                                       EXT20488
 .2438E-30.0        7.4581E 00.0                                                             EXT20489
0.0         2.4766E 00.0                                                                     EXT20490
 43  2                                                                                       EXT20491
4.1398E-20.0        2.2015E 10.0                                                             EXT20492
0.0         0.0         4.7066E 0                                                            EXT20493
 43  3                                                                                       EXT20494
6.1276E-10.0        7.7699E 10.0                                                             EXT20495
0.0         0.0         0.0                                                                  EXT20496
 44  1                                                                                       EXT20497
3.0467E-30.0        2.0394E 00.0                                                             EXT20498
0.0         7.1607E-30.0                                                                     EXT20499
 44  2                                                                                       EXT20500
1.4371E-20.0        1.3794E 00.0                                                             EXT20501
0.0         0.0         1.2011E-2                                                            EXT20502
 44  3                                                                                       EXT20503
2.1166E-10.0        1.5991E 00.0                                                             EXT20504
```

```
0.0          0.0          0.0                                                                              EXT20505
 45   1                                                                                                    EXT20506
3.6428E-30.0              8.0176E 00.0                                                                     EXT20507
0.0          2.7762E 00.0                                                                                  EXT20508
 45   2                                                                                                    EXT20509
4.0418E-20.0              2.2003E 10.0                                                                     EXT20510
0.0          0.0          4.5923E 0                                                                        EXT20511
 45   3                                                                                                    EXT20512
6.1276E-10.0              7.7699E 10.0                                                                     EXT20513
0.0          0.0          0.0                                                                              EXT20514
 46   1                                                                                                    EXT20515
3.4945E-30.0              8.0340E 00.0                                                                     EXT20516
0.0          2.7121E 00.0                                                                                  EXT20517
 46   2                                                                                                    EXT20518
3.8902E-20.0              2.1953E 10.0                                                                     EXT20519
0.0          0.0          4.3424E 0                                                                        EXT20520
 46   3                                                                                                    EXT20521
6.1276E-10.0              7.7699E 10.0                                                                     EXT20522
0.0          0.0          0.0                                                                              EXT20523
 47   1                                                                                                    EXT20524
3.8794E-30.0              8.0138E 00.0                                                                     EXT20525
0.0          3.0305E 00.0                                                                                  EXT20526
 47   2                                                                                                    EXT20527
4.3928E-20.0              2.2099E 10.0                                                                     EXT20528
0.0          0.0          5.1276E 0                                                                        EXT20529
 47   3                                                                                                    EXT20530
6.1276E-10.0              7.7699E 10.0                                                                     EXT20531
0.0          0.0          0.0                                                                              EXT20532
 48   1                                                                                                    EXT20533
3.0827E-30.0              2.0098E 00.0                                                                     EXT20534
0.0          8.8612E-30.0                                                                                  EXT20535
 48   2                                                                                                    EXT20536
1.5235E-20.0              1.3804E 00.0                                                                     EXT20537
0.0          0.0          1.3473E-2                                                                        EXT20538
 48   3                                                                                                    EXT20539
2.1166E-10.0              1.5991E 00.0                                                                     EXT20540
```

```
0.0         0.0         0.0                                                                                     EXT20541
 49  1                                                                                                          EXT20542
3.8567E-30.0            7.6667E 00.0                                                                            EXT20543
0.0         2.3724E 00.0                                                                                        EXT20544
 49  2                                                                                                          EXT20545
3.8773E-20.0            2.1957E 10.0                                                                            EXT20546
0.0         0.0         4.3394E 0                                                                               EXT20547
 49  3                                                                                                          EXT20548
6.1276E-10.0            7.7699E 10.0                                                                            EXT20549
0.0         0.0         0.0                                                                                     EXT20550
 50  1                                                                                                          EXT20551
2.9202E-30.0            2.0670E 00.0                                                                            EXT20552
0.0         6.7902E-30.0                                                                                        EXT20553
 50  2                                                                                                          EXT20554
1.3464E-20.0            1.3783E 00.0                                                                            EXT20555
0.0         0.0         1.1070E-2                                                                               EXT20556
 50  3                                                                                                          EXT20557
2.1166E-10.0            1.5991E 00.0                                                                            EXT20558
0.0         0.0         0.0                                                                                     EXT20559
 51  1                                                                                                          EXT20560
2.5773E-30.0            7.0489E 00.0                                                                            EXT20561
0.0         6.5528E-10.0                                                                                        EXT20562
 51  2                                                                                                          EXT20563
2.5709E-50.0            8.3246E 00.0                                                                            EXT20564
0.0         0.0         6.0911E-1                                                                               EXT20565
 51  3                                                                                                          EXT20566
9.8633E-40.0            1.2816E 10.0                                                                            EXT20567
0.0         0.0         0.0                                                                                     EXT20568
 52  1                                                                                                          EXT20569
3.1038E-30.0            1.9280E 00.0                                                                            EXT20570
0.0         1.3310E-20.0                                                                                        EXT20571
 52  2                                                                                                          EXT20572
1.4689E-20.0            1.3797E 00.0                                                                            EXT20573
0.0         0.0         1.3308E-2                                                                               EXT20574
 52  3                                                                                                          EXT20575
2.1166E-10.0            1.5991E 00.0                                                                            EXT20576
```

```
0.0         0.0         0.0                                                                EXT20577
 53  1                                                                                     EXT20578
0.0         0.0         3.1243E 00.0                                                       EXT20579
0.0         1.1079E-10.0                                                                   EXT20580
 53  2                                                                                     EXT20581
1.0224E-40.0            4.4025E 00.0                                                       EXT20582
0.0         0.0         1.2339E-1                                                          EXT20583
 53  3                                                                                     EXT20584
2.9912E-30.0            4.7187E 00.0                                                       EXT20585
0.0         0.0         0.0                                                                EXT20586
 54  1                                                                                     EXT20587
2.8567E-30.0            2.0758E 00.0                                                       EXT20588
0.0         6.6215E-30.0                                                                   EXT20589
 54  2                                                                                     EXT20590
1.2907E-20.0            1.3776E 00.0                                                       EXT20591
0.0         0.0         1.0003E-2                                                          EXT20592
 54  3                                                                                     EXT20593
2.1166E-10.0            1.5991E 00.0                                                       EXT20594
0.0         0.0         0.0                                                                EXT20595
 55  1                                                                                     EXT20596
2.9237E-30.0            2.0380E 00.0                                                       EXT20597
0.0         8.1833E-30.0                                                                   EXT20598
 55  2                                                                                     EXT20599
1.3662E-20.0            1.3785E 00.0                                                       EXT20600
0.0         0.0         1.1252E-2                                                          EXT20601
 55  3                                                                                     EXT20602
2.1166E-10.0            1.5991E 00.0                                                       EXT20603
0.0         0.0         0.0                                                                EXT20604
                                                                                           EXT20605
MITR11 EQUILIBRIUM ADJOINT FUNCTION                                                        EXT20606
                         1                                                     0 1         EXT20607
 0 0 0 0                                                                                   EXT20608
  1 24                                                                                     EXT20609
1.990E-92.317E-74.545E-6                                                                   EXT20610
                                                                                           EXT20611
                                                                                           EXT20612
```

/*

EXT20613

290

APPENDIX J

PROGRAM S1

(Photoneutrons Generated By Photons Having Had One and Only One Collision from U^{235} Fission Products on D_2O)

```
// 'TOLGA YARMAN',CLASS=A
/*MITID USER=(M3696,9441)
/*SRI LOW
/*MAIN   TIME=02,LINES=10
//STEP1 EXEC FORCGO
//C.SYSIN   DD  *
C PROGRAM S1
C
C STUDY OF PHOTONEUTRONS GENERATED BY PHOTONS HAVING HAD ONE AND ONLY ONE
C COLLISION,FROM AN ATOM OF U235 FISSIONNING IN THE MIDDLE OF AN INFINTE MEDIUM
C OF D2O(CF. EQUATION A-22 OF APPENDIX A).
C
      DIMENSION A(5),SIGMA(5),DELTA(5),SIGD(5),SLAM(5)
C
      DATA SND2O,NZ,RO,EO/3.32E22,10,2.818E-13,0.51/
C
      NAMELIST/IN/A,SIGMA,DELTA,SIGD,SLAM
      NAMELIST/OUT/S1
C
      READ(5,IN)
      SUM2=0.
      DO 500 LP=1,4
      AS=A(LP)/SIGMA(LP)
      L1=LP+1
      SUM1=0.
      DO 400 L=L1,5
      PAR=(SLAM(L)/SLAM(LP))*(SLAM(L)/SLAM(LP))*
     1((SLAM(LP)/SLAM(L))+(SLAM(L)/SLAM(LP))-1.+EO*EO*
     2((1./EO)+(1./SLAM(L))-(1./SLAM(LP)))**2)*DELTA(L)/
     3(SLAM(L)*SLAM(L))*SIGD(L)/SIGMA(L)
      SUM1=SUM1+PAR
  400 CONTINUE
      DEH=SUM1*AS
      SUM2=SUM2+DEH
  500 CONTINUE
      S1=SUM2*3.1416*SND2O*SND2O*NZ*RO*RO*EO
```

```
      WRITE(6,OUT)
      STOP
      END
/*
//G.SYSIN   DD  *
 &IN A=0.0692,0.141,0.0518,0.0804,0.08,
 SIGMA=0.04,0.0366,0.0405,0.0424,0.0448,
 DELTA=2.,1.,0.25,0.25,0.27,
 SIGD=4.E-27,4.50E-27,3.4E-27,2.4E-27,1.2E-27
 SLAM=5.,3.5,2.875,2.625,2.365
 &END
/*
```

APPENDIX K

APPROXIMATE CORRECTION FACTORS FOR THE DELAYED NEUTRON FRACTIONS

We intended to approximate the Eq. (6-24) by applying a neutron balance argument to the already available fifteen-group Exterminator-II output for MITR-II.

The central idea of this method is to compute the ratio of the probability of causing fission of a delayed neutron to the probability of causing fission of a prompt neutron.

For this purpose neutrons born in the first six groups of a fifteen-group scheme are considered. These neutrons may cause fission, or may be absorbed, or may leak out of the core, or may scatter to a lower group. The probability for these events can be computed by a balance argument. The probability of causing fission of a neutron of group y in the core is for instance the number of fissions per sec. caused in the core by the neutrons of group g over the number of neutrons gained (or lost -if the reactor is at a steady state critical condition-) per sec. in the core in group g.

The neutrons born in group g are followed throughout their story until they become thermalized and the number of fissions caused by these neutrons is counted. The ratio of the final number of fissions caused by the neutrons born in group g - during the thermalization process - to the number of neutrons born in group g give the global probability of causing fission of a neutron born in group g throughout its entire lifetime.

This probability PFISS(g), g=1, ..., 6, is computed for all the six groups of neutrons and averaged over the prompt neutron spectrum. This yields, PRTHP, the global probability of causing fission of a prompt fission neutron over a lifetime period.

Assuming that the delayed neutrons are born in the fifth end sixth energy group of the fifteen-group scheme, the correction factor that we seek is then

$$C_{F_j} = \frac{\text{PFISS}(5)}{\text{PRTHP}} \, , \; j = 1, \ldots 5, \qquad \text{(K-1)}$$

$$C_{F_G} = \frac{\text{PFISS}(6)}{\text{PRTHP}} \, , \qquad \text{(K-2)}$$

where j refers to the j^{th} delayed group.

The details of the calculations can be followed from the code written for this purpose (cf. Appendix L).

PFISS(g), g = 1, ..., 6, is shown in Table K-1.

Table K-1 PFISS(g), g=1,...,6

g	PFISS(g)
1	0.30629
2	0.40506
3	0.50895
4	0.57297
5	0.65779
6	0.70902

PRTHP is found to be 0.45959

To cross check this result the eigenvalue of the reactor may be computed by simply multiplying PRTHP by ν, the average number of neutrons generated through the fission. If this is done a discrepancy of about 8% is found as compared to the eigenvalue given in the relevant Exterminator-II output. It is believed, this is due to the bad convergence of the fluxes.

Nevertheless it is anticipated that an error of the same order of magnitude may be introduced in each of the probabilities PFISS(g)'s. In this case C_{F_j}'s would not be affected by the fact that we had to work with badly converged fluxes.

APPENDIX L

PROGRAM BTCR

(Like BETA - Delayed Neutron Fractions - Correction Factor)

```
// 'TOLGA YARMAN',REGION=128K,CLASS=A
/*MITIC USER=(M8696,9441)
/*SRI LOW
/*MAIN LINES=20,CARDS=00,TIME=5
//STEP1 EXEC FORCGC
//C.SYSIN DD *
C PROGRAM BTCR
C
C THIS PROGRAM COMPUTES THE RATIO OF THE PROBABILITY OF A DELAYED NEUTRON(BORN
C WITHIN THE 5TH OR 6TH GROUP OF THE 15-GROUP SCHEME) TO CAUSE FISSION,TO THE
C PROBABILITY OF A FISSION NEUTRON TO CAUSE FISSSON.THIS RATIO WILL BE USED AS A
C CORRECTION FACTOR FOR THE DELAYED NEUTRON FRACTIONS IN FEW GROUP SCHEME WHERE
C PROMPT AND DELAYED NEUTRONS ARE BORN WITHIN THE SAME -FAST- GROUP
C
      COMMON/P/PSI(15,29)
      COMMON/A/ ALEAK1(15),ALEAK2(15),ALEAK3(15),SOLT(15)
      COMMON/ABS/ABSP(15)
      COMMON/S/SCAT(15,29,15)
      COMMON/ABC/ABSPC(15,7)
      COMMON/FC/FISSC(15,7)
      COMMON/STC/STINC(15,7)
      COMMON/OTC/OTSTC(15,7)
      COMMON/KB/KHIF(15),BETA(6)
      COMMON/SR/SRCE(15)
      COMMON/URTAK1/ALEAK(15),PLRC
      COMMON/URTAK2/PF(15),PLCR(14),PSR(14,15),PSC(14,15)
      COMMON/MSTUDY/MF,SRT,LLL,MH(14),KKK
C
      DIMENSION S0(6),S1(6),S2(6),S3(6),S4(6),S5(6),S6(6),S7(6),S8(6),
     1S9(6),S10(5),S11(4),S12(3),S13(2),S( 6,15),C(6),STH(6),FIS(6),PFIS
     2S(6)
C
      REAL KHIF
C
      EQUIVALENCE ( MH(1),MH1),(MH(2),MH2),(MH(3),MH3),(MH(4),MH4),
     1(MH(5),MH5),(MH(6),MH6),(MH(7),MH7),(MH(8),MH8),(MH(9),MH9),
```

```
     2(MH(10),MH10),(MH(11),MH11),(MH(12),MH12),(MH(13),MH13),(MH(14),
     3MH14)
C
      EQUIVALENCE (S0(1),S(1,1))
      EQUIVALENCE (S1(1),S(1,2))
      EQUIVALENCE (S2(1),S(1,3))
      EQUIVALENCE (S3(1),S(1,4))
      EQUIVALENCE (S4(1),S(1,5))
      EQUIVALENCE (S5(1),S(1,6))
      EQUIVALENCE (S6(1),S(1,7))
      EQUIVALENCE (S7(1),S(1,8))
      EQUIVALENCE (S8(1),S(1,9))
      EQUIVALENCE (S9(1),S(1,10))
      EQUIVALENCE (S10(1),S(1,11))
      EQUIVALENCE (S11(1),S(1,12))
      EQUIVALENCE (S12(1),S(1,13))
      EQUIVALENCE (S13(1),S(1,14))
      EQUIVALENCE (S14,S(1,15))
C
      NAMELIST/OUTK/KKK
      NAMELIST/OUTSTH/STH
      NAMELIST/OUTS0/S0
      NAMELIST/OUTS1/S1
      NAMELIST/OUTS2/S2
      NAMELIST/OUTS3/S3
      NAMELIST/OUTS4/S4
      NAMELIST/OUTS5/S5
      NAMELIST/OUTS6/S6
      NAMELIST/OUTS7/S7
      NAMELIST/OUTS8/S8
      NAMELIST/OUTS9/S9
      NAMELIST/OUTS10/S10
      NAMELIST/OUTS11/S11
      NAMELIST/OUTS12/S12
      NAMELIST/OUTS13/S13
      NAMELIST/OUTS14/S14
```

```
      NAMELIST/OUTF/FIS
      NAMELIST/OUTFFS/PFISS
      NAMELIST/OPRTHP/PRTHP
      NAMELIST/OUTC1/C1
      NAMELIST/OUTC2/C2
      NAMELIST/OUTE/BETA
C
C ALEAK(I) ; NUMBER OF NEUTRONS THAT LEAK OUT FROM GROUP I/SEC
C SOUT(I) ; NUMBER OF NEUTRONS THAT SCATTER OUT FROM GROUP I/SEC
C ABSP(I) ; NUMBER OF NEUTRONS THAT ARE ABSORBED IN GROUP I/SEC
C SCAT(MG,MC,MH) ; MACROSCOPIC SCATTERING CROSS SECTION FROM GROUP MG INTO
C GROUP MH IN COMPOSITION MC
C KHIF ; DESCRIBES THE FISSION SPECTRUM
C MC.EQ.1 CORRESPONDS TO MATERIEL 1,2 TO 3,3 TO 4,4 TO 5,5 TO 6,6 TO 13,7 TO 14
C OF THE CORE
C ABSPC(I,MC);ABSORPTS /SEC,IN MATERIEL MC OF THE CORE,OF NEUTRONS OF GROUP I
C FISSC(I,MC);FISSIONS/SEC CAUSED BY NEUTRONS OF GROUP I IN MATERIEL MC
C STINC(I,MC);NUMBER OF NEUTRONS SCATTERED IN GROUP I/SEC WITHIN THE MATERIEL
C MC OF THE CORE
C OTSTC(I,MC);NUMBER OF NEUTRONS SCATTERED OUT OF GROUP I/SEC WITHIN THE
C MATERIEL MC OF THE CORE
C
      KKK=0
      DO 80 I=1,15
   80 ALEAK(I)=ALEAK1(I)+ALEAK2(I)+ALEAK3(I)
C
      CALL PROB
C
      MF=5
      DO 300 I=1,6
      IF (KKK.LT.1000000000) GO TO 893
      WRITE(6,OUTK)
      KKK=0
  893 CONTINUE
      SRT=0.
      SUM1=0.
```

```
      SUM2=0.
      SUM3=0.
      SUM4=0.
      SUM5=0.
      SUM6=0.
      SUM7=0.
      SUM8=0.
      SUM9=0.
      SUM10=0.
      SUM11=0.
      SUM12=0.
      SUM13=0.
      SUM14=0.
C
C YET NO COLLISION FOR NEUTRONS BORN IN ENERGY GROUP I THAT WOULD SCATTER
C THEM INTO A LOWER ENERGY GROUP;
C
      SCO=SRCE(I)
C
C WE ARE INTERESTED IN THESE NEUTRONS EITHER CAUSING FISSION,
C
      SUM0=SCO*PF(I)
C
C OR LEAKING OUT OF THE CORE AND CONTINUING FROM THERE ON,
C
      SRO=SCO*PLCR(I)
C
C OR SCATTERING(THAT MAY HAPPEN IN THE CORE OF IN THE REFLECTOR)-FIRST COLLISION
C IN I- INTO A LOWER ENERGY GROUP MH1,AND CONTINUING FROM THERE ON.
C
      I1=I+1
      IF=I+MF
      DO 200 MH1=I1,IF
      SC1=SCO*PSC(I,MH1)
      SUM1=SUM1+SC1*PF(MH1)
C
```

```
C THE REFLECTOR SOURCE OF GROUP MH1 IS FED BY NEUTRONS OF GROUP MH1 LEAKING
C FROM THE CORE AND NEUTRONS SCATTERING (IN THE REFLECTOR) INTO MH1 FROM UPPER
C GROUPS.HOWEVER IF MH1 CORRESPONDS TO THE THERMAL GROUP(WHICH IS NOT TRUE AT
C THIS LEVEL EVEN IF I WERE 6 AND THERE WERE SCATTERING TO FIVE LOWER GROUPS;
C NEVERTHELESS WE WILL PERSUE THE THOUGHT TO INITIATE THE CHAIN OF REASONING)
C THERE WILL BE NO LEAKAGE OUT OF THE CORE,AND THERE WILL BE ONE FROM OUTSIDE
C OF THE CORE INTO THE CORE FOR WHICH WE BUILD UP THE THERMAL
C REFLECTOR SOURCE TERM SRT.
C
      IF (MH1.EQ.15) GO TO 5
      SR1=SC1*PLCR(MH1)+SRO*PSR(I,MH1)
      GO TO 6
    5 SRT=SRT+SRO*PSR(I,MH1)
C
C IF WE COUNT ON THE SECOND COLLISION TO BRING THE NEUTRON TO THE 15TH
C GROUP (THE GREATEST),MH1(WHERE THE SECOND COLLISION WILL EVENTUALLY
C OCCUR) CAN NOT BE BIGER THAN 14 (HERE AGAIN,WHILE MH1 IS NEVER GREATER
C THAN 14,WE WANT TO INITIATE THE CHAIN OF REASONING).
C
    6 IF(MH1.GT.14) GO TO 200
      MH1B=MH1+1
      MH1F=MH1+MF
      DO 200 MH2=MH1B,MH1F
C
C SECOND COLLISION IN MH1,STUDY OF MH2
C
      CALL STUDY(SC1,SR1,SC2,SR2,SUM2,2,MH21,MH2F)
      IF (LLL.EQ.0) GO TO 200
      DO 200 MH3=MH21,MH2F
C
C AND SO ON
C
      CALL STUDY(SC2,SR2,SC3,SR3,SUM3,3,MH31,MH3F)
      IF (LLL.EQ.0) GO TO 200
      DO 200 MH4=MH31,MH3F
C
```

```
      CALL STUDY( SC3,SR3,SC4,SR4,SUM4,4,MH41,MH4F)
      IF (LLL.EQ.0) GO TO 200
      DO 200 MH5=MH41,MH4F
C
      CALL STUDY(SC4,SR4,SC5,SR5,SUM5,5,MH51,MH5F)
      IF (LLL.EQ.0) GO TO 200
      DO 200 MH6=MH51,MH5F
C
      CALL STUDY( SC5,SR5,SC6,SR6,SUM6,6,MH61,MH6F)
      IF (LLL.EQ.0) GO TO 200
      DO 200 MH7=MH61,MH6F
C
      CALL STUDY(SC6,SR6,SC7,SR7,SUM7,7,MH71,MH7F)
      IF (LLL.EQ.0) GO TO 200
      DO 200 MH8=MH71,MH7F
C
      CALL STUDY( SC7,SR7,SC8,SR8,SUM8,8,MH81,MH8F)
      IF (LLL.EQ.0) GO TO 200
      DO 200 MH9=MH81,MH8F
C
      CALL STUDY(SC8,SR8,SC9,SR9,SUM9,9,MH91,MH9F)
C
C EVEN IF THE NEUTRON HAS BEEN SCATTERED ALWAYS TO THE CLOSEST GROUP STARTING
C FROM THE 6TH GROUP AFTER 9 COLLISIONS IT WOULD BE NOW AT THE 15 TH GROUP;
C THEN WE KEEP IT ASIDE.
C
      IF((I.EQ.6).OR.(LLL.EQ.0)) GO TO 200
      DO 200 MH10=MH91,MH9F
C
      CALL STUDY(SC9,SR9,  SC10,SR10,SUM10,10,MH101,MH10F)
      IF((I.EQ.5).OR.(LLL.EQ.0)) GO TO 200
      DO 200 MH11=MH101,MH10F
C
      CALL STUDY(SC10,SR10,SC11,SR11,SUM11,11,MH111,MH11F)
      IF((I.EQ.4).OR.(LLL.EQ.0)) GO TO 200
      DO 200 MH12=MH111,MH11F
```

```
C
      CALL STUDY(SC11,SR11,SC12,SR12,SUM12,12,MH121,MH12F)
      IF((I.EQ.3).OR.(LLL.EQ.0)) GO TO 200
      DO 200 MH13=MH121,MH12F
C
      CALL STUDY(SC12,SR12,SC13,SR13,SUM13,13,MH131,MH13F)
      IF((I.EQ.2).OR.(LLL.EQ.0)) GO TO 200
      DO 200 MH14=MH131,MH13F
C
      CALL STUDY(SC13,SR13,SC14,SR14,SUM14,14,MH141,MH14F)
  200 CONTINUE
      STH(I)=SRT
      S0(I)=SUM0
      S1(I)=SUM1
      S2(I)=SUM2
      S3(I)=SUM3
      S4(I)=SUM4
      S5(I)=SUM5
      S6(I)=SUM6
      S7(I)=SUM7
      S8(I)=SUM8
      S9(I)=SUM9
      IF (I.EQ.6) GO TO 300
      S10(I)=SUM10
      IF (I.EQ.5) GO TO 300
      S11(I)=SUM11
      IF (I.EQ.4) GO TO 300
      S12(I)=SUM12
      IF (I.EQ.3) GO TO 300
      S13(I)=SUM13
      IF (I.EQ.2) GO TO 300
      S14=SUM14
  300 CONTINUE
      WRITE(6,OUTK)
      WRITE(6,OUTSTH)
      WRITE(6,OUTS0)
```

```
      WRITE(6,OUTS1)
      WRITE(6,OUTS2)
      WRITE(6,OUTS3)
      WRITE(6,OUTS4)
      WRITE(6,OUTS5)
      WRITE(6,OUTS6)
      WRITE(6,OUTS7)
      WRITE(6,OUTS8)
      WRITE(6,OUTS9)
      WRITE(6,OUTS10)
      WRITE(6,OUTS11)
      WRITE(6,OUTS12)
      WRITE(6,OUTS13)
      WRITE(6,OUTS14)
C
C TOTAL NUMBER OF NEUTRONS THAT STARTED UP IN GROUP I(1.LE.I.LE.6)
C AND CAUSE EVENTUALLY FISSION
C
      DO 500 I=1,6
      KCR=17-I
      SUM=0.
      DO 400 K=1,15
      IF (K.GE.KCR) GO TO 400
      SUM=SUM+S(I,K)
  400 CONTINUE
      FIS(I)=SUM+STH(I)*PLRC*PF(15)
  500 CONTINUE
      WRITE(6,OUTF)
C
C THE PROBABILITY THAT A NEUTRON BORN IN GROUP I GIVES EVENTUALLY RISE TO A
C FISSION
C
      DO 510 I=1,6
  510 PFISS(I)=FIS(I)/SRCE(I)
      WRITE(6,OUTPFS)
C
```

```
C NEUTRONS IN THIS SCHEME ARE SUPPSED TO BE BORN IN SIX ENERGY GROUPS AND
C WE WANT TO AVERAGE THE ABOVE PROBABILITY OVER THE FISSION SPECTRUM;
C
      PRTHP=0.
      DO 520 I=1,6
  520 PRTHP=PRTHP+PFISS(I)*KHIF(I)
      WRITE(6,OPRTHP)
C
C THE CORRECTION FACTOR WE ARE SEEKING FOR THE FRACTION OF DELAYED NEUTRONS
C OF THE NTH GROUP(TIME WISE) IS FINALLY;
C
      C1=PFISS(5)/PRTHP
      C2=PFISS(4)/PRTHP
      WRITE(6,OUTC1)
      WRITE(6,OUTC2)
      C(1)=C1
      DO 66 M=2,6
   66 C(M)=C2
C
C THE CORRECTED BETA VALUES ARE THEN
C
      DO 550 N=1,6
  550 BETA(N)=BETA(N)*C(N)
      WRITE(6,OUTB)
      STOP
      END
      BLOCK DATA
C
      COMMON/P/ PSI1(15),PSI2(15),PSI3(15),PSI4(15),PSI5(15),PSI6(15),
     1PSI7(15),PSI8(15),PSI9(15),PSI10(15),PSI11(15),PSI12(15),PSI13(15
     2),PSI14(15),PSI15(15),PSI16(15),PSI17(15),PSI18(15),PSI19(15),
     3PSI20(15),PSI21(15),PSI22(15),PSI23(15),PSI24(15),PSI25(15),PSI26
     4(15),PSI27(15),PSI28(15),PSI29(15)
      COMMON/A/ ALEAK1(15),ALEAK2(15),ALEAK3(15),SOUT(15)
      COMMON/ABS/ABSP(15)
      COMMON/S/ SCAT1(15,29),SCAT2(15,29),SCAT3(15,29),SCAT4(15,29),
```

```
     2SCAT5(15,29),SCAT6(15,29),SCAT7(15,29),SCAT8(15,29),SCAT9(15,29),
     3SCAT10(15,29),SCAT11(15,29),SCAT12(15,29),SCAT13(15,
     429),SCAT14(15,29),SCAT15(15,29)
      COMMON/ABC/ABSPC1(15),ABSPC2(15),ABSPC3(15),ABSPC4(15),ABSPC5(15),
     1ABSPC6(15),ABSPC7(15)
      COMMON/FC/FISSC1(15),FISSC2(15),FISSC3(15),FISSC4(15),FISSC5(15),
     1FISSC6(15),FISSC7(15)
      COMMON/STC/STINC1(15),STINC2(15),STINC3(15),STINC4(15),STINC5(15),
     1STINC6(15),STINC7(15)
      COMMON/CTC/CTSTC1(15),CTSTC2(15),CTSTC3(15),CTSTC4(15),CTSTC5(15),
     1CTSTC6(15),CTSTC7(15)
      COMMON/KB/KHIF(15),BETA(6)
      COMMON/SR/SRCE(15)
C
      REAL KHIF
C
C AVERAGE FLUX IN MATERIEL NUMBERED 1 FOR 15 GROUPS
C
      DATA PSI1/1.00737E13,2.23071E13,1.18319E13,1.76862E13,
     11.78534E13,1.25523E13,9.69910E12,8.69193E12,8.34772E12,
     25.54323E12,4.87979E12,5.07788E12,4.51213E12,3.58995E12,
     33.09949E13/
C
C AVERAGE FLUX IN MATERIEL NUMBERED 2 FOR 15 GROUPS
C
      DATA PSI2/7.13232E11,1.62687E12,7.77294E11,1.18596E12,
     11.30902E12,1.00939E12,8.29590E11,7.80258E11,7.85932E11,5.49627E11,
     25.00281E11,5.34657E11,4.83793E11,3.94693E11,1.05229E13/
C
C AND SO ON
C
      DATA PSI3/1.27551E13,2.89790E13,1.54629E13,2.35919E13,
     12.38825E13,1.69370E13,1.30778E13,1.17095E13,1.12181E13,
     27.44364E12,6.52920E12,6.76325E12,5.98542E12,4.74891E12,
     33.85021E13/
C
```

```
      DATA PSI4/1.71227E13,3.96525E13,2.05659E13,3.16724E13,           BTCR0361
     13.24365E13,2.31479E13,1.78172E13,1.58380E13,1.49665E13,9.74154E12,BTCR0362
     28.41021E12,8.58567E12,7.50363E12,5.84070E12,2.68752E13/           BTCR0363
C                                                                       BTCR0364
      DATA PSI5/1.45549E13,3.29063E13,1.68575E13,2.54005E13,2.60652E13, BTCR0365
     11.85560E13,1.42987E13,1.27317E13,1.20567E13,7.84387E12,6.78769E12,BTCR0366
     26.95031E12,6.08968E12,4.75007E12,2.16459E13/                      BTCR0367
C                                                                       BTCR0368
      DATA PSI6/9.88098E12,2.21733E13,1.14855E13,1.72909E13,1.75745E13, BTCR0369
     11.22013E13,9.39882E12,8.39353E12,8.03255E12,5.30221E12,           BTCR0370
     24.65178E12,4.82862E12,4.27763E12,3.34948E12,2.17280E13/           BTCR0371
C                                                                       BTCR0372
      DATA PSI7/1.51137E11,3.06827E11,1.34340E11,2.47386E11,            BTCR0373
     15.05956E11,5.45318E11,5.28815E11,5.26329E11,5.44502E11,3.93885E11,BTCR0374
     23.66978E11,4.08846E11,3.79416E11,3.52016E11,3.62643E13/           BTCR0375
C                                                                       BTCR0376
      DATA PSI8/1.20144E13,2.84534E13,1.50317E13,2.36870E13,            BTCR0377
     12.40741E13,1.73901E13,1.33255E13,1.18493E13,1.12134E13,7.36938E12,BTCR0378
     26.35423E12,6.48740E12,5.68764E12,4.41452E12,2.24688E13/           BTCR0379
C                                                                       BTCR0380
      DATA PSI9/1.50146E12,3.58446E12,1.77785E12,2.73737E12,            BTCR0381
     13.05101E12,2.39223E12,1.94321E12,1.80874E12,1.76625E12,1.17805E12,BTCR0382
     21.06644E12,1.13439E12,1.00268E12,6.22961E11,3.90013E11/           BTCR0383
C                                                                       BTCR0384
      DATA PSI10/1.56417E13,3.60170E13,1.85488E13,2.83327E13,           BTCR0385
     12.91862E13,2.08403E13,1.61003E13,1.43636E13,1.36231E13,8.8824E12, BTCR0386
     27.69509E12,7.88080E12,6.89826E12,5.35424E12,2.67592E13/           BTCR0387
C                                                                       BTCR0388
      DATA PSI11/4.65987E12,1.07289E13,5.55235E12,8.48465E12,           BTCR0389
     19.05601E12,6.63210E12,5.29852E12,4.85433E12,4.74320E12,3.19684E12,BTCR0390
     22.85435E12,3.00461E12,2.67725E12,2.03224E12,1.92446E13/           BTCR0391
C                                                                       BTCR0392
      DATA PSI12/2.44550E12,5.57977E12,2.66179E12,4.24124E12,           BTCR0393
     15.48086E12,4.46704E12,3.71362E12,3.47187E12,3.46546E12,2.41814E12,BTCR0394
     22.20282E12,2.36435E12,2.13292E12,1.74126E12,5.40822E13/           BTCR0395
C                                                                       BTCR0396
```

```
      DATA PSI13/6.93262E12,1.63319E13,8.21708E12,1.27142E13,1.32311E13,
     19.66926E12,7.56880E12,6.82197E12,6.49332E12,4.22544E12,3.67926E12,
     23.79062E12,3.31885E12,2.39604E12,7.04389E12/
C
      DATA PSI14/5.51701E12,1.26775E13,6.30738E12,9.52943E12,
     19.88196E12,7.09271E12,5.52900E12,4.97879E12,4.76316E12,
     23.12083E12,2.72414E12,2.81461E12,2.48035E12,1.89559E12,
     37.84037E12/
C
      DATA PSI15/2.83592E9,5.53228E9,2.1419E9,3.85601E9,
     18.45488E9,1.19461E10,1.51236E10,1.96665E10,2.58602E10,2.18789E10,
     22.29989E10,2.84099E10,2.90990E10,2.70993E10,9.94618E12/
C
      DATA PSI16/2.55197E8,8.86992E8,3.67096E8,6.17273E8,
     11.10916E9,1.46164E9,1.68106E9,2.08979E9,2.65010E9,2.21534E9,
     22.33090E9,2.89865E9,2.99767E9,2.73959E9,2.15733E12/
C
      DATA PSI17/2.38627E12,5.21569E12,2.38901E12,3.90725E12,
     15.61735E12,4.70592E12,3.93748E12,3.66121E12,3.65511E12,2.57785E12,
     22.35870E12,2.55382E12,2.32249E12,2.01416E12,9.41901E13/
C
      DATA PSI18/9.99961E9,2.29717E10,8.79224E9,1.30877E10,
     11.48976E10,1.19969E10,1.02758E10,1.00958E10,1.06745E10,7.79902E9,
     27.36367E9,8.15255E9,7.61416E9,6.31105E9,3.68421E11/
C
      DATA PSI19/4.69802E10,1.07163E11,4.26929E10,6.39392E10,
     17.26767E10,5.90273E10,5.03304E10,4.92060E10,5.15745E10,3.72584E10,
     23.49577E10,3.84597E10,3.56174E10,2.88146E10,1.76375E12/
C
      DATA PSI20/2.92986E12,6.48734E12,3.10695E12,4.83535E12,
     15.88415E12,4.82943E12,4.09801E12,3.92453E12,4.00831E12,2.84567E12,
     22.61498E12,2.82121E12,2.57460E12,2.15952E12,8.82265E13/
C
      DATA PSI21/2.79272E12,6.41947E12,3.15487E12,4.93465E12,
     14.93872E12,4.76330E12,3.96308E12,3.72960E12,3.73572E12,2.59872E12,
     22.35888E12,2.51551E12,2.26435E12,1.81786E12,4.46644E13/
```

```
C
      DATA PSI22/15*0./
C
      DATA PSI23/7.30400E10,1.59244E11,6.33609E10,1.00316E11,
     11.33994E11,1.17226E11,1.05928E11,1.07670E11,1.16894E11,8.71505E10,
     28.33669E10,9.36818E10,8.86947E10,7.66278E10,8.54001E12/
C
      DATA PSI24/6.57385E12,1.46396E13,7.38030E12,1.12008E13,
     11.19848E13,9.05311E12,7.3486E12,6.83381E12,6.80922E12,4.72257E12,
     24.25975E12,4.50770E12,4.05123E12,3.32159E12,7.32432E13/
C
      DATA PSI25/5.79924E11,1.14494E12,4.82339E11, 9.10516E11,
     11.93840E12,2.04278E12,1.90154E12,1.82458E12,1.83840E12,1.31154E12,
     21.21184E12,1.34153E12,1.23831E12,1.14720E12,8.87780E13/
C
      DATA PSI26/1.90676E11,3.45018E11,1.42709E11,2.88850E11,
     17.49914E11,9.43641E11,9.88051E11,1.01437E12,1.06279E12,7.74108E11,
     27.24443E11,8.12987E11,7.58574E11,7.15832E11,7.18332E13/
C
      DATA PSI27/5.44443E10,9.02989E10,3.67989E10,7.64669E10,
     12.22783E11,3.26632E11,3.88721E11,4.39476E11,4.95380E11,3.77230E11,
     23.64096E11,4.20310E11,4.01508E11,3.85550E11,5.44373E13/
C
      DATA PSI28/1.09570E10,1.73024E10,6.98252E9,1.44094E10,
     14.28526E10,6.84570E10,8.99937E10,1.12109E11,1.38318E11,1.12020E11,
     21.13418E11,1.36955E11,1.36171E11,1.33562E11,3.27973E13/
C
      DATA PSI29/4.21734E8,1.83346E9,7.75283E8,1.30522E9,
     12.28654E9,2.97064E9,3.35040E9,4.08927E9,5.08521E9,4.20670E9,
     24.39746E9,5.45074E9,5.63666E9,5.16516E9,3.58462E12/
C
C OVERALL TOP LEAKAGE FOR 15 GROUPS
C
      DATA ALEAK1/1.889440E13,3.153295E13,5.987261E12,6.845539E12,
     15.600768E12,3.234598E12,2.337979E12,2.154750E12,2.169184E12,
     21.524452E12,1.466040E12,1.650620E12,1.475029E12,9.392717E11,
```

```
     39.824966E14/
C
C OVERALL RIHGT LEAKAGE FOR 15 GROUPS
C
      DATA ALEAK2/4.552575E11,3.632165E12,1.019874E12,1.368641E12,
     11.947569E12,2.153000E12,2.277313E12,2.747096E12,3.229789E12,
     22.561373E12,2.579727E12,3.016094E12,3.028231E12,2.669834E12,
     35.464075E15/
C
C OVERALL BOTTOM LEAKAGE FOR 15 GROUPS
C
      DATA ALEAK3/1.221791E12,1.807827E12,4.596729E11,7.703967E11,
     11.99357E12,3.489477E12,4.676534E12,6.200280E12,8.251115E12,
     27.073027E12,7.518418E12,9.545074E12,9.946090E12,8.713511E12,
     39.291814E15/
C
C OVERALL ABSORPTION FOR 15 GROUPS
C
      DATA ABSP/1.88522E15,1.662308E15,9.366816E14,1.514466E15,
     11.855078E15,1.978965E15,2.041348E15,3.105764E15,6.613305E15,
     21.020215E16,8.413368E15,7.673170E15,6.260898E15,1.051310E16,
     33.176098E17/
C
COVERALL SCATTERING OUT FOR 15 GROUPS
C
      DATA SOUT/7.952307E16,1.867122E17,1.566322E17,2.434807E17,
     13.155958E17,3.362193E17,3.297101E17,3.239994E17,3.183894E17,
     22.671682E17,2.505562E17,2.581691E17,2.433807E17,2.187724E17,
     30./
C
C MACROSCOPIC SCATTERING CROSS SECTIONS FROM GROUP 1 INTO FIFTEEN GROUPS FOR
C 29 MATERIELS
C
      DATA SCAT1/435*0./
C
      DATA SCAT2/5.06E-2, 14*0. ,4.93E-2, 14*0. ,5.16E-2, 14*0.,4.91E-2,
```

```
     114*0.,4.80E-2,14*0.,5.06E-2,14*0.,4.96E-2,14*0.,2.31E-3,          BTCR0505
     214*0.,2.87E-2,14*0.,3.37E-2,14*0.,3.37E-2,14*0.,3.37E-2,          BTCR0506
     314*0.,4.91E-2,14*0.,4.80E-2,14*0.,4.93E-2,14*0.,4.29E-2,          BTCR0507
     414*0.,4.23E-2,14*0.,6.55E-2,14*0.,6.33E-2,14*0.,6.55E-2,          BTCR0508
     514*0.,6.55E-2,14*0.,15*0.,6.24E-2,14*0.,6.23E-2,                  BTCR0509
     614*0.,4.96E-2,14*0.,4.96E-2,14*0.,4.96E-2,                        BTCR0510
     714*0.,4.96E-2,14*0.,4.29E-2,14*0./                                BTCR0511
C                                                                       BTCR0512
      DATA SCAT3/1.13E-2,3.63E-2,13*0.,1.09E-2,3.29E-2,13*0.,1.16E-2,   BTCR0513
     13.73E-2,13*0.,1.10E-2,3.28E-2,13*0.,1.07E-2,3.16E-2,13*0.,        BTCR0514
     21.13E-2,3.63E-2,13*0.,1.32E-2,4.15E-2,13*0.,1.58E-2,2.04E-3,      BTCR0515
     313*0.,5.12E-3,1.18E-2,13*0.,6.02E-3,1.38E-2,13*0.,6.02E-3,        BTCR0516
     41.38E-2,13*0.,6.02E-3,1.38E-2,13*0.,1.10E-2,3.28E-2,13*0.,        BTCR0517
     51.07E-2,3.16E-2,13*0.,1.09E-2,3.29E-2,14*0.,2.62E-2,              BTCR0518
     613*0.,9.74E-3,2.80E-2,13*0.,1.60E-2,5.25E-2,13*0.,1.53E-2,        BTCR0519
     75.01E-2,13*0.,1.60E-2,5.25E-2,13*0.,1.60E-2,5.25E-2,13*0.,        BTCR0520
     815*0.,1.50E-2,4.86E-2,13*0.,1.50E-2,4.86E-2,13*0.,1.32E-2,        BTCR0521
     94.15E-2,13*0.,1.32E-2,4.15E-2,13*0.,1.32E-2,4.15E-2,13*0.,        BTCR0522
     11.32E-2,4.15E-2,14*0.,2.62E-2,13*0./                              BTCR0523
C                                                                       BTCR0524
      DATA SCAT4/8.58E-3,2.85E-2,8.20E-2,12*0.,8.81E-3,2.61E-2,8.58E-2, BTCR0525
     112*0.,9.01E-3,2.95E-2,8.57E-2,12*0.,9.03E-3,2.62E-2,8.53E-2,      BTCR0526
     212*0.,8.60E-3,2.50E-2,8.15E-2,12*0.,8.58E-3,2.85E-2,8.20E-2,      BTCR0527
     312*0.,1.78E-2,4.17E-2,1.05E-1,12*0.,1.34E-2,8.57E-3,2.40E-3,      BTCR0528
     412*0.,1.54E-3,5.63E-3,1.94E-2,12*0.,1.81E-3,6.62E-3,2.29E-2,      BTCR0529
     512*0.,1.81E-3,6.62E-3,2.29E-2,12*0.,1.81E-3,6.62E-3,2.29E-2,      BTCR0530
     612*0.,9.03E-3,2.62E-2,8.53E-2,12*0.,8.60E-3,2.50E-2,8.15E-2,      BTCR0531
     712*0.,8.81E-3,2.61E-2,8.58E-2,14*0.,7.13E-2,                      BTCR0532
     812*0.,9.87E-3,2.44E-2,6.45E-2,12*0.,1.60E-2,4.61E-2,1.50E-1,      BTCR0533
     912*0.,1.51E-2,4.37E-2,1.42E-1,12*0.,1.60E-2,4.61E-2,1.50E-1,      BTCR0534
     112*0.,1.60E-2,4.61E-2,1.50E-1,27*0.,                              BTCR0535
     21.46E-2,4.22E-2,1.37E-1,12*0.,1.45E-2,4.21E-2,1.37E-1,            BTCR0536
     312*0.,1.78E-2,4.17E-2,1.05E-1,12*0.,1.78E-2,4.17E-2,1.05E-1,      BTCR0537
     412*0.,1.78E-2,4.17E-2,1.05E-1,12*0.,1.78E-2,4.17E-2,1.05E-1,12*0.,BTCR0538
     52*0.,7.13E-2,12*0./                                               BTCR0539
C                                                                       BTCR0540
```

```
      DATA SCAT5/4.63E-3,1.41E-2,3.87E-2,1.04E-1,11*0.,4.77E-3,1.43E-2,       BTCR0541
     13.98E-2,1.10E-1,11*0.,4.92E-3,1.48E-2,4.05E-2,1.10E-1,11*0.,            BTCR0542
     24.92E-3,1.44E-2,3.96E-2,1.09E-1,11*0.,4.63E-3,1.36E-2,3.77E-2,          BTCR0543
     31.04E-1,11*0.,4.63E-3,1.41E-2,3.87E-2,1.04E-1,11*0.,7.24E-4,            BTCR0544
     42.21E-2,6.35E-2,1.38E-1,11*0.,3.62E-3,3.29E-3,4.28E-3,2.27E-3,          BTCR0545
     512*0.,1.02E-3,7.17E-3,1.28E-2,12*0.,1.20E-3,8.43E-3,1.51E-2,            BTCR0546
     612*0.,1.20E-3,8.43E-3,1.51E-2,12*0.,1.20E-3,8.43E-3,1.51E-2,11*0.,      BTCR0547
     74.92E-3,1.44E-2,3.96E-2,1.09E-1,11*0.,4.63E-3,1.36E-2,3.77E-2,          BTCR0548
     81.04E-1,11*0.,4.77E-3,1.43E-2,3.98E-2,1.10E-1,14*0.,                    BTCR0549
     95.03E-2,11*0.,3.64E-4,1.17E-2,3.62E-2,7.74E-2,11*0.,9.62E-3,            BTCR0550
     12.77E-2,7.19E-2,2.07E-1,11*0.,9.05E-3,2.61E-2,6.81E-2,1.96E-1,          BTCR0551
     211*0.,9.62E-3,2.77E-2,7.19E-2,2.07E-1,11*0.,9.62E-3,2.77E-2,            BTCR0552
     37.19E-2,2.07E-1,26*0.,8.66E-3,2.51E-2,6.56E-2,                          BTCR0553
     41.88E-1,11*0.,8.66E-3,2.51E-2,6.55E-2,1.88E-1,11*0.,7.24E-4,            BTCR0554
     52.20E-2,6.35E-2,1.38E-1,11*0.,7.24E-4,2.21E-2,6.35E-2,1.38E-1,          BTCR0555
     611*0.,7.24E-4,2.21E-2,6.34E-2,1.38E-1,11*0.,7.24E-4,2.21E-2,            BTCR0556
     76.35E-2,1.38E-1,14*0.,5.03E-2,11*0./                                    BTCR0557
C                                                                             BTCR0558
      DATA SCAT6/1.54E-3,3.66E-3,9.65E-3,2.41E-2,1.36E-1,10*0.,1.62E-3,       BTCR0559
     13.87E-3,1.02E-2,2.58E-2,1.43E-1,10*0.,1.63E-3,3.88E-3,1.02E-2,          BTCR0560
     22.56E-2,1.43E-1,10*0.,1.63E-3,3.86E-3,1.01E-2,2.56E-2,1.42E-1,          BTCR0561
     310*0.,1.54E-3,3.63E-3,9.59E-3,2.41E-2,1.34E-1,10*0.,1.54E-3,            BTCR0562
     43.66E-3,9.65E-3,2.41E-2,1.36E-1,13*0.,1.40E-2,9.91E-2,10*0.,            BTCR0563
     52*1.32E-3,3.62E-3,0.,3.46E-3,14*0.,7.17E-3,14*0.,8.43E-3,               BTCR0564
     614*0.,8.43E-3,14*0.,8.43E-3,10*0.,1.63E-3,3.86E-3,1.01E-2,              BTCR0565
     72.56E-2,1.42E-1,10*0.,1.54E-3,3.63E-3,9.59E-3,2.41E-2,1.34E-1,          BTCR0566
     810*0.,1.62E-3,3.87E-3,1.02E-2,2.58E-2,1.43E-1,14*0.,3.61E-2,            BTCR0567
     212*0.,3.12E-4,7.01E-3,5.41E-2,10*0.,3.27E-3,7.75E-3,2.00E-2,            BTCR0568
     15.22E-2,2.81E-1,10*0.,3.08E-3,7.29E-3,1.89E-2,4.91E-2,2.65E-1,          BTCR0569
     210*0.,3.27E-3,7.75E-3,2.00E-2,5.22E-2,2.81E-1,10*0.,3.27E-3,7.75E-      BTCR0570
     33,2.00E-2,5.22E-2,2.81E-1,25*0.,2.95E-3,6.98E-3,1.81E-2,4.70E-2,        BTCR0571
     42.54E-1,10*0.,2.95E-3,6.98E-3,1.81E-2,4.69E-2,2.54E-1,13*0.,            BTCR0572
     51.40E-2,9.91E-2,13*0.,1.40E-2,9.91E-2,13*0.,1.40E-2,9.91E-2,            BTCR0573
     613*0.,1.40E-2,9.91E-2,14*0.,3.61E-2,10*0./                              BTCR0574
C                                                                             BTCR0575
      DATA SCAT7/0.,6.16E-4,1.60E-3,4.07E-3,2.11E-2,1.93E-1,9*0.,0.,          BTCR0576
```

```
      16.62E-4,1.72E-3,4.37E-3,2.26E-2,2.05E-1,9*0.,0.,6.55E-4,1.70E-3,          BTCR0577
      24.32E-3,2.24E-2,2.05E-1,10*0.,6.55E-4,1.70E-3,4.32E-3,2.24E-2,            BTCR0578
      32.03E-1,11*0.,1.60E-3,4.07E-3,2.11E-2,1.91E-1,10*0.,0.,                   BTCR0579
      41.60E-3,4.07E-3,2.11E-2,1.93E-1,14*0.,9.56E-2,11*0.,1.32E-3,              BTCR0580
      52*0.,4.04E-3,14*0.,3.58E-3,14*0.,4.22E-3,14*0.,4.22E-3,14*0.,             BTCR0581
      64.22E-3,10*0.,0.,1.70E-3,4.32E-3,2.24E-2,2.03E-1,11*0.,                   BTCR0582
      71.60E-3,4.07E-3,2.11E-2,1.91E-1,10*0.,6.62E-4,1.72E-3,4.37E-3,2.26        BTCR0583
      8E-2,2.05E-1,14*0.,3.34E-2,14*0.,5.02E-2,10*0.,1.34E-3,                    BTCR0584
      93.47E-3,8.82E-3,4.57E-2,4.10E-1,10*0.,1.26E-3,3.27E-3,8.30E-3,            BTCR0585
      14.30E-2,3.86E-1,10*0.,1.34E-3,3.47E-3,8.82E-3,4.57E-2,4.10E-1,            BTCR0586
      210*0.,1.34E-3,3.47E-3,8.82E-3,4.57E-2,4.10E-1,25*0.,                      BTCR0587
      31.20E-3,3.13E-3,7.94E-3,4.11E-2,3.70E-1,10*0.,1.20E-3,3.13E-3,            BTCR0588
      47.94E-3,4.11E-2,3.70E-1,13*0.,7.90E-4,9.56E-2,13*0.,7.90E-4,              BTCR0589
      59.56E-2,14*0.,9.56E-2,13*0.,7.90E-4,9.56E-2,                              BTCR0590
      614*0.,3.34E-2,9*0./                                                       BTCR0591
C                                                                                BTCR0592
       DATA SCAT8/2*0.,3.70E-4,6.78E-4,3.60E-3,3.22E-2,2.33E-1,10*0.,            BTCR0593
      13.97E-4,7.28E-4,3.87E-3,3.46E-2,2.50E-1,12*0.,                            BTCR0594
      23.83E-3,3.42E-2,2.47E-1,10*0.,2*0.,3.83E-3,3.42E-2,                       BTCR0595
      32.47E-1,12*0.,3.60E-3,3.22E-2,3.33E-1,12*0.,3.60E-3,                      BTCR0596
      43.22E-2,2.33E-1,13*0.,2.04E-3,9.75E-2,14*0.,                              BTCR0597
      54.45E-3,14*0.,3.22E-3,14*0.,3.79E-3,14*0.,3.79E-3,                        BTCR0598
      614*0.,3.79E-3,12*0.,3.83E-3,3.42E-2,2.47E-1,12*0.,                        BTCR0599
      73.60E-3,3.22E-2,2.33E-1,12*0.,3.87E-3,3.46E-2,2.50E-1,14*0.,              BTCR0600
      83.57E-2,13*0.,1.02E-3,5.09E-2,11*0.,1.47E-3,7.82E-3,6.98E-2,              BTCR0601
      95.01E-1,11*0.,1.38E-3,7.35E-3,6.57E-2,4.72E-1,11*0.,1.47E-3,              BTCR0602
      17.82E-3,6.98E-2,5.E-1,11*0.,1.47E-3,7.82E-3,6.98E-2,5.E-1,23*0.,          BTCR0603
      23*0.,1.32E-3,7.04E-3,6.29E-2,4.51E-1,11*0.,1.32E-3,7.03E-3,               BTCR0604
      36.28E-2,4.51E-1,13*0.,2.04E-3,9.75E-2,13*0.,2.04E-3,9.75E-2,              BTCR0605
      413*0.,2.04E-3,9.75E-2,13*0.,2.04E-3,9.75E-2,14*0.,3.57E-2,8*0./           BTCR0606
C                                                                                BTCR0607
       DATA SCAT9/5*0.,5.76E-3,4.16E-2,2.49E-1,12*0.,6.19E-3,4.46E-2,            BTCR0608
      12.67E-1,12*0.,6.12E-3,4.42E-2,2.64E-1,12*0.,6.12E-3,4.42E-2,              BTCR0609
      22.64E-1,12*0.,5.76E-3,4.16E-2,2.49E-1,12*0.,5.76E-3,4.16E-2,              BTCR0610
      32.49E-1,13*0.,2.44E-3,9.97E-2,14*0.,4.55E-3,14*0.,3.07E-3,                BTCR0611
      414*0.,3.61E-3,14*0.,3.61E-3,14*0.,3.61E-3,12*0.,6.12E-3,4.42E-2,          BTCR0612
```

```
     52.64E-1,12*0.,5.76E-3,4.16E-2,2.49E-1,12*0.,6.19E-3,4.46E-2,
     62.67E-1,14*0.,3.57E-2,13*0.,1.22E-3,5.20E-2,11*0.,1.44E-3,1.25E-2,
     79.01E-2,5.35E-1,11*0.,1.36E-3,1.17E-2,8.48E-2,5.04E-1,11*0.,
     81.44E-3,1.25E-2,9.01E-2,5.35E-1,11*0.,1.44E-3,1.25E-2,9.01E-2,
     95.35E-1,26*0.,1.30E-3,1.12E-2,8.11E-2,4.82E-1,11*0.,1.30E-3,
     11.12E-2,8.11E-2,4.82E-1,13*0.,2.43E-3,9.97E-2,13*0.,
     22.43E-3,9.97E-2,13*0.,2.43E-3,9.97E-2,13*0.,2.43E-3,9.97E-2,
     314*0.,3.57E-2,7*0./
C
      DATA SCAT10/6*0.,6.44E-3,3.76E-2,2.13E-1,12*0.,6.92E-3,4.04E-2,
     12.29E-1,12*0.,6.84E-3,3.99E-2,2.26E-1,12*0.,6.84E-3,3.99E-2,
     22.26E-1,12*0.,6.44E-3,3.76E-2,2.13E-1,12*0.,6.44E-3,3.76E-2,
     32.13E-1,13*0.,2.43E-3,9.01E-2,14*0.,4.65E-3,14*0.,3.07E-3,14*0.,
     43.61E-3,14*0.,3.61E-3,14*0.,3.61E-3,12*0.,6.84E-3,3.99E-2,2.26E-1,
     512*0.,6.44E-3,3.76E-2,2.13E-1,12*0.,6.92E-3,4.04E-2,2.29E-1,14*0.,
     63.57E-2,13*0.,1.22E-3,4.72E-2,11*0.,1.98E-3,1.40E-2,8.15E-2,
     74.58E-1,11*0.,1.86E-3,1.31E-2,7.67E-2,4.31E-1,
     811*0.,1.98E-3,1.40E-2,8.15E-2,4.58E-1,11*0.,1.98E-3,1.40E-2,
     98.15E-2,4.58E-1,6*0.,20*0.,1.78E-3,1.26E-2,7.34E-2,4.13E-1,
     111*0.,1.78E-3,1.26E-2,7.33E-2,4.12E-1,13*0.,2.44E-3,9.01E-2,13*0.,
     22.43E-3,9.01E-2,13*0.,2.43E-3,9.01E-2,13*0.,2.43E-3,9.01E-2,14*0.,
     33.57E-2,6*0./
C
      DATA SCAT11/6*0.,1.87E-3,1.11E-2,5.92E-2,2.47E-1,11*0.,2.01E-3,
     11.19E-2,6.35E-2,2.65E-1,11*0.,1.99E-3,1.18E-2,6.28E-2,2.63E-1,
     211*0.,1.99E-3,1.18E-2,6.28E-2,2.63E-1,11*0.,1.87E-3,1.11E-2,
     35.91E-2,2.47E-1,11*0.,1.87E-3,1.11E-2,5.91E-2,2.47E-1,13*0.,
     41.16E-2,1.10E-1,14*0.,4.64E-3,14*0.,4.30E-3,14*0.,5.06E-3,14*0.,
     55.06E-3,14*0.,5.06E-3,11*0.,1.99E-3,1.18E-2,6.28E-2,2.63E-1,11*0.,
     61.87E-3,1.11E-2,5.91E-2,2.47E-1,11*0.,2.01E-3,1.19E-2,6.35E-2,
     72.66E-1,14*0.,5.02E-2,13*0.,5.85E-3,5.793E-2,11*0.,4.06E-3,
     82.40E-2,1.28E-1,5.31E-1,11*0.,3.82E-3,2.26E-2,1.21E-1,5.00E-1,
     911*0.,4.06E-3,2.40E-2,1.28E-1,5.31E-1,11*0.,4.06E-3,2.40E-2,
     11.28E-1,5.31E-1,5*0.,15*0.,6*0.,3.66E-3,2.16E-2,1.15E-1,4.78E-1,
     211*0.,3.65E-3,2.16E-2,1.15E-1,4.78E-1,13*0.,1.16E-2,1.10E-1,13*0.,
     31.16E-2,1.10E-1,13*0.,1.16E-2,1.10E-1,13*0.,1.16E-2,1.10E-1,14*0.,
```

```
     45.02E-2,5*0./
C
      DATA SCAT12/7*0.,3.76E-3,2.09E-2,8.38E-2,2.71E-1,10*0.,1.00E-3,
     14.04E-3,2.25E-2,9.00E-2,2.91E-1,11*0.,3.99E-3,2.23E-2,8.90E-2,
     22.88E-1,11*0.,3.99E-3,2.22E-2,8.90E-2,2.88E-1,11*0.,3.76E-3,
     32.09E-2,8.38E-2,2.71E-1,11*0.,3.76E-3,2.09E-2,8.38E-2,2.71E-1,
     413*0.,2.08E-2,1.21E-1,14*0.,4.65E-3,14*0.,4.71E-3,14*0.,5.54E-3,
     514*0.,5.54E-3,14*0.,5.54E-3,11*0.,3.99E-3,2.22E-2,8.90E-2,2.88E-1,
     611*0.,3.76E-3,2.09E-2,8.38E-2,2.71E-1,10*0.,1.01E-3,4.04E-3,
     72.25E-2,9.00E-2,2.91E-1,14*0.,5.52E-2,13*0.,1.04E-2,6.35E-2,
     810*0.,2.03E-3,8.15E-3,4.54E-2,1.82E-1,5.81E-1,10*0.,1.91E-3,
     97.67E-3,4.27E-2,1.71E-1,5.47E-1,10*0.,2.03E-3,8.15E-3,4.54E-2,
     11.82E-1,5.81E-1,10*0.,2.03E-3,8.15E-3,4.54E-2,1.82E-1,5.81E-1,
     24*0.,15*0.,6*0.,1.83E-3,7.34E-3,4.09E-2,1.63E-1,5.24E-1,10*0.,
     31.83E-3,7.33E-3,4.09E-2,1.63E-1,5.24E-1,13*0.,2.08E-2,1.21E-1,
     413*0.,2.08E-2,1.21E-1,13*0.,2.08E-2,1.21E-1,13*0.,2.08E-2,
     51.21E-1,14*0.,5.52E-2,4*0./
C
      DATA SCAT13/7*0.,1.60E-3,5.91E-3,2.40E-2,7.45E-2,2.52E-1,10*0.,
     11.72E-3,6.35E-3,2.58E-2,8.00E-2,2.70E-1,10*0.,1.70E-3,6.28E-3,
     22.55E-2,7.91E-2,2.67E-1,10*0.,1.70E-3,6.28E-3,2.55E-2,7.91E-2,
     32.67E-1,10*0.,1.60E-3,5.91E-3,2.40E-2,7.45E-2,2.52E-1,10*0.,
     41.60E-3,5.91E-3,2.40E-2,7.45E-2,2.52E-1,13*0.,1.79E-2,1.10E-1,
     514*0.,4.64E-3,14*0.,4.30E-3,14*0.,5.06E-3,14*0.,5.06E-3,14*0.,
     65.06E-3,10*0.,1.70E-3,6.28E-3,2.55E-2,7.91E-2,2.67E-1,10*0.,
     71.60E-3,5.91E-3,2.40E-2,7.45E-2,2.52E-1,10*0.,1.72E-3,6.35E-3,
     82.58E-2,8.00E-2,2.70E-1,14*0.,5.13E-2,13*0.,9.00E-3,5.79E-2,
     910*0.,3.47E-3,1.28E-2,5.21E-2,1.61E-1,5.41E-1,10*0.,3.27E-3,
     11.21E-2,4.90E-2,4.52E-1,5.09E-1,10*0.,3.47E-3,1.28E-2,4.21E-2,
     21.61E-1,5.41E-1,10*0.,3.47E-3,1.28E-2,5.21E-2,1.61E-1,5.41E-1,
     33*0.,15*0.,7*0.,3.13E-3,1.15E-2,4.69E-2,1.45E-1,4.87E-1,10*0.,
     43.13E-3,1.15E-2,4.69E-2,1.45E-1,4.87E-1,13*0.,1.79E-2,1.10E-1,
     513*0.,1.79E-2,1.10E-1,13*0.,1.79E-2,1.10E-1,13*0.,1.79E-2,1.10E-1,
     614*0.,5.13E-2,3*0./
C
      DATA SCAT14/8*0.,2.96E-3,7.14E-3,2.21E-2,7.28E-2,2.38E-1,10*0.,
```

```
     13.18E-3,7.68E-3,2.38E-2,7.82E-2,2.55E-1,10*0.,3.14E-3,7.59E-3,
     22.35E-2,7.74E-2,2.52E-1,10*0.,3.14E-3,7.59E-3,2.35E-3,7.74E-2,
     32.52E-1,10*0.,2.96E-3,7.14E-3,2.21E-2,7.28E-2,2.38E-1,10*0.,
     42.96E-3,7.14E-3,2.21E-2,7.28E-2,2.38E-1,13*0.,2.03E-2,1.21E-1,
     514*0.,4.65E-3,14*0.,4.81E-3,14*0.,5.66E-3,14*0.,5.66E-3,14*0.,
     65.66E-3,10*0.,3.14E-3,7.59E-3,2.35E-2,7.74E-2,2.52E-1,10*0.,
     72.96E-3,7.14E-3,2.21E-2,7.28E-2,2.38E-1,10*0.,3.18E-3,7.67E-3,
     82.38E-2,7.82E-2,2.55E-1,14*0.,5.64E-2,13*0.,1.02E-2,6.35E-2,
     910*0.,6.41E-3,1.55E-2,4.80E-2,1.58E-1,5.09E-1,10*0.,6.03E-3,
     11.46E-2,4.52E-2,1.49E-1,4.79E-1,10*0.,6.41E-3,1.55E-2,4.80E-2,
     21.58E-1,5.09E-1,10*0.,6.41E-3,1.55E-2,4.80E-2,1.58E-1,5.09E-1,
     32*0.,15*0.,8*0.,5.77E-3,1.39E-2,4.32E-2,1.42E-1,4.59E-1,10*0.,
     45.77E-3,1.39E-2,4.32E-2,1.42E-1,4.58E-1,13*0.,2.03E-2,1.21E-1,
     513*0.,2.03E-2,1.21E-1,13*0.,2.03E-2,1.21E-1,13*0.,2.03E-2,
     61.21E-1,14*0.,5.64E-2,2*0./
C
      DATA SCAT15/9*0.,4.80E-3,1.48E-2,4.83E-2,1.52E-1,4.21E-1,10*0.,
     15.16E-3,1.59E-2,5.19E-2,1.63E-1,4.52E-1,10*0.,5.10E-3,1.57E-2,
     25.13E-2,1.61E-1,4.47E-1,10*0.,5.10E-3,1.57E-2,5.13E-2,1.61E-1,
     34.47E-1,10*0.,4.80E-3,1.48E-2,4.83E-2,1.51E-1,4.21E-1,10*0.,
     44.80E-3,1.48E-2,4.82E-2,1.51E-1,4.21E-1,13*0.,1.79E-2,1.53E-1,
     514*0.,4.64E-3,14*0.,5.89E-3,14*0.,6.93E-3,14*0.,6.93E-3,14*0.,
     66.93E-3,10*0.,5.10E-3,1.57E-2,5.13E-2,1.61E-1,4.47E-1,10*0.,4.8E-3
     7,1.48E-2,4.83E-2,1.52E-1,4.21E-1,10*0.,5.16E-3,1.59E-2,5.19E-2,
     81.63E-1,4.52E-1,14*0.,6.77E-2,13*0.,9.00E-3,8.07E-2,10*0.,1.04E-2,
     93.20E-2,1.05E-1,3.29E-1,9.06E-1,10*0.,9.80E-3,3.02E-2,9.86E-2,
     13.10E-1,8.53E-1,10*0.,1.04E-2,3.20E-2,1.05E-1,3.29E-1,9.06E-1,
     210*0.,1.04E-2,3.20E-2,1.05E-1,3.29E-1,9.06E-1,25*0.,9.38E-3,
     32.89E-2,9.44E-2,2.96E-1,8.17E-1,10*0.,9.37E-3,2.88E-2,9.43E-2,
     42.96E-1,8.16E-1,13*0.,1.79E-2,1.53E-1,13*0.,1.79E-2,1.53E-1,13*0.,
     51.79E-2,1.53E-1,13*0.,1.79E-2,1.53E-1,14*0.,6.78E-2,0./
C
C FISSION SPECTRUM
C
      DATA KHIF/0.2040,0.3440,0.1680,0.1800,0.0900,0.0140,9*0./
C
```

```
C THE BETA VALUES THAT ARE TO BE CORRECTED
C
      DATA BETA/0.215E-3,1.424E-3,1.274E-3,2.568E-3,0.748E-3,
     10.273E-3/
C
C OVERALL ABSORPTIONS OVER THE CORE MATERIEL NUMBER 1
C
      DATA ABSPC1/4.905E13,3.634E13,1.863E13,2.839E13,3.67E13,5.035E13,
     16.210E13,1.112E14,2.515E14,4.124E14,3.528E14,3.236E14,2.461E14,
     23.411E14,1.6219E16/
C
      DATA ABSPC2/5.065E12,3.935E12,2.030E12,3.150E12,4.071E12,5.615E12,
     16.974E12,1.250E13,2.820E13,4.622E13,3.938E13,3.592E13,2.716E13,
     23.754E13,1.67832E15/
C
      DATA ABSPC3/7.480E13,5.821E13,2.982E13,4.652E13,6.082E13,8.441E13,
     11.045E14,1.859E14,4.139E14,6.653E14,5.579E14,5.016E14,3.745E14,
     25.010E14,1.07130E16/
C
      DATA ABSPC4/5.668E14,4.206E14,2.132E14,3.260E14,4.290E14,5.953E14,
     17.321E14,1.302E15,2.905E15,4.667E15,3.924E15,3.542E15,2.656E15,
     23.611E15,7.60956E16/
C
      DATA ABSPC5/1.445E14,1.085E14,5.431E13,8.333E13,1.086E14,1.470E14,
     11.807E14,3.223E14,7.267E14,1.184E15,1.010E15,9.240E14,7.006E14,
     29.556E14,3.41424E16/
C
      DATA ABSPC6/2.478E13,1.962E13,9.749E12,1.528E13,2.030E13,2.885E13,
     13.633E13,6.553E13,1.469E14,2.361E14,1.997E14,1.812E14,1.355E14,
     21.708E14,2.29734E15/
C
      DATA ABSPC7/2.418E14,1.824E14,8.979E13,1.376E14,1.830E14,2.561E14,
     13.186E14,5.731E14,1.292E15,2.090E15,1.772E15,1.614E15,1.218E15,
     21.625E15,3.07011E16/
C
C OVERALL FISSIONS IN CORE MATERIEL NUMBER 1
```

```
C
      DATA FISSC1/1.701E13,3.365E13,1.686E13,3.314E13,2.886E13,3.519E13,
     14.568E13,7.701E13,1.638E14,2.467E14,1.992E14,1.668E14,1.761E14,
     22.656E14,1.28138E16/
C
      DATA FISSC2/1.799E12,3.650E12,1.840E12,3.691E12,3.224E12,3.964E12,
     15.143E12,8.664E12,1.838E13,2.767E13,2.225E13,1.855E13,1.950E13,
     22.934E13,1.32918E15/
C
      DATA FISSC3/2.656E13,5.494E13,2.692E13,5.451E13,4.816E13,
     15.960E13,7.707E13,1.289E14,2.697E14,3.983E14,3.153E14,2.591E14,
     22.689E14,3.973E14,8.43590E15/
C
      DATA FISSC4/1.966E14,3.969E14,1.921E14,3.806E14,3.369E14,4.160E14,
     15.385E14,9.021E14,1.892E15,2.792E15,2.215E15,1.826E15,1.900E15,
     22.812E15,5.98862E16/
C
      DATA FISSC5/5.011E13,1.004E14,4.915E13,9.729E13,8.530E13,1.027E14,
     11.329E14,2.233E14,4.732E14,7.087E14,5.701E14,4.764E14,5.012E14,
     27.441E14,2.69741E16/
C
      DATA FISSC6/8.710E12,1.851E13,8.710E12,1.790E13,1.607E13,2.037E13,
     12.679E13,4.543E13,9.574E13,1.414E14,1.129E14,9.359E13,9.732E13,
     21.334E14,1.80902E15/
C
      DATA FISSC7/8.386E13,1.721E14,8.089E13,1.607E14,1.438E14,1.789E14,
     12.343E14,3.970E14,8.411E14,1.250E15,1.001E15,8.322E14,8.710E14,
     21.263E15,2.41131E16/
C
C OVERALL SCATTERINGS IN,IN CORE MATERIEL NUMBER 1
C
      DATA STINC1/0.,1.424E15,2.580E15,4.725E15,7.428E15,8.542E15,
     18.106E15,7.664E15,7.407E15,6.091E15,5.542E15,5.593E15,5.137E15,
     24.507E15,7.098E15/
C
      DATA STINC2/0.,1.459E14,2.723E14,5.091E15,8.221E14,9.582E14,
```

```
     19.195E14,8.711E14,8.415E14,6.904E14,6.277E14,6.3180E14,5.779E14,    BTCR0793
     25.050E14,7.933E14/                                                  BTCR0794
C                                                                         BTCR0795
      DATA STINC3/0.,2.051E15,3.627E15,7.188E15,1.203E16,1.416E16,        BTCR0796
     11.371E16,1.306E16,1.254E16,1.016E16,9.098E15,9.022E15,8.126E15,     BTCR0797
     27.011E15,1.084E16/                                                  BTCR0798
C                                                                         BTCR0799
      DATA STINC4/0.,1.561E16,2.667E16,5.186E16,8.452E16,9.849E16,        BTCR0800
     19.487E16,9.034E16,8.686E16,7.055E16,6.318E16,6.274E16,5.666E16,     BTCR0801
     24.901E16,7.592E16/                                                  BTCR0802
C                                                                         BTCR0803
      DATA STINC5/0.,4.195E15,7.689E15,1.390E16,2.182E16,2.522E16,        BTCR0804
     12.370E16,2.232E16,2.150E16,1.761E16,1.595E16,1.604E16,1.469E16,     BTCR0805
     21.285E16,2.003E16/                                                  BTCR0806
C                                                                         BTCR0807
      DATA STINC6/0.,6.794E14,1.220E15,2.377E15,3.960E15,4.715E15,        BTCR0808
     14.667E15,4.522E15,4.404E15,3.510E15,3.227E15,3.219E15,2.924E15,     BTCR0809
     22.532E15,3.754E15/                                                  BTCR0810
C                                                                         BTCR0811
      DATA STINC7/0.,6.661E15,1.154E16,2.208E16,3.580E16,4.197E16,        BTCR0812
     14.075E16,3.923E16,3.814E16,3.129E16,2.820E16,2.822E16,2.572E16,     BTCR0813
     22.239E16,3.434E16/                                                  BTCR0814
C                                                                         BTCR0815
C OVERALL SCATTERINGS OUT,IN CORE MATERIEL NUMBER 1                       BTCR0816
C                                                                         BTCR0817
      DATA OTSTC1/2.158E15,5.180E15,4.371E15,6.575E15,8.033E15,8.139E15,  BTCR0818
     17.69E15,7.350E15,7.040E15,5.684E15,5.210E15,5.292E15,4.905E15,      BTCR0819
     24.225E15,0./                                                        BTCR0820
C                                                                         BTCR0821
      DATA OTSTC2/2.227E14,5.535E14,4.750E14,7.352E14,9.031E14,9.249E14,  BTCR0822
     18.738E14,8.349E14,7.976E14,6.434E14,5.877E14,5.942E14,5.485E14,     BTCR0823
     24.711E14,0./                                                        BTCR0824
C                                                                         BTCR0825
      DATA OTSTC3/3.161E15,7.531E15,6.878E15,1.082E16,1.338E16,1.381E16,  BTCR0826
     11.309E16,1.242E16,1.171E16,9.263E15,8.327E15,8.297E15,7.565E15,     BTCR0827
     26.374E15,0./                                                        BTCR0828
```

```
C
      DATA OTSTC4/2.389E16,5.472E16,4.923E16,7.527E16,9.290E16,9.553E16,
     19.062E16,8.610E16,8.131E16,6.432E16,5.796E16,5.792E16,5.294E16,
     24.471E16,0./
C
      DATA OTSTC5/6.356E15,1.546E16,1.274E16,1.930E16,2.374E16,
     12.376E16,2.237E16,2.131E16,2.034E16,1.633E16,1.491E16,1.511E16,
     21.396E16,1.184E16,0./
C
      DATA OTSTC6/1.047E15,2.538E15,2.248E15,3.555E15,4.465E15,
     14.722E15,4.551E15,4.377E15,4.155E15,3.287E15,2.980E15,2.997E15,
     22.737E15,2.139E15,0./
C
      DATA OTSTC7/1.019E16,2.373E16,2.073E16,3.178E16,3.964E16,4.109E16,
     13.944E16,3.789E16,3.615E16,2.880E16,2.618E16,2.640E16,2.427E16,
     22.008E16,0./
C
C TOTAL NUMBER OF NEUTRONS BORN IN VARIOUS GROUPS/SEC
C
      DATA SRCE/8.121976E16,1.369589E17,6.688694E16,
     17.166452E16,3.583228E16,5.573905E15,9*0./
C
      END
      SUBROUTINE PROB
C
C VARIOUS PROBABILITIES WE NEED
C
      COMMON/ORTAK1/ALEAK(15),PLRC
      COMMON/P/PSI(15,29)
      COMMON/A/ ALEAK1(15),ALEAK2(15),ALEAK3(15),SOUT(15)
      COMMON/S/SCAT(15,29,15)
      COMMON/ABC/AESPC(15,7)
      COMMON/FC/FISSC(15,7)
      COMMON/STC/STINC(15,7)
      COMMON/OTC/OTSTC(15,7)
      COMMON/ORTAK2/PF(15),FLCR(14),PSR(14,15),PSC(14,15)
```

```
      COMMON/SR/SRCE(15)
      COMMON/AES/AESP(15)
C
      DIMENSION TSTINC(15),TGC(15),TABSPC(15),V(29),
     1SNR(15,15),SNC(15,15),SDR(15),SDC(15),TSCA(15,29),TOTSTC(15),
     2DENR(15),PSOUTC(14),PSOUTR(14)
C
C  VOLUMES(FOR 29 MATERIELS)
C
      DATA V/2.792E3,7.246E4,2.217E2,2.439E3,
     12.233E4,8.384E3,9.452E5,2.412E3,6.333E3,1.011E3,
     21.520E4,9.395E3,1.995E3,2.513E4,1.717E5,
     35.381E6,7.915E2,2.090E5,6.271E4,4.991E3,
     42.150E4,0.,1.048E5,7.534E2,1.031E4,
     51.776E4,1.519E4,2.918E4,5.692E5/
C
      NAMELIST/OUTSTC/TSTINC
      NAMELIST/OUTPF/PF
      NAMELIST/OUTPLC/PLCR
      NAMELIST/OUTFRC/FUTRC,FUTRCC
      NAMELIST/OUTPRC/PLRC
      NAMELIST/OUTPSR/PSR
      NAMELIST/OUTPSC/PSC
      NAMELIST/OPSTC/PSOUTC
      NAMELIST/OPSTR/PSOUTR
C
C  COMPUTATION OF THE PROBABILITY THAT A NEUTRON OF ENERGY GROUP I
C  CAUSES FISSION WHILE IT IS WITHIN THE ENERGY GROUP I
C
      DO 30 I=1,15
      SUMN=0.
      SUMD=0.
      DO 20 M=1,7
      SUMN=SUMN+FISSC(I,M)
      SUMD=SUMD+STINC(I,M)
   20 CONTINUE
```

```
      TSTINC(I)=SUMD
      TGC(I)=SUMD+SRCE(I)
      PF(I)=SUMN/TGC(I)
   30 CONTINUE
C
C TSTINC(I);TOTAL NUMBER OF NEUTRONS SCATTERED INTO ENERGY GROUP I
C WITHIN THE CORE/SEC
C TGC(I);TOTAL GAIN IN ENERGY GROUP I IN THE CORE /SEC
C PF(I);PROBABILITY THAT A NEUTRON OF ENERGY GROUP I CAUSES FISSION WHILE IT
C IS STILL IN ENERGY GROUP I
C
      WRITE(6,OUTSTC)
      WRITE(6,OUTPF)
C
C PRBABILITY THAT A NEUTRON OF ENERGY GROUP I LEAKS OUT OF THE CORE
C
      DO 31 I=1,15
      SUMA=0.
      SUMO=0.
      DO 21 M=1,7
      SUMA=SUMA+ABSPC(I,M)
      SUMO=SUMO+OTSTC(I,M)
   21 CONTINUE
      TABSPC(I)=SUMA
      TOTSTC(I)=SUMO
      FUITEC=-(SUMA+SUMO-TGC(I))
      IF (I.EQ.15) GO TO 31
      PLCR(I)=FUITEC/TGC(I)
   31 CONTINUE
      WRITE(6,OUTPLC)
C
C ABSORPTION OUTSIDE OF THE CORE FOR THERMAL NEUTRONS
C
      ABSPR=ABSP(15)-TABSPC(15)
C
C SCATTERING INTO THE 15 TH GROUP OUTSIDE OF THE CORE
```

```
C
      SINTH=3.357790E17
      STINR=SINTH-TSTINC(15)
C
C LEAKAGE FROM THE REFLECTOR REGION FOR THERMAL NEUTRONS
C
      FUITR=-(ABSPR-STINR)
C
C LEAKAGE FROM THE REFLECTOR TO THE CORE FOR THERMAL NEUTRONS
C
      FUTRC=FUITR-ALEAK(15)
C
C SAME LEAKAGE  COMPUTED BASED ON THE NUMBERS RELEVANT TO THE CORE(CROSS
C CHECKING)
C
      FUTRCC=TABSPC(15)-TSTINC(15)
      WRITE(6,OUTFRC)
C
C PROBABILITY THAT A THERMAL NEUTRON LEAKS FROM THE REFLECTOR TO THE CORE
C
      PLRC=FUTRCC/STINR
      WRITE(6,OUTPRC)
C
C PROBABILITY THAT A NEUTRON SCATTERS OUT OF GROUP I IN THE CORE AND IN THE
C REFLECTOR
C
      DO 720 I=1,14
      DENR(I)=SOUT(I)-TOTSTC(I)+ABSP(I)-TABSPC(I)+ALEAK(I)
      PSOUTC(I)=TOTSTC(I)/TOC(I)
  720 PSOUTR(I)=(SOUT(I)-TOTSTC(I))/DENR(I)
      WRITE(6,OPSTC)
      WRITE(6,OPSTR)
C
C COMPUTATION OF THE PROBABILITY OF SCATTERING FROM GROUP MG TO GROUP MH
C IN THE CORE AND OUTSIDE OF THE CORE,WHEN THERE IS A SCATTERING
C
```

```
      DO 32 MC=1,29                                                     BTCR0973
      DO 32 MG=1,14                                                     BTCR0974
      SUM=0.                                                            BTCR0975
      DO 22 MH=1,15                                                     BTCR0976
   22 SUM=SUM+SCAT(MG,MC,MH)                                            BTCR0977
   32 TSCA(MG,MC)=SUM                                                   BTCR0978
      DO 50 MG=1,14                                                     BTCR0979
      DO 50 MH=1,15                                                     BTCR0980
      SUMNC=0.                                                          BTCR0981
      SUMNR=0.                                                          BTCR0982
      DO 45 MC=1,29                                                     BTCR0983
      IF ((MC.EQ.1).OR.(MC.EQ.3).OR.(MC.EQ.4).OR.(MC.EQ.6).OR.(MC.EQ.5). BTCR0984
     1OR.(MC.EQ.13).OR.(MC.EQ.14)) GO TO 44                            BTCR0985
      SUMNR=SUMNR+SCAT(MG,MC,MH)*V(MC)*PSI(MG,MC)                       BTCR0986
      GO TO 45                                                          BTCR0987
   44 SUMNC=SUMNC+SCAT(MG,MC,MH)*V(MC)*PSI(MG,MC)                       BTCR0988
   45 CONTINUE                                                          BTCR0989
      SNR(MG,MH)=SUMNR                                                  BTCR0990
   50 SNC(MG,MH)=SUMNC                                                  BTCR0991
      DO 60 MG=1,14                                                     BTCR0992
      SUMDR=0.                                                          BTCR0993
      SUMDC=0.                                                          BTCR0994
      DO 55 MC=1,29                                                     BTCR0995
      IF ((MC.EQ.1).OR.(MC.EQ.3).OR.(MC.EQ.4).OR.(MC.EQ.6).OR.(MC.EQ.5). BTCR0996
     1OR.(MC.EQ.13).OR.(MC.EQ.14)) GO TO 54                            BTCR0997
      SUMDR=SUMDR+FSI(MG,MC)*TSCA(MG,MC)*V(MC)                          BTCR0998
      GO TO 55                                                          BTCR0999
   54 SUMDC=SUMDC+FSI(MG,MC)*TSCA(MG,MC)*V(MC)                          BTCR1000
   55 CONTINUE                                                          BTCR1001
      SDR(MG)=SUMDR                                                     BTCR1002
   60 SDC(MG)=SUMDC                                                     BTCR1003
C                                                                       BTCR1004
C PROBABILITY OF SCATTERING FROM MG TO MH IN THE CORE AND OUTSIDE OF THE CORE BTCR1005
C                                                                       BTCR1006
      DO 70 MG=1,14                                                     BTCR1007
      DO 70 MH=1,15                                                     BTCR1008
```

```
      PSR(MG,MH)=SNR(MG,MH)/SDR(MG)*PSCUTR(MG)
   70 PSC(MG,MH)=SNC(MG,MH)/SDC(MG)*PSCUTC(MG)
      WRITE(6,OUTPSR)
      WRITE(6,OUTPSC)
      RETURN
      END
      SUBROUTINE STUDY(SC1,SR1,SC2,SR2,SUM2,JJ,MH21,MH2F)
C
      COMMON/MSTUDY/MF,SRT,LLL,MH(14),KKK
      COMMON/URTAK2/PF(15),PLCR(14),PSR(14,15),PSC(14,15)
C
      MG1=MH(JJ-1)
      MG2=MH(JJ)
      SC2=SC1*PSC(MG1,MG2)
      SUM2=SUM2+SC2*PF(MG2)
      IF (MG2.EQ.15) GO TO 5
      SR2=SC2*PLCR(MG2)+SR1*PSR(MG1,MG2)
      GO TO 6
    5 SRT=SRT+SR1*PSR(MG1,MG2)
    6 DO 7 J=1,JJ
      JN=14-JJ+J
      IF (MH(J).GT.JN) GO TO 8
    7 CONTINUE
      MH21=MG2+1
      MH2F=MG2+MF
      IF (MH2F.LE.15) GO TO 71
      MH2F=15
   71 LLL=1
      KKK=KKK+1
      RETURN
    8 LLL=0
      KKK=KKK+1
      RETURN
      END
@
```

APPENDIX M

PROGRAM INVA

(Like Averaged Inverse Velocity)

```
// 'TOLGA YARMAN',CLASS=A,REGION=128K
/*MITID USER=(M8696,9441)
/*MAIN TIME=2,LINES=20,CARDS=0
/*SRI LOW
//STEP1 EXEC FORCGO
//C.SYSIN DD *
C PROGRAM INVA
C
C COMPUTATION OF AN INVERSE VELOCITY
C
      DIMENSION PSI1(15),PSI2(15),PSI3(15),PSI4(15),PSI5(15),PSI6(15),
     1PSI7(15),PSI8(15),PSI9(15),PSI10(15),PSI11(15),PSI12(15),PSI13(15
     2),PSI14(15),PSI15(15),PSI16(15),PSI17(15),PSI18(15),PSI19(15),
     3PSI20(15),PSI21(15),PSI22(15),PSI23(15),PSI24(15),PSI25(15),PSI26
     4(15),PSI27(15),PSI29(15),PSI28(15),PSI(15,29)
      DIMENSION V(15),V1(15),NMGI(2),NMGF(2),V1AV(2),V11(2)
C
      EQUIVALENCE (PSI1(1),PSI(1,1))
      EQUIVALENCE (PSI2(1),PSI(1,2))
      EQUIVALENCE (PSI3(1),PSI(1,3))
      EQUIVALENCE (PSI4(1),PSI(1,4))
      EQUIVALENCE (PSI5(1),PSI(1,5))
      EQUIVALENCE (PSI6(1),PSI(1,6))
      EQUIVALENCE (PSI7(1),PSI(1,7))
      EQUIVALENCE (PSI8(1),PSI(1,8))
      EQUIVALENCE (PSI9(1),PSI(1,9))
      EQUIVALENCE (PSI10(1),PSI(1,10))
      EQUIVALENCE (PSI11(1),PSI(1,11))
      EQUIVALENCE (PSI12(1),PSI(1,12))
      EQUIVALENCE (PSI13(1),PSI(1,13))
      EQUIVALENCE (PSI14(1),PSI(1,14))
      EQUIVALENCE (PSI15(1),PSI(1,15))
      EQUIVALENCE (PSI16(1),PSI(1,16))
      EQUIVALENCE (PSI17(1),PSI(1,17))
      EQUIVALENCE (PSI18(1),PSI(1,18))
      EQUIVALENCE (PSI19(1),PSI(1,19))
```

```
      EQUIVALENCE (PSI20(1),PSI(1,20))
      EQUIVALENCE (PSI21(1),PSI(1,21))
      EQUIVALENCE (PSI22(1),PSI(1,22))
      EQUIVALENCE (PSI23(1),PSI(1,23))
      EQUIVALENCE (PSI24(1),PSI(1,24))
      EQUIVALENCE (PSI25(1),PSI(1,25))
      EQUIVALENCE (PSI26(1),PSI(1,26))
      EQUIVALENCE (PSI27(1),PSI(1,27))
      EQUIVALENCE (PSI28(1),PSI(1,28))
      EQUIVALENCE (PSI29(1),PSI(1,29))
C
      NAMELIST/OUT0/V
      NAMELIST/OUT1/V1AV
      NAMELIST/OUT2/V11
C
      DATA PSI1/1.00737E13,2.23071E13,1.18319E13,1.76862E13,
     11.76534E13,1.25523E13,9.69910E12,8.69193E12,8.34772E12,
     25.54323E12,4.87979E12,5.07788E12,4.51213E12,3.58995E12,
     33.09949E13/
C
      DATA PSI2/7.13232E11,1.62687E12,7.77294E11,1.18596E12,
     11.30902E12,1.00939E12,8.29590E11,7.80258E11,7.85932E11,5.49627E11,
     25.00281E11,5.34657E11,4.83793E11,3.94693E11,1.05229E13/
C
      DATA PSI3/1.27551E13,2.89790E13,1.54629E13,2.35919E13,
     12.38825E13,1.69370E13,1.30778E13,1.17095E13,1.12181E13,
     27.44364E12,6.52920E12,6.76325E12,5.98542E12,4.74891E12,
     33.85021E13/
C
      DATA PSI4/1.71227E13,3.96525E13,2.05659E13,3.16724E13,
     13.24365E13,2.31479E13,1.78172E13,1.58380E13,1.49665E13,9.74154E12,
     28.41021E12,8.58567E12,7.50363E12,5.84070E12,2.68752E13/
C
      DATA PSI5/1.45549E13,3.29063E13,1.68575E13,2.54005E13,2.60652E13,
     11.85560E13,1.42987E13,1.27317E13,1.20567E13,7.84387E12,6.78769E12,
     26.95031E12,6.08968E12,4.75007E12,2.16459E13/
```

```
C                                                                         INVA0073
      DATA PSI6/9.88098E12,2.21733E13,1.14855E13,1.72909E13,1.75745E13,   INVA0074
     11.22013E13,9.39882E12,8.39353E12,8.03255E12,5.30221E12,             INVA0075
     24.65178E12,4.82862E12,4.27763E12,3.34948E12,2.17280E13/             INVA0076
C                                                                         INVA0077
      DATA PSI7/1.51137E11,3.06827E11,1.34340E11,2.47386E11,              INVA0078
     15.05956E11,5.45318E11,5.28815E11,5.26329E11,5.44502E11,3.93885E11,  INVA0079
     23.66978E11,4.03846E11,3.79416E11,3.52016E11,3.62643E13/             INVA0080
C                                                                         INVA0081
      DATA PSI8/1.20144E13,2.84534E13,1.50317E13,2.36870E13,              INVA0082
     12.40741E13,1.73901E13,1.33255E13,1.18493E13,1.12134E13,7.36938E12,  INVA0083
     26.35423E12,6.48740E12,5.68764E12,4.41452E12,2.24688E13/             INVA0084
C                                                                         INVA0085
      DATA PSI9/1.50146E12,3.58446E12,1.77785E12,2.73737E12,              INVA0086
     13.05101E12,2.39223E12,1.94321E12,1.80874E12,1.76625E12,1.17805E12,  INVA0087
     21.06644E12,1.13439E12,1.00268E12,6.22961E11,3.90013E11/             INVA0088
C                                                                         INVA0089
      DATA PSI10/1.56417E13,3.60170E13,1.85488E13,2.83327E13,             INVA0090
     12.91862E13,2.08403E13,1.61003E13,1.43636E13,1.36231E13,8.8824E12,   INVA0091
     27.69509E12,7.88080E12,6.39826E12,5.35424E12,2.67592E13/             INVA0092
C                                                                         INVA0093
      DATA PSI11/4.65987E12,1.07289E13,5.55235E12,8.48465E12,             INVA0094
     19.05601E12,6.63210E12,5.29852E12,4.85433E12,4.74320E12,3.19684E12,  INVA0095
     22.85435E12,3.00461E12,2.67725E12,2.03224E12,1.92446E13/             INVA0096
C                                                                         INVA0097
      DATA PSI12/2.44550E12,5.57977E12,2.66179E12,4.24124E12,             INVA0098
     15.48086E12,4.46704E12,3.71362E12,3.47187E12,3.46546E12,2.41814E12,  INVA0099
     22.20282E12,2.36435E12,2.13292E12,1.74126E12,5.40822E13/             INVA0100
C                                                                         INVA0101
      DATA PSI13/6.93262E12,1.63319E13,8.21708E12,1.27142E13,1.32311E13,  INVA0102
     19.66926E12,7.56880E12,6.82197E12,6.49332E12,4.22544E12,3.67926E12,  INVA0103
     23.79062E12,3.31885E12,2.39604E12,7.04389E12/                        INVA0104
C                                                                         INVA0105
      DATA PSI14/5.51701E12,1.26775E13,6.30738E12,9.52943E12,             INVA0106
     19.88196E12,7.09271E12,5.52900E12,4.97879E12,4.76316E12,             INVA0107
     23.12083E12,2.72414E12,2.81461E12,2.48035E12,1.89559E12,             INVA0108
```

```
     37.84037E12/
C
      DATA PS115/2.83592E9,5.53228E9,2.1419E9,3.85601E9,
     18.45488E9,1.19461E10,1.51236E10,1.96665E10,2.58602E10,2.18789E10,
     22.29989E10,2.84099E10,2.90990E10,2.70993E10,9.94618E12/
C
      DATA PS116/2.55197E8,8.86992E8,3.67096E8,6.17273E8,
     11.10915E9,1.46164E9,1.68106E9,2.08979E9,2.65010E9,2.21534E9,
     22.33090E9,2.89865E9,2.99767E9,2.73959E9,2.15733E12/
C
      DATA PS117/2.38627E12,5.21569E12,2.38901E12,3.90725E12,
     15.61735E12,4.70592E12,3.93748E12,3.66121E12,3.65511E12,2.57785E12,
     22.35870E12,2.55382E12,2.32249E12,2.01416E12,9.41901E13/
C
      DATA PS118/9.99961E9,2.29717E10,8.79224E9,1.30877E10,
     11.48976E10,1.19969E10,1.02758E10,1.00958E10,1.06745E10,7.79902E9,
     27.36367E9,8.15255E9,7.61416E9,6.31105E9,3.68421E11/
C
      DATA PS119/4.69802E10,1.07163E11,4.26929E10,6.39392E10,
     17.26767E10,5.90273E10,5.03304E10,4.92060E10,5.15745E10,3.72584E10,
     23.49577E10,3.84597E10,3.56174E10,2.88146E10,1.76375E12/
C
      DATA PS120/2.92986E12,6.48734E12,3.10695E12,4.83535E12,
     15.88415E12,4.82943E12,4.09801E12,3.92453E12,4.00831E12,2.84567E12,
     22.61498E12,2.82121E12,2.57460E12,2.15952E12,8.82265E13/
C
      DATA PS121/2.79272E12,6.41947E12,3.15487E12,4.93465E12,
     14.93672E12,4.76330E12,3.96308E12,3.72960E12,3.73572E12,2.59872E12,
     22.35888E12,2.51551E12,2.26435E12,1.81786E12,4.46644E13/
C
      DATA PS122/15*0./
C
      DATA PS123/7.30400E10,1.59244E11,6.33609E10,1.00316E11,
     11.33994E11,1.17226E11,1.05928E11,1.07670E11,1.16894E11,8.71505E10,
     28.33669E10,9.36818E10,8.86947E10,7.66278E10,8.54001E12/
C
```

```
      DATA PSI24/6.57385E12,1.46396E13,7.38030E12,1.12008E13,
     11.19848E13,9.05311E12,7.3486E12,6.83381E12,6.80922E12,4.72257E12,
     24.25975E12,4.50770E12,4.05123E12,3.32159E12,7.32432E13/
C
      DATA PSI25/5.79924E11,1.14494E12,4.82339E11, 9.10516E11,
     11.93840E12,2.04278E12,1.90154E12,1.82458E12,1.83840E12,1.31154E12,
     21.21184E12,1.34153E12,1.23831E12,1.14720E12,8.87780E13/
C
      DATA PSI26/1.90676E11,3.45018E11,1.42709E11,2.88850E11,
     17.49914E11,9.43641E11,9.88051E11,1.01437E12,1.06279E12,7.74108E11,
     27.24443E11,8.12987E11,7.58574E11,7.15832E11,7.18332E13/
C
      DATA PSI27/5.44443E10,9.02989E10,3.67989E10,7.64669E10,
     12.22783E11,3.26632E11,3.38721E11,4.39476E11,4.95380E11,3.77230E11,
     23.64096E11,4.20310E11,4.01508E11,3.85550E11,5.44373E13/
C
      DATA PSI28/1.09570E10,1.73024E10,6.98252E9,1.44094E10,
     14.28526E10,6.84570E10,8.99937E10,1.12109E11,1.38318E11,1.12020E11,
     21.13418E11,1.36955E11,1.36171E11,1.33562E11,3.27973E13/
C
      DATA PSI29/4.21734E8,1.83346E9,7.75283E8,1.30522E9,
     12.28654E9,2.97064E9,3.35040E9,4.08927E9,5.08521E9,4.20670E9,
     24.39746E9,5.45074E9,5.63666E9,5.16516E9,3.58462E12/
C
      DATA V/28.5E8,19.9E8,14.7E8,11.0E8,6.7E8,2.9E8,1.14E8,
     10.48E8,0.206E8,0.101E8,0.0566E8,0.0319E8,0.0179E8,0.0109E8,
     20.004E+08/
C
      DATA NMGI/1,8/
C
      DATA NMGF/7,14/
C
      DO 100 MG=1,15
  100 VI(MG)=1./V(MG)
      DO 300 K=1,2
      MGI=NMGI(K)
```

```
      MGF=NMGF(K)
      SUMN=0.
      SUMD=0.
      DO 200 MM=1,29
      DO 200 MG=MGI,MGF
      SUMN=SUMN+V1(MG)*PSI(MG,MM)
      SUMD=SUMD+PSI(MG,MM)
  200 CONTINUE
      V1AV(K)=SUMN/SUMD
      V11(K)=1./V1AV(K)
  300 CONTINUE
      WRITE(6,OUT0)
      WRITE(6,OUT1)
      WRITE(6,OUT2)
      STOP
      END
/*
```

APPENDIX N

BRIEF DESCRIPTION OF THE INPUT TO OZAN

All the input is in NAMELIST format. That is the class name is introduced by an ampersand sign in the column 2 and the class is terminated by a card bearing &END in columns 2 to 5.

A complete listing of the input is shown in Appendix O.

The input consists of (in this order)

Card type 1, class name INNM;

NMODES: number of trial shapes;

NOEKIN may be input 1 if the cross sections are ready on tapes to be used by OZAN. A zero indicates that the cross sections will be prepared on tapes throughout the run;

KSREX: 1 for this variable indicates that the eigenvalue(s) for the trial shape(s) will be computed in an integral sense by OZAN. If 0 is input the eigenvalue(s) must be supplied in card INSKEF (see below);

KSROZ: 1 for this variable indicates that an eigenvalue for the first trial shape will be computed to compensate the photoneutrons and make the (11) element of the initial value of the reactivity matrix vanish if the reactor is critical at the beginning of the transient. If 0 is input the eigenvalue of the critical reactor must be supplied in card INSKOZ (see below);

COEFIC: The correction factor for the photoneutrons. If this number is input 0, the photoneutrons will be ignored;

LFINAL: Denotes the number of the time zone(s);

INPC: 1 for this variable indicates that the initial value(s) of the first precursor amplitude function(s) will be input to the code (generally when the reactor is not at a steady state at the beginning of the transient). 0 indicates that the initial value(s) of the precursor amplitude function(s) will be computed in the code;

LPSN: 1 for this variable indicates that the absorption cross sections will be increased by OMEG X V1(MG) (Input in the next type of card, MG being the neutron group, MG = 1,2,3) for the computation in an integral sense of the eigenvalue of the second shape; otherwise 0 should be input;

LBYD: 1 for this parameter indicates that we intend to continue computations beyond the end of the time zone (TMAX; see below) established to study the transient with the proposed method;

<u>Card type 2, class name INV1</u>;

V1: Neutron inverse velocities, the first one belonging to the fast group;

OMEG: ω, the estimated inverse period that the reactor will assume by the end of the transient;

<u>Card type 3, class name INHU</u>;

HU: the mesh intervals in the r direction;

Card type 4, class name INHV;

HV: the mesh intervals in the z direction;

Card type 5, class name INYL;

YIEL: Relative yields of photons of interest, the first one belonging to the most energetic group of photons;

Card type 6, class name INYJ;

YIEJ: Probabilities of photoneutrons to show up in various - time wise - groups;

NZRO: Total number of photons of interest generated per fission of U^{235};

Card type 7, class name INBA;

BETA: the delayed neutron

NBETA1: number of delayed neutron group fraction(s);

NBETA2: number of delayed photoneutron group(s);

Card type 8, class name INF;

FIJ: the initial conditions for the time coefficients;

FAMLAM: Decay constant(s) for the delayed neutron(s) [and photoneutron(s)];

Card type 9, class name INATT1;

ATT1: The attenuation coefficients for the various attenuation zones

Card type 10, class name INMVU;

An edit of the time dependent flux will be made for the region framed by the mesh points MV1, MVV in the z direction and, MU1, MUU in the r direction;

Card types 11,12,13,14, class names INUI, INUF, INVI, INVF;

MRUI (1), MRUF(1), MRVI(1), MRVF(1) are the mesh points framing the first attenuation zone (the first two numbers in the r direction and the last two ones in the z direction);

Card type 15, class name INGLK;

MGLK: Number of groups for D, Σ_a, $\nu\Sigma_F$, Σ_F, $SGCS_1$ (first group of photons), $SGCS_2$ (second group of photons), Σ_s, and Σ_D;

Card type 16, Class name INDV;

MDVIC: Input output device numbers for in this order, D(0), $\Sigma_a(0)$, $\nu\Sigma_F(0)$, $\Sigma_F(0)$, $SGCS_1(0)$, $SGCS_2(0)$, $\Sigma_s(0)$,

$\Sigma_D(0)$, D(T), $\Sigma_a(T)$, $\nu\Sigma_F(T)$, $\Sigma_F(T)$, $SGCS_1(T)$,

$SGCS_2(T)$, $\Sigma_s(T)$, $\Sigma_D(T)$, D_2, Σ_{a_2}, $\nu\Sigma_{F_2}$,

(Here enter three any numbers to fill a blank in the array), Σ_{s_2}, (another any number to fill a blank in the array), D_1, Σ_{a_1} , $\nu\Sigma_{F_1}$, (any three numbers), Σ_{s_1}, (any number), where 0 stands for the beginning of the transient, T the end of the transient, 1 for the first trial shape and 2 for the second trial shape.

Card type 17, class name INT;

TMIN: time at which the transient starts;

IJUMP: After Every IJUMP times GONCA (the subroutine solving the multimode kinetics Equations) is called, the time dependent solutions will be printed out;

TUP: is built up out of times at which a complete edit will be made;

NINT: Number of times a complete edit will be made; TUP (NINT) is the end of the time zone established for studying the transient with the proposed method;

NCM1: Degree of the polynomial expansion used in determining the time coefficients (cf. Appendix F);

EPS2: Criteria insuring the convergence of the time coefficients (1. E-1 is good enough for this purpose);

Card type 18, class name IN1;

X1: Macroscopic diffusion coefficients and cross sections in various materials. Input three (-group-) diffusion coefficients for all the materials. Do the same thing for Σ_a, $\nu\Sigma_F$, Σ_F, $SGCS_1$ and $SGCS_2$.

Card type 19, class name IN2;

X2: Macroscopic scattering cross sections in various materials. Input first the scattering cross section from group one to group 2 [$\Sigma_s(1\to 1)$], then the scattering cross section from group 2 to group 3 [$\Sigma_s(2\to 3)$] for the first material. Do the same thing for the other materials.

Card type 20, class name IN3:

X3: Macroscopic photoneutron reaction cross sections for various materials;

Card type 21, class name INCS;

NCS: If the first, or the second, or the third, or the seventh element of this array is 2, D_2, or Σ_{a_2}, or $\nu\Sigma_{F_2}$ or Σ_{s_2} (in this order) - relative to the second trial shape - is the same as compared to D_1, or Σ_{a_1}, or $\nu\Sigma_{F_1}$ or Σ_{s_1} (in this order) - relative to the first trial shape. If 1 is input for any of these elements the corresponding cross sections relative to the second trial shape are not equal to those relative to the first trial shape.

Card type 22, class name INNCS;

ND=1, NSSGA=1, NUNSF=2, NSCRT=1,

Correspond to NCS (1) = 1, NCS(2) = 1, NCS(3) = 2, NCS(7) = 1 (see above Card type 21);

Card type 23, 24, 25, 26, class names INNRK1, INNRK2, INNRK3, INNRK7;

NRK1: Number of regions in which D_2 is different as compared to D_1.

NRUI1(1), NRUF1(1), NRVI1(1), NRVF1(1)frame the first region (the first two numbers in the r direction, and the last two ones in the z direction) where D_2 is different as compared to D_1. NRCC1(1) = 1 is the material number in this region;

XT1(1): the new diffusion coefficients relative to the trial shape in this region;

The same thing is repeated for INNRK2, INNRK3 and INNRK7 relative respectively to Σ_{a_2}, $\nu\Sigma_{F_2}$ and Σ_{s_2}. If any of D_2,

Σ_{a_2}, $\nu\Sigma_{F_2}$ and Σ_{s_2} do not differ from those relative to the first trial shape, the corresponding cards can be dismissed;

Card type 27, class name INSKEF;

SKEF: The eigenvalue(s) of the trial shapes computed in an integral sense. This card is read in only if KSREX is 1 (cf. first type of cards);

Card type 28, class name INSKOZ;

SKOZN: Eigenvalue of the critical reactor, computed in an integral sense;

Card type 29, class name INCDNC;

CSC: This array has eight elements that correspond respectively to D, Σ_a $\nu\Sigma_F$, Σ_F, $SGCS_1$, $SGCS_2$, Σ_s and Σ_D. If during the transient any of these cross section sets receive a ramp change 1 will be input in the place of the element of interest. Otherwise 2 will be input;

Card type 30, class name INDDNC;

DC, SIGAC, UNSFC, SIGFC, SGCSC, SCATC, SPNRC

These variables are treated the same way the elements of the CSC array (see above Card type 23) are treated. DC=1 will then mean that the diffusion coefficient-set receives a ramp change during the transient;

Card type 31, 32, 33, 34, 35, 36, 37, 38, class names INMRK1, INMRK2, INMRK3, INMRK4, INMRK5, INMRK6, INMRK7, INMRK8 (D, Σ_a, $\nu\Sigma_F$, Σ_F, $SCGS_1$, $SGCS_2$, Σ_s, Σ_D);

Confer Card type 21 with the only difference that the values at the end of the transient, t = TUP(NINT), for those cross sections that vary during the transient will now be input.

Cards, for those cross sections that do not receive any change during the transient, can be dismissed;

Card types 39, 40, 41, 42, 43, 44, 45, 46, 47, 48, class names INSPC, INSTP, INMSK1, INMSK2, INMSK3, INMSK4, INMSK5, INMSK6, INMSK7, INMSK8;

The test that is made for a ramp change through card types 29 up to 38 is now made for a step change.

If LBYD is greater than 1, then the class INT is repeated to characterize the output beyond the time TUP(NINT) input through the first INT (see above, card type A).

APPENDIX O

PROGRAM OZAN

ALONG WITH REQUIRED PREPARATIONS,

PROGRAM RHO1

(The Ramp Change Slope of the Reactivity Matrix Computed through a Perturbation type of Approach)

ALLO Set Up

(Like Allocate)

```
ALLOCATE SPACE TO SAVE VARIOUS CROSS SECTIONS

// 'TOLGA YARMAN',REGION=128K,CLASS=A
/*MITID USER=(M8696,9441)
/*MAIN LINES=20,CARDS=00,TIME=5
//STEP1 EXEC PGM=IEFBR14
//DD1 DD DSNAME=USERFILE.M8696.9441.EQD.IF,
// DCB=MIT.STANDARD.SOURCE,SPACE=(1600,(50,5),RLSE),                X
// UNIT=3330,VOL=REF=RENTDISK,DISP=(NEW,CATLG)
//DD2 DD DSNAME=USERFILE.M8696.9441.ESI.GA,
// DCB=MIT.STANDARD.SOURCE,SPACE=(1600,(50,5),RLSE),                X
// UNIT=3330,VOL=REF=RENTDISK,DISP=(NEW,CATLG)
//DD3 DD DSNAME=USERFILE.M8696.9441.FUN.SF,
// DCB=MIT.STANDARD.SOURCE,SPACE=(1600,(50,5),RLSE),                X
// UNIT=3330,VOL=REF=RENTDISK,DISP=(NEW,CATLG)
//DD4 DD DSNAME=USERFILE.M8696.9441.ESC.AT,
// DCB=MIT.STANDARD.SOURCE,SPACE=(1600,(40,4),RLSE),                X
// UNIT=3330,VOL=REF=RENTDISK,DISP=(NEW,CATLG)
//DD14 DD DSNAME=USERFILE.M8696.9441.FQD.IF,
// DCB=MIT.STANDARD.SOURCE,SPACE=(1600,(50,5),RLSE),                X
// UNIT=3330,VOL=REF=RENTDISK,DISP=(NEW,CATLG)
//DD15 DD DSNAME=USERFILE.M8696.9441.FSI.GA,
// DCB=MIT.STANDARD.SOURCE,SPACE=(1600,(50,5),RLSE),                X
// UNIT=3330,VOL=REF=RENTDISK,DISP=(NEW,CATLG)
//DD16 DD DSNAME=USERFILE.M8696.9441.FUN.SF,
// DCB=MIT.STANDARD.SOURCE,SPACE=(1600,(50,5),RLSE),                X
// UNIT=3330,VOL=REF=RENTDISK,DISP=(NEW,CATLG)
//DD17 DD DSNAME=USERFILE.M8696.9441.FIS.GF,
// DCB=MIT.STANDARD.SOURCE,SPACE=(1600,(50,5),RLSE),                X
// UNIT=3330,VOL=REF=RENTDISK,DISP=(NEW,CATLG)
//DD18 DD DSNAME=USERFILE.M8696.9441.TRD.IF,
// DCB=MIT.STANDARD.SOURCE,SPACE=(1600,(50,5),RLSE),                X
// UNIT=3330,VOL=REF=RENTDISK,DISP=(NEW,CATLG)
//DD19 DD DSNAME=USERFILE.M8696.9441.TSI.GA,
// DCB=MIT.STANDARD.SOURCE,SPACE=(1600,(50,5),RLSE),                X
```

```
// UNIT=3330,VOL=REF=RENTDISK,DISP=(NEW,CATLG)                          ALL00037
//DD22 DD DSNAME=USERFILE.M8696.9441.FSC.AT,                            ALL00038
// DCB=MIT.STANDARD.SOURCE,SPACE=(1600,(40,4),RLSE),           X        ALL00039
// UNIT=3330,VOL=REF=RENTDISK,DISP=(NEW,CATLG)                          ALL00040
//DD23 DD DSNAME=USERFILE.M8696.9441.TSC.AT,                            ALL00041
// DCB=MIT.STANDARD.SOURCE,SPACE=(1600,(40,4),RLSE),           X        ALL00042
// UNIT=3330,VOL=REF=RENTDISK,DISP=(NEW,CATLG)                          ALL00043
//DD24 DD DSNAME=USERFILE.M8696.9441.FSG.CS,                            ALL00044
// DCB=MIT.STANDARD.SOURCE,SPACE=(1600,(100,10),RLSE),         X        ALL00045
// UNIT=3330,VOL=REF=RENTDISK,DISP=(NEW,CATLG)                          ALL00046
//DD26 DD DSNAME=USERFILE.M8696.9441.FSP.NR,                            ALL00047
// DCB=MIT.STANDARD.SOURCE,SPACE=(1600,(40,4),RLSE),           X        ALL00048
// UNIT=3330,VOL=REF=RENTDISK,DISP=(NEW,CATLG)                          ALL00049
//DD28 DD DSNAME=USERFILE.M8696.9441.HED.IF,                            ALL00050
// DCB=MIT.STANDARD.SOURCE,SPACE=(1600,(50,5),RLSE),           X        ALL00051
// UNIT=3330,VOL=REF=RENTDISK,DISP=(NEW,CATLG)                          ALL00052
//DD29 DD DSNAME=USERFILE.M8696.9441.HSI.GA,                            ALL00053
// DCB=MIT.STANDARD.SOURCE,SPACE=(1600,(50,5),RLSE),           X        ALL00054
// UNIT=3330,VOL=REF=RENTDISK,DISP=(NEW,CATLG)                          ALL00055
//DD31 DD DSNAME=USERFILE.M8696.9441.HSC.AT,                            ALL00056
// DCB=MIT.STANDARD.SOURCE,SPACE=(1600,(40,4),RLSE),           X        ALL00057
// UNIT=3330,VOL=REF=RENTDISK,DISP=(NEW,CATLG)                          ALL00058
/*                                                                      ALL00059
```

TRSF Set Up

(Like Transfer)

```
TRANSFER VARIOUS FLUXES(FIRST SHAPE AND ITS ADJOINT,ETC) TO THE CORRESPONDING
DATA SETS IN ORDER TO MAKE USE OF THEM DURING THE ,, OZAN ,, RUN


// 'TOLGA YARMAN',REGION=128K,CLASS=A
/*MITID USER=(M8696,9441)
/*MAIN LINES=20,CARDS=00,TIME=3
/*SRI LOW
//STEP1 EXEC FORCGO
//C.SYSIN DD *
C PROGRAM TRANSFER
C
C COPY FROM EXTERMINATOR 2'S DATA SET THE FIRST SHAPE AND ITS ADJOINT WITH
C NECESSARY MODIFICATIONS ONTO TAPES WHICH WILL BE USED BY ,,OZAN,,
C
      DIMENSION PSI(40,3,48),PHI(3,48,40)
C
      REWIND 20
      DO 100 I=1,48
      READ(20) ((PSI(J,K,I),J=1,40),K=1,3)
  100 CONTINUE
 1000 FORMAT(1P5E14.6)
      DO 200 MG=1,3
      DO 200 MV=1,48
      DO 200 MU=1,40
  200 PHI(MG,MV,MU)=PSI(MU,MG,MV)
      DO 210 MG=1,3
      DO 210 MV=1,48
  210 PHI(MG,MV,1)=PHI(MG,MV,2)
      REWIND 10
      WRITE(10,1000) PHI
      REWIND 10
      DO 125 J=1,2
      READ(20)
  125 CONTINUE
      DO 150 I=1,48
```

```
      READ(20) ((PSI(J,K,I),J=1,40),K=1,3)                              TRSF0037
  150 CONTINUE                                                          TRSF0038
      DO 300 MG=1,3                                                     TRSF0039
      DO 300 MV=1,48                                                    TRSF0040
      DO 300 MU=1,40                                                    TRSF0041
  300 PHI(MG,MV,MU)=PSI(MU,MG,MV)                                       TRSF0042
      DO 310 MG=1,3                                                     TRSF0043
      DO 310 MV=1,48                                                    TRSF0044
  310 PHI(MG,MV,1)=PHI(MG,MV,2)                                         TRSF0045
      REWIND 11                                                         TRSF0046
      WRITE(11,1000) PHI                                                TRSF0047
      REWIND 11                                                         TRSF0048
      STOP                                                              TRSF0049
      END                                                               TRSF0050
/*                                                                      TRSF0051
//G.FT20F001 DD DSNAME=USERFILE.M8696.9441.DENGEA.KISI,DISP=(OLD,PASS)  TRSF0052
//G.FT10F001 DD DSNAME=USERFILE.M8696.9441.EQP.SI,DISP=OLD              TRSF0053
//G.FT11F001 DD DSNAME=USERFILE.M8696.9441.FQA.DJ,DISP=OLD              TRSF0054
/*                                                                      TRSF0055
```

PROGRAM OZAN

```
// 'TOLGA YARMAN',REGION=325K,CLASS=A
/*SRI LOW
/*MITID USER=(M8696,9441)
/*MAIN LINES=20,CARDS=30,TIME=25
//STEP1 EXEC FORCGC
//C.SYSIN DD *
C      PROGRAM OZAN
C
C      ,,OZAN,, MEANS POET IN TURKISH
C
      COMMON/OZ0/SIGA,UNSF,SGCS,SCAT,PSI,W
      COMMON/OZ11/C,DNC,KSRCZ,SKOZN,NDPSI,NDW,HU,HV,R
      COMMON/OZ12/CC,SIGAC,UNSFC,SIGFC,SGCSC,SCATC,SFNRC,ATTC
      COMMON/OZ2/NMODES,II,KK
      COMMON/OZ3/TMIN,TMAX
      COMMON/OZ4/NBETA1,NBETA2,NBETA,NBET1
      COMMON/OZEK/MGLK,MDVIC
      COMMON/OZETA/NHS,NHK,NHUI,NHUF,NHVI,NHVF,NHCC,XOZ
      COMMON/FOZ11/LLL,LFINAL,KSREX,FLAP1,ALAP1,DIFF1,SKEF
      COMMON/FOZ12/ISD,ISSA,ISUF,ISSF,ISSG,ISST,ISSP,ISATT
      COMMON/FOZ13/ND,NSIGA,NUNSF,NSCAT
      COMMON/OZ2FZ1/V1
      COMMON/OZ3FZ1/GENTME
      COMMON/OZ4FZ1/LAPN,VLAPN
      COMMON/FCFA/COEF,MCOF
      COMMON/OZFZ2/BETA,E,FMAR,VFMAR,BETR,VBETR,BEC11,BEC21
      COMMON/F2F4/WSC,JNPC
      COMMON/OZ1FZ3/NZRO,COEFIC,S1,YIEL,YIEJ,MRUI,MRUF,MRVI,MRVF,ATT
      COMMON/OZ2FZ3/PHPR,VPHPR,DPPR,VDPPR,BEC12,BEC22
      COMMON/OZFZ4/FIJ,FAMLAM,ROC1,ROC2,ROC3,BEC1,BEC2,BEC3,FAMPRE,INPC
      COMMON/FZ4HT/BE
      COMMON/OZGON/IJUMP,EPS2,NCM1,NCOEF,RCJ,BATA,J3
      COMMON/OZGOHT/FAMCLM
      COMMON/GOZHT/FIF
      COMMON/OZHST/ATT1,ATT2,MU1,MUU,MV1,MVV
C
```

```
      INTEGER C,DNC
      INTEGER DC,SIGAC,UNSFC,SIGFC,SCATC,SGCSC,SPNRC,ATTC
      REAL NZRC
      REAL LAPN
C
      DIMENSION SIGA(3,47,39),SCAT(2,47,39),SGCS(2,3,47,39),HU(39),
     1HV(47),R(40),V1(3),ATT(2,10),ATT1(10),ATT2(10),MRUI(10),MRUF(10),
     2MRVI(10),MRVF(10),YIEL(2),YIEJ(9),BETA(6),TUP(20),FIJ(2),FIF(2),
     3NDW(2),NDPSI(2),SKEF(2),FAMLAM(15),FAMPRE(2,15),FAMCLM(2,15),
     4BEC11(2,2,6),BEC21(2,2,6),BEC12(2,2,9),BEC22(2,2,9),DPPR(2,2),
     5VDPPR(2,2),GENTME(2,2),BEC1(2,2,15),BEC2(2,2,15),BEC3(2,2,15),
     6BATA(2,2,15),ROC1(2,2),ROC2(2,2),ROC3(2,2),RCJ(2,2)
      DIMENSION PFULL(4,4),PHALF(4,4),BFULL(4),BHALF(4),BETR(2,2),VBETR
     1(2,2),LAPN(2,2),VLAPN(2,2),FMAR(2,2),VFMAR(2,2),PHPR(2,2),VPHPR
     2(2,2),MGLK(8),MDVIC(32),NHS(8),NHK(8),NCSCU(8),NHUI(20,8),
     3NHUF(20,8),NHVI(20,8),NHVF(20,8),NHCC(20,8),XOZ(3,20,8)
      DIMENSION PSI(3,48,40),W(3,48,40),UNSF(3,47,39),S1(2,10),
     1COEF(3,47,39),WSC(2),LBYD(5)
C
      C=1
      DNC=2
C
C C LIKE CHANGE,DNC LIKE DOES NOT CHANGE(DURING THE TRANSIENT)
C
      NDPSI(1)=10
      NDPSI(2)=12
      NDW(1)=11
      NDW(2)=13
C
      NAMELIST/INNM/NMODES,NCEKIN,KSREX,KSRCZ,COEFIC,LFINAL,INPC,LPSN,
     1LBYD
      NAMELIST/INV1/V1,OMEG
      NAMELIST/INHU/HU
      NAMELIST/INHV/HV
      NAMELIST/INYL/YIEL
      NAMELIST/INYJ/YIEJ,NZRO
```

```
      NAMELIST/INBA/BETA,NBETA1,NBETA2
      NAMELIST/INF/FIJ,FAMLAM,FAMPRE
      NAMELIST/INMVU/MV1,MVV,MU1,MUU
      NAMELIST/INATT1/ATT1
      NAMELIST/INATT2/ATT2
      NAMELIST/INUI/MRUI
      NAMELIST/INUF/MRUF
      NAMELIST/INVI/MRVI
      NAMELIST/INVF/MRVF
      NAMELIST/INGLK/MGLK
C
C MGLK(1) IS THE NUMBER OF GROUPS FOR D
C
      NAMELIST/INDV/MDVIC
C
C MDVIC(1) IS THE INPUT OUTPUT DEVICE FOR D AT THE BEGINNING OF THE TRANSIENT
C
      NAMELIST/INSKEF/SKEF
      NAMELIST/INSKOZ/SKOZN
      NAMELIST/INT/TMIN,IJUMP,TUP,NINT,NCM1,EPS2
C
      READ(5,INNM)
      READ(5,INV1)
      READ(5,INHU)
      READ(5,INHV)
      READ(5,INYL)
      READ(5,INYJ)
      READ(5,INBA)
      READ(5,INF)
      READ(5,INATT1)
      READ(5,INMVU)
      READ(5,INUI)
      READ(5,INUF)
      READ(5,INVI)
      READ(5,INVF)
      READ(5,INGLK)
```

```
      READ(5,INCV)
      READ(5,INT)
C
 1000 FORMAT(7E11.5)
  600 FORMAT (1H ,20X,'INPUT OPTIONS'///)
  601 FORMAT (1H ,'THE NUMBER OF THE TRIAL FUNCTION(S) USED IS ',I1)
  602 FORMAT (1H ,'CROSS SECTION ARRAYS WILL BE SENT ON TAPES'/)
  603 FORMAT (1H ,'CROSS SECTION ARRAYS ARE SUPPOSEDLY READY ON TAPES'/)
  604 FORMAT (1H ,'A SEARCH FOR THE EIGENVALUE(S) OF THE TRIAL FUNCTION(
     1S) WILL BE MADE TROUGH THE CODE')
  605 FORMAT (1H ,'THE EIGENVALUE(S) OF THE TRIAL FUNCTION(S) ARE SUPPOS
     1EDLY KNOWN')
  606 FORMAT (1H ,'CONSIDERING THE PHOTONEUTRONS A SEARCH FOR THE EIGENV
     1ALUE OF THE STEADY STATE SHAPE WILL BE MADE TROUGH THE CODE'/)
  607 FORMAT (1H ,'THE PHOTONEUTRONS HAVE BEEN ESTIMATED TO BE NOT IMPOR
     1TANT FOR THE TRANSIENT STUDIED'/)
  608 FORMAT(1H ,'IT HAS BEEN CHOSEN',I2,' TIME ZONE(S) FOR THE TRANSIEN
     1T STUDIED')
 6081 FORMAT (/1X,'THE PRECURSOR CONCENTRATIONS WILL BE COMPUTED WITHIN
     1THE CODE'/)
 6082 FORMAT (1H ,'THE PRECURSOR CONCENTRATIONS ARE INPUT TO THE CODE')
 6083 FORMAT (1H ,'THE REACTOR WILL BE UNIFORMLY POISONED FOR COMPUTATIO
     1N OF THE EIGENVALUE OF THE SECOND SHAPE'/)
  609 FORMAT(1H ,'THE INITIAL CONDITION FOR THE  FIRST TRIAL FUNCTION IS
     1   ',E11.5)
  610 FORMAT(1H ,'THE INITIAL CONDITION FOR THE SECOND TRIAL FUNCTION IS
     1   ',E11.5)
  611 FORMAT (/1X,'AN EDIT OF THE TIME DEPENDENT FLUX WILL BE MADE(IF NM
     1ODES.GT.1)AT THE SELECTED POINT(S) LOCATED BETWEEN THE MESHES'//7X
     2,I2,',',I2,' IN THE Z DIRECTION AND '/7X,I2,',',I2,' IN THE R DIRE
     3CTION'//)
  612 FORMAT(1X,'FIRST TIME ZONE'//7X,'TIME ORIGIN IS AT ',F10.8/7X,'AMP
     1LITUDE FUNCTIONS PRINTED AT INCREMENTS OF ',I2/7X,'A COMPLETE EDIT
     2 WILL BE MADE(IF NMODES.GT.1) AT TIMES;'//(7X,10(F8.6,2X))/(7X,10(
     3F8.6,2X))/)
 6121 FORMAT (/7X,'THERE ARE THEN ',I2,' TIME STEPS'///)
```

```
 620 FORMAT (1H1,/////21X,'SEARCH FOR THE EIGENVALUE (S) OF THE TRIAL F
    1UNCTION (S) '///)
 621 FORMAT (/////1X,'KEFF1=',F10.8,4X,'  KEFF2=',F10.8//)
 622 FORMAT (1H1,/////21X,'SEARCH FOR THE EIGENVALUE OF THE STEADY STAT
    1E SHAPE CONSIDERING THE PHOTONEUTRONS'///)
 623 FORMAT (/////1X,'KEFFOZAN=',F10.8//)
 624 FORMAT(1H1,'NEW TIME ZONE'/7X,'TIME ORIGIN AT ',F10.8/7X,'AMPLITUD
    1E FUNCTIONS PRINTED AT INCREMENTS OF ',I2/7X,'A COMPLETE EDIT WILL
    2 BE MADE(IF NMODES.GT.1) AT TIMES;'//(7X,10(F8.6,2X))/(7X,10(F8.6,
    32X))/)
7024 FORMAT (/////1X,'THE REACTOR HAS ALREADY BLOWN UP '/7X,'NO NEED TO
    1 CONTINUE..')
7025 FORMAT (///////7X,'THE CRITERIUM(EPS2) INSURING THE TIME DEPENDENT
    1 SOLUTION(S) TO CONVERGE ,IS TOO SMALL')
C
     WRITE (6,600)
     WRITE (6,601) NMODES
     IF (NOEKIN.EQ.1) GO TO 613
     WRITE(6,602)
     GO TO 614
 613 WRITE(6,603)
 614 IF (KSREX.EQ.1) GO TO 615
     WRITE(6,605)
     GO TO 616
 615 WRITE(6,604)
 616 IF (KSROZ.EQ.1) GO TO 617
     IF (COEFIC.NE.0.) GO TO 618
     WRITE(6,607)
     GO TO 618
 617 WRITE(6,606)
 618 WRITE(6,608) LFINAL
     IF (INPC.EQ.1) GO TO 6181
     WRITE(6,6081)
     GO TO 6182
6181 WRITE(6,6082)
6182 CONTINUE
```

```
      IF (LPSN.EQ.0) GO TO 6192
      WRITE(6,6083)
 6192 WRITE(6,609) FIJ(1)
      IF (NMODES.EQ.1) GO TO 619
      WRITE(6,610) FIJ(2)
      WRITE(6,611) MV1,MVV,MU1,MUU
  619 WRITE(6,612) TMIN,IJUMP,(TUP(IT),IT=1,NINT)
      WRITE(6,6121) NINT
      NBETA=NBETA1+NBETA2
      NBET1=NBETA1+1
      DO 2022 MR=1,10
      ATT(1,MR)=ATT1(MR)
 2022 CONTINUE
      IF(ATTC .EQ.0) GO TO 1024
      GO TO 1025
 1024 READ(5,INATT2)
      DO 2023 MR=1,10
 2023 ATT(2,MR)=ATT2(MR)
 1025 CONTINUE
C
C     CALCULATION OF R(MU)
C
      R(1)=0.
      DO 1030 MU=2,40
      R(MU)=R(MU-1)+HU(MU-1)
 1030 CONTINUE
      II=NMODES
      KK=II
      LLL=1
      MMM=0
      JNPC=INPC
      TMAX=TUP(NINT)
      NDIM=NMODES*NCM1
      NCOEF=NCM1+1
      IF (NDEKIN.EQ.1) GO TO 511
C
```

```
      CALL EKIN(COEFIC,SIGA,SGCS,SCAT)
C
      READ(14,1000) SIGA
      REWIND 14
      WRITE(1,1000) SIGA
      REWIND 1
      READ(15,1000) SIGA
      REWIND 15
      WRITE(2,1000) SIGA
      REWIND 2
      READ(16,1000) SIGA
      REWIND 16
      WRITE(3,1000) SIGA
      REWIND 3
      READ(22,1000) SCAT
      REWIND 22
      WRITE(4,1000) SCAT
      REWIND 4
C
  511 CALL DATA3(DNC)
      CALL THEEND(NGLK,MCVIC,DNC,SIGA,SCAT)
C
      IF ((NMODES.EQ.1).OR.(LPSN.NE.1)) GO TO 5111
C
      CALL POISON(SIGA,OMEG,V1)
C
 5111 CONTINUE
      IF (KSREX.EQ.1) GO TO 500
      READ(5,INSKEF)
      GO TO 502
  500 CONTINUE
      WRITE(6,620)
C
      CALL FILIZ1
C
      WRITE(6,621) (SKEF(IS),IS=1,NMODES)
```

```
  502 IF (KSROZ.EQ.1) GO TO 504
      IF (COEFIC.EQ.0.) GO TO 5021
      READ(5,INSKOZ)
      GO TO 506
 5021 SKOZN=SKEF(1)
  506 KSREX=0
      KSROZ=0
C
  507 CALL DATA2(DNC)
C
      IF (LLL.EQ.1) GO TO 509
C
      CALL PASS(NCSKO,DNC,MDVIC,SIGA,SGCS,SCAT)
  509 CALL CHANGE(MGLK,MDVIC,DNC,SIGA,SGCS,SCAT,NCSCO)
      CALL DATA1(DNC)
      CALL STEP(MGLK,MDVIC,DNC,SIGA,SGCS,SCAT)
C
      IF (LLL.EQ.1) GO TO 503
      READ(5,INT)
      WRITE(6,624) TMIN,IJUMP,(TUP(IT),IT=1,NINT)
      WRITE(6,6121) NINT
      TMAX=TUP(NINT)
C
  503 CALL FILIZ1
      CALL FILIZ2
C
      IF (COEFIC.NE.0.) GO TO 508
      DO 520 I=1,II
      DO 520 K=1,KK
      PHPR(I,K)=0.
      VPHPR(I,K)=0.
      DPPR(I,K)=0.
      VDPPR(I,K)=0.
      DO 520 J=1,NBETA2
      BEC12(I,K,J)=0.
      BEC22(I,K,J)=0.
```

```
  520 CONTINUE
      GO TO 510
C
  508 CALL FILIZ3
  510 CALL FILIZ4
C
      GO TO 512
  504 CONTINUE
      WRITE(6,622)
      II=1
      KK=1
C
      CALL FILIZ3
C
      SKOZN=-FLAP1/(ALAP1-DIFF1-PHPR(1,1)-DPPR(1,1))
      WRITE(6,623) SKOZN
      II=NMODES
      KK=NMODES
      GO TO 506
  512 TMAX=TUP(1)
      IF (MMM.EQ.0) GO TO 1094
      DO 1093 I=1,II
      DO 1093 K=1,KK
      ROC1(I,K)=ROJ(I,K)
      DO 1093 J=1,NBETA
 1093 BEC1(I,K,J)=BATA(I,K,J)
 1094 CONTINUE
C
      CALL GONCA(NDIM,PFULL,PHALF,BFULL,BHALF)
C
      IF (J3.GE.30) GO TO 5900
      DO 5041 I=1,II
      FIFM=FIF(I)
 5041 IF ((ABS(FIFM).GE.1.E35).OR.(ABS(FIFM).LE.1.E-35)) GO TO 5800
      IF (NMODES.EQ.1) GO TO 513
C
```

```
      CALL HASAT(BATA,GENTME,ROJ)
C
  513 IF (NINT.LT.2) GO TO 7032
      DO 1032 NI=2,NINT
      TMIN=TMAX
      TMAX=TUP(NI)
      DO 1031 I=1,II
      DO 1031 K=1,KK
      ROC1(I,K)=ROJ(I,K)
      DO 1031 J=1,NBETA
      BFC1(I,K,J)=BATA(I,K,J)
 1031 CONTINUE
C
      CALL GONCA(NDIM,PFULL,PHALF,BFULL,BHALF)
C
      IF (J3.GE.30) GO TO 5900
      DO 5042 I=1,II
      FIFM=FIF(I)
 5042 IF ((ABS(FIFM).GE.1.E35).OR.(ABS(FIFM).LE.1.E-35)) GO TO 5800
      IF (NMODES.EQ.1) GO TO 1032
C
      CALL HASAT(BATA,GENTME,ROJ)
C
 1032 CONTINUE
 7032 CONTINUE
      IF (LBYD(LLL).EQ.0) GO TO 1033
      READ(5,INT)
      WRITE(6,624) TMIN,IJUMP,(TUP(IT),IT=1,NINT)
      WRITE(6,6121) NINT
      LBYD(LLL)=0
      MMM=1
      GO TO 512
 1033 IF (LLL.EQ.LFINAL) GO TO 5000
      LLL=LLL+1
      GO TO 507
 5800 WRITE(6,7024)
```

```
      GO TO 5000
 5900 WRITE(6,7025)
 5000 CONTINUE
      STOP
      END
      SUBROUTINE EKIN(COEFIC,D,SGCS,SCAT)
C
C THIS SUBROUTINE WILL MAKE UP THE CROSS SECTION ARRAYS AND WILL SEND THE
C RESULTS TO THE DATA CELLS
C
C ,, EKIN ,, MEANS SEED IN TURKISH
C
C A PROVERB SAYS ,,WHATSOEVER A MAN SOWETH THAT ALSO SHALL HE REAP,,
C
      COMMON/OZEK/MGLK,MDVIC
C
      DIMENSION X1(3,23,6),X2(2,23),X3(2,23),X(3,23,8),D(3,47,39),
     1SGCS(2,3,47,39),SCAT(2,47,39),MGLK(8),MDVIC(32)
C
C DATA FOR D,SIGA,NUSIGF,SIGF,SECONDARY GAMMA RAY CROSS SECTION
C PHOTON GROUP 1 AND PHOTON GROUP 2 (STEADY STATE)
C
      NAMELIST/IN1/X1
C
C DATA FOR SCAT; SCATTERING CROSS SECTION  (STEADY STATE)
C
      NAMELIST/IN2/X2
C
C DATA FOR SPNR; PHOTONEUTRON REACTION CROSS SECTION (STEADY STATE)
C
      NAMELIST/IN3/X3
 9000 FORMAT(7E11.5)
      READ(5,IN1)
      READ(5,IN2)
      READ(5,IN3)
C
```

```
C STEADY STATE PICTURE
C
      DO 153 K=1,8
      IF ((COEFIC.EQ.0.).AND.((K.EQ.4).OR.(K.EQ.5).OR.(K.EQ.6).OR.
     1(K.EQ.8))) GO TO 153
      MDEVC=MDVIC(K)
      MGL=MGLK(K)
      IF (K.EQ.7) GO TO 17
      IF (K.EQ.8) GO TO 18
      DO 80 MC=1,23
      DO 80 LG=1,MGL
      X(LG,MC,K)=X1(LG,MC,K)
   80 CONTINUE
      GO TO 20
   17 DO 85 MC=1,23
      DO 85 LG=1,MGL
      X(LG,MC,K)=X2(LG,MC)
   85 CONTINUE
      GO TO 20
   18 DO 86 MC=1,23
      DO 86 LG=1,MGL
      X(LG,MC,K)=X3(LG,MC)
   86 CONTINUE
   20 DO 250 LG=1,MGL
C
      CALL SU(K,LG,X,D)
C
      IF(K.EQ.5) GO TO 212
      IF(K.EQ.6) GO TO 214
      IF (K.GT.6) GO TO 215
      IF (LG.LT.MGL) GO TO 250
      WRITE(MDEVC,9000) D
      REWIND MDEVC
      GO TO 250
  212 DO 300 MV=1,47
      DO 300 MU=1,39
```

```
      SGCS(1,LG,MV,MU)=D(LG,MV,MU)
  300 CONTINUE
      GO TO 250
  214 DO 310 MV=1,47
      DO 310 MU=1,39
      SGCS(2,LG,MV,MU)=D(LG,MV,MU)
  310 CONTINUE
      IF (LG.LT.MGL) GO TO 250
      WRITE(MDEVC,9000) SGCS
      REWIND MDEVC
      GO TO 250
  215 DO 315 MV=1,47
      DO 315 MU=1,39
      SCAT(LG,MV,MU)=D(LG,MV,MU)
  315 CONTINUE
      IF (LG.LT.MGL) GO TO 250
      WRITE(MDEVC,9000) SCAT
      REWIND MDEVC
  250 CONTINUE
  153 CONTINUE
      RETURN
      END
      SUBROUTINE SU(K,LG,X,Y)
C
C ,,SU,, MEANS WATER IN TURKISH
C
      DIMENSION X(3,23,8),Y(3,47,39)
      DIMENSION MRUI(99),MRUF(99),MRVI(99),MRVF(99),MRCC(99)
C
C FOR MV=1,MU=1 THE CROSS SECTION OF THE 18TH MATERIEL IS SAID TO BELONG TO THE
C MESH VOLUMES ENCLOSED IN MU=1,MU=18(IN THE R DIRECTION) AND MV=1,MV=2(IN THE Z
C DIRECTION)
C
      DATA MRUI/1,19,20,21,20,22,35,34,1,22,31,33,1,7,
     122,1,3,5,7,17,23,22,26,27,3,5,6,7,11,3,7,3,7,3,7,1,23,22,
     221,23,19,18,20,17,1,8,11,14,19,17,25,26,2*25,3*24,3*23,22,
```

```
     320,21,22,20,18,19,17,16,17,13,14,15,10,11,12,13,5,6,7,8,9,
     410,1,5,2*26,25,24,23,21,20,18,16,3*1,27,1/
C
      DATA MRUF/18,19,20,21,20,33,39,34,18,30,32,33,4,16,
     132,2,4,6,16,18,25,22,26,32,4,5,6,10,16,4,16,4,16,4,2*16,24,2*22,
     223,2*22,21,2*19,17,16,15,20,17,25,26,2*25,3*24,23,2*23,
     322,20,21,22,20,18,19,17,16,17,13,14,15,10,11,12,13,5,6,7,8,9,10,
     44,7,9*26,12,9,4,2*33/
C
      DATA MRVI/4*1,12,3*1,4*3,3*4,2*5,4,5,4,4*5,
     110,2*8,2*10,2*20,2*24,2*25,26,2*19,21,2*22,24,2*27,
     229,30,31,32,21,24,2*19,20,21,22,23,2*24,25,26,27,3*28,29,2*30,
     331,2*32,3*33,4*32,6*31,2*30,20,21,22,25,27,29,30,31,2*33,
     432,31,7,34/
C
      DATA MRVF/2,20,11,2*20,2,2*47,3*3,6,3*4,25,9,7,9,
     123,3*18,6,19,2*25,2*19,2*23,2*24,2*25,28,21,20,21,2*23,26,27,
     228,29,30,31,32,21,26,2*19,20,21,22,23,2*24,25,26,27,3*28,29,
     32*30,31,2*32,3*33,4*32,6*31,2*30,20,21,24,26,28,29,30,32,
     42*33,32,31,33,47/
C
      DATA MRCC/18,21,9,2*21,18,16,15,2*2,19,22,2*2,
     119,8,13,9,14,11,21,2*12,22,4,2*10,5,6,3,1,2*2,2*23,2,21,2*20,
     221,8*20,2*11,2,17,4*12,17,2,3*12,2,2*17,3*12,2,12,2*17,
     32*12,17,2*12,2,3*17,2*12,2,12,2,14*7/
C
      DO 90 MR=1,99
      MUI=MRUI(MR)
      MUF=MRUF(MR)
      MVI=MRVI(MR)
      MVF=MRVF(MR)
      MCC=MRCC(MR)
      DO 90 MU=MUI,MUF
      DO 90 MV=MVI,MVF
      Y(LG,MV,MU)=X(LG,MCC,K)
   90 CONTINUE
```

```
      RETURN
      END
      SUBROUTINE DATA1(DNC)
C
C STEP CHANGE AT THE BEGINNING OF THE TIME STEP
C
      COMMON/FOZ12/ISD,ISSA,ISUF,ISSF,ISSG,ISST,ISSP,ISATT
      COMMON/OZDTA/ISTPC,MSK1,MSK2,MSK3,MSK4,MSK5,MSK6,MSK7,MSK8,MSUI1,
     1MSUI2,MSUI3,MSUI4,MSUI5,MSUI6,MSUI7,MSUI8,MSUF1,MSUF2,MSUF3,MSUF4,
     2MSUF5,MSUF6,MSUF7,MSUF8,MSVI1,MSVI2,MSVI3,MSVI4,MSVI5,MSVI6,MSVI7,
     3MSVI8,MSVF1,MSVF2,MSVF3,MSVF4,MSVF5,MSVF6,MSVF7,MSVF8,MSCC1,MSCC2,
     4MSCC3,MSCC4,MSCC5,MSCC6,MSCC7,MSCC8,XS1,XS2,XS3,XS4,XS5,XS6,XSS7,
     5XSS8
C
      INTEGER DNC
C
      DIMENSION XS1(3,20),XS2(3,20),XS3(3,20),XS4(3,20),XS5(3,20),
     1XS6(3,20),XS7(2,20),XS8(2,20),ISTPC(8),XSS7(3,20),XSS8(3,20)
      DIMENSION MSUI1(20),MSUI2(20),MSUI3(20),MSUI4(20),MSUI5(20
     2),MSUI6(20),MSUI7(20),MSUI8(20),MSUF1(20),MSUF2(20),MSUF3(20),MSUF
     34(20),MSUF5(20),MSUF6(20),MSUF7(20),MSUF8(20),MSVI1(20),MSVI2(20),
     4MSVI3(20),MSVI4(20),MSVI5(20),MSVI6(20),MSVI7(20),MSVI8(20),
     5MSVF1(20),MSVF2(20),MSVF3(20),MSVF4(20),MSVF5(20),MSVF6(20),MSVF7(
     620),MSVF8(20),MSCC1(20),MSCC2(20),MSCC3(20),MSCC4(20),MSCC5(20),
     7MSCC6(20),MSCC7(20),MSCC8(20)
C
      EQUIVALENCE(XS7(1,1),XSS7(1,1)),(XS8(1,1),XSS8(1,1))
C
      NAMELIST/INSFC/ISTPC
      NAMELIST/INSTP/ISD,ISSA,ISUF,ISSF,ISSG,ISST,ISSP,ISATT
      NAMELIST/INMSK1/MSK1,MSUI1,MSUF1,MSVI1,MSVF1,MSCC1,XS1
      NAMELIST/INMSK2/MSK2,MSUI2,MSUF2,MSVI2,MSVF2,MSCC2,XS2
      NAMELIST/INMSK3/MSK3,MSUI3,MSUF3,MSVI3,MSVF3,MSCC3,XS3
      NAMELIST/INMSK4/MSK4,MSUI4,MSUF4,MSVI4,MSVF4,MSCC4,XS4
      NAMELIST/INMSK5/MSK5,MSUI5,MSUF5,MSVI5,MSVF5,MSCC5,XS5
      NAMELIST/INMSK6/MSK6,MSUI6,MSUF6,MSVI6,MSVF6,MSCC6,XS6
```

```
      NAMELIST/INMSK7/MSK7,MSUI7,MSUF7,MSVI7,MSVF7,MSCC7,XS7
      NAMELIST/INMSK8/MSK8,MSUI8,MSUF8,MSVI8,MSVF8,MSCC8,XS8
C
C MSK1 GIVES THE NUMBER OF REGIONS IN WHICH DURING THE TRANSIENT D- THE
C DIFFUSION COEFFICIENT- CHANGES.
C
C      ( K.EQ.1 CORRES TO D)
C      ( K.EQ.2 CORRES TO SIGA)
C      ( K.EQ.3 CORRES TO UNSF)
C      ( K.EQ.4 CORRES TO SIGF)
C      ( K.EQ.5 CORRES TO SGCS -PHOTON GROUP 1-)
C      ( K.EQ.6 CORRES TO SGCS -PHOTON GROUP 2-)
C      ( K.EQ.7 CORRES TO SCAT)
C      ( K.EQ.8 CORRES TO SPNR)
C
C THE REGION MSK1(MR) IS BORDERED BY MSUI1(MR),MSUF1(MR) (IN THE R DIRECTION)
C AND MSVI1(MR),MSVF1(MR) (IN THE Z DIRECTION),ENCLOSES THE MATERIEL MSCC1(MR).
C
C XS1 IS THE NEW CROSS SECTION ARRAY FOR D(BEGINNING OF THE TRANSIENT -STEP
C CHANGE-)
C
      READ(5,INSPC)
      READ(5,INSTP)
      IF (ISD.EQ.DNC) GO TO 704
      READ(5,INMSK1)
  704 IF (ISSA.EQ.DNC) GO TO 705
      READ(5,INMSK2)
  705 IF (ISUF .EQ.DNC) GO TO 706
      READ(5,INMSK3)
  706 IF (ISSF .EQ.DNC) GO TO 707
      READ(5,INMSK4)
  707 IF (ISSG .EQ.DNC) GO TO 708
      READ(5,INMSK5)
      READ(5,INMSK6)
  708 IF (ISST .EQ.DNC) GO TO 709
      READ(5,INMSK7)
```

```
  709 IF (ISSP .EQ.DNC) GO TO 710
      READ(5,INMSK8)
  710 CONTINUE
      RETURN
      END
      SUBROUTINE DATA2(DNC)
C
C CHANGE -THE END OF THE TIME STEP-
C
      COMMON/OZ12/DC,SIGAC,UNSFC,SIGFC,SGCSC,SCATC,SPNRC,ATTC
      COMMON/OZDTA/ CSC ,MRK1,MRK2,MRK3,MRK4,MRK5,MRK6,MRK7,MRK8,MRUI1,
     1MRUI2,MRUI3,MRUI4,MRUI5,MRUI6,MRUI7,MRUI8,MRUF1,MRUF2,MRUF3,MRUF4,
     2MRUF5,MRUF6,MRUF7,MRUF8,MRVI1,MRVI2,MRVI3,MRVI4,MRVI5,MRVI6,MRVI7,
     3MRVI8,MRVF1,MRVF2,MRVF3,MRVF4,MRVF5,MRVF6,MRVF7,MRVF8,MRCC1,MRCC2,
     4MRCC3,MRCC4,MRCC5,MRCC6,MRCC7,MRCC8,XK1,XK2,XK3,XK4,XK5,XK6,XKK7,
     5XKK8
C
      INTEGER DNC
      INTEGER DC,SIGAC,UNSFC,SIGFC,SGCSC,SCATC,SPNRC,ATTC
      INTEGER CSC
C
      DIMENSION XK1(3,20),XK2(3,20),XK3(3,20),XK4(3,20),XK5(3,20),
     1XK6(3,20),XK7(2,20),XK8(2,20),CSC(8),XKK7(3,20),XKK8(3,20)
      DIMENSION MRUI1(20),MRUI2(20),MRUI3(20),MRUI4(20),MRUI5(20
     2),MRUI6(20),MRUI7(20),MRUI8(20),MRUF1(20),MRUF2(20),MRUF3(20),MRUF
     34(20),MRUF5(20),MRUF6(20),MRUF7(20),MRUF8(20),MRVI1(20),MRVI2(20),
     4MRVI3(20),MRVI4(20),MRVI5(20),MRVI6(20),MRVI7(20),MRVI8(20),
     5MRVF1(20),MRVF2(20),MRVF3(20),MRVF4(20),MRVF5(20),MRVF6(20),MRVF7(
     620),MRVF8(20),MRCC1(20),MRCC2(20),MRCC3(20),MRCC4(20),MRCC5(20),
     7MRCC6(20),MRCC7(20),MRCC8(20)
C
      EQUIVALENCE(XK7(1,1),XKK7(1,1)),(XK8(1,1),XKK8(1,1))
C
      NAMELIST/INCDNC/CSC
C
C IF THE FIRST ELEMENT OF CSC .EQ. 1,DURING THE TRANSIENT D CHANGES
```

```
C
      NAMELIST/INDDNC/DC,SIGAC,UNSFC,SIGFC,SGCSC,SCATC,SPNRC,ATTC
      NAMELIST/INMRK1/MRK1,MRUI1,MRUF1,MRVI1,MRVF1,MRCC1,XK1
      NAMELIST/INMRK2/MRK2,MRUI2,MRUF2,MRVI2,MRVF2,MRCC2,XK2
      NAMELIST/INMRK3/MRK3,MRUI3,MRUF3,MRVI3,MRVF3,MRCC3,XK3
      NAMELIST/INMRK4/MRK4,MRUI4,MRUF4,MRVI4,MRVF4,MRCC4,XK4
      NAMELIST/INMRK5/MRK5,MRUI5,MRUF5,MRVI5,MRVF5,MRCC5,XK5
      NAMELIST/INMRK6/MRK6,MRUI6,MRUF6,MRVI6,MRVF6,MRCC6,XK6
      NAMELIST/INMRK7/MRK7,MRUI7,MRUF7,MRVI7,MRVF7,MRCC7,XK7
      NAMELIST/INMRK8/MRK8,MRUI8,MRUF8,MRVI8,MRVF8,MRCC8,XK8
C
      READ(5,INCDNC)
      READ(5,INDDNC)
      IF (DC.EQ.DNC) GO TO 714
      READ(5,INMRK1)
  714 IF (SIGAC.EQ.DNC) GO TO 715
      READ(5,INMRK2)
  715 IF (UNSFC.EQ.DNC) GO TO 716
      READ(5,INMRK3)
  716 IF (SIGFC.EQ.DNC) GO TO 717
      READ(5,INMRK4)
  717 IF (SGCSC.EQ.DNC) GO TO 718
      READ(5,INMRK5)
      READ(5,INMRK6)
  718 IF (SCATC.EQ.DNC) GO TO 719
      READ(5,INMRK7)
  719 IF (SPNRC.EQ.DNC) GO TO 720
      READ(5,INMRK8)
  720 CONTINUE
      RETURN
      END
      SUBROUTINE DATA3(DNC)
C
C THE END OF THE TRANSIENT
C
      COMMON/FOZ13/ND,NSIGA,NUNSF,NSCAT
```

```
      COMMON/OZDTA/ NCS ,NRK1,NRK2,NRK3,NRK4,NRK5,NRK6,NRK7,NRK8,NRUI1,
     1NRUI2,NRUI3,NRUI4,NRUI5,NRUI6,NRUI7,NRUI8,NRUF1,NRUF2,NRUF3,NRUF4,
     2NRUF5,NRUF6,NRUF7,NRUF8,NRVI1,NRVI2,NRVI3,NRVI4,NRVI5,NRVI6,NRVI7,
     3NRVI8,NRVF1,NRVF2,NRVF3,NRVF4,NRVF5,NRVF6,NRVF7,NRVF8,NRCC1,NRCC2,
     4NRCC3,NRCC4,NRCC5,NRCC6,NRCC7,NRCC8,XT1,XT2,XT3,XT4,XT5,XT6,XTT7,
     5XTT8
C
      INTEGER DNC
C
      DIMENSION XT1(3,20),XT2(3,20),XT3(3,20),XT4(3,20),XT5(3,20),
     1XT6(3,20),XT7(2,20),XT8(2,20),NCS(8),XTT7(3,20),XTT8(3,20)
      DIMENSION NRUI1(20),NRUI2(20),NRUI3(20),NRUI4(20),NRUI5(20
     2),NRUI6(20),NRUI7(20),NRUI8(20),NRUF1(20),NRUF2(20),NRUF3(20),NRUF
     34(20),NRUF5(20),NRUF6(20),NRUF7(20),NRUF8(20),NRVI1(20),NRVI2(20),
     4NRVI3(20),NRVI4(20),NRVI5(20),NRVI6(20),NRVI7(20),NRVI8(20),
     5NRVF1(20),NRVF2(20),NRVF3(20),NRVF4(20),NRVF5(20),NRVF6(20),NRVF7(
     620),NRVF8(20),NRCC1(20),NRCC2(20),NRCC3(20),NRCC4(20),NRCC5(20),
     7NRCC6(20),NRCC7(20),NRCC8(20)
C
      EQUIVALENCE(XT7(1,1),XTT7(1,1)),(XT8(1,1),XTT8(1,1))
C
C DATA RELIATED TO THE SECOND TRIAL FUNCTION IF NOT THE SAME AS COMPARED
C TO THE STEADY STATE ONE
C
      NAMELIST/INCS/NCS
      NAMELIST/INNCS/ND,NSIGA,NUNSF,NSCAT
      NAMELIST/INNRK1/NRK1,NRUI1,NRUF1,NRVI1,NRVF1,NRCC1,XT1
      NAMELIST/INNRK2/NRK2,NRUI2,NRUF2,NRVI2,NRVF2,NRCC2,XT2
      NAMELIST/INNRK3/NRK3,NRUI3,NRUF3,NRVI3,NRVF3,NRCC3,XT3
      NAMELIST/INNRK7/NRK7,NRUI7,NRUF7,NRVI7,NRVF7,NRCC7,XT7
C
      READ(5,INCS)
      READ(5,INNCS)
      IF (ND.EQ.DNC) GO TO 725
      READ(5,INNRK1)
  725 IF (NSIGA.EQ.DNC) GO TO 726
```

```
      READ(5,INNRK2)
  726 IF (NUNSF.EQ.DNC) GO TO 727
      READ(5,INNRK3)
  727 IF (NSCAT.EQ.DNC) GO TO 728
      READ(5,INNRK7)
  728 CONTINUE
      RETURN
      END
      SUBROUTINE STEP(MGLK,MDVIC,DNC,Y,SGCS,Z)
C
C STEP CHANGE AT THE BEGINNING OF THE TIME STEP
C
      COMMON/OZCTA/ISTPC,MSK,MSUI,MSUF,MSVI,MSVF,MSCC,XS
C
      DIMENSION MDVIC(32),MSK(8),MSUI(20,8),MSUF(20,8),MSVI(20,8),
     1MSVF(20,8),MSCC(20,8),XS(3,20,8),Y(3,47,39),SGCS(2,3,47,39),Z(2,
     247,39),ISTPC(8),MGLK(8)
C
      INTEGER DNC
C
 9000 FORMAT(7E11.5)
      DO 153 K=1,8
      MDEVC=MDVIC(K)
      MGL=MGLK(K)
      IF (ISTPC(K).EQ.DNC) GO TO 153
      IF (K.EQ.5) GO TO 853
      IF (K.EQ.6) GO TO 855
      IF (K.GT.6) GO TO 854
      READ(MDEVC,9000) Y
      REWIND MDEVC
      GO TO 855
  853 READ(MDEVC,9000) SGCS
      REWIND MDEVC
      GO TO 855
  854 READ(MDEVC,9000) Z
      REWIND MDEVC
```

```
855 MRR=MSK(K)
    DO 8000 LG=1,MGL
    DO 320 MR=1,MRR
    MUI=MSUI(MR,K)
    MUF=MSUF(MR,K)
    MVI=MSVI(MR,K)
    MVF=MSVF(MR,K)
    MCC=MSCC(MR,K)
    DO 320 MV=MVI,MVF
    DO 320 MU=MUI,MUF
    IF (K.EQ.5) GO TO 412
    IF (K.EQ.6) GO TO 414
    IF (K.GT.6) GO TO 415
    GO TO 416
412 SGCS(1,LG,MV,MU)=XS(LG,MCC,K)
    GO TO 320
414 SGCS(2,LG,MV,MU)=XS(LG,MCC,K)
    IF ((MR.LT.MRR).OR.(LG.LT.MGL)) GO TO 320
    WRITE(MDEVC,9000) SGCS
    REWIND MDEVC
    GO TO 153
415 Z(LG,MV,MU)=XS(LG,MCC,K)
    IF ((MR.LT.MRR).OR.(LG.LT.MGL)) GO TO 320
    WRITE(MDEVC,9000) Z
    REWIND MDEVC
    GO TO 153
416 Y(LG,MV,MU)=XS(LG,MCC,K)
320 CONTINUE
    IF (LG.LT.MGL) GO TO 8000
    WRITE(MDEVC,9000) Y
    REWIND MDEVC
8000 CONTINUE
153 CONTINUE
    RETURN
    END
    SUBROUTINE CHANGE(MGLK,MDVIC,DNC,Y,SGCS,Z,NCSCO)
```

```
C
C CHANGE- THE END OF THE TIME STEP-
C
      COMMON/OZDTA/CSC,MRK,MRUI,MRUF,MRVI,MRVF,MRCC,XC
C
      INTEGER CSC
      INTEGER DNC
C
      DIMENSION MDVIC(32),MRK(8),MRUI(20,8),MRUF(20,8),MRVI(20,8),
     1MRVF(20,8),MRCC(20,8),XC(3,20,8),Y(3,47,39),SGCS(2,3,47,39),
     2Z(2,47,39),NCSCO(8),CSC(8),MGLK(8)
C
 9000 FORMAT(7E11.5)
      DO 153 K=1,8
      MDEVC=MDVIC(K)
      MGL=MGLK(K)
      IF(CSC(K).EQ.DNC) GO TO 153
      IF (K.EQ.5) GO TO 853
      IF (K.EQ.6) GO TO 855
      IF (K.GT.6) GO TO 854
      READ(MDEVC,9000) Y
      REWIND MDEVC
      GO TO 855
  853 READ(MDEVC,9000) SGCS
      REWIND MDEVC
      GO TO 855
  854 READ(MDEVC,9000) Z
      REWIND MDEVC
  855 MRR=MRK(K)
      MDEVC=MDVIC(K+8)
      DO 8000 LG=1,MGL
      DO 320 MR=1,MRR
      MUI=MRUI(MR,K)
      MUF=MRUF(MR,K)
      MVI=MRVI(MR,K)
      MVF=MRVF(MR,K)
```

```
      MCC=MRCC(MR,K)                                                    OZAN0793
      DO 320 MV=MVI,MVF                                                 OZAN0794
      DO 320 MU=MUI,MUF                                                 OZAN0795
      IF (K.EQ.5) GO TO 412                                             OZAN0796
      IF (K.EQ.6) GO TO 414                                             OZAN0797
      IF (K.GT.6) GO TO 415                                             OZAN0798
      GO TO 416                                                         OZAN0799
  412 SGCS(1,LG,MV,MU)=XC(LG,MCC,K)                                     OZAN0800
      GO TO 320                                                         OZAN0801
  414 SGCS(2,LG,MV,MU)=XC(LG,MCC,K)                                     OZAN0802
      IF ((MR.LT.MFR).OR.(LG.LT.MGL)) GO TO 320                         OZAN0803
      WRITE(MDEVC,9000) SGCS                                            OZAN0804
      REWIND MDEVC                                                      OZAN0805
      GO TO 8000                                                        OZAN0806
  415 Z(LG,MV,MU)=XC(LG,MCC,K)                                          OZAN0807
      IF ((MR.LT.MFR).OR.(LG.LT.MGL)) GO TO 320                         OZAN0808
      WRITE(MDEVC,9000) Z                                               OZAN0809
      REWIND MDEVC                                                      OZAN0810
      GO TO 8000                                                        OZAN0811
  416 Y(LG,MV,MU)=XC(LG,MCC,K)                                          OZAN0812
  320 CONTINUE                                                          OZAN0813
      IF (LG.LT.MGL) GO TO 8000                                         OZAN0814
      WRITE(MDEVC,9000) Y                                               OZAN0815
      REWIND MDEVC                                                      OZAN0816
 8000 CONTINUE                                                          OZAN0817
      NCSCC(K)=CSC(K)                                                   OZAN0818
  153 CONTINUE                                                          OZAN0819
      RETURN                                                            OZAN0820
      END                                                               OZAN0821
      SUBROUTINE  THEEND(MGLK,MDVIC,DNC,Y,Z)                            OZAN0822
C                                                                       OZAN0823
C THE END OF THE TRANSIENT                                              OZAN0824
C                                                                       OZAN0825
      COMMON/OZDTA/NCS,NRK,NRUI,NRUF,NRVI,NRVF,NRCC,XT                  OZAN0826
C                                                                       OZAN0827
      DIMENSION MDVIC(32),NRK(8),NRUI(20,8),NRUF(20,8),NRVI(20,8),NRVF( OZAN0828
```

```
     120,8),NRCC(20,8),XT(3,20,8),Y(3,47,39),Z(2,47,39),NCS(8),MGLK(8)
C
      INTEGER DNC
C
 9000 FORMAT(7E11.5)
      DO 153 K=1,8
      IF ((K.EQ.4).OR.(K.EQ.5).OR.(K.EQ.6).OR.(K.EQ.8)) GO TO 153
      IF (NCS (K).EQ.DNC) GO TO 153
      MDEVC=MDVIC(K)
      MGL=MGLK(K)
      IF (K.EQ.7) GO TO 854
      READ(MDEVC,9000) Y
      REWIND MDEVC
      GO TO 855
  854 READ(MDEVC,9000) Z
      REWIND MDEVC
  855 MRR=NRK(K)
      MDEVC=MDVIC(K+16)
      DO 8000 LG=1,MGL
      DO 321 MR=1,MRR
      MUI=NRUI(MR,K)
      MUF=NRUF(MR,K)
      MVI=NRVI(MR,K)
      MVF=NRVF(MR,K)
      MCC=NRCC(MR,K)
      DO 321 MV=MVI,MVF
      DO 321 MU=MUI,MUF
      IF (K.NE.7) GO TO 856
      Z(LG,MV,MU)=XT(LG,MCC,K)
      IF((MR.LT.MRR).OR.(LG.LT.MGL)) GO TO 321
      WRITE(MDEVC,9000) Z
      REWIND MDEVC
      GO TO 153
  856 Y(LG,MV,MU)=XT(LG,MCC,K)
  321 CONTINUE
      IF (LG.LT.MGL) GO TO 8000
```

```
      WRITE(MDEVC,9000) Y
      REWIND MDEVC
 8000 CONTINUE
  153 CONTINUE
      RETURN
      END
      SUBROUTINE POISON(SIGA,OMEG,V1)
C
C  POISON THE REACTOR UNIFORMLY
C
      DIMENSION SIGA(3,47,39),V1(3)
C
 1000 FORMAT (7E11.5)
      READ(29,1000) SIGA
      REWIND 29
      DO 289 MG=1,3
      DO 289 MV=1,47
      DO 289 MU=1,39
      SIGA(MG,MV,MU)=SIGA(MG,MV,MU)+OMEG*V1(MG)
  289 CONTINUE
      WRITE(29,1000) SIGA
      REWIND 29
      RETURN
      END
      SUBROUTINE PASS(NCSCO,DNC,MOVIC,D,SGCS,SCAT)
C
C THE END OF THE  FIRST TIME STEP IS THE BEGINNING OF THE SECOND ONE(NATURALLY)
C
      DIMENSION NCSCO(8),MOVIC(32),D(3,47,39),SGCS(2,3,47,39),SCAT(2,47,
     139)
C
      INTEGER DNC
C
 9000 FORMAT(7E11.5)
      DO 153 K=1,8
      IF (NCSCO(K).EQ.DNC) GO TO 153
```

```
      MDEVC2=MDVIC(K+8)
      MDEVC1=MDVIC(K)
      IF(K.EQ.5) GO TO 605
      IF (K.EQ.6) GO TO 153
      IF (K.GT.6) GO TO 606
      READ(MDEVC2,9000) D
      REWIND MDEVC2
      WRITE(MDEVC1,9000) D
      REWIND MDEVC1
      GO TO 153
  605 READ(MDEVC2,9000) SGCS
      REWIND MDEVC2
      WRITE(MDEVC1,9000) SGCS
      REWIND MDEVC1
      GO TO 153
  606 READ(MDEVC2,9000) SCAT
      REWIND MDEVC2
      WRITE(MDEVC1,9000) SCAT
      REWIND MDEVC1
  153 CONTINUE
      RETURN
      END
      SUBROUTINE FILIZ1
C
C     THIS SUBROUTINE CALCULATES SOME OF THE COEFFICIENTS FOR THE FINAL POINT
C     KINETICS TYPE OF EQUATIONS(GENERATION TIME MATRIX AND LEAKAGE MATRIX)
C
C     "FILIZ" MEANS "NYMPH" IN TURKISH
C
      COMMON/OZO/SIGA,UNSF,SGCS,SCAT,PSI,W
      COMMON/OZ11/C,DNC,KSFCZ,SKOZN,NDPSI,NDW,HU,HV,R
      COMMON/OZ12/DC,SIGAC,UNSFC,SIGFC,SGCSC,SCATC,SFNRC,ATTC
      COMMON/FOZ11/LLL,LFINAL,KSREX,FLAP1,ALAP1,DIFF1,SKEF
      COMMON/FOZ12/ISD,ISSA,ISUF,ISSF,ISSG,ISST,ISSF,ISATT
      COMMON/FOZ13/ND,NSIGA,NUNSF,NSCAT
      COMMON/OZ2/NMODES,II,KK
```

```
      COMMON/OZ3/TMIN,TMAX
      COMMON/OZ2FZ1/V1
      COMMON/OZ3FZ1/GENTME
      COMMON/OZ4FZ1/LAPN,VLAPN
      COMMON/FCFA/COEF,MCOF
C
      DIMENSION PSI(3,48,40),W(3,48,40),SIGA(3,47,39),UNSF(3,47,39),SCAT
     1(2,47,39),COEF(3,47,39),HU(39),HV(47),R(40),V1(3),NDW(2),NDPSI(2),
     2SKEF(2),GENTME(2,2),LAPN(2,2),VLAPN(2,2),FLAP(2),ALAP(2),DIFFP(2),
     3SGCS(2,3,47,39),SF(2,2),SA(2,2)
C
      REAL LAPN
      INTEGER C,DNC
      INTEGER DC,SIGAC,UNSFC,SIGFC,SCATC,SGCSC,SPNRC,ATTC
C
 1000 FORMAT(7E11.5)
 2000 FORMAT(1P5E14.6)
  625 FORMAT (1H1,'GENERATION TIME MATRIX'/)
  626 FORMAT (1X,2(E15.8,3X)/(1X,2(E15.8,3X))//)
  627 FORMAT (/1X,'LEAKAGE MATRIX(INITIAL VALUE)'/)
  628 FORMAT (/1X,'LEAKAGE MATRIX (RAMP CHANGE SLOPE)'/)
 6291 FORMAT(/1X,'LEAKAGE INTEGRAL(S)'/)
 6292 FORMAT (/1X,'ABSORPTION INTEGRAL(S)'/)
 6293 FORMAT (/1X,'FISSION INTEGRAL(S)'/)
C
      IF (KSREX.EQ.1) GO TO 58
C
C CALCULATION OF THE GENERATION TIME MATRIX
C
      DO 2 I=1,II
      NN=NDW(I)
C
C NDW LIKE INPUT DEVICE NUMBER FOR W
C
      READ(NN,2000) W
      REWIND NN
```

```
      DO 2 K=1,KK
      NN=NDPSI(K)
C
C NDPSI LIKE INPUT DEVICE NUMBER FOR PSI
C
      READ(NN,2000) PSI
      REWIND NN
C
      CALL GTM(W,PSI,HU,HV,F,V1,GEN1)
C
    2 GENTME(I,K)=GEN1*1.5708
      WRITE(6,625)
      WRITE(6,626) ((GENTME(I,K),K=1,KK),I=1,II)
   58 CONTINUE
C
C CALCULATION OF THE LEAKAGE MATRIX
C
C AT THE BEGINNING OF THE TIME STEP
C
      TIME=TMIN
  108 DO 4 K=1,KK
      NN=NDPSI(K)
      READ(NN,2000) PSI
      REWIND NN
      IF (K.EQ.1) GO TO 102
      IF (ND.EQ.DNC) GO TO 102
C
C DIFFUSION COEFFICIENT ARRAY FOR THE SECOND TRIAL FUNCTION
C
      READ(28,1000) SIGA
      REWIND 28
      IF (KSPEX.EQ.1) GO TO 170
      GO TO 106
C
C DIFFUSION COEFFICIENT ARRAY FOR THE FIRST TRIAL FUNCTION
C
```

```
  102 READ(1,1000) SIGA
      REWIND 1
      IF (KSREX.EQ.1) GO TO 109
  106 IF (TIME.EQ.TMAX) GO TO 107
C
C DIFFUSION COEFFICIENT ARRAY AT THE BEGINNING OF THE TIME STEP
C
      READ(14,1000) UNSF
      REWIND 14
      GO TO 109
C
C D AT THE END OF THE TIME STEP
C
  107 READ(18,1000) UNSF
      REWIND 18
C
  109 CALL COF(KSREX,K,TIME,TMAX,LFINAL,ISD,DNC,ND,LLL,DC,TMIN,UNSF,SIGA
     1)
C
      IF (KSREX.EQ.0) GO TO 169
      IF (K.NE.1 ) GO TO 170
      READ(11,2000) W
      REWIND 11
C
  170 CALL FILIZO(W,PSI,SIGA,HU,HV,R,SUM25)
C
      DIFF=SUM25*3.1416
      DIFFP(K)=DIFF
  169 IF (K.EQ.1) GO TO 112
C
C SSKEF COMES OUT OF EXTERMINATOR 2 RUN OR ADJUSTED THROUGH OZAN AND IS THE KEFF
C FOR THE TRIAL FUNCTION IN QUESTION
C
      SSKEF=SKEF(K)
      IF (NSIGA.EQ.DNC) GO TO 114
      READ(29,1000) SIGA
```

```
      REWIND 29
      GO TC 714
  114 READ(2,1000) SIGA
      REWIND 2
  714 IF (NUNSF.EQ.DNC) GC TO 115
      READ(30,1000) UNSF
      REWIND 30
      GO TC 715
  115 READ(3,1000) UNSF
      REWIND 3
  715 IF (NSCAT.EQ.DNC) GO TO 171
      READ(31,1000) SCAT
      REWIND 31
      GO TO 171
  112 SSKEF=SKEF(K)
      READ(2,1000) SIGA
      REWIND 2
      READ(3,1000) UNSF
      REWIND 3
      READ(4,1000) SCAT
      REWIND 4
  171 DO 4 I=1,II
      IF ((KSREX.EQ.1).AND.(I.NE.1 )) GO TO 4
      IF (KSREX.EQ.1) GO TC 172
      NN=NDW(I)
      READ(NN,2000) W
      REWIND NN
  172 MCF1=1
      MCF2=1
      IF ((TIME.EQ.TMAX).AND.(UNSFC.EQ.DNC)) GC TO 62
C
      CALL FISS(W,PSI,UNSF,FL,HV,R,MCF1,SUM21)
C
      IF (KSREX.EQ.0) GO TC 61
      FLAP(K)=SUM21*1.5708
      IF (KSREX.EQ.1) GO TO 62
```

```
 61 SUM21=SUM21/SSKEF
    SF(I,K)=SUM21
    IF ((TIME.EQ.TMAX).AND.(SIGAC.EQ.DNC).AND.(SCATC.EQ.DNC)) GO TO 11
 62 CONTINUE
C
    CALL ABSP(W,PSI,SIGA,SCAT,HU,HV,R,MCF2,SUM22)
C
    SA(I,K)=SUM22
    IF (KSREX.EQ.0) GO TO 63
    ALAP(K)=SUM22*1.5708
    IF ((KSREX.EQ.1).AND.(K.EQ.KK)) GO TO 131
    IF (KSREX.EQ.1) GO TO 4
 63 IF(TIME.EQ.TMAX) GO TO 11
    LAPN(I,K)=(SF(I,K)+SA(I,K))*1.5708
    GO TO 4
 11 VLAPN(I,K)=((SF(I,K)+SA(I,K))*1.5708-LAPN(I,K))/(TMAX-TMIN)
  4 CONTINUE
    IF (TIME.EQ.TMAX) GO TO 10
    WRITE(6,627)
    WRITE(6,626) ((LAPN(I,K),K=1,KK),I=1,II)
    IF (DC.EQ.DNC) GO TO 12
C
C   AT TMAX
C
    TIME=TMAX
    GO TO 108
 10 WRITE(6,628)
    WRITE(6,626) ((VLAPN(I,K),K=1,KK),I=1,II)
    GO TO 14
 12 DO 13 I=1,II
    DO 13 K=1,KK
 13 VLAPN(I,K)=0.
    GO TO 14
131 DIFF1=DIFFP(1)
    FLAP1=FLAP(1)
    ALAP1=ALAP(1)
```

```
      WRITE(6,6291)
      WRITE(6,626)(DIFFP(I),I=1,II)
      WRITE(6,6293)
      WRITE(6,626)(FLAP(I),I=1,II)
      WRITE(6,6292)
      WRITE(6,626)(ALAP(I),I=1,II)
      DO 24 K=1,KK
   24 SKEF(K)=FLAP(K)/(+DIFFP(K)-ALAP(K))
   14 CONTINUE
      RETURN
      END
      SUBROUTINE GTM(W,PSI,HU,HV,R,V1,GEN1)
C
C GENERATION TIME MATRIX
C
      DIMENSION W(3,48,40),PSI(3,48,40),HU(39),HV(47),R(40),V1(3)
C
      GEN1=0.
      DO 3 MG=1,3
      SUM1=0.
      DO 1 MV=2,47
      MU=1
      GEN=W(MG,MV,MU)*PSI(MG,MV,MU)*(HV(MV-1)+HV(MV))*HU(MU)*(R(MU)+HU(M
     1U)/4)
      SUM1=SUM1+GEN
      DO 1 MU=2,39
      GEN=W(MG,MV,MU)*PSI(MG,MV,MU)*
     1(HV(MV-1)+HV(MV))*(HU(MU-1)*(R(MU)-HU(MU-1)/4)+HU(MU)*
     2(R(MU)+HU(MU)/4))
      SUM1=SUM1+GEN
    1 CONTINUE
    3 GEN1=SUM1*V1(MG)+GEN1
      RETURN
      END
      SUBROUTINE CCF(KSREX,K,TIME,TMAX,LFINAL,ISD,DNC,NC,LLL,DC,TMIN,D,
     1DPSI)
```

```
C
      COMMON/FCFA/COEF,MCOF
C
      DIMENSION D(3,47,39),DPSI(3,47,39),COEF(3,47,39)
C
      INTEGER DNC
C
      MCOF=1
      IF (KSREX.EQ.1) GO TO 123
      IF (K.EQ.1) GO TO 120
      IF (TIME.EQ.TMAX) GO TO 121
      IF (LFINAL.EQ.1) GO TO 122
  135 DO 130 MV=1,47
      DO 130 MU=1,39
      DO 130 IK=1,3
      COEF(IK,MV,MU)=D(IK,MV,MU)/DPSI(IK,MV,MU)
  130 CONTINUE
      RETURN
  122 IF ((ISD.EQ.DNC).AND.(ND.EQ.DNC)) GO TO 123
      GO TO 135
  121 IF (LFINAL.EQ.1) GO TO 123
      IF (LLL.EQ.LFINAL) GO TO 123
      GO TO 135
  120 IF (TIME.NE.TMAX) GO TO 124
      IF ((ISD.EQ.DNC).AND.(DC.EQ.DNC).AND.(LLL.EQ.1)) GO TO 123
      GO TO 135
  124 IF ((ISD.EQ.DNC).AND.(TMIN.EQ.0.)) GO TO 123
      GO TO 135
  123 MCOF=0
      RETURN
      END
      SUBROUTINE FILIZO(W,PSI,D,HU,HV,R,SUM25)
C
C EQUIVALENT OF THE LEAKAGE TERM FOR THE TRIAL FUNCTION IN QUESTION
C
      DIMENSION PSI(3,48,40),W(3,48,40),D(3,47,39),HU(39),HV(47),
```

```
     1R(40)
C
      REAL LAP
C
      SUM25=0.
      DO 5 MG=1,3
      DO 5 MV=2,47
      HV1=HV(MV-1)
      HV2=HV(MV)
      MU=1
      HU2=HU(MU)
      HR2=R(MU)+HU(MU)/4
      HR4=R(MU)+HU(MU)/2
      LAP=W(MG,MV,MU)*((D(MG,MV-1,MU)*HV1+D(MG,MV,MU)*HV2)*HR4*PSI(MG,
     1MV,MU+1)/HU2+(D(MG,MV-1,MU)*HU2*HR2)*PSI(MG,MV-1,MU)/HV1+(D(MG,MV,
     2MU)*HU2*HR2)*PSI (MG,MV+1,MU)/HV2-((D(MG,MV-1,MU)*HV1+D(MG,MV,MU)
     3*HV2)*HR4/HU2+(D(MG,MV-1,MU)*HU2*HR2)/HV1+(D(MG,MV,MU)*HU2*HR2)/HV
     42)*PSI(MG,MV,MU))
      SUM25=SUM25+LAP
      DO 5 MU=2,39
      HU1=HU(MU-1)
      HU2=HU(MU)
      HR1=R(MU)-HU(MU-1)/4
      HR2=R(MU)+HU(MU)/4
      HR3=R(MU)-HU(MU-1)/2
      HR4=R(MU)+HU(MU)/2
      LAP=W(MG,MV,MU)*((D(MG,MV-1,MU)*HV1+D(MG,MV,MU)*HV2)*HR4*PSI(MG,
     1MV,MU+1)/HU2+(D(MG,MV-1,MU)*HU2*HR2+D(MG,MV-1,MU-1)*HU1*HR1)*
     2PSI(MG,MV-1,MU)/HV1+(D(MG,MV-1,MU-1)*HV1+D(MG,MV,MU-1)*HV2)*
     3HR3*PSI(MG,MV,MU-1)/HU1+(D(MG,MV,MU-1)*HU1*HR1+D(MG,MV,MU)*HU2*
     4HR2)*PSI(MG,MV+1,MU)/HV2-((D(MG,MV-1,MU)*HV1+D(MG,MV,MU)*HV2)*
     5HR4/HU2+(D(MG,MV-1,MU)*HU2*HR2+D(MG,MV-1,MU-1)*HU1*HR1)/HV1+
     6(D(MG,MV-1,MU-1)*HV1+D(MG,MV,MU-1)*HV2)*HR3/HU1+(D(MG,MV,MU-1)*
     7HU1*HR1+D(MG,MV,MU)*HU2*HR2)/HV2)*PSI(MG,MV,MU))
      SUM25=SUM25+LAP
    5 CONTINUE
```

```
      RETURN
      END
      SUBROUTINE FISS(W,PSI,UNSF,HU,HV,R,MCF1,SUM21)
C
C FISS LIKE FISSION(PRODUCTION) INTEGRATED OVER THE REACTOR
C VOLUME AFTER BEING WEIGHTED
C
      COMMON/FCFA/COEF,MCOF
C
      DIMENSION W(3,48,40),PSI(3,48,40),UNSF(3,47,39),HU(39),HV(47),
     1R(40),COEF(3,47,39)
C
      SUM21=0.
      IF ((MCF1.EQ.1).AND.(MCOF.EQ.1)) GO TO 14
      CF11=1.
      CF12=1.
      CF13=1.
      CF14=1.
   14 DO 7 MV=5,24
      HV1=HV(MV-1)
      HV2=HV(MV)
      DO 7 MU=3,17
      W1=W(1,MV,MU)
      PI1=PSI(1,MV,MU)
      PI2=PSI(2,MV,MU)
      PI3=PSI(3,MV,MU)
      UF11=UNSF(1,MV-1,MU-1)
      UF12=UNSF(1,MV,MU-1)
      UF13=UNSF(1,MV-1,MU)
      UF14=UNSF(1,MV,MU)
      UF21=UNSF(2,MV-1,MU-1)
      UF22=UNSF(2,MV,MU-1)
      UF23=UNSF(2,MV-1,MU)
      UF24=UNSF(2,MV,MU)
      UF31=UNSF(3,MV-1,MU-1)
      UF32=UNSF(3,MV,MU-1)
```

```
      UF33=UNSF(3,MV-1,MU)
      UF34=UNSF(3,MV,MU)
      HR1=(R(MU)-HU(MU-1)/4)*HU(MU-1)
      HR2=(R(MU)+HU(MU)/4)*HU(MU)
      IF ((MCF1.EQ.0).OR.(MCOF.EQ.0)) GO TO 16
      CF11=COEF(1,MV-1,MU-1)
      CF12=COEF(1,MV,MU-1)
      CF13=COEF(1,MV-1,MU)
      CF14=COEF(1,MV,MU)
   16 FIS=-W1*((((UF11*CF11*HV1+UF12*CF12*HV2)*HR1+(UF13*CF13*
     1HV1+UF14*CF14*HV2)*HR2)*PI1+((UF21*CF11*HV1+UF22*CF12
     2*HV2)*HR1+(UF23*CF13*HV1+UF24*CF14*HV2)*HR2)*PI2+
     3((UF31*CF11*HV1+UF32*CF12*HV2)*HR1+(UF33*CF13*HV1+
     4UF34*CF14*HV2)*HR2)*PI3)
      SUM21=SUM21+FIS
    7 CONTINUE
      RETURN
      END
      SUBROUTINE ABSP(W,PSI,SIGA,SCAT,HU,HV,R,MCF2,SUM22)
C
C ABSP LIKE ABSORPTION(AND ALSO SCATTERING)INTEGRATED OVER THE
C REACTOR VOLUME AFTER BEING WEIGHTED
C
      COMMON/FCFA/COEF,MCOF
C
      DIMENSION W(3,48,40),PSI(3,48,40),SIGA(3,47,39),SCAT(2,47,39),
     1HU(39),HV(47),R(40),COEF(3,47,39)
C
      SUM22=0.
      IF ((MCF2.EQ.1).AND.(MCOF.EQ.1)) GO TO 16
      CF11=1.
      CF12=1.
      CF13=1.
      CF14=1.
      CF21=1.
      CF22=1.
```

```
      CF23=1.
      CF24=1.
      CF31=1.
      CF32=1.
      CF33=1.
      CF34=1.
   16 DO 6 MV=2,47
      HV1=HV(MV-1)
      HV2=HV(MV)
      MU=1
      W1=W(1,MV,MU)
      W2=W(2,MV,MU)
      W3=W(3,MV,MU)
      PI1=PSI(1,MV,MU)
      PI2=PSI(2,MV,MU)
      PI3=PSI(3,MV,MU)
      SA13=SIGA(1,MV-1,MU)
      SA14=SIGA(1,MV,MU)
      SA23=SIGA(2,MV-1,MU)
      SA24=SIGA(2,MV,MU)
      SA33=SIGA(3,MV-1,MU)
      SA34=SIGA(3,MV,MU)
      ST13=SCAT(1,MV-1,MU)
      ST14=SCAT(1,MV,MU)
      ST23=SCAT(2,MV-1,MU)
      ST24=SCAT(2,MV,MU)
      HR2=(R(MU)+HU(MU)/4)*HU(MU)
      IF ((MCF2.EQ.0).OR.(MCOF.EQ.0)) GO TO 18
      CF13=COEF(1,MV-1,MU)
      CF14=COEF(1,MV,MU)
      CF23=COEF(2,MV-1,MU)
      CF24=COEF(2,MV,MU)
      CF33=COEF(3,MV-1,MU)
      CF34=COEF(3,MV,MU)
   18 ASB=(W1*((SA13+ST13)*CF13*HV1+(SA14+ST14)*CF14*HV2)*PI1+
     1W2*(-(ST13*CF23*HV1+ST14*CF24*HV2)*PI1+((SA23+ST23)*CF23*
```

```
     2HV1+(SA24+ST24)*CF24*HV2)*PI2)+W3*(-(ST23*CF33*HV1+
     3ST24*CF34*HV2)*PI2+(SA33*CF33*HV1+SA34*CF34*HV2)*
     4PI3))*HR2
      SUM22=SUM22+ASB
      DO 6 MU=2,39
      W1=W(1,MV,MU)
      W2=W(2,MV,MU)
      W3=W(3,MV,MU)
      PI1=PSI(1,MV,MU)
      PI2=PSI(2,MV,MU)
      PI3=PSI(3,MV,MU)
      SA13=SIGA(1,MV-1,MU)
      SA14=SIGA(1,MV,MU)
      SA23=SIGA(2,MV-1,MU)
      SA24=SIGA(2,MV,MU)
      SA33=SIGA(3,MV-1,MU)
      SA34=SIGA(3,MV,MU)
      ST13=SCAT(1,MV-1,MU)
      ST14=SCAT(1,MV,MU)
      ST23=SCAT(2,MV-1,MU)
      ST24=SCAT(2,MV,MU)
      HR2=(R(MU)+HU(MU)/4)*HU(MU)
      SA11=SIGA(1,MV-1,MU-1)
      SA12=SIGA(1,MV,MU-1)
      SA21=SIGA(2,MV-1,MU-1)
      SA22=SIGA(2,MV,MU-1)
      SA31=SIGA(3,MV-1,MU-1)
      SA32=SIGA(3,MV,MU-1)
      ST11=SCAT(1,MV-1,MU-1)
      ST12=SCAT(1,MV,MU-1)
      ST21=SCAT(2,MV-1,MU-1)
      ST22=SCAT(2,MV,MU-1)
      HR1=(R(MU)-HU(MU-1)/4)*HU(MU-1)
      IF ((MCF2.EQ.0).OR.(MCOF.EQ.0)) GO TO 20
      CF13=COEF(1,MV-1,MU)
      CF14=COEF(1,MV,MU)
```

```
      CF23=COEF(2,MV-1,MU)
      CF24=COEF(2,MV,MU)
      CF33=COEF(3,MV-1,MU)
      CF34=COEF(3,MV,MU)
      CF11=COEF(1,MV-1,MU-1)
      CF12=COEF(1,MV,MU-1)
      CF21=COEF(2,MV-1,MU-1)
      CF22=COEF(2,MV,MU-1)
      CF31=COEF(3,MV-1,MU-1)
      CF32=COEF(3,MV,MU-1)
   20 ASB=W1*(((SA11+ST11)*CF11*HV1+(SA12+ST12)*CF12*HV2)*HR1+((SA13+ST1
     13)*CF13*HV1+(SA14+ST14)*CF14*HV2)*HR2)*PI1+W2*(-((ST11*CF21*HV1+ST
     212*CF22*HV2)*HR1+(ST13*CF23*HV1+ST14*CF24*HV2)*HR2)*PI1+(((SA21+ST
     321)*CF21*HV1+(SA22+ST22)*CF22*HV2)*HR1+((SA23+ST23)*CF23*HV1+(SA24
     3+ST24)*CF24*HV2)*HR2)*PI2)+W3*(-((ST21*CF31*HV1+ST22*CF32*HV2)*HR1
     4+(ST23*CF33*HV1+ST24*CF34*HV2)*HR2)*PI2+((SA31*CF31*HV1+SA32*CF32*
     5HV2)*HR1+(SA33*CF33*HV1+SA34*CF34*HV2)*HR2)*PI3)
      SUM22=SUM22+ASB
    6 CONTINUE
      RETURN
      END
      SUBROUTINE FILIZ2
C
C FISSION MATRIX AND ABSORPTION MATRIX
C
      COMMON/OZO/SIGA,UNSF,SGCS,SCAT,PSI,W
      COMMON/OZ11/C,DNC,KSRCZ,SKOZN,NDPSI,NDW,HU,HV,R
      COMMON/OZ12/EC,SIGAC,UNSFC,SIGFC,SGCSC,SCATC,SPNRC,ATTC
      COMMON/OZ2/NMODES,II,KK
      COMMON/OZ3/TMIN,TMAX
      COMMON/OZ4/NBETA1,NBETA2,NBETA,NBET1
      COMMON/OZFZ2/BETA,E,FMAR,VFMAR,BETR,VBETR,BEC11,BEC21
      COMMON/F2F4/WSC,JNPC
C
      DIMENSION PSI(3,48,40),W(3,48,40),SIGA(3,47,39),UNSF(3,47,39),
     1SCAT(2,47,39),HU(39),HV(47),R(40),BETA(6),NDW(2),NDPSI(2),
```

```
     1BEC11(2,2,6),BEC21(2,2,6),BETR(2,2),VBETR(2,2),FMAR(2,2),VFMAR(2,2
     2),SGCS(2,3,47,39),SF(2,2),SA(2,2),WSC(2)
C
      INTEGER C,DNC
      INTEGER DC,SIGAC,UNSFC,SIGFC,SCATC,SGCSC,SPNRC,ATTC
C
C     CALCULATION OF FMAR -VT*(OMBA*KI*NU*SIGMAFT-A)*PSI(MATRIX)INTEGRATED OVER
C     THE REACTOR VOLUME-AND CALCULATION OF BEC11 AND BEC21(J=1,6)
C
 1000 FORMAT(7E11.5)
 2000 FORMAT(1P5E14.6)
 2001 FORMAT (1X,8E12.5/(1X,8E12.5))
  626 FORMAT (1X,2(E15.8,3X)/(1X,2(E15.8,3X))//)
  629 FORMAT(/1X,'FISSION MINUS ABSORPTION MATRIX(INITIAL VALUE)'/)
  630 FORMAT (/1X,'FISSION MINUS ABSORPTION MATRIX(RAMP CHANGE SLOPE)'/)
  631 FORMAT (/1X,'DELAYED NEUTRON FRACTION MATRICES'/)
 6311 FORMAT (/1X,'DELAYED NEUTRON FRACTIONS'/)
  632 FORMAT (12X,I2,3(26X,I2))
 6321 FORMAT (1X,4(2(E12.5,1X),2X))
 6322 FORMAT (/1X,'RAMP CHANGE SLOPE OF THE DELAYED NEUTRON FRACTION MAT
     1RICES'/)
 6323 FORMAT (/1X,'RAMP CHANGE SLOPE OF THE DELAYED NEUTRON FRACTIONS'/)
  633 FORMAT(/1X,'PRODUCTION TERM WHICH WILL DIVIDE ALL THE MATRIX ELEME
     1NTS'/)
C
C     AT THE BEGINNING OF THE TIME STEP
C
      MCF1=0
      MCF2=0
      TIME=TMIN
      READ(15,1000) SIGA
      REWIND 15
      READ(16,1000) UNSF
      REWIND 16
      READ(22,1000) SCAT
      REWIND 22
```

```
  158 DO 121 I=1,II
      NN=NDW(I)
      READ(NN,2000) W
      REWIND NN
      IF((NMODES.EQ.1).OR.(TIME.EQ.TMAX).OR.(JNPC.EQ.0)) GO TO 159
      WSC(I)=0.
C
      CALL WCOEF(I,W,HU,HV,F,WSC)
C
      WSC(I)=WSC(I)*1.5708
  159 DO 121 K=1,KK
      NN=NDPSI(K)
      READ(NN,2000) PSI
      REWIND NN
      IF((TIME.EQ.TMAX).AND.(UNSFC.EQ.DNC)) GO TO 56
C
      CALL FISS(W,PSI,UNSF,HU,HV,R,MCF1,SUM61)
C
      SF(I,K)=-SUM61/SKOZN
      IF ((TIME.EQ.TMAX).AND.(SIGAC.EQ.DNC).AND.(SCATC.EQ.DNC))
     1GO TO 42
   56 CONTINUE
C
      CALL ABSP(W,PSI,SIGA,SCAT,HU,HV,R,MCF2,SUM62)
C
      SA(I,K)=-SUM62
  393 IF (TIME.EQ.TMAX) GO TO 42
      FMAR(I,K)=(SF(I,K)+SA(I,K))*1.5708
      BETR(I,K)=SF(I,K)*1.5708
      IF ((I.EQ.1).AND.(K.EQ.1)) GO TO 591
      GO TO 592
  591 E=BETR(I,K)
      WRITE(6,633)
      WRITE(6,626) E
  592 CONTINUE
C
```

```
C DELAYED NEUTRON FRACTION MATRIX
C
      DO 120 J=1,NBETA1
  120 BEC11(I,K,J)=BETA(J)*BETR(I,K)
      GO TO 121
   42 IF ((SIGAC.EQ.DNC).AND.(SCATC.EQ.DNC)) GO TO 421
      VFMAR(I,K)=((SF(I,K)+SA(I,K))*1.5708-FMAR(I,K))/(TMAX-TMIN)
      GO TO 422
  421 VFMAR(I,K)=0.
  422 IF (UNSFC.EQ.DNC) GO TO 125
      VBETR(I,K)=(SF(I,K)*1.5708-BETR(I,K))/(TMAX-TMIN)
      DO 63 J=1,NBETA1
   63 BEC21(I,K,J)=BETA(J)*VBETR(I,K)
      GO TO 121
  125 DO 126 J=1,NBETA1
  126 BEC21(I,K,J)=0.
  121 CONTINUE
      IF (TIME.EQ.TMAX) GO TO 64
      WRITE(6,629)
      WRITE(6,626) ((FMAR(I,K),K=1,KK),I=1,II)
      IF (NMODES.EQ.1) GO TO 6327
      WRITE(6,631)
      WRITE(6,632) (J,J=1,4)
      DO 7323 I=1,II
 7323 WRITE(6,6321) (((BEC11(I,K,J),K=1,KK),J=1,4))
      WRITE(6,632) (J,J=5,6)
      DO 6324 I=1,II
 6324 WRITE(6,6321) (((BEC11(I,K,J),K=1,KK),J=5,NBETA1))
      GO TO 6328
 6327 WRITE(6,6311)
      WRITE(6,2001) ((((BEC11(I,K,J),I=1,II),K=1,KK),J=1,NBETA1))
 6328 IF ((SIGAC.EQ.DNC). AND.(UNSFC.EQ.DNC).AND.(SCATC.EQ.DNC))
     1GO TO 43
C
C     AT TMAX
C
```

```
      TIME=TMAX
      IF (SIGAC.EQ.DNC) GO TO 164
      READ(19,1000) SIGA
      REWIND 19
  164 IF (UNSFC.EQ.DNC) GO TO 168
      READ(20,1000) UNSF
      REWIND 20
  168 IF (SCATC.EQ.DNC) GO TO 172
      READ(23,1000) SCAT
      REWIND 23
  172 CONTINUE
      GO TO 158
   64 WRITE(6,630)
      WRITE(6,626) ((VFMAR(I,K),K=1,KK),I=1,II)
      IF (NMODES.EQ.1) GO TO 6329
      WRITE(6,6322)
      WRITE(6,632) (J,J=1,4)
      DO 6325 I=1,II
 6325 WRITE(6,6321) (((BEC21(I,K,J),K=1,KK),J=1,4))
      WRITE(6,632) (J,J=5,6)
      DO 6326 I=1,II
 6326 WRITE(6,6321) (((BEC21(I,K,J),K=1,KK),J=5,NBETA1))
      GO TO 6330
 6329 WRITE(6,6323)
      WRITE(6,2001) ((((BEC21(I,K,J),I=1,II),K=1,KK),J=1,NBETA1))
 6330 CONTINUE
      GO TO 45
   43 DO 44 I=1,II
      DO 44 K=1,KK
      VFMAR(I,K)=0.
      DO 44 J=1,NBETA1
   44 BEC21(I,K,J)=0.
   45 CONTINUE
      RETURN
      END
      SUBROUTINE WCOEF(I,W,HU,HV,R,WSC)
```

```
C
C INTEGRATE THE WEIGHTING FUNCTIONS OVER THE REACTOR VOLUME-FIRST GROUP ONLY-
C
      DIMENSION W(3,48,40),HU(39),HV(47),R(40),WSC(2)
C
      SUM=0.
      MG=1
      DO 3 MV=2,47
      MU=1
      GE=W(MG,MV,MU)*(HV(MV-1)+HV(MV))*HU(MU)*(R(MU)+HU(MU)/4)
      SUM=SUM+GE
      DO 3 MU=2,39
      GE=W(MG,MV,MU)*(HV(MV-1)+HV(MV))*(HU(MU-1)*(R(MU)-HU(MU-1)/4)+
     1HU(MU)*(R(MU)+HU(MU)/4))
      SUM=SUM+GE
    3 CONTINUE
      WSC(I)=SUM
      RETURN
      END
      SUBROUTINE FILIZ3
C
C PROMPT AND DELAYED PHOTONEUTRONS
C THIS SUBROUTINE IS CALLED IF IT IS BELIEVED THAT THE PHOTONEUTRONS ARE NOT UN
C IMPORTANT IN THE TRANSIENT STUDIED(COEFIC.NE.0.)
C
      COMMON/OZ0/SIGA,UNSF,SGCS,SCAT,PSI,W
      COMMON/OZ11/C,DNC,KSFCZ,SKOZN,NDPSI,NDW,HU,HV,R
      COMMON/OZ12/DC,SIGAC,UNSFC,SIGFC,SGCSC,SCATC,SFNRC,ATTC
      COMMON/OZ2/NMODES,II,KK
      COMMON/OZ3/TMIN,TMAX
      COMMON/OZ4/NBETA1,NBETA2,NBETA,NBET1
      COMMON/OZ1FZ3/NZRO,COEFIC,S1,YIEL,YIEJ,MRUI,MRUF,MRVI,MRVF,ATT
      COMMON/OZ2FZ3/PHPR,VPHPR,DPPR,VDPPR,BEC12,BEC22
C
      REAL NZRO
      INTEGER C,DNC
```

```
      INTEGER DC,SIGAC,UNSFC,SIGFC,SCATC,SGCSC,SPNRC,ATTC
C
      DIMENSION PSI(3,48,40),W(3,48,40),SGCS(2,3,47,39),UNSF(3,47,39),
     1ATT(2,10),AT(10),SCAT(2,47,39),HU(39),HV(47),R(40),MRUI(10),
     2MRUF(10),MRVI(10),MRVF(10),YIEL(2),YIEJ(9),NDW(2),NDPSI(2),
     3PHPR(2,2),VPHPR(2,2),DPPR(2,2),VDPPR(2,2),BEC12(2,2,9),BEC22(2,
     42,9),BDN(2,2),PHP1(2,2),DPP1(2),SUM4IL(2,10,2),S1(2,10),SIGA(3,47,
     539),SUM41(2),SUM42(2)
C
 1000 FORMAT(7E11.5)
 2000 FORMAT(1P5E14.6)
 2001 FORMAT (1X,8E12.5/(1X,8E12.5))
  626 FORMAT (1X,2(E15.8,3X)/(1X,2(E15.8,3X))//)
  634 FORMAT (/1X,'PROMPT PHOTON PRODUCTION MATRIX'/)
  635 FORMAT (/1X,'DELAYED PHOTON PRODUCTION MATRIX'/)
  636 FORMAT(/1X,'PROMPT PHOTONEUTRON PRODUCTION MATRIX(INITIAL VALUE)'/
     1)
  637 FORMAT (/1X,'DELAYED PHOTONEUTRON PRODUCTION MATRIX(INITIAL VALUE)
     1'/)
 6371 FORMAT (/1X,'DELAYED PHOTONEUTRON FRACTIONS'/)
  638 FORMAT (/1X,'PROMPT PHOTONEUTRON PRODUCTION MATRIX(RAMP CHANGE SLO
     1PE)'/)
  639 FORMAT (/1X,'DELAYED PHOTONEUTRON PRODUCTION MATRIX(RAMP CHANGE SL
     1OPE)'/)
  640 FORMAT (/1X,'DELAYED PHOTONEUTRON FRACTION MATRICES'/)
  632 FORMAT (12X,I2,3(26X,I2))
 6321 FORMAT (1X,4(2(E12.5,1X),2X))
  643 FORMAT (/1X,'RAMP CHANGE SLOPE OF THE DELAYED PHOTONEUTRON FRACTIO
     1N MATRICES'/)
 6431 FORMAT (/1X,'RAMP CHANGE SLOPE OF THE DELAYED PHOTONEUTRON FRACTIO
     1NS'/)
C
C  AT TMIN
C
      MTI=1
      TIME=TMIN
```

```
      READ(24,1000) SGCS
      REWIND 24
C
C UNSF ; THE FISSION CROSS SECTION ARRAY
C
      READ(17,1000) UNSF
      REWIND 17
C
C THE PHOTONEUTRON REACTION CROSS SECTION ARRAY
C
      READ(26,1000) SCAT
      REWIND 26
   27 CONTINUE
      IF ((TIME.EQ.TMAX).AND.(SGCSC.EQ.DNC).AND.(SIGFC.EQ.DNC)) GO TO
     1291
      DO 2956 K=1,KK
      DO 2955 L=1,2
 2955 PHP1(K,L)=0.
      DPP1(K)=0.
      NN=NDPSI(K)
      READ(NN,2000) PSI
      REWIND NN
      IF ((TIME.EQ.TMAX).AND.(SGCSC.EQ.DNC)) GO TO 290
C
      CALL PPN1(K,PSI,SGCS,HU,HV,R,PHP1)
C
      IF ((TIME .EQ.TMAX).AND.(SIFC.EQ.DNC)) GO TO 291
C
  290 CALL DPN1(PSI,UNSF,HU,HV,R,SUM8)
C
      DPP1(K)=SUM8*1.5708
      IF (KSROZ.EQ.1) GO TO 291
      DPP1(K)=DPP1(K)/SKOZN
 2956 CONTINUE
  291 CONTINUE
      WRITE(6,634)
```

```
      WRITE(6,626) ((PHP1(K,L),L=1,2),K=1,KK)
      WRITE(6,635)
      WRITE(6,626) (DPP1(K),K=1,KK)
      IF ((TIME.EQ.TMAX ).AND.(ATTC.EQ.DNC)) GO TO 7215
      DO 215 MR=1,10
  215 AT(MR)=ATT(MTI,MR)
 7215 CONTINUE
      DO 34 I=1,II
      NN=NDW(I)
      READ(NN,2000) W
      REWIND NN
C
C     INTEGRATE OVER THE D2O REFLECTOR WITH APPROXIMATE ATTENUATION FACTORS
C
      DO 308 K=1,KK
  308 SUM41(K)=0.
      SUM91=0.
      DO 33 MR=1,10
      DO 309 K=1,KK
  309 SUM42(K)=0.
      SUM92=0.
      MUI=MRUI(MR)
      MUF=MRUF(MR)
      MVI=MRVI(MR)
      MVF=MRVF(MR)
      DO 311 L=1,2
      IF ((SPNRC.EQ.DNC).AND.(TIME.EQ.TMAX)) GO TO 310
      SUM4=0.
C
      CALL PDN2(L,MUI,MUF,MVI,MVF,W,SCAT,HU,HV,R,SUM4)
C
      SUM4IL(L,MR,I)=SUM4
      S1(L,MR)=SUM4IL(L,MR,1)
  310 SUM92=SUM4IL(L,MR,I)*YIEL(L)+SUM92
      DO 311 K=1,KK
      SUM42(K)=SUM4IL(L,MR,I)*PHP1(K,L)+SUM42(K)
```

```
  311 CONTINUE
      SUM91=SUM92*AT(MR)+SUM91
      DO 33 K=1,KK
      SUM41(K)=SUM42(K)*AT(MR)+SUM41(K)
   33 CONTINUE
      DO 34 K=1,KK
      IF (TIME.EQ.TMAX) GO TO 36
C
C     PHPR LIKE PROMPT PHOTONEUTRON PRODUCTION OVER THE REACTOR VOLUME
C
      PHPR(I,K)=SUM41(K)*1.5708*COEFIC
C
C     DPPR LIKE DELAYED PHOTONEUTRON PRODUCTION OVER THE REACTOR VOLUME
C
      DPPR(I,K)=SUM91*NZRO*1.5708*DPP1(K)*COEFIC
      IF (KSROZ.EQ.1) GO TO 35
      GO TO 34
   36 IF ((SGCSC.EQ.DNC).AND.(SPNRC.EQ.DNC )) GO TO 361
      VPHPR(I,K)=(SUM41(K)*1.5708*COEFIC-PHPR(I,K))/(TMAX-TMIN)
  361 IF ((SGCSC.EQ.DNC).AND.(SIGFC.EQ.DNC)) GO TO 34
      VDPPR(I,K)=(SUM91*NZRO*1.5708-DPPR(I,K))/(TMAX-TMIN)
      DO 88 J=1,NBETA2
   88 BEC22(I,K,J)=YIEJ(J)*VDPPR(I,K)
   34 CONTINUE
      IF (TIME.EQ.TMAX) GO TO 89
   35 WRITE(6,636)
      WRITE(6,626) ((PHPR(I,K),K=1,KK),I=1,II)
      WRITE(6,637)
      WRITE(6,626) ((DPPR(I,K),K=1,KK),I=1,II)
      IF (KSROZ.EQ.1) GO TO 391
C
C SINCE THE SUMMATION OF YIEJ(J) OVER J IS 1,DPPR(I,K) IS NATURALLY
C THE TOTAL DELAYED PHOTONEUTRON FRACTION MATRIX
C
      DO 85 I=1,II
      DO 85 K=1,KK
```

```
C
C     CALCULATION OF BEC12 AND BEC22 (J=7,15)
C
      DO 85 J=1,NBETA2
   85 BEC12(I,K,J)=DPPR(I,K)*YIEJ(J)
      IF (NMODES.EQ.1) GO TO 6344
      WRITE(6,640)
      WRITE(6,632) (J,J=1,4)
      DO 6341 I=1,II
 6341 WRITE(6,6321)(((BEC12(I,K,J),K=1,KK),J=1,4))
      WRITE(6,632) (J,J=5,8)
      DO 6342 I=1,II
 6342 WRITE(6,6321)(((BEC12(I,K,J),K=1,KK),J=5,8))
      WRITE(6,632) (J,J=9,NBETA2)
      DO 6343 I=1,II
 6343 WRITE(6,6321)(((BEC12(I,K,J),K=1,KK),J=9,NBETA2))
      GO TO 6345
 6344 WRITE(6,6371)
      WRITE(6,2001) ((((BEC12(I,K,J),I=1,II),K=1,KK),J=1,NBETA2))
 6345 CONTINUE
      IF ((SGCSC.EQ.DNC).AND.(SPNRC.EQ.DNC).AND.(SIGFC.EQ.DNC)) GO TO
     137
C
C     AT TMAX
C
      MTI=2
      TIME=TMAX
      IF (SIGFC.EQ.DNC) GO TO 340
      READ(21,1000) UNSF
      REWIND 21
  340 IF (SGCSC.EQ.DNC) GO TO 341
      READ(25,1000) SGCS
      REWIND 25
      IF (SPNRC.EQ.DNC) GO TO 342
  341 READ(27,1000) SCAT
      REWIND 27
```

```
  342 CONTINUE
      GO TO 27
   89 WRITE(6,638)
      WRITE(6,626) ((VPHPR(I,K),K=1,KK),I=1,II)
      WRITE(6,639)
      WRITE(6,626) ((VDPPR(I,K),K=1,KK),I=1,II)
      IF (NMODES.EQ.1) GO TO 6346
      WRITE(6,643)
      WRITE(6,632) (J,J=1,4)
      DO 7431 I=1,II
 7431 WRITE(6,6321)(((BEC22(I,K,J),K=1,KK),J=1,4))
      WRITE(6,632) (J,J=5,8)
      DO 6432 I=1,II
 6432 WRITE(6,6321)(((BEC22(I,K,J),K=1,KK),J=5,8))
      WRITE(6,632) (J,J=9,NBETA2)
      DO 6433 I=1,II
 6433 WRITE(6,6321)(((BEC22(I,K,J),K=1,KK),J=9,NBETA2))
      GO TO 6347
 6346 WRITE(6,6431)
      WRITE(6,2001) ((((BEC22(I,K,J),I=1,II),K=1,KK),J=1,NBETA2))
 6347 CONTINUE
      GO TO 391
   37 DO 381 I=1,II
      DO 381 K=1,KK
      VPHPR(I,K)=0.
      VDPPR(I,K)=0.
      DO 381 J=1,NBETA2
  381 BEC22(I,K,J)=0.
  391 CONTINUE
      RETURN
      END
      SUBROUTINE PFN1(K,PSI,SGCS,HU,HV,R,PHP1)
C
C PHP LIKE PROMPT PHOTON PRODUCTION
C
      DIMENSION PSI(3,48,40),SGCS(2,3,47,39),HU(39),HV(47),R(40),PHP1(2,
```

```
     12)
C
      DO 29 L=1,2
      SUM3=0.
      DO 28 MG=1,3
      DO 28 MV=2,47
      HV1=HV(MV-1)
      HV2=HV(MV)
      MU=1
      PHP=PSI(MG,MV,MU)*((SGCS(L,MG,MV-1,MU)*HV(MV-1)+SGCS(L,MG,MV,MU)*H
     1V(MV))*HU(MU)*(R(MU)+HU(MU)/4))
      SUM3=SUM3+PHP
      DO 28 MU=2,39
      HR1=(R(MU)-HU(MU-1)/4)*HU(MU-1)
      HR2=(R(MU)+HU(MU)/4)*HU(MU)
      PHP=PSI(MG,MV,MU)*((SGCS(L,MG,MV-1,MU-1)*HV1+SGCS(L,MG,MV,MU-1)
     1*HV2)*HR1+(SGCS(L,MG,MV-1,MU)*HV1+SGCS(L,MG,MV,MU)*HV2)*HR2)
      SUM3=SUM3+PHP
   28 CONTINUE
      PHP1(K,L)=SUM3*1.5708
   29 CONTINUE
      RETURN
      END
      SUBROUTINE DPN1(PSI,UNSF,HU,HV,R,SUM8)
C
C     DPP LIKE DELAYED PHOTON PRODUCTION
C
      DIMENSION PSI(3,48,40),UNSF(3,47,39),HU(39),HV(47),R(40)
C
      SUM8=0.
      DO 78 MG=1,3
      DO 78 MV=5,24
      DO 78 MU=3,17
      DPP=PSI(MG,MV,MU)*((UNSF(MG,MV-1,MU-1)*HV(MV-1)+UNSF(MG,MV,MU-1)*
     1HV(MV))*HU(MU-1)*(R(MU)-HU(MU-1)/4)+(UNSF(MG,MV-1,MU)*HV(MV-1)+UNS
     2F(MG,MV,MU)*HV(MV))*HU(MU)*(R(MU)+HU(MU)/4))
```

```
      SUM8=SUM8+DPF
   78 CONTINUE
      RETURN
      END
      SUBROUTINE  PDN2(L,MUI,MUF,MVI,MVF,W,SCAT,HU,HV,R,SUM4)
C
C PHOTONEUTRON REACTION INTEGRATION
C
      DIMENSION W(3,48,40),SCAT(2,47,39),HU(39),HV(47),R(40)
C
      DO 31 MV=MVI,MVF
      IF (MUI.NE.1) GO TO 30
      MU=1
      PNR=W(1,MV,MU)*((SCAT(L,MV-1,MU)*HV(MV-1)+SCAT(L,MV,MU)*HV(MV))*HU
     1(MU)*(R(MU)+HU(MU)/4))
      SUM4=SUM4+PNR
      MUI=2
   30 DO 31 MU=MUI,MUF
      PNR=W(1,MV,MU)*((SCAT(L,MV-1,MU-1)*HV(MV-1)+SCAT(L,MV,MU-1)*HV(MV)
     1)*HU(MU-1)*(R(MU)-HU(MU-1)/4)+(SCAT(L,MV-1,MU)*HV(MV-1)+SCAT(L,MV,
     2MU)*HV(MV))*HU(MU)*(R(MU)+HU(MU)/4))
      SUM4=SUM4+PNR
   31 CONTINUE
      RETURN
      END
      SUBROUTINE FILIZ4
C
C FINAL STEP BEFORE THE TIME DEPENDENT EQUATIONS
C
      COMMON/OZ2/NMODES,II,KK
      COMMON/OZ4/NBETA1,NBETA2,NBETA,NBET1
      COMMON/OZ3FZ1/GENTME
      COMMON/OZ4FZ1/LAPN,VLAPN
      COMMON/OZFZ2/BETA,E,FMAR,VFMAR,BETR,VBETR,BEC11,BEC21
      COMMON/OZ2FZ3/PHPR,VPHPR,DPPR,VDPPR,BEC12,BEC22
      COMMON/F2F4/WSC,JNPC
```

```
      COMMON/OZFZ4/FIJ,FAMLAM,ROC1,ROC2,ROC3,BEC1,BEC2,BEC3,FAMPRE,INPC
      COMMON/FZ4HT/BE
C
      REAL LAPN
C
      DIMENSION FIJ(2),FAMLAM(15),BEC11(2,2,6),BEC21(
     12,2,6),BEC12(2,2,9),BEC22(2,2,9),DPPR(2,2),VDPPR(2,2),GENTME(2,2),
     2BEC1(2,2,15),BEC2(2,2,15),BEC3(2,2,15),ROC1(2,2),ROC2(2,2),
     3ROC3(2,2),BATA(2,2,15),ROJ(2,2),LAPN(2,2),VLAPN(2,2),FMAR(2,2),
     4VFMAR(2,2),PHPR(2,2),VPHPR(2,2),BETR(2,2),VBETR(2,2),FAMPRE(2,15),
     5BETA(6),WSC(2),BETRX(2,2),DPPRX(2,2)
C
 2001 FORMAT (1X,8E12.5/(1X,8E12.5))
  626 FORMAT (1X,2(E15.8,3X)/(1X,2(E15.8,3X))//)
  644 FORMAT (1H1,21X,'FINAL STEP BEFORE THE TIME DEPENDENT EQUATIONS'//
     1/)
  625 FORMAT (1H ,'GENERATION TIME MATRIX'/)
  645 FORMAT (/1X,'THE REACTIVITY MATRIX(INITIAL VALUE)'/)
  646 FORMAT (/1X,'THE REACTIVITY MATRIX(RAMP CHANGE SLOPE)'/)
  647 FORMAT (/1X,'DELAYED NEUTRON(AND PHOTONEUTRON) FRACTION MATRICES(I
     1NITIAL VALUE)'/)
 6471 FORMAT (/1X,'DELAYED NEUTRON(AND PHOTONEUTRON) FRACTIONS'/)
  632 FORMAT (12X,I2,3(26X,I2))
 6321 FORMAT (1X,4(2(E12.5,1X),2X))
  648 FORMAT(1H1 ,'DELAYED NEUTRON(AND PHOTONEUTRON) FRACTION MATRICES(R
     1AMP CHANGE SLOPE)'/)
 6481 FORMAT (/1X,'DELAYED NEUTRON(AND PHOTONEUTRON) FRACTIONS(RAMP CHAN
     1GE SLOPE)'/)
 6461 FORMAT (/1X,'TOTAL DELAYED NEUTRON FRACTION MATRIX'/)
 6462 FORMAT (/1X,'TOTAL DELAYED PHOTONEUTRON FRACTION MATRIX'/)
  222 FORMAT (5X,2(E12.5,1X)/)
 2221 FORMAT(//1X,'INTEGRAL OF THE WEIGHTING FUNCTIONS OVER THE REACTOR
     1VOLUME-FIRST GROUP ONLY-'/)
  113 FORMAT(/1X,'INITIAL PRECURSOR AMPLITUDES'/)
C
      BE=0.
```

```
      DO 90 J=1,NBETA1
   90 EE=BETA(J)+BE
C
C     CALCULATION OF ROC1 AND ROC2
C
      DO 50 I=1,II
      DO 50 K=1,KK
      ROC1(I,K)=LAPN(I,K)+FMAR(I,K)+PHPR(I,K)+DPPR(I,K)
      ROC2(I,K)=VLAPN(I,K)+VFMAR(I,K)+VPHPR(I,K)+VDPPR(I,K)
      ROC3(I,K)=0.
      GENTME(I,K)=GENTME(I,K)/E
      ROC1(I,K)=ROC1(I,K)/E
      ROC2(I,K)=ROC2(I,K)/E
      BETRX(I,K)=BETR(I,K)/E*BE
      DPPRX(I,K)=DPPR(I,K)/E
   50 CONTINUE
      WRITE(6,644)
      WRITE(6,625)
      WRITE(6,626) ((GENTME(I,K),K=1,KK),I=1,II)
      WRITE(6,645)
      WRITE(6,626)((ROC1(I,K),K=1,KK),I=1,II)
      WRITE(6,646)
      WRITE(6,626)((ROC2(I,K),K=1,KK),I=1,II)
      WRITE(6,6461)
      WRITE(6,626) ((BETRX(I,K),K=1,KK),I=1,II)
      WRITE(6,6462)
      WRITE(6,626) ((DPPRX(I,K),K=1,KK),I=1,II)
C
C     CALCULATION OF BEC1 AND BEC2
C
      DO 99 I=1,II
      DO 99 K=1,KK
      DO 98 J=1,NBETA1
      BEC1(I,K,J)=BEC11(I,K,J)
      BEC2(I,K,J)=BEC21(I,K,J)
      BEC3(I,K,J)=0.
```

```
      BEC1(I,K,J)=BEC1(I,K,J)/E
      BEC2(I,K,J)=BEC2(I,K,J)/E
   98 CONTINUE
      DO 99 J=NBET1,NBETA
      JJ=J-NBETA1
      BEC1(I,K,J)=BEC12(I,K,JJ)
      BEC2(I,K,J)=BEC22(I,K,JJ)
      BEC1(I,K,J)=BEC1(I,K,J)/E
      BEC2(I,K,J)=BEC2(I,K,J)/E
      BEC3(I,K,J)=0.
   99 CONTINUE
      IF (NMODES.EQ.1) GO TO 6485
      WRITE(6,647)
      WRITE(6,632) (J,J=1,4)
      DO 7471 I=1,II
 7471 WRITE(6,6321)(((BEC1 (I,K,J),K=1,KK),J=1,4))
      WRITE(6,632) (J,J=5,8)
      DO 6472 I=1,II
 6472 WRITE(6,6321)(((BEC1 (I,K,J),K=1,KK),J=5,8))
      WRITE(6,632) (J,J=9,12)
      DO 6473 I=1,II
 6473 WRITE(6,6321)(((BEC1 (I,K,J),K=1,KK),J=9,12))
      WRITE(6,632) (J,J=13,15)
      DO 6474 I=1,II
 6474 WRITE(6,6321)(((BEC1 (I,K,J),K=1,KK),J=13,NBETA))
      WRITE(6,648)
      WRITE(6,632) (J,J=1,4)
      DO 7481 I=1,II
 7481 WRITE(6,6321)(((BEC2 (I,K,J),K=1,KK),J=1,4))
      WRITE(6,632) (J,J=5,8)
      DO 6482 I=1,II
 6482 WRITE(6,6321)(((BEC2 (I,K,J),K=1,KK),J=5,8))
      WRITE(6,632) (J,J=9,12)
      DO 6483 I=1,II
 6483 WRITE(6,6321)(((BEC2 (I,K,J),K=1,KK),J=9,12))
      WRITE(6,632) (J,J=13,15)
```

```
      DO 6484 I=1,II
 6484 WRITE(6,6321)(((BEC2 (I,K,J),K=1,KK),J=13,NBETA))
      GO TO 6486
 6485 WRITE(6,6471)
      WRITE(6,2001) ((((BEC1(I,K,J),I=1,II),K=1,KK),J=1,NBETA))
      WRITE(6,6481)
      WRITE(6,2001) ((((BEC2(I,K,J),I=1,II),K=1,KK),J=1,NBETA))
 6486 CONTINUE
C
C     CALCULATION OF STEADY STATE PRECURSOR CONCENTRATIONS
C
      IF (INPC.EQ.1) GO TO 112
      DO 105 I=1,II
      DO 105 J=1,NBETA
  105 FAMPRE(I,J)=0.
      DO 110 J=1,NBETA
      DO 110 I=1,II
      DO 110 K=1,KK
  110 FAMPRE(I,J)=BEC1(I,K,J)*FIJ(I)/FAMLAM(J)+FAMPRE(I,J)
      GO TO 4999
  112 CONTINUE
      IF (NMODES .EQ.1) GO TO 4999
      DO 499 J=1,NBETA
      IF (J.NE.NBETA) GO TO 498
      WRITE(6,2221)
      WRITE(6,626)(WSC(I),I=1,II)
      FAMPRE(2,J)=FAMPRE(1,J)*WSC(2)/WSC(1)
      GO TO 499
  498 FAMPRE(2,J)=FAMPRE(1,J)*BEC1(2,1,J)/BEC1(1,1,J)
  499 CONTINUE
 4999 WRITE(6,113)
      DO 500 J=1,NBETA
  500 WRITE(6,222)(FAMPRE(I,J),I=1,II)
      RETURN
      END
      SUBROUTINE GCNCA(NDIM,PFULL,PHALF,BFULL,BHALF)
```

```
C
C THIS SUBROUTINE WILL SOLVE THE POINT KINETIC TYPE OF EQUATIONS USING THE WEIGH
C TED RESIDUAL TECHNIQUE(SUBDOMAIN WEIGHTING)-ANL 7565 P.68-KNOWING THE MATRICES
C EQUIVALENT TO THE CONVENTINAL GENERATION TIME(LAMBDA),REACTIVITY(RHO) AND THE
C DELAYED NEUTRON(ALSO THE DELAYED PHOTONEUTRON) GROUP FRACTIONS(BETA'S) IN OR-
C DER TO GET THE UNKNOWM TIME COEFFICIENTS
C
C I HAVE BARROWED THIS SUBROUTINE (WITH FEW CHANGES) FROM WEIRD -EDWARD FULLER-.
C THE ORIGINAL NAME OF THE SUBROUTINE WAS MOVER
C
C ,, GONCA ,, MEANS BUD IN TURKISH
C
      COMMON/OZ2/NMODES,II,KK
      COMMON/OZ3/TMIN,TMAX
      COMMON/OZ4/NBETA1,NBETA2,NBETA,NBET1
      COMMON/OZ3FZ1/GENTME
      COMMON/OZFZ4/FIJ,FAMLAM,ROC1,ROC2,ROC3,BEC1,BEC2,BEC3,FAMPRE,INPC
      COMMON/OZGON/IJUMP,EPS2,NCM1,NCOEF,ROJ,BATA,JJ33
      COMMON/OZGOHT/FAMCLM
      COMMON/GOZHT/FIF
C
      DIMENSION FAMLAM(15),FAMPRE(2,15),FIJ(2),GENTME(2,2),BETA(6),ROC1(
     12,2),ROC2(2,2),ROC3(2,2),BEC1(2,2,15),BEC2(2,2,15),BEC3(2,2,15),AC
     2(5),Q(20,15,5),ROJ(2,2),BATA(2,2,15),FAMCLM(2,15),SUMCI(2),SUMRO(2
     3,2,3),SUMB(2,2,3),CBURN(2,15),BINT(2,2,3),SUINIT(2),FIF(2),CCMP(6,
     42),PFULL(NDIM,NDIM),PHALF(NDIM,NDIM),BFULL(NDIM),BHALF(NDIM),COFE(
     52,2,6),A(3,2,20),ENFULL(6,2),ENHALF(6,2),SENFLL(2),SENHAF(2),SQN(
     62),T(20,8),IPOWR(30),DBURN(2,15),SUMRB(2,2,3),EPS(2),BIFIJ(2),
     7SUMNB(2),TERMNB(2),ENBINT(2)
C
      EQUIVALENCE (J3,JJ33)
C
  450 FORMAT(35H THE TIME STEP IMPOSED IS TOO LARGE)
  500 FORMAT(15H          TIME=E18.10)
  501 FORMAT(15H MAXIMUM ERROR=E18.10)
  502 FORMAT(51H MODE       AMPLITUDE FUNCTION       ERROR IN AMPLITUDE)
```

```
  503 FORMAT(I4,2E23.10)
  504 FORMAT(18H TIME STEP NUMBER I6)
 1000 FORMAT(4H J3=I3)
 1001 FORMAT (1X,'J3=*',I2)
 1500 FORMAT(1H1,//21X,'THE TIME DEPENDENT FUNCTION(S)'///)
 1600 FORMAT (////1X,'PROGRAM RETURNED FROM SIMQ WITH NO RESULT')
C
      WRITE(6,1500)
      NBET=NBETA
      NPP1=NMODES*NCOEF
      IMAX=NCOEF+2
      TJUMP=TMAX-TMIN
      EPS1=.1*EPS2
      TIME=TMIN
      TOME=TMIN
      ISTEP=1
      ICUT=1
      J3=1
      J5=1
      NPR1=1
      J6=NCOEF
      NN=1073741824
      INC=1073741824
      A0(1)=1.
      DO 81 I=2,IMAX
      XI=I
   81 A0(I)=1./XI
      DO 11 IN=1,NMODES
      DO 11 IM=1,NMODES
      DO 103 I=1,NBET
      FAMCLM(IM,I)=FAMPRE(IM,I)*FAMLAM(I)
  103 BATA(IM,IN,I)=BEC1(IM,IN,I)
   11 RCJ(IM,IN)=RCC1(IM,IN)
      TEX=TJUMP
   90 DO 61 J=J5,J6
      T(J,1)=TEX
```

```
      DO 82 I=2,IMAX                                                    OZAN2089
   82 T(J,I)=T(J,I-1)*T(J,1)                                            OZAN2090
      DO 62 K=1,NBET                                                    OZAN2091
      DO 12 I=1,IMAX                                                    OZAN2092
   12 Q(J,K,I)=0.                                                       OZAN2093
      X=FAMLAM(K)*T(J,1)                                                OZAN2094
      IF(ABS(X)-1.) 2,1,1                                               OZAN2095
    1 RX=1./FAMLAM(K)                                                   OZAN2096
      IF (.NOT.(X.GE.150.)) GO TO 15                                    OZAN2097
      WRITE(6,450)                                                      OZAN2098
      PRINT 500,TONE                                                    OZAN2099
      GO TO 139                                                         OZAN2100
   15 Q(J,K,1)=(1.-EXP(-X))*RX                                          OZAN2101
      DO 7 JJ=2,IMAX                                                    OZAN2102
      XI=JJ                                                             OZAN2103
    7 Q(J,K,JJ)=(T(J,JJ-1)-(XI-1.)*Q(J,K,JJ-1))*RX                      OZAN2104
      GO TO 62                                                          OZAN2105
    2 SUM=AO(IMAX)*T(J,IMAX)                                            OZAN2106
      APS=SUM*1.E-20                                                    OZAN2107
      ACOEF=NCOEF                                                       OZAN2108
      FJ2=ACOEF+3.                                                      OZAN2109
      TERM=SUM                                                          OZAN2110
    3 TERM=-X*TERM/FJ2                                                  OZAN2111
      IF(ABS(TERM)-APS) 5,5,4                                           OZAN2112
    4 SUM=SUM+TERM                                                      OZAN2113
      FJ2=FJ2+1.                                                        OZAN2114
      GO TO 3                                                           OZAN2115
    5 Q(J,K,IMAX)=SUM                                                   OZAN2116
      DO 8 JJ=2,IMAX                                                    OZAN2117
      I2=IMAX+1-JJ                                                      OZAN2118
      XI=I2                                                             OZAN2119
    8 Q(J,K,I2)=(T(J,I2)-FAMLAM(K)*Q(J,K,I2+1))*AO(I2)                  OZAN2120
   62 CONTINUE                                                          OZAN2121
   61 TEX=.5*TEX                                                        OZAN2122
  111 TSTEP=T(J3,1)                                                     OZAN2123
      J4=J3                                                             OZAN2124
```

```
      DO 60 J1=1,NCOEF                                                  OZAN2125
      J2=J3-1+J1                                                        OZAN2126
      DO 104 IM=1,NMODES                                                OZAN2127
  104 SUMCI(IM)=0.                                                      OZAN2128
      DO 10 I1=1,NCOEF                                                  OZAN2129
      DO 10 IN=1,NMODES                                                 OZAN2130
      DO 10 IM=1,NMODES                                                 OZAN2131
      SUMRC(IM,IN,I1)=AO(I1)*T(J2,I1)*ROJ(IM,IN)+AO(I1+1)*T(J2,I1+1)*(RO OZAN2132
     1 C2(IM,IN)+2.*ROC3(IM,IN)*TIME)+AO(I1+2)*T(J2,I1+2)*ROC3(IM,IN)   OZAN2133
   10 SUMB(IM,IN,I1)=0.                                                 OZAN2134
      DO 80 I=1,NBET                                                    OZAN2135
      DO 80 IM=1,NMODES                                                 OZAN2136
      CBURN(IM,I)=FAMCLM(IM,I)*Q(J2,I,1)                                OZAN2137
      SUMCI(IM)=SUMCI(IM)+CBURN(IM,I)                                   OZAN2138
      DO 80 IN=1,NMODES                                                 OZAN2139
      DO 80 I1=1,NCOEF                                                  OZAN2140
      BINT(IM,IN,I1)=BATA(IM,IN,I)*Q(J2,I,I1)+(BEC2(IM,IN,I)+2.*BEC3(IM, OZAN2141
     1 IN,I)*TIME)*Q(J2,I,I1+1)+BEC3(IM,IN,I)*Q(J2,I,I1+2)              OZAN2142
      SUMB(IM,IN,I1)=SUMB(IM,IN,I1)+BINT(IM,IN,I1)                      OZAN2143
   80 CONTINUE                                                          OZAN2144
      DO 105 I1=1,NCOEF                                                 OZAN2145
      DO 105 IN=1,NMODES                                                OZAN2146
      DO 105 IM=1,NMODES                                                OZAN2147
  105 SUMRB(IM,IN,I1)=SUMRC(IM,IN,I1)-SUMB(IM,IN,I1)                    OZAN2148
      DO 106 IM=1,NMODES                                                OZAN2149
      SUINIT(IM)=0.                                                     OZAN2150
      DO 107 IP=1,NMODES                                                OZAN2151
      TEINIT=SUMRB(IM,IP,1)*FIJ(IP)                                     OZAN2152
  107 SUINIT(IM)=SUINIT(IM)+TEINIT                                      OZAN2153
      COMP(J1,IM)=SUINIT(IM)+SUMCI(IM)                                  OZAN2154
      DO 106 IN=1,NMODES                                                OZAN2155
      DO 106 I1=2,NCOEF                                                 OZAN2156
  106 COFE(IM,IN,I1)=GENTME(IM,IN)*T(J2,I1-1)-SUMRB(IM,IN,I1)           OZAN2157
      DO 113 IM=1,NMODES                                                OZAN2158
      JK=2                                                              OZAN2159
  112 JL=JK-1                                                           OZAN2160
```

```
      DO 114 IN=1,NMODES
      LNMODS=(JL-1)*NMODES
      IY=LNMODS+IN
  114 A(J1,IM,IY)=COFE(IM,IN,JK)
      IF(IY.EQ.NDIM) GO TO 113
  110 JK=JK+1
      GO TO 112
  113 CONTINUE
   60 CONTINUE
      DO 121 IY=1,NDIM
      J1=1
  122 MNMODS=(J1-1)*NMODES
      DO 118 IM=1,NMODES
      IX=MNMODS+IM
      IF(J1.EQ.NCOEF) GO TO 117
  119 PFULL(IX,IY)=A(J1,IM,IY)
      BFULL(IX)=COMP(J1,IM)
  117 IZ=IX-NMODES
      IF(IZ.GT.0) GO TO 115
      GO TO 118
  115 PHALF(IZ,IY)=A(J1,IM,IY)
      BHALF(IZ)=COMP(J1,IM)
  118 CONTINUE
      IF(IX.EQ.NPP1) GO TO 121
  120 J1=J1+1
      GO TO 122
  121 CONTINUE
C
C SIMQ IS A GENERAL MATRIX INVERSION SUBROUTINE ACCOMPANIED BY THE SOLUTION OF
C THE LINEAR SYSTEM OF EQUATIONS
C
      CALL SIMQ(PFULL,BFULL,NDIM,KS)
      CALL SIMQ(PHALF,BHALF,NDIM,KS)
C
      IF (KS.EQ.0) GO TO 8000
      WRITE(6,1600)
```

```
      RETURN
 8000 CONTINUE
      J1=1
  124 MNMODS=(J1-1)*NMODES
      DO 123 IM=1,NMODES
      IX=MNMODS+IM
      ENFULL(J1,IM)=BFULL(IX)
  123 ENHALF(J1,IM)=BHALF(IX)
      IF(IX-NDIM) 126,125,125
  126 J1=J1+1
      GO TO 124
  125 CONTINUE
      DO 128 IM=1,NMODES
      SENFUL(IM)=FIJ(IM)
      SENHAF(IM)=FIJ(IM)
      DO 128 J1=1,NCM1
      TERFUL=ENFULL(J1,IM)*TSTEP**J1
      TERHAF=ENHALF(J1,IM)*TSTEP**J1
      SENFUL(IM)=SENFUL(IM)+TERFUL
  128 SENHAF(IM)=SENHAF(IM)+TERHAF
      SEPS=0.
      SSQN=0.
      DO 127 IM=1,NMODES
      EPS(IM)=(SENHAF(IM)-SENFUL(IM))**2
      SQN(IM)=(SENHAF(IM))**2
      SEPS=SEPS+EPS(IM)
      SSQN=SSQN+SQN(IM)
      EPS(IM)=EPS(IM)/SQN(IM)
  127 CONTINUE
      EPSLON=SQRT(SEPS/SSQN)
      EPSILN=EPSLON
      IF(EPSILN.GT.EPS2) GO TO 72
      IF(EPSILN.LT.EPS1) GO TO 63
      GO TO 64
   72 J3=J3+1
      PRINT 1000,J3
```

```
 73 IF(J3.LE.NPR1) GO TO 111
    IF (J3.GT.30) GO TO 71
    J5=J6+1
    J6=J5
    NPR1=J3
    GO TO 90
 71 CONTINUE
    PRINT 1000,J3
    RETURN
 63 CONTINUE
    IF (J3.EQ.1) GO TO 64
    J3=J3-1
    PRINT 1000,J3
 64 TOME=TOME+TSTEP
    J2=J4
    DO 133 IM=1,NMODES
    FIF(IM)=SENFUL(IM)
    FIFM=FIF(IM)
    ITIME=ISTEP
    IF((ABS(FIFM).GE.1.E35).OR.(ABS(FIFM).LE.1.E-35)) GO TO 140
    DO 65 I=1,NBET
    SUMNB(IM)=0.
    TERMNB(IM)=0.
    DBURN(IM,I)=FAMCLM(IM,I)*Q(J2,I,1)
    DO 91 IN=1,NMODES
    DO 180 I1=1,NCOEF
180 BINT(IM,IN,I1)=BATA(IM,IN,I)*Q(J2,I,I1)+(BEC2(IM,IN,I)+2.*BEC3(IM,
   1 IN,I)*TIME)*Q(J2,I,I1+1)+BEC3(IM,IN,I)*Q(J2,I,I1+2)
    BIFIJ(IM)=BINT(IM,IN,1)*FIJ(IN)
    SUMNB(IM)=SUMNB(IM)+BIFIJ(IM)
    DO 91 JM=2,NCOEF
    ENBINT(IM)=BINT(IM,IN,JM)*ENFULL(JM-1,IN)
 91 TERMNB(IM)=TERMNB(IM)+ENBINT(IM)
    SUMNB(IM)=SUMNB(IM)+TERMNB(IM)
    FAMPRE(IM,I)=FAMPRE(IM,I)-DBURN(IM,I)+SUMNB(IM)
 65 FAMCLM(IM,I)=FAMPRE(IM,I)*FAMLAM(I)
```

```
133  FIJ(IM)=FIF(IM)
     IJCT=IJUMP*ICUT
     IF(ISTEP.EQ.IJCT) GO TO 135
     GO TO 136
135  PRINT 504,ISTEP
     IOUT=IOUT+1
     PRINT 500,TOME
     PRINT 501,EPSILN
     PRINT 502
     DO 137 IM=1,NMODES
     PRINT 503,IM,FIF(IM),EPS(IM)
137  CONTINUE
136  ISTEP=ISTEP+1
     TIME=TIME+TSTEP
     TEMI=TIME-TMIN
     DO 134 IM=1,NMODES
     DO 134 IN=1,NMODES
     ROJ(IM,IN)=ROC1(IM,IN)+TEMI*(ROC2(IM,IN)+TEMI*ROC3(IM,IN))
     DO 134 I=1,NBET
     BATA(IM,IN,I)=BEC1(IM,IN,I)+TEMI*(BEC2(IM,IN,I)+TEMI*BEC3(IM,IN,I)
    1 )
134  CONTINUE
     IPOWR(J3)=2**(J3-1)
     IPOWR(J4)=2**(J4-1)
     INC=NN/IPOWR(J3)
     INC=INC-NN/IPOWR(J4)
     IF(TOME.GE.TMAX) GO TO 138
     GO TO 68
138  ITIME=ISTEP-1
140  PRINT 504,ITIME
     PRINT 500,TOME
     PRINT 501,EPSILN
     PRINT 502
     DO 139 IM=1,NMODES
     PRINT 503,IM,FIF(IM),EPS(IM)
139  CONTINUE
```

```
      RETURN
   68 CONTINUE
      IF(IND.LE.INC) GO TO 73
      IND=IND/2
      J3=J3+1
      PRINT 1001,J3
      GO TO 68
      END
      SUBROUTINE HASAT(BATA,GENTME,ROJ)
C
C     THIS SUBROUTINE GIVES THE FINAL TIME DEPENDENT FLUX AT THE END OF THE
C     TRANSIENT AS WELL AS SOME OF THE CONVENTIONEL PARAMETERS WHICH ALLOW A
C     COMPARISON OF OUR RESULTS WITH THOSE OBTAINED TROUGH A POINT KINETICS
C     TYPE APPROACH
C
C     ,, HASAT ,, MEANS HARVEST IN TURKISH
C
      COMMON/OZO/SIGA,UNSF,SGCS,SCAT,PSI,W
      COMMON/OZ11/C,DNC,KSFCZ,SKOZN,NDPSI,NDW,HU,HV,R
      COMMON/OZ2/NMODES,II,KK
      COMMON/OZ4/NBETA1,NBETA2,NBETA,NBET1
      COMMON/FZ4HT/BE
      COMMON/OZGOHT/FAMCLM
      COMMON/GCZHT/FIF
      COMMON/OZHST/ATT1,ATT2,MU1,MUU,MV1,MVV
C
      DIMENSION PSI(3,48,40),W(3,48,40),HU(39),HV(47),R(40),SIGA(3,47,
     139),UNSF(3,47,39),SCAT(2,47,39),ATT1(10),ATT2(10),
     2FIF(2),BATA(2,2,15),GENTME(2,2),BATA1(2),ROJ(2,2),BATAT(2),
     3PHLUX(3,48,40),NDW(2),NDPSI(2),SGCS(2,3,47,39),FAMCLM(2,15),
     4SBETA(2)
C
 1000 FORMAT(7E11.5)
 5000 FORMAT(1P5E14.6)
  649 FORMAT (1H1,/////21X,'TIME DEPENDENT FRUITS')
 6501 FORMAT(////1X,'AMPLITUDE FUNCTION',24X'=',E13.6///' REACTIVITY',3
```

```
     12X,'=',E13.6/' OMEGA',37X,'=',E13.6//' GENERATION TIME',27X,'=',E1
     23.6/' TOTAL DELAYED NEUTRON FRACTION',12X,'=',E13.6/' TOTAL PRECUR
     3SOR ACTIVITY',18X,'=',E13.6/)
 651 FORMAT (1H1,'TIME DEPENDENT FLUX GROUP ',I1/)
 652 FORMAT (8X,I2,9(9X,I2))
 653 FORMAT (/1X,I2,3X,10(E9.3,2X))
     DEL=0.
     IF (KK.NE.1) GO TO 179
     READ(10,5000) PSI
     REWIND 10
     DO 178 MV=1,48
     DO 178 MU=1,40
     DO 178 MG=1,3
 178 PHLUX(MG,MV,MU)=PSI(MG,MV,MU)*FIF(1)
     GO TO 192
 179 DO 180 MV=1,48
     DO 180 MU=1,40
     DO 180 MG=1,3
     PHLUX(MG,MV,MU)=0.
 180 CONTINUE
     KKK=0
     DO 190 K=1,KK
     KKK=K+1-KKK
     NN=NDPSI(KKK)
     READ(NN,5000) PSI
     REWIND NN
     DO 190 MV=1,48
     DO 190 MU=1,40
     DO 190 MG=1,3
 190 PHLUX(MG,MV,MU)=PSI(MG,MV,MU)*FIF(KKK)+PHLUX(MG,MV,MU)
 192 CONTINUE
     DO 60 K=1,KK
     SUM1=0.
     DO 50 J=1,NBETA1
     SUM1=SUM1+BATA(1,K,J)
  50 CONTINUE
```

```
      SBETA(K)=SUM1                                                     OZAN2377
      BATA1(K)=SUM1/BE                                                  OZAN2378
   60 CONTINUE                                                          OZAN2379
      DO 70 K=1,KK                                                      OZAN2380
      SUM2=SBETA(K)                                                     OZAN2381
      DO 65 J=NBET1,NBETA                                               OZAN2382
      SUM2=SUM2+BATA(1,K,J)                                             OZAN2383
   65 CONTINUE                                                          OZAN2384
      BATAT(K)=SUM2                                                     OZAN2385
   70 CONTINUE                                                          OZAN2386
      AMP=FIF(1)+GENTME(1,2)/GENTME(1,1)*FIF(2)                         OZAN2387
      DEN=BATA1(1)*FIF(1)+BATA1(2)*FIF(2)                               OZAN2388
      GENN=AMP*GENTME(1,1)/DEN                                          OZAN2389
      RHO=(ROJ(1,1)*FIF(1)+ROJ(1,2)*FIF(2))/DEN                         OZAN2390
      BETAT=(BATAT(1)*FIF(1)+BATAT(2)*FIF(2))/DEN                       OZAN2391
      DO 230 J=1,NBETA                                                  OZAN2392
      DEL=FAMCLM(1,J)+DEL                                               OZAN2393
  230 CONTINUE                                                          OZAN2394
      ALFA=((RHO-BETAT)*AMP+DEL)/(GENN*AMP)                             OZAN2395
      WRITE(6,6501) AMP,RHO,ALFA,GENN,BETAT,DEL                         OZAN2396
      MX=(MUU-MU1+1)/10                                                 OZAN2397
      MY=(MVV-MV1+1)/25                                                 OZAN2398
      MX1=MX+1                                                          OZAN2399
      MY1=MY+1                                                          OZAN2400
      NEX=MUU-MU1+1-MX*10                                               OZAN2401
      NEY=MVV-MV1+1-MY*25                                               OZAN2402
      DO 30 MG=1,3                                                      OZAN2403
      MUF=MU1-1                                                         OZAN2404
      MUI=MU1-10                                                        OZAN2405
      DO 30 MXX=1,MX1                                                   OZAN2406
      IF ((MX.EQ.0).OR.(MXX.EQ.MX1)) GO TO 10                           OZAN2407
      MUI=MUI+10                                                        OZAN2408
      MUF=MUF+10                                                        OZAN2409
      GO TO 15                                                          OZAN2410
   10 MUF=MUF+NEX                                                       OZAN2411
      MUI=MUF-NEX+1                                                     OZAN2412
```

```
   15 MVF=MV1-1
      MVI=MV1-25
      DO 30 MYY=1,MY1
      IF ((MY.EQ.0).OR.(MYY.EQ.MY1)) GO TO 20
      MVI=MVI+25
      MVF=MVF+25
      GO TO 25
   20 MVF=MVF+NEY
      MVI=MVF-NEY+1
   25 WRITE(6,651) MG
      WRITE(6,652) (MU,MU=MUI,MUF)
      DO 30 MV=MVI,MVF
      WRITE(6,653) MV,(PHLUX(MG,MV,MU),MU=MUI,MUF)
   30 CONTINUE
      RETURN
      END
/*
//G.FT10F001 DD DSNAME=USERFILE.M8696.9441.EQP.SI,DISP=OLD
//G.FT11F001 DD DSNAME=USERFILE.M8696.9441.FQA.DJ,DISP=OLD
//G.FT12F001 DD DSNAME=USERFILE.M8696.9441.TRP.SI,DISP=OLD
//G.FT13F001 DD DSNAME=USERFILE.M8696.9441.TRA.DJ,DISP=OLD
//G.FT14F001 DD DSNAME=USERFILE.M8696.9441.FQD.IF,DISP=OLD
//G.FT15F001 DD DSNAME=USERFILE.M8696.9441.FSI.GA,DISP=OLD
//G.FT16F001 DD DSNAME=USERFILE.M8696.9441.FUN.SF,DISP=OLD
//G.FT17F001 DD DSNAME=USERFILE.M8696.9441.FIS.GF,DISP=OLD
//G.FT18F001 DD DSNAME=USERFILE.M8696.9441.TRD.IF,DISP=OLD
//G.FT19F001 DD DSNAME=USERFILE.M8696.9441.TSI.GA,DISP=OLD
//G.FT22F001 DD DSNAME=USERFILE.M8696.9441.FSC.AT,DISP=OLD
//G.FT23F001 DD DSNAME=USERFILE.M8696.9441.TSC.AT,DISP=OLD
//G.FT24F001 DD DSNAME=USERFILE.M8696.9441.FSG.CS,DISP=OLD
//G.FT26F001 DD DSNAME=USERFILE.M8696.9441.FSP.NR,DISP=OLD
//G.FT01F001 DD DSNAME=USERFILE.M8696.9441.EQD.IF,DISP=OLD
//G.FT02F001 DD DSNAME=USERFILE.M8696.9441.ESI.GA,DISP=OLD
//G.FT03F001 DD DSNAME=USERFILE.M8696.9441.EUN.SF,DISP=OLD
//G.FT04F001 DD DSNAME=USERFILE.M8696.9441.ESC.AT,DISP=OLD
//G.FT28F001 DD DSNAME=USERFILE.M8696.9441.HED.IF,DISP=OLD
```

```
//C.FT29F001 DD DSNAME=USERFILE.M8696.9441.HSI.GA,DISP=OLD
//G.FT31F001 DD DSNAME=USERFILE.M8696.9441.HSC.AT,DISP=OLD
//C.SYSIN DD *
 &INNM NMODES=2,NOEKIN=1,KSFEX=1,KSROZ=1,COEFIC=10.,LFINAL=1,INPC=1,LPSN=1,
 LEYD=1
 &END
 &INV1 V1=0.199030E-8,0.231703E-6,0.454545E-5,OMEG=17.262131
 &END
 &INHU
 HU=  3.7799997      ,  1.8639994      ,  1.3639994      ,  1.3639994      ,
  0.31699997     , 0.31699997     ,  1.6139994      ,  1.6139994      ,
   1.6139994     ,  1.6139994     , 0.97700000      , 0.97700000      ,
  0.97700000     , 0.97700000     ,  1.5959997      , 0.95400000      ,
  0.95400000     , 0.95400000     , 0.15899998      , 0.63499999      ,
  0.15899998     , 0.47599999     , 0.68699998      , 0.68699998      ,
  0.68699998     , 0.63499999     ,  4.4099998      ,  4.4099998      ,
   4.4099998     ,  4.4099998     ,  4.4099998      ,  4.4099998      ,
   4.4099998     ,  3.0000000     ,  9.6599998      ,  9.6599998      ,
   15.240000     ,  15.240000     ,  15.240000
 &END
 &INHV
 HV=  10.160000      ,  10.160000      ,  10.160000      ,  5.0799999      ,
   5.0799999     ,  5.0799999     ,  7.6199999      ,  2.5400000      ,
   2.5400000     ,  2.5400000     ,  2.5400000      ,  2.5400000      ,
   2.5400000     ,  2.5400000     ,  2.5400000      ,  2.5400000      ,
   2.5400000     ,  2.5400000     ,  2.5400000      ,  1.2699995      ,
   1.2699995     ,  1.2699995     ,  1.2699995      ,  1.2699995      ,
  0.63499999     ,  1.1639996     ,  1.1639996      ,  1.1639996      ,
  0.63499999     , 0.63499999     , 0.63499999      , 0.63499999      ,
  0.63499999     , 0.95199996     , 0.99699998      , 0.99699998      ,
  0.99699998     , 0.99699998     , 0.99699998      , 0.99699998      ,
  0.99699998     ,  1.2699995     ,  1.2699995      ,  1.2699995      ,
   15.240000     ,  15.240000     ,  15.240000
 &END
 &INYL
 YIEL= 0.23999995      , 0.75999999
```

```
&END
&INYJ
YIEJ= 0.64699996     , 0.20249999     , 0.69699943E-01, 0.33399999E-01,
 0.20499997E-01, 0.23100000E-01, 0.31899998E-02, 0.10080000E-02,
 0.0            ,NZRC=          0.5
&END
&INBA
BETA= 0.30099996E-03, 0.17090000E-02, 0.15289998E-02, 0.30820000E-02,
 0.89799985E-03, 0.32799994E-03,NBETA1=            6,NBETA2=           9
&END
&INF
FIJ= 0.41499995E-08, 0.0            ,FAMLAM= 0.12399998E-01, 0.30499998E-01,
 0.11099994     , 0.30100000     , 1.1399994      , 3.0099993      ,
 0.27699995     , 0.16899999E-01, 0.48099980E-02, 0.14999998E-02,
 0.42800000E-03, 0.11699999E-03, 0.43699998E-04, 0.36299998E-05,
 0.99999978E-13,FAMPRE= 0.10100000E-10, 0.0            , 0.38499995E-10,
 0.0            , 0.20099991E-10, 0.0            , 0.23899993E-10,
 0.0            , 0.26999999E-11, 0.0            , 0.42099999E-12,
 0.0            , 0.97999994E-12, 0.0            , 0.10899996E-11,
 0.0            , 0.77399995E-12, 0.0            , 0.93599954E-12,
 0.0            , 0.18299997E-11, 0.0            , 0.73199996E-11,
 0.0            , 0.26899993E-11, 0.0            , 0.10200000E-10,
 0.0            , 236.00000     , 0.0
&END
&INATT1 ATT1=0.4E-4,2*0.24E-4,2*0.1E-4,0.27E-4,2*0.1E-4,2*0.03E-4
&END
&INMVU MV1= 9,MVV=15,MU1=17,MUU=24
&END
&INUI MRUI=1,9,1,16,23,25,28,1,31,1
&END
&INUF MRUF=8,15,15,22,27,27,30,30,33,33
&END
&INVI MRVI=31,32,35,28,23,7,7,40,7,45
&END
&INVF MRVF=34,34,39,39,39,22,39,44,44,47
&END
```

```
&INGLK MGLK=6*3,2*2                                                                  OZAN2521
&END                                                                                 OZAN2522
&INDV MDVIC=14,15,16,17,2*24,22,26,18,19,20,21,2*25,23,27,28,29,30,3*5,31,5,         OZAN2523
1,2,3,3*5,4,5                                                                        OZAN2524
&END                                                                                 OZAN2525
&INT                                                                                 OZAN2526
TMIN= 0.0            ,IJUMP=            15,TUP=  1.0000000      ,  2.0000000     ,   OZAN2527
 3.0000000     ,3.5,3.77         ,-0.72370051E 76,-0.72370051E 76,                  OZAN2528
-0.72370051E 76,-0.72370051E 76,-0.72370051E 76,-0.72370051E 76,NINT=               OZAN2529
          5,NCM1=             2,EPS2= 1.E-01                                         OZAN2530
&END                                                                                 OZAN2531
&IN1                                                                                 OZAN2532
X1=  1.6391191     , 0.84075296     , 0.26702499     ,  1.7610798     ,              OZAN2533
 0.82282799     , 0.24985999     ,  1.6004200     , 0.80091798     ,                 OZAN2534
 0.25264597     ,  1.7538595     , 0.80182099     , 0.29360098     ,                 OZAN2535
  1.8078394     , 0.84202498     , 0.30796999     ,  1.6420193     ,                 OZAN2536
 0.84117997     , 0.26702499     ,  1.4325495     ,  1.2150497     ,                 OZAN2537
 0.78971696     ,  1.7206993     , 0.90859997     , 0.90892595     ,                 OZAN2538
  2.2368097     ,  2.2575293     , 0.16682897E-01,  2.6548691     ,                  OZAN2539
  4.0194197     ,  3.6016798     ,  2.6661196     ,  4.0173798     ,                 OZAN2540
  3.4609098     ,  2.7155800     ,  4.0147591     ,  3.4609098     ,                 OZAN2541
  1.7501698     , 0.80236799     , 0.29360098     ,  1.8089199     ,                 OZAN2542
 0.84150797     , 0.31006700     ,  1.4184895     , 0.80972195     ,                 OZAN2543
 0.24985999     ,  1.2845392     , 0.90837896     , 0.84762394     ,                 OZAN2544
  1.9194298     ,  1.8468199     ,  1.2728996     ,  1.3544693     ,                 OZAN2545
 0.45275295     , 0.12844497     ,  1.3857098     , 0.47886795     ,                 OZAN2546
 0.13622695     ,  1.2447691     , 0.45357698     , 0.12844497     ,                 OZAN2547
  1.2422295     , 0.45460399     , 0.12844497     ,  1.3167696     ,                 OZAN2548
 0.49528897     , 0.14204597     , 0.93908399     , 0.44860697     ,                 OZAN2549
 0.13706499     , 0.98881382E-03, 0.17965499E-01, 0.18742299     ,                  OZAN2550
 0.15144500E-03, 0.10632100E-02, 0.16516399E-01, 0.10329299E-02,                    OZAN2551
 0.18816397E-01, 0.19662899     , 0.11386098E-02, 0.18559597E-01,                   OZAN2552
 0.16346496     , 0.98922686E-03, 0.17698400E-01, 0.15745395     ,                   OZAN2553
 0.94003393E-03, 0.17886300E-01, 0.17972100     , 0.82731087E-04,                   OZAN2554
 0.32893495E-05, 0.37151593E-04, 0.10228300E-03, 0.28404780E-03,                    OZAN2555
 0.15815999E-02, 0.44388499E-01, 0.10759300     ,  14.910100     ,                  OZAN2556
```

```
0.17204099E-03, 0.74323779E-03, 0.95205493E-02, 0.17205899E-03,                  OZAN2557
0.77738799E-03, 0.12748297E-01, 0.17609399E-03, 0.82286191E-03,                  OZAN2558
0.12748297E-01, 0.10397998E-02, 0.18528499E-01, 0.16346496    ,                  OZAN2559
0.99201780E-03, 0.17791998E-01, 0.15583497    , 0.13150199E-03,                  OZAN2560
0.14228399E-02, 0.65863691E-02, 0.0           , 0.85815200E-05,                  OZAN2561
0.24928595E-03, 0.14938500E-03, 0.43912092E-03, 0.66200979E-02,                  OZAN2562
0.11576400E-04, 0.14110799E-02, 0.20466197E-01, 0.16839287E-04,                  OZAN2563
0.13444198E-02, 0.19896597E-01, 0.12166999E-03, 0.13499600E-02,                  OZAN2564
0.20466197E-01, 0.11671599E-03, 0.12993298E-02, 0.20466197E-01,                  OZAN2565
0.13525199E-03, 0.14130299E-02, 0.19705400E-01, 0.29181596E-03,                  OZAN2566
0.19776600E-02, 0.31167798E-01, 0.17254699E-02, 0.26332997E-01,                  OZAN2567
0.34060895    , 0.0           , 0.0           , 0.0           ,                  OZAN2568
0.18209699E-02, 0.27617998E-01, 0.35820794    , 0.21680598E-02,                  OZAN2569
0.27194899E-01, 0.29608798    , 0.17302500E-02, 0.25900196E-01,                  OZAN2570
0.28195298    , 0.17218299E-02, 0.26197199E-01, 0.34060895    ,                  OZAN2571
0.0           , 0.0           , 0.0           , 0.0           ,                  OZAN2572
0.0           , 0.0           , 0.0           , 0.0           ,                  OZAN2573
0.0           , 0.0           , 0.0           , 0.0           ,                  OZAN2574
0.0           , 0.0           , 0.0           , 0.0           ,                  OZAN2575
0.0           , 0.0           , 0.18366198E-02, 0.27019199E-01,                  OZAN2576
0.29608798    , 0.17352998E-02, 0.25992598E-01, 0.28154099    ,                  OZAN2577
0.0           , 0.0           , 0.0           , 0.0           ,                  OZAN2578
0.0           , 0.0           , 0.0           , 0.0           ,                  OZAN2579
0.0           , 0.0           , 0.0           , 0.0           ,                  OZAN2580
0.0           , 0.0           , 0.0           , 0.0           ,                  OZAN2581
0.0           , 0.0           , 0.0           , 0.0           ,                  OZAN2582
0.0           , 0.0           , 0.0           , 0.0           ,                  OZAN2583
0.0           , 0.0           , 0.0           , 0.69583580E-03,                  OZAN2584
0.10751199E-01, 0.13947999    , 0.0           , 0.0           ,                  OZAN2585
0.0           , 0.73542190E-03, 0.11275899E-01, 0.14668596    ,                  OZAN2586
0.10543198E-02, 0.11103097E-01, 0.12124795    , 0.69754990E-03,                  OZAN2587
0.10574497E-01, 0.11545998    , 0.69418992E-03, 0.10695796E-01,                  OZAN2588
0.13947999    , 0.0           , 0.0           , 0.0           ,                  OZAN2589
0.0           , 0.0           , 0.0           , 0.0           ,                  OZAN2590
0.0           , 0.0           , 0.0           , 0.0           ,                  OZAN2591
0.0           , 0.0           , 0.0           , 0.0           ,                  OZAN2592
```

```
0.0           , 0.0           , 0.0           , 0.74138585E-03,                         OZAN2593
0.11030897E-01, 0.12124795    , 0.69927284E-03, 0.10612298E-01,                         OZAN2594
0.11529100    , 0.0           , 0.0           , 0.0           ,                         OZAN2595
0.0           , 0.0           , 0.0           , 0.0           ,                         OZAN2596
0.0           , 0.0           , 0.0           , 0.0           ,                         OZAN2597
0.0           , 0.0           , 0.0           , 0.0           ,                         OZAN2598
0.0           , 0.0           , 0.0           , 0.0           ,                         OZAN2599
0.0           , 0.0           , 0.0           , 0.0           ,                         OZAN2600
0.0           , 0.0           , 0.0           , 0.0           ,                         OZAN2601
0.18389999E-03, 0.24020998E-02, 0.24629999E-01, 0.51889991E-04,                         OZAN2602
0.15922000E-03, 0.22634999E-02, 0.18999999E-03, 0.25079998E-02,                         OZAN2603
0.25649000E-01, 0.18999999E-03, 0.25079998E-02, 0.25649000E-01,                         OZAN2604
0.18389999E-03, 0.24020998E-02, 0.24629999E-01, 0.18389999E-03,                         OZAN2605
0.24020998E-02, 0.24629999E-01, 0.82433995E-04, 0.17221992E-05,                         OZAN2606
0.15021999E-04, 0.51730995E-05, 0.14428800E-04, 0.80397993E-04,                         OZAN2607
0.85492991E-02, 0.20836998E-01, 2.8643999     , 0.68459995E-04,                         OZAN2608
0.31861640E-03, 0.45292899E-02, 0.68459995E-04, 0.31861640E-03,                         OZAN2609
0.45292899E-02, 0.68459995E-04, 0.31861640E-03, 0.45292899E-02,                         OZAN2610
0.18999999E-03, 0.25079998E-02, 0.25649000E-01, 0.18389999E-03,                         OZAN2611
0.24020998E-02, 0.24629999E-01, 0.51889991E-04, 0.15922000E-03,                         OZAN2612
0.22634999E-02, 0.45356830E-03, 0.64307578E-05, 0.18659195E-03,                         OZAN2613
0.76715020E-04, 0.16548185E-03, 0.23476621E-02, 0.35671183E-04,                         OZAN2614
0.0           , 0.0           , 0.36990969E-05, 0.15933460E-04,                         OZAN2615
0.22649999E-03, 0.35671183E-04, 0.0           , 0.0           ,                         OZAN2616
0.35671183E-04, 0.0           , 0.0           , 0.38882892E-04,                         OZAN2617
0.31845761E-04, 0.45270380E-03, 0.68463400E-04, 0.31861593E-03,                         OZAN2618
0.45292862E-02, 0.37063519E-03, 0.62334538E-02, 0.67583025E-01,                         OZAN2619
0.25855988E-04, 0.12039990E-03, 0.17126899E-02, 0.38682180E-03,                         OZAN2620
0.65378174E-02, 0.70840955E-01, 0.38682180E-03, 0.65378174E-02,                         OZAN2621
0.70840955E-01, 0.37063519E-03, 0.62334538E-02, 0.67583025E-01,                         OZAN2622
0.37063519E-03, 0.62334538E-02, 0.67583025E-01, 0.13919998E-06,                         OZAN2623
0.64799895E-06, 0.92177997E-05, 0.0           , 0.0           ,                         OZAN2624
0.0           , 0.10344677E-01, 0.25197700E-01, 3.4759436     ,                         OZAN2625
0.51737545E-04, 0.24091981E-03, 0.34270864E-02, 0.51737545E-04,                         OZAN2626
0.24091981E-03, 0.34270864E-02, 0.51737545E-04, 0.24091981E-03,                         OZAN2627
0.34270864E-02, 0.38682180E-03, 0.65378174E-02, 0.70840955E-01,                         OZAN2628
```

```
 0.37063519E-03, 0.62334538E-02, 0.67583025E-01, 0.25855988E-04,        OZAN2629
 0.12039990E-03, 0.17126899E-02, 0.0           , 0.21408077E-05,         OZAN2630
 0.62225066E-04, 0.26800786E-04, 0.12479989E-03, 0.17752799E-02,         OZAN2631
 0.46759973E-70, 0.0           , 0.0           , 0.26312991E-05,         OZAN2632
 0.12047990E-04, 0.17138277E-03, 0.46759973E-70, 0.0           ,         OZAN2633
 0.0           , 0.46759973E-70, 0.0           , 0.0           ,         OZAN2634
 0.52113164E-05, 0.24079898E-04, 0.34253765E-03, 0.51737545E-04,         OZAN2635
 0.24091931E-03, 0.34270864E-02                                          OZAN2636
&END                                                                     OZAN2637
&IN2                                                                     OZAN2638
X2= 0.32783300E-01, 0.62555254E-01, 0.40656097E-01, 0.73466957E-01,      OZAN2639
 0.35542600E-01, 0.65780759E-01, 0.35764698E-01, 0.62729299E-01,         OZAN2640
 0.33167597E-01, 0.59441298E-01, 0.32431398E-01, 0.61510999E-01,         OZAN2641
 0.22293299E-01, 0.20518899E-01, 0.47938898E-03, 0.38426300E-03,         OZAN2642
 0.36893692E-03, 0.42748777E-03, 0.37100399E-03, 0.57322090E-03,         OZAN2643
 0.39881282E-03, 0.60247979E-03, 0.49287989E-03, 0.67770784E-03,         OZAN2644
 0.36979698E-01, 0.61235998E-01, 0.33640597E-01, 0.60008898E-01,         OZAN2645
 0.10335898    , 0.10833299    , 0.94007365E-02, 0.10357499E-01,         OZAN2646
 0.74656084E-02, 0.96096471E-02, 0.81225395E-01, 0.16196996    ,         OZAN2647
 0.77860951E-01, 0.14796394    , 0.92724979E-01, 0.15338296    ,         OZAN2648
 0.90584099E-01, 0.14503598    , 0.91204584E-01, 0.15430897    ,         OZAN2649
 0.71723163E-01, 0.13110900                                              OZAN2650
&END                                                                     OZAN2651
&IN3  X3=                                                                OZAN2652
12*0.,15.32E-5,7.501E-5,18*0.,7.69E-5,3.76E-5,12*0.                      OZAN2653
&END                                                                     OZAN2654
&INCS  NCS=1,1,2,3*0,1,0                                                 OZAN2655
&END                                                                     OZAN2656
&INNCS  ND=1,NSIGA=1,NUNSF=2,NSCAT=1                                     OZAN2657
&END                                                                     OZAN2658
&INNRK1  NRK1=1,NRUI1=20,NRLF1=20,NRVI1=11,NRVF1=11,NRCC1=1,             OZAN2659
       XT1=1.24223,4.5461E-1,1.28445E-01                                 OZAN2660
&END                                                                     OZAN2661
&INNRK2  NRK2=1,NRUI2=20,NRLF2=20,NRVI2=11,NRVF2=11,NRCC2=1,             OZAN2662
       XT2=1.16716E-4,1.29933E-3,2.04662E-02                             OZAN2663
&END                                                                     OZAN2664
```

```
&INNRK7 NRK7=1,NRUI7=20,NRUF7=20,NRVI7=11,NRVF7=11,NRCC7=1,
        XT7=9.05841E-2,1.45036E-01
&END
&INSKEF SKEF=1.01737499,0.39372498
&END
&INSKCZ SKOZN=1.01795673
&END
&INCDNC CSC=2*1,4*2,1,2
&END
&INDDNC DC=1,SIGAC=1,UNSFC=2,SIGFC=2,SGCSC=2,SCATC=1,SPNRC=2
&END
&INMRK1 MRK1=1,MRUI1=20,MRUF1=20,MRVI1=11,MRVF1=11,MRCC1=1,
        XK1=1.24223,4.5461E-1,1.28445E-01
&END
&INMRK2 MRK2=1,MRUI2=20,MRUF2=20,MRVI2=11,MRVF2=11,MRCC2=1,
        XK2=1.16716E-4,1.29933E-3,2.04662E-02
&END
&INMRK7 MRK7=1,MRUI7=20,MRUF7=20,MRVI7=11,MRVF7=11,MRCC7=1,
        XK7=9.05841E-2,1.45036E-01
&END
&INSPC ISTPC=8*2
&END
&INSTP ISD=2,ISSA=2,ISUF=2,ISSF=2,ISSG=2,ISST=2,ISSP=2,ISATT=2
&END
&INT
TMIN= 3.77            ,IJUMP=          15,TUP=  5.0000000    ,  7.0000000     ,
-0.72370051E 76,-0.72370051E 76,-0.72370051E 76,-0.72370051E 76,NINT=
         4,NCM1=            2,EPS2= 1.E-01
&END
/*
```

DELT Set Up

(Like Delete)

DELETE THE SPACE ALLOCATED FOR VARIOUS CROSS SECTIONS IF IT IS NOT INTENDED TO
MAKE ANY FURTHER USE OF THEM

```
// 'TOLGA YARMAN',REGION=128K,CLASS=A
/*MITID USER=(M8696,9441)
/*SRI LOW
/*MAIN LINES=20,CARDS=00,TIME=3
//STEP1 EXEC PGM=IEFBR14
//DD1 DD DSNAME=USERFILE.M8696.9441.EQD.IF,
// DISP=(OLD,DELETE)
//DD2 DD DSNAME=USERFILE.M8696.9441.ESI.GA,
// DISP=(OLD,DELETE)
//DD3 DD DSNAME=USERFILE.M8696.9441.EUN.SF,
// DISP=(OLD,DELETE)
//DD4 DD DSNAME=USERFILE.M8696.9441.ESC.AT,
// DISP=(OLD,DELETE)
//DD14 DD DSNAME=USERFILE.M8696.9441.FQD.IF,
// DISP=(OLD,DELETE)
//DD15 DD DSNAME=USERFILE.M8696.9441.FSI.GA,
// DISP=(OLD,DELETE)
//DD16 DD DSNAME=USERFILE.M8696.9441.FUN.SF,
// DISP=(OLD,DELETE)
//DD17 DD DSNAME=USERFILE.M8696.9441.FIS.GF,
// DISP=(OLD,DELETE)
//DD18 DD DSNAME=USERFILE.M8696.9441.TRD.IF,
// DISP=(OLD,DELETE)
//DD19 DD DSNAME=USERFILE.M8696.9441.TSI.GA,
// DISP=(OLD,DELETE)
//DD22 DD DSNAME=USERFILE.M8696.9441.FSC.AT,
// DISP=(OLD,DELETE)
//DD23 DD DSNAME=USERFILE.M8696.9441.TSC.AT,
// DISP=(OLD,DELETE)
//DD24 DD DSNAME=USERFILE.M8696.9441.FSG.CS,
// DISP=(OLD,DELETE)
//DD26 DD DSNAME=USERFILE.M8696.9441.FSP.NR,
```

```
// DISP=(OLD,DELETE)
//DD28 DD DSNAME=USERFILE.M8696.9441.HED.IF,
// DISP=(OLD,DELETE)
//DD29 DD DSNAME=USERFILE.M8696.9441.HSI.GA,
// DISP=(OLD,DELETE)
//DD31 DD DSNAME=USERFILE.M8696.9441.HSC.AT,
// DISP=(OLD,DELETE)
/*
```

PROGRAM RHO1

(The Ramp Change Slope of the Reactivity Matrix Computed Through a Perturbation Type of Approach)

```
// 'TOLGA YARMAN',REGION=200K,CLASS=A
/*MITID USER=(M8696,9441)
/*SRI LOW
/*MAIN LINES=20,CARDS=00,TIME=5
//STEP1 EXEC FORCGO
//C.SYSIN DD *
C PROGRAM RHO1
C
C CALCULATION OF THE RAMP CHANGE SLOPE OF THE REACTIVITY MATRIX BY A
C PERTURBATION TYPE OF APPROACH (IN ORDER TO CROSS CHECK ,, OZAN ,,)
C
      COMMON/FCFA/COEF,MCOF
C
      DIMENSION PSI(3,48,40),W(3,48,40),SIGA(3,47,39),
     1SCAT(2,47,39),HU(39),HV(47),R(40),ALFA(2,2),NDW(2),NDPSI(2),
     2COEF(3,47,39),D1(3),D2(3),ABO(2,2),DD(2,2)
C
      DATA NDW/11,13/
      DATA NDPSI/10,12/
      DATA DELT,D1,D2/3.77,2.23681,2.25753,1.66829E-2,1.24223,
     14.54610E-1,1.28445E-1/
C
 1000 FORMAT (1P5E14.6)
 2000 FORMAT (7E11.5)
C
      NAMELIST/INHU/HU
      NAMELIST/INHV/HV
      NAMELIST/OUT/ALFA,ABO,DD
C
      READ(5,INHU)
      READ(5,INHV)
      R(1)=0.
      DO 1030 MU=2,40
      R(MU)=R(MU-1)+HU(MU-1)
 1030 CONTINUE
      SIGA(1,11,20)=-4.4271784E-2
```

```
      SIGA(2,11,20)=-1.0629367E-1
      SIGA(3,11,20)=-1.48896338E+01
      DO 650 MG=1,3
      DO 640 MV=10,12
      SIGA(MG,MV,19)=0.
      COEF(MG,MV,19)=0.
      SIGA(MG,MV,21)=0.
  640 COEF(MG,MV,21)=0.
      SIGA(MG,10,20)=0.
      COEF(MG,10,20)=0.
      SIGA(MG,12,20)=0.
  650 COEF(MG,12,20)=0.
      SCAT(1,11,20)=9.0215163E-2
      SCAT(2,11,20)=1.44608512E-1
      DO 670 MG=1,2
      DO 660 MV=10,12
      SCAT(MG,MV,19)=0.
  660 SCAT(MG,MV,21)=0.
      SCAT(MG,10,20)=0.
  670 SCAT(MG,12,20)=0.
      MCOF=0
      MCF2=1
      DO 100 I=1,2
      NN=NDW(I)
      READ(NN,1000) W
      REWIND NN
      DO 100 K=1,2
      MM=NDPSI(K)
      READ(MM,1000) PSI
      REWIND MM
C
      CALL ABSP(W,PSI,SIGA,SCAT,HU,HV,R,MCF2,SUM22)
C
      ABO(I,K)=-SUM22*1.5708/DELT
  100 CONTINUE
      MCOF=1
```

```
      DO 200 I=1,2
      NN=NDW(I)
      READ(NN,1000) W
      REWIND NN
      DO 200 K=1,2
      MM=NDPSI(K)
      READ(MM,1000) PSI
      REWIND MM
      IF (K.EQ.1) GO TO 750
      READ(29,2000) SIGA
      REWIND 29
      READ(31,2000) SCAT
      REWIND 31
      DO 500 MG=1,3
      COEF(MG,11,20)=(D2(MG)-D1(MG))/D2(MG)
  500 CONTINUE
      GO TO 850
  750 CONTINUE
      READ(2,2000) SIGA
      REWIND 2
      READ(4,2000) SCAT
      REWIND 4
      DO 550 MG=1,3
  550 COEF(MG,11,20)=(D2(MG)-D1(MG))/D1(MG)
  850 CONTINUE
C
      CALL ABSP(W,PSI,SIGA,SCAT,HU,HV,R,MCF2,SUM22)
C
      DD(I,K)=SUM22*1.5708/DELT
      ALFA(I,K)=(ABO(I,K)+DD(I,K))
  200 CONTINUE
      WRITE(6,OUT)
      STOP
      END
      SUBROUTINE ABSP(W,PSI,SIGA,SCAT,HU,HV,R,MCF2,SUM22)
C
```

```
C ABSP LIKE ABSORPTION(AND ALSO SCATTERING)INTEGRATED OVER THE
C REACTOR VOLUME AFTER BEING WEIGHTED
C
      COMMON/FCFA/COEF,MCOF
C
      DIMENSION W(3,48,40),PSI(3,48,40),SIGA(3,47,39),SCAT(2,47,39),
     1HU(39),HV(47),R(40),COEF(3,47,39)
C
      SUM22=0.
      IF ((MCF2.EQ.1).AND.(MCOF.EQ.1)) GO TO 16
      CF11=1.
      CF12=1.
      CF13=1.
      CF14=1.
      CF21=1.
      CF22=1.
      CF23=1.
      CF24=1.
      CF31=1.
      CF32=1.
      CF33=1.
      CF34=1.
   16 DO 6 MV=11,12
      HV1=HV(MV-1)
      HV2=HV(MV)
      DO 6 MU=20,21
      W1=W(1,MV,MU)
      W2=W(2,MV,MU)
      W3=W(3,MV,MU)
      PI1=PSI(1,MV,MU)
      PI2=PSI(2,MV,MU)
      PI3=PSI(3,MV,MU)
      SA13=SIGA(1,MV-1,MU)
      SA14=SIGA(1,MV,MU)
      SA23=SIGA(2,MV-1,MU)
      SA24=SIGA(2,MV,MU)
```

```
      SA33=SIGA(3,MV-1,MU)                                              RH010145
      SA34=SIGA(3,MV,MU)                                                RH010146
      ST13=SCAT(1,MV-1,MU)                                              RH010147
      ST14=SCAT(1,MV,MU)                                                RH010148
      ST23=SCAT(2,MV-1,MU)                                              RH010149
      ST24=SCAT(2,MV,MU)                                                RH010150
      HR2=(R(MU)+HU(MU)/4)*HU(MU)                                       RH010151
      SA11=SIGA(1,MV-1,MU-1)                                            RH010152
      SA12=SIGA(1,MV,MU-1)                                              RH010153
      SA21=SIGA(2,MV-1,MU-1)                                            RH010154
      SA22=SIGA(2,MV,MU-1)                                              RH010155
      SA31=SIGA(3,MV-1,MU-1)                                            RH010156
      SA32=SIGA(3,MV,MU-1)                                              RH010157
      ST11=SCAT(1,MV-1,MU-1)                                            RH010158
      ST12=SCAT(1,MV,MU-1)                                              RH010159
      ST21=SCAT(2,MV-1,MU-1)                                            RH010160
      ST22=SCAT(2,MV,MU-1)                                              RH010161
      HR1=(R(MU)-HU(MU-1)/4)*HU(MU-1)                                   RH010162
      IF ((MCF2.EQ.0).OR.(MCOF.EQ.0)) GO TO 20                          RH010163
      CF13=COEF(1,MV-1,MU)                                              RH010164
      CF14=COEF(1,MV,MU)                                                RH010165
      CF23=COEF(2,MV-1,MU)                                              RH010166
      CF24=COEF(2,MV,MU)                                                RH010167
      CF33=COEF(3,MV-1,MU)                                              RH010168
      CF34=COEF(3,MV,MU)                                                RH010169
      CF11=COEF(1,MV-1,MU-1)                                            RH010170
      CF12=COEF(1,MV,MU-1)                                              RH010171
      CF21=COEF(2,MV-1,MU-1)                                            RH010172
      CF22=COEF(2,MV,MU-1)                                              RH010173
      CF31=COEF(3,MV-1,MU-1)                                            RH010174
      CF32=COEF(3,MV,MU-1)                                              RH010175
   20 ASB=W1*(((SA11+ST11)*CF11*HV1+(SA12+ST12)*CF12*HV2)*HR1+((SA13+ST1RH010176
     13)*CF13*HV1+(SA14+ST14)*CF14*HV2)*HR2)*PI1+W2*(-((ST11*CF21*HV1+ST RH010177
     212*CF22*HV2)*HR1+(ST13*CF23*HV1+ST14*CF24*HV2)*HR2)*PI1+(((SA21+ST RH010178
     321)*CF21*HV1+(SA22+ST22)*CF22*HV2)*HR1+((SA23+ST23)*CF23*HV1+(SA24 RH010179
     3+ST24)*CF24*HV2)*HR2)*PI2)+W3*(-((ST21*CF31*HV1+ST22*CF32*HV2)*HR1 RH010180
```

```
     4+(ST23*CF33*HV1+ST24*CF34*HV2)*HR2)*PI2+((SA31*CF31*HV1+SA32*CF32*
     5HV2)*HR1+(SA33*CF33*HV1+SA34*CF34*HV2)*HR2)*PI3)
      SUM22=SUM22+ASB
    6 CONTINUE
      RETURN
      END
/*
//G.FT10F001 DD DSNAME=USERFILE.M8696.9441.EQP.SI,DISP=OLD
//G.FT11F001 DD DSNAME=USERFILE.M8696.9441.FQA.DJ,DISP=OLD
//G.FT12F001 DD DSNAME=USERFILE.M8696.9441.TRP.SI,DISP=OLD
//G.FT13F001 DD DSNAME=USERFILE.M8696.9441.TRA.DJ,DISP=OLD
//G.FT01F001 DD DSNAME=USERFILE.M8696.9441.EQD.IF,DISP=OLD
//G.FT02F001 DD DSNAME=USERFILE.M8696.9441.ESI.GA,DISP=OLD
//G.FT04F001 DD DSNAME=USERFILE.M8696.9441.ESC.AT,DISP=OLD
//G.FT28F001 DD DSNAME=USERFILE.M8696.9441.HED.IF,DISP=OLD
//G.FT29F001 DD DSNAME=USERFILE.M8696.9441.HSI.GA,DISP=OLD
//G.FT31F001 DD DSNAME=USERFILE.M8696.9441.HSC.AT,DISP=OLD
//G.SYSIN DD *
 &INHU
      HU=3.78,1.864,2*1.364,2*0.317,4*1.614,4*0.977,1.596,3*0.954,0.159,0.635,
         0.159,0.476,3*0.687,0.635,7*4.41,3.,2*9.66,3*15.24
 &END
 &INHV
      HV=3*10.16,3*5.080,7.62,12*2.54,5*1.27,0.635,3*1.164,5*0.635,0.952,
         7*0.997,3*1.27,3*15.24
 &END
/*
```